

THE EXPANSION OF KNOWLEDGE ON EVAPOTRANSPIRATION AND STREAM FLOW REDUCTION OF DIFFERENT CLONES/ HYBRIDS TO IMPROVE THE WATER USE ESTIMATION OF SFRA SPECIES (I.E. PINUS, EUCALYPTUS AND WATTLE SPECIES).

Clulow, A.D., Kunz, R.P., Gokool, S., Toucher, M.L., Schutte, S., Schulze, R.E., Horan, R., Everson, C.E, Thornton-Dibb, S.L.C., Horan, M.J.C., Kaptein, N., Clark, D.J. and Germishuizen, I

VOLUME 2: SFRA ASSESSMENT UTILITY



TT 898/2/22



THE EXPANSION OF KNOWLEDGE ON
EVAPOTRANSPIRATION AND STREAM FLOW REDUCTION OF
DIFFERENT CLONES/HYBRIDS TO IMPROVE THE WATER USE
ESTIMATION OF SFRA SPECIES (I.E. PINUS, EUCALYPTUS
AND WATTLE SPECIES):

VOLUME 2: SFRA ASSESSMENT UTILITY

Report to the
WATER RESEARCH COMMISSION

Prepared by: Clulow, A.D.¹, Kunz, R.P.¹, Gokool, S.¹, Toucher, M.L.^{1,2}, Schutte, S.¹, Schulze, R.E.¹,
Horan, R.¹, Thornton-Dibb, S.L.C.¹, Horan, M.J.C.¹, Kaptein, N.^{1,3},
Clark, D.J.⁴, Germishuizen, I.³ and Everson, C.E.¹

¹ Centre for Water Resources Research

² South African Environmental Observation Network

³ Institute for Commercial Forestry Research

⁴ South African Sugar Association

WRC Report no. TT 898/2/22
ISBN 978-0-6392-0355-3

February 2023



VOLUME 2:

SFRA ASSESSMENT UTILITY

Prepared by:

Clulow, A.D., Kunz, R.P., Gokool, S., Toucher, M.L., Schutte, S., Schulze, R.E., Horan, R., Thornton-Dibb, S.L.C., Horan, M.J.C., Kaptein, N., Clark, D.J. and Germishuizen, I., Everson, C.E.

Report to the:

WATER RESEARCH COMMISSION

Physical Address:

Lynnwood Bridge Office Park
Bloukrans Building,
4 Daventry Street, Lynnwood Manor
PRETORIA

Postal Address:

Private Bag X03
GEZINA, 0031, South Africa

Project Leader:

Dr Alistair Clulow

This report has been reviewed by the Water Research Commission (WRC) and approved for publication.

Approval does not signify that the contents necessarily reflect the views and policies of the WRC, nor does mention of trade names or commercial products constitute endorsement or recommendation for use.

Obtainable from:

Water Research Commission, Private Bag X03
GEZINA, 0031

orders@wrc.org.za or download from www.wrc.org.za

© Water Research Commission

EXECUTIVE SUMMARY

BACKGROUND

The impacts of commercial trees on South Africa's water resources is a topic of significant concern to many from varying points of view, from policy and decision makers, to the forestry industry and stakeholder concerned about the impacts at their local scale. In particular, the ongoing disputes surrounding genus exchange has resulted in increased conflict surrounding the impacts of commercial forestry on water resources. Under the National Water Act of 1998, the use of land for commercial afforestation is a streamflow reduction activity (SFRA). The tools used in the SFRA assessment have developed over time. The most recent prior to this project, was the development the SFRA Assessment Utility to assist in water use licensing by Jewitt et al. (2009). The SFRA Assessment Utility provided estimates of reductions at a finer scaler and an improved consideration of low flows. However, as the regulation of afforestation needs to be achieved within an environment that is continually changing and evolving with regard to legal, social and biophysical characteristics, an update to the SFRA Assessment Utility was required to address and include the following,

- The utility estimates the streamflow reductions of three commercial forestry species, namely *Pinus patula*, *Eucalyptus grandis* and *Acacia mearnsii*. However, as the forestry industry currently uses more than 40 species, hybrids and clones, there is a pressing need to expand the knowledge on the water use of the different species, clones and hybrids used by the forestry industry.
- Update the hydrological baseline against which the impacts of afforestation are assessed to the CWRR clusters as developed by WRC project K5/2437 (Toucher et al., 2020).
- As Leaf Area Index (LAI) was used to determine the water use parameters for the CWRR clusters, expand the LAI database for the commercial forestry species.
- Include into the SFRA Assessment Utility the updated quinary catchments climate and soils database, as well as updates to the ACRU model.

The outcomes of the project are captured in two final reports, Deliverable 8 which details the field-based studies to expand the knowledge of the water use of different commercial tree species and this Deliverable 9 which details the updates and advances made to the inputs and parameters used in the ACRU model runs. The outputs of the ACRU model runs are contained in the updated SFRA Assessment Utility.

PROJECT AIMS

The following were the aims of the project:

1. To expand the knowledge of the estimates of water use of different clones and hybrids of eucalypt, wattle and pine species (e.g. clones/hybrids most commonly used, clones/hybrids planted in optimal sites).
2. To address shortcomings in the availability of leaf area index information for different SFRA species, clones and hybrids.
3. To improve existing tools used for the estimation of the impacts of SFRA through the inclusion of improved soils data and baseline land cover data, as well as the inclusion of the latest process results related to water use (i.e. evapotranspiration) of SFRA clones, hybrids and species.

The outcomes, findings and products of the project are comprised of two final reports. This document details the research that contributes to the SFRA Utility to address Aims 3 and 4, while the other deliverable speaks to Aim 1, which focuses on the improved water use estimation of SFRA species.

Given the structure of the report as stand-alone Chapters, a summary of each is provided.

CHAPTER 2: MAPPING SOIL HYDROLOGICAL ATTRIBUTES AT TERRAIN UNIT SPATIAL RESOLUTION FOR THE SOUTH AFRICAN PRODUCTION FORESTRY INDUSTRY

The soils used in the quinary catchments database, prior to this project, were based on the Agricultural Research Council (ARC) and Institute for Soil-Climate-Water (ISCW) division of the country at 1 in 250 000 scale into zones of similar broad soil categories referred to as land types. Any particular land type is made up of many different (although similar) soil series, and with the committee-based knowledge of the water holding capacities of the individual soils within a land type, through a process of area weighting, land type specific values of the hydrological parameters were derived. With advances in GIS and computing, it has become possible to subdivide landscapes in catenal sequences using elevation, slope, aspect and surface curvature and spatially identify the position of the terrain unit (i.e. crest, scarp, mid slope, foot slope and valley floor). As the ARC not only included the breakdown of land types as a whole by ratio of soil series, but also the percentages of each catenal sequence in the land type, as well as the soil series percentages for each catenal stage, the soil series per terrain unit was identified as well as the location of each terrain unit. Thus, the country was divided into small homogeneous areas of, for example, crests, mid slopes, with their associated soil mixes.

For the key soils physical attributes of

- Thicknesses of Topsoil and Subsoil Horizons
- Soil Water Content at the Soil's Permanent Wilting Point
- Soil Water Content at the Soil's Drained Upper Limit
- Soil Water Content when Soils are at Total Porosity
- Saturated Redistribution Rates

Algorithms and working rules were established to determine the parameters for each terrain unit and its associated Land Type soils series.

The outcome was that significant spatial information gain was obtained when using TU level information compared with the use of Land Type information (Figure A), which has aggregated and, as such, has area-averaged much the detail available on the soils of South Africa.

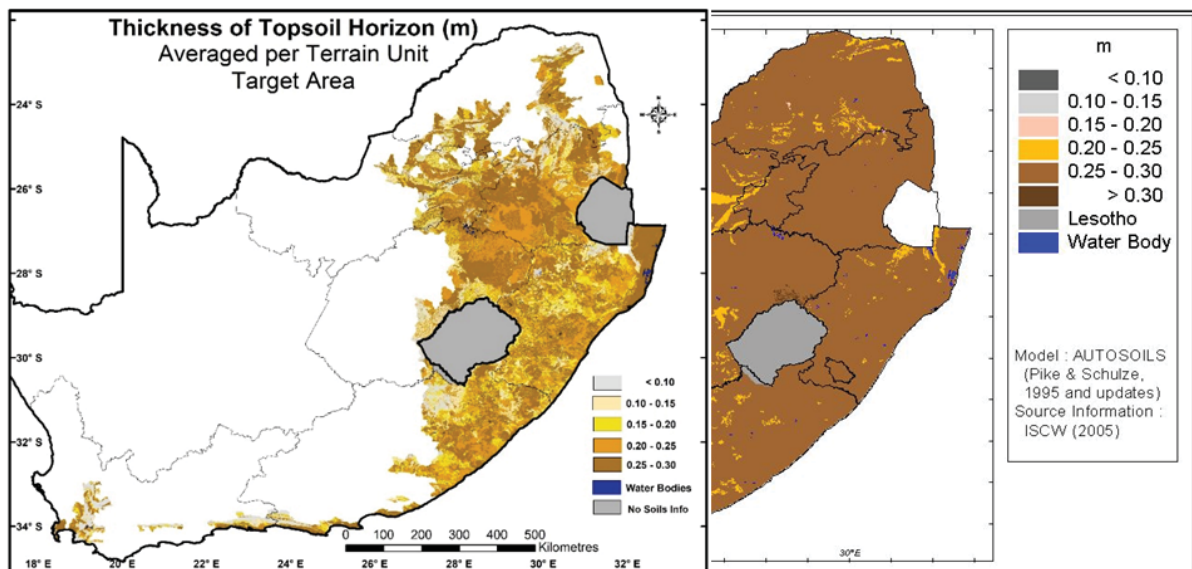


Figure A: Example of the spatial information gain when utilising terrain unit information (left) compared with detail when using area-averaged Land Type information (right map: Schulze and Horan, 2008)

CHAPTER 3: INVESTIGATION OF THE POTENTIAL USE OF THE ROOT ZONE STORAGE CONCEPT

This chapter did not speak directly to the aims of the project but was supplement and undertaken to potentially advance knowledge related to an alternative approach to modelling the root zone. The question addressed was “Can the root zone storage concept be used to determine the root zone storage capacity and thus the soil depth under commercial tree species?”

Soil and rooting depth are key parameters in hydrological and land-surface modelling; however, the distribution of soil and rooting depths are largely unknown due to the difficulties in measurement and the high variance between soil type, plant species and combinations thereof within modelling units. A common trait amongst many plant species is a deep complex rooting system. The rooting systems are essential in the determination of the soil pedogenesis, soil water partitioning and soil chemistry processes. Further, research efforts are focused on shallow root systems whilst the study of deep root systems are scant, due to challenging procedures to observe and measure deep systems. Studies show that the majority of the soils are deeper than 1.2 metres and many plants grow beyond this depth. However, the depth of 1.2 metres is often considered as the maximum soil depth in literature and hydrological modelling, e.g. the ACRU model. The misrepresentation of soil and root depths in hydrological models causes uncertainty in hydrological prediction and land-surface modelling.

Root-zone storage capacity can be considered as a volume of water per unit area within the range of plant roots and available for transpiration. Vegetation survives by extracting plant available water between the field capacity and wilting point of their immediate soil, thereby creating a moisture storage volume known as the root-zone storage capacity. The vegetative roots structurally adapt to establish an equilibrium resulting in the avoidance of water shortage within the ecosystem, whilst minimising root growth necessary to avoid water stress. Thus, climate has a strong influence on the hydrologically active root-zone, whilst periods of drought and flood are critical situations that affect the establishment of the root-zone.

Successful studies have been performed internationally using the root-zone concept but not as yet in South African conditions. The most accurate and popular method of estimating the root-zone capacity is using the water balance principle. Of the eight current studies using the water balance method, the methods by Nijzink et al. (2016), Wang-Erlandsson et al. (2014) and the DiCaSM routine are the most appropriate under South African conditions and for the potential use in ACRU. Thus, these were further investigated for two well-monitored catchments, viz. the Two Streams and Cathedral Peak Catchment VI.

The ACRU model was set up and calibrated for both catchment using data that is readily available (i.e. maximum and minimum temperature, precipitation and streamflow) to identify the weaknesses within a common modelling environment. As the purpose was to use commonly available information as a way of determining the model adequacy under typical conditions, the observed evaporation and soil moisture data that was available in this case was used solely for the purpose of validation and not in the model calibration.

The methodology followed was:

1. The ACRU model was run using daily observed precipitation and maximum and minimum temperatures. Hargreaves and Samani daily was used internally to estimate the potential evaporation. The daily observed streamflow was used in the calibration of the model.
2. As observed, actual evaporation and soil moisture are not commonly available, these were not used in the calibration of the model. In the calibration process, only parameters were that were known or could be estimated with use of the ACRU manual were adjusted.
3. The calibration statistics were calculated on the best fit of streamflow obtained only from commonly available input data and parameters. Once all the parameters and information that would be commonly available for South African catchments were adjusted, the calibration process ceased.
4. The simulated actual evaporation and soil water was validated against observed data.

5. The root zone storage calculations were undertaken with both the observed and the simulated actual evaporation, observed precipitation, interception and observed streamflow. This was to test the robustness of the methodology to data scarcity.
6. The observed gravimetric water content, permanent wilting point and field capacity were converted to a depth of water using the soil depth before being compared to the root-zone storage capacity. To validate the root-zone storage capacity estimations, the estimations needed to be adjusted to reflect a water content within the soil profile using the permanent wilting point as the lower limit of the water in the root zone.

The results showed that the ACRU model performed poorly at Cathedral Peak VI and more so at Two Streams. The streamflow simulations at Cathedral Peak Catchment VI were fair. However, the actual evaporation and soil water simulations were poor. At Two Streams the simulation of the streamflow, actual evaporation and soil water were all poor. The poor performance could be the conceptualisation of and uncertainty with the use of the crop coefficient in the estimation of actual evaporation in the ACRU model and consequently the soil water. Added to this, the lack of adequate root depth and distribution information, and poor soils data further compounds the poor estimation of the soil water.

Three methods were used to estimate the root-zone storage capacity for each of the catchments, however, validation was only undertaken for the Two Streams catchment. Across the soil profile, the root-zone storage capacity methods produced better simulation of the soil water than the ACRU model at the Two Streams catchment. The goodness of fit statistics showed a poor simulation for all the root-zone storage capacity methods and the ACRU simulation compared to the observed data. However, the estimated root-zone storage capacity methods produced better statistics compared to the ACRU simulation. The estimated root-zone storage capacity methods all produce an accurate bias, which indicates that the volume of water within the soil profile was comparable to observed values, but the root zone storage capacities were substantially more reactive to the rainfall compared to the observed data. The goodness of fit statistics suggest that the DiCaSM method produced the best simulation of the observed soil water although all three methods produced less variance than the observed data.

The root-zone storage capacity is a core component in determining a dynamic hydrological response and could be a valuable concept in improving the development of dynamic models. The concept of root-zone storage in hydrological modelling would need to be treated as a dynamically evolving parameter as a function of vegetation and climate. The use of the root-zone storage concept within the ACRU model could limit the model uncertainty. The method could allow areas of limited soils and rooting data to be modelled more accurately and the implication of afforestation be fully understood. However, the study was limited to two small catchments and the data used for validation was for a short time. A more spatially and temporally explicit study would improve the understanding and confidence in the methodology and concept. Although this study has its limitations, it could be considered as proposing a step forward in the modelling of soil water in South Africa

CHAPTER 4: THE CWRR CLUSTERS AS A HYDROLOGICAL BASELINE

The previously accepted hydrological baseline against which the impacts of SFRA activities were assessed was the Acocks (1988) Veld Types. The Acocks (1988) Veld Types which were mapped at a coarse resolution were agriculturally based, with a veld type defined as “an agro-ecological unit of vegetation whose range of variation is small enough to permit the whole of it to have the same farming potentialities” (Acocks, 1953). The South African National Biodiversity Institute (SANBI) produced a finer scale vegetation map (SANBI, 2012) using a “sound theoretical classification of the vegetation of South Africa” that describes and maps the vegetation diversity across South Africa, based on the current knowledge of vegetation structure and biogeographical patterns (Mucina and Rutherford, 2006). The SANBI (2012) vegetation maps have been broadly accepted by numerous disciplines as a good representation of natural vegetation. The WRC project K5/2437 (Toucher et al., 2020) clustered the vegetation units of the SANBI (2012) map into hydrologically

relevant clusters to which vegetation and water-use parameters, for use in the ACRU model, were assigned using a consistent and repeatable methodology. Importantly, the crop coefficients were derived using a method which made use of LAI. The recommendation of the project was to assess SFRA impacts relative to the CWRR clusters for which consistent vegetation and water use parameters had been determined.

CHAPTER 5: ADDRESSING THE SHORTCOMINGS IN THE AVAILABILITY OF LEAF AREA INDEX INFORMATION FOR COMMERCIAL TREE SPECIES

There is an urgent need to more adequately understand and better represent the biophysical characteristics of commercial forestry species, hybrids and clones in the tools that are used as decision support systems so that their hydrological impacts can be more accurately quantified. For such purposes, Leaf Area Index (LAI) is a key parameter as it is often used to characterize vegetation biophysical properties and plays an important regulatory role in terrestrial-atmospheric exchanges.

LAI is often a critical data input to various evapotranspiration, hydrological and climatic models. However, LAI data is seldom available in SA at spatio-temporal scales that can be used to guide and inform management decisions for localised applications due to the challenges experienced with traditional in-situ data acquisition approaches. While remote sensing represents a suitable alternative to traditional approaches, the global satellite-based LAI products that are used most frequently may be too coarse to provide representative estimates of LAI within the various commercial forestry compartments. Statistical approaches which utilize satellite-derived vegetation indices (VIs) to estimate LAI have been most frequently applied to address this limitation, as VIs can be generated relatively easily at various spatio-temporal resolutions and are often used in conjunction with or as a surrogate to LAI to account for vegetation characteristics. Despite the success and relative simplicity of these approaches, the acquisition, storage, processing and analysis of the large volumes of satellite data that are now available can prove to be a barrier to users that lack the computational resources and technical skills required to effectively utilize this data. With the emergence of geospatial cloud computing platforms and convenient machine learning packages many of the aforementioned barriers have now been removed. In light of these advancements, we proposed a methodology to acquire moderate resolution LAI (LAI_{MR}) estimates using the Google Earth Engine (GEE) cloud computing platform and machine learning.

Fifteen sites distributed within the KwaZulu-Natal and Mpumalanga provinces of South Africa were selected as study areas. Coarse spatial resolution MODIS LAI and vegetation index (VI) products were acquired for each of these sites to establish the LAI-VI relationship which was then used to develop machine learning-based models (MLBMs) to estimate LAI_{MR} using VIs derived from Landsat or Sentinel-2 data. All satellite-based datasets were accessed within the GEE platform and were further processed prior to their export for further analysis. The caret and caretEnsemble packages available in R statistical software were then used to develop and test the MLBMs using these datasets. A mix of simple and complex machine learning algorithms which included i) generalized linear model (GLM), ii) decision tree (CART), iii) k nearest neighbour (kNN), iv) random forest (RF) and v) support vector machine (SVM) was selected for application. Additionally, two new MLBMs were developed using an ensembling approach which involved using the aforementioned algorithms as base algorithms and stacking these algorithms to combine their predictions. Model performance was first assessed by performing a 10-fold cross validation with 3 repeats on the data reserved for training. Thereafter, the 3 best performing models were selected and applied using the data reserved for validation. Following this two-step process the best performing model was then selected to estimate LAI using estimates of NDVI and EVI.

The finer spatial resolution NDVI and EVI estimates were first upscaled to the MODIS LAI spatial resolution prior to their use in the selected MLBM. The rationale for this was so that the estimated LAI could be evaluated against MODIS LAI product values, as these were the only long-term records available. During each of these various phases the performance of the MLBMs were evaluated using commonly applied

machine learning performance metrics. Upon completion of the MLBM evaluations, LAI_{MR} was estimated using the NDVI and EVI estimates derived at the original Landsat and Sentinel-2 spatial resolutions.

During the validation and testing phases of the study, LAI estimates were compared against the corresponding MODIS LAI product values. The results of these investigations demonstrated that MLBMs performed satisfactorily across the majority of the study sites, producing correlation coefficients ranging from 0.62-0.97 and 0.29-0.84 for the validation and testing phases, respectively. Comparisons between the LAI estimates derived using the different finer spatial resolution VIs showed that there were no major drop-offs in performance of the MLBMs when using Landsat- and Sentinel-derived VIs to estimate LAI, which is possibly a consequence of the compatibility of the bands between these sensors.

Despite the satisfactory performance of the MLBMs during the various phases of the study, it should be noted that a major limitation of the methods applied herein is that the accuracy of the estimated LAI will largely be influenced by the accuracy of a coarse spatial resolution LAI product. Furthermore, it was also noted that there was a decrease in the performance of the MLBMs when using VIs derived from Landsat or Sentinel-2 data to estimate LAI as compared to the use of MODIS derived VIs. This can be largely attributed to inherent limitations associated with the proposed methodology, such as i) the lack of moderate-high spatial resolution LAI records that could be used for training and testing purposes, and ii) saturation effects associated with the use of VIs. Notwithstanding these limitations, the proposed methodology has been shown to be flexible and robust and can be a useful approach to acquire LAI_{MR} estimates with fairly reasonable accuracy in data limited circumstances. Furthermore, the synergistic use of geospatial cloud computing platforms and convenient machine learning packages provide users with greater opportunities to more effectively utilize information rich satellite datasets which in turn can serve enhance the capabilities of existing decision support tools used to guide and inform water resources management decisions.

CHAPTER 6: DETERMINING CROP COEFFICIENTS FOR COMMERCIAL TREE SPECIES

The accurate quantification of evapotranspiration (ET), which is a key variable within ACRU and many other hydrological models, forms a crucial component of modelling hydrological response under various land uses. While many ET estimation procedures exist, the use of the Food and Agricultural Organization method (FAO-56) which is based on the reference evapotranspiration and crop coefficient (K_c) remains one of the most widely used approaches and is the method used in most hydrological models including ACRU. However, the lack of well-established K_c coefficients in these non-cropping environments derived from conventional measurement approaches is limited. To address this situation, alternate K_c estimation procedures have been recommended/proposed to derive K_c as a function of variables which directly influence it. One of the variables that is most frequently utilized for such purposes is LAI.

Since remote sensing-based methods provide a pragmatic approach to fairly easily acquire spatially and temporally explicit LAI data across large geographic extents, there exists great potential for utilizing these datasets to derive K_c in non-agricultural and natural environments. Considering the recent advancements in geospatial cloud computing and machine learning, the focus of this study was to leverage the processing and analysis capabilities of these platforms to derive K_c estimates for various commercial forest species, clones and hybrids which are presently lacking but urgently required and necessary to improve the management and regulation of this activity.

In this study we applied and evaluated two approaches to estimate K_c as a function of satellite-derived LAI estimates, i.e. a relatively simplistic conventional estimation procedure and a machine learning based approach. For this purpose, K_c was initially quantified through daily in-situ measurements of ET and ET_0 to account for vegetation characteristics and weather conditions at two sites. The daily ET and ET_0 were then scaled up to monthly totals and these values were used to create a monthly time series of K_c for each of the sites. Thereafter, the GEE platform was used to acquire MODIS LAI data for the two sites. This data was

then summarized to create a time-series of average monthly values that was consistent with the K_{cObs} dataset.

For the estimation of K_c using a machine learning-based approach, the monthly K_{cObs} and LAI dataset for each of the sites were combined into a single dataset to maximize the use of the relatively limited data that was available whilst also allowing for the development of a generic model that could be used to estimate K_c for various forestry species, hybrids and clones in the region when only LAI data is available. The caret and caretEnsemble packages available in R statistical software were used to develop and test the machine learning based models (MLBMs). A mix of simple and complex machine learning algorithms which included i) generalized linear model (GLM), ii) decision tree (CART), iii) k nearest neighbour (kNN), iv) random forest (RF), and v) support vector machine (SVM) was selected for application. Additionally, a new MLBM was developed using an ensembling approach which involved using the aforementioned algorithms as base algorithms and stacking these algorithms to combine their predictions. Model performance was assessed by performing a k-fold cross validation approach. Thereafter, the best performing model was then selected to estimate the average monthly K_c using the average monthly LAI values for each of the sites. Once the average monthly K_c was derived for each of the sites using both the conventional and machine learning-based approaches, these values were used in conjunction with the daily ET_o to estimate daily ET. The daily ET estimates were then scaled up to monthly totals and these values along with the monthly K_c were then compared against the corresponding values measured in-situ. Estimated K_c and ET were evaluated through comparisons against in-situ measurements using commonly applied performance metrics.

The results of our investigations demonstrated that K_c could be estimated relatively accurately using satellite-derived LAI estimates as inputs to both a conventional and machine-learning based estimation approach. The range of the estimated K_c -RMSE values (0.06-0.20) when compared against K_{cObs} , are within the range of published values (0.04-0.30). Furthermore, both techniques were found to perform relatively well during the winter months. This is particularly noteworthy, as it is during the drier periods when forest species are likely to have greater impacts on available water resources, therefore, this is when it is particularly important to accurately estimate ET.

The estimation of ET using the aforementioned K_c estimates was also quite promising with simulated values being in good agreement with the measured values, producing R^2 values ranging from 0.72 and 0.89. Overall, the results of the investigations demonstrated the utility of using satellite-derived estimates of LAI for the estimation of K_c . Both the conventional and machine learning based approaches showed good levels of performance, however, the ability of the machine learning based approaches to more adequately account for complex relationships between variables can prove to be invaluable when attempting to estimate K_c by extrapolating K_c -LAI models to ungauged or data scarce sites.

Despite the success of the investigations, the methods employed herein are limited by the assumptions that were factored into the analyses as well as the reliance on in-situ measurements. Nevertheless, in this study we demonstrated how the use of geospatial cloud computing and machine learning based approaches can provide a robust and efficient means to handle large volumes of data and optimally utilize this data. Furthermore, through the development of a generic K_c -LAI model in this study, K_c values for the various commercial forest species, clones and hybrids can be seamlessly generated using easily accessible and readily available satellite-based estimates of LAI. This can prove to be particularly advantageous for future hydrological modelling applications and may allow for improved understanding and estimation of the hydrological impacts of commercial forestry in the region.

Using the MLBM described above, K_c values were derived. With using an LAI based approach, the record of LAI obtained from the satellite imagery needs to be as long as possible and the forestry compartment had to be as large as possible. Together with ICFR, a compartment database that gave the compartment size, species and age, was used to select appropriate sites. Not all the forestry species could be included, as for some suitable compartments where the trees had been planted a few years back to give a long enough

record of LAI could not be identified. However, 15 sites to represent the dominant species were included and differences in same species grown in different ICFR climate zones were included.

For each of the sites, MODIS LAI (MCD15A3H V6 level 4, 500 m spatial and 4-day temporal resolution), Landsat 7 and 8 (Collection 1 Tier 1 calibrated top-of-atmosphere reflectance, 30 m spatial and 16-day temporal resolution) and Sentinel-2 (MultiSpectral Instrument, Level-1C, 10 m spatial and 5-day temporal resolution) images were imported into GEE. Using the MLBM LAI values from the Landsat and Sentinel-2 VI's were estimated. Following which the MLBM was applied to estimate the K_c values for the 15 sites for the three LAI products. The K_c values were averaged monthly. The K_c estimated using the three LAI products were generally similar (Figure B), and the variation between the maximum and minimum K_c values across all species and LAI products is 0.15. The greatest variation between the maximum and minimum K_c value for a species is for *E. grandis x nitens* in both a warm temperate dry (WTD) and cool temperate moist (CTM) climate zone, and when using the Landsat or Sentinel-2 LAI products. Overall, the variation between the minimum and maximum K_c values was less when using the MODIS LAI product. Negligible variation occurred between the minimum and maximum K_c values for *E. grandis* warm temperate moist (WTM), *E. grandis x urophylla* WTM and *P. elliottii x caribaea* WTM. K_c values estimated using MODIS LAI will be the primary set of K_c values used. It must be noted that these are FAO-reference potential related, non-standard K_c values.

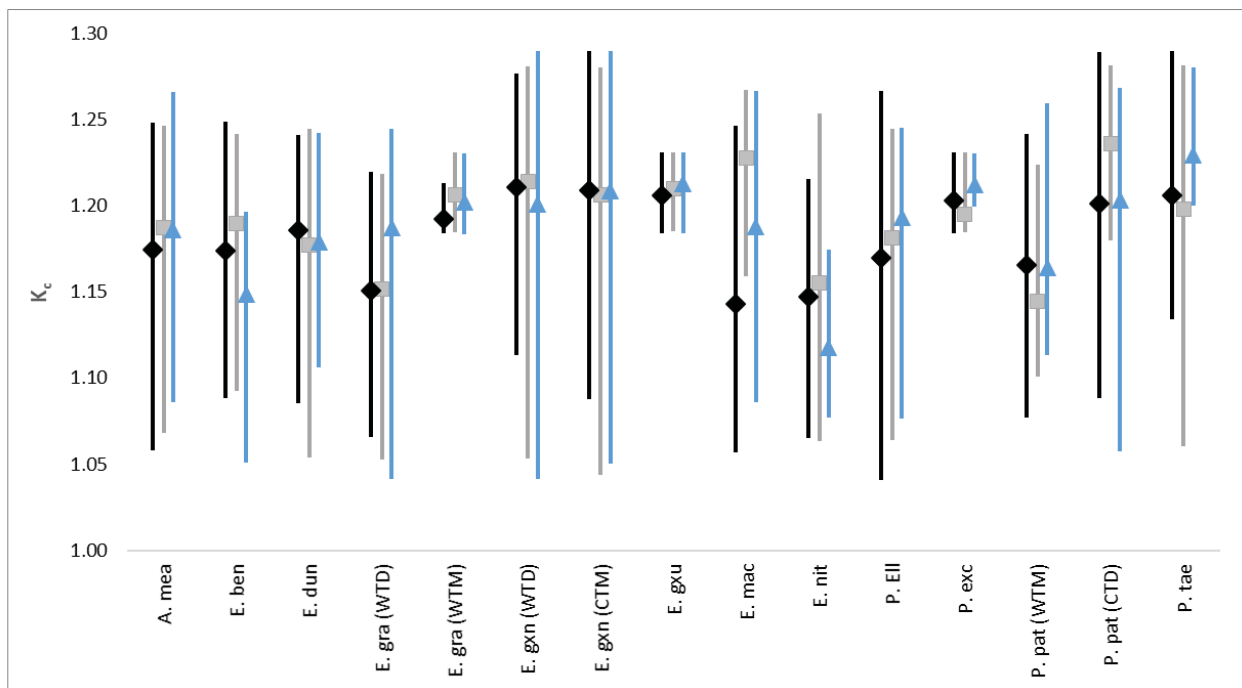


Figure B: Maximum (top of line), minimum (bottom of line) and average (marker) K_c values estimated with the MODIS LAI (black), Landsat LAI (grey) and Sentinel LAI (blue)

CHAPTER 7: OTHER ACRU INPUT PARAMETERS

In addition to the monthly K_c (CAY) values, ACRU requires further vegetation related parameters, namely the monthly vegetation interception loss (VEGINT in $\text{mm}\cdot\text{rainday}^{-1}$), coefficient of initial abstraction (COIAM), percentage surface cover (PCSUCO), fraction of active roots in the topsoil horizon (ROOTA), the effective rooting depth (EFRDEP), degree of root colonisation in the subsoil (COLON), and fraction of the soil's plant available water (PAW) at which total evaporation is assumed to drop below maximum evaporation due to drying of the soil (CONST). These were determined using remotely sensed, field-based data (where possible) or literature via a clearly documented and repeatable methodology. Further to this, ACRU requires streamflow response parameters to be input which are used to govern the portion of generated stormflow exiting a catchment on a particular day, as well as the portion of baseflow originating from the groundwater store, which contributes to streamflow. As a summary, all parameters are provided in Table A.

Table A: Vegetation input parameters and streamflow response variables

Parameter	Value	Method/evidence
VEGINT	Varies per species (MODIS LAI for 15 sites used) and per quinary catchment (as rainfall dependent).	Two methods were considered: <ol style="list-style-type: none"> 1. the simplistic Von Hoyningen-Huene Method and 2. the more complex "variable storage Gash model". LAI is a primary input to both methodologies. The decision was made to utilise the Von Hoyningen-Huene estimates, which matches the approach taken in the baseline project. Hence, the same method was used to estimate VEGINT in ACRU for both natural vegetation and for the forest species, hybrids and clones, thus facilitating a fair comparison.
ROOTA	0.65 across all months and species	Literature based. Studies (mostly international) related to the roots of the commercial tree species grown in South Africa typically tend to focus on the depth of the tree roots, or the root distribution profile. Common findings were that <ul style="list-style-type: none"> - A significant portion of the active roots were found in the upper soil horizons; - Distribution of the root profile was heavily dependent and influenced by site characteristics. Using the literature available and given the limited information relating the fine root distribution, the site dependence of the rooting distribution and the low sensitivity of the ACRU model to the parameter, a consistent monthly ROOTA value was selected.
EFRDEP	0 across all months and species	Setting EFRDEP to 0 defaults the EFRDEP to combined depth of the input soil horizons. The combined soil depths of the input horizons do not exceed 3 m. However, several studies provided evidence of active root depths for the commercial tree species grown in South Africa to depths of 8 m and deeper. Therefore, the EFRDEP for all the tree species was set to 0 to default to the maximum permitted effective root depth.
CONST	0.2 for eucalypts, 0.3 for pines, and 0.4 for wattle.	Allen et al. (1998) provides average fractions of total available soil water content (called the depletion fraction or p) that can be depleted from the root zone before plant stress occurs for various crops and vegetation types. As CONST is the fraction of plant available water in a soil horizon when total evaporation is reduced, it can be defined as the inverse of p , i.e. $\text{CONST} = 1 - p$. According to Allan et al. (1998), p ranges from 0.1 to 0.8 and provided a value of 0.7 for conifer trees ($\text{CONST} = 0.3$), compared to 0.2 ($\text{CONST} = 0.8$) for drought sensitive vegetable crops. These values were used as limits for CONST values,

Parameter	Value	Method/evidence
		as well as the findings by Dye (1996) of the drought tolerance of Eucalypts.
COIAM	0.35 across all months and species	The working rule defined by Schulze (2004) that for dense forests COIAM = 0.35 throughout the year, because the deep litter layer enhances initial infiltration before stormflow commences was used.
PCSUCO	100.00	Schulze (2004) assumed that a greater above-ground biomass resulted in higher litter cover, and through consultation with the National Biodiversity Institute developed a sigmoidal relationship between PCSUCO and maximum K_c , where for a K_c of greater than 0.85, PCSUCO = 100.00. The maximum K_c value for all commercial forestry species exceeded 0.85.
COLON	100.00	A COLON value of 100% for a given soil horizon implies that the roots in that horizon can access water from 100% of the horizon, provided water is available in the soil. Within the ACRU model, the root colonisation of the topsoil A-horizon is assumed to be 100% and thus, monthly input values of COLON are only required for the B-horizon (ACRU FDSS Workshop No3, 1995). As the maximum soil depth is limited to 1.2 m within the ACRU model, and trees have been found to root to 8 m, COLON was assumed to be 100%.
SMDDEP	0 (default to depth of A-horizon)	SMDDEP was set to the thickness of the topsoil, which is the suggested default value (Smithers and Schulze, 1995). Hence, the effective soil depth from which stormflow is generated is the topsoil depth. The same value was used in the baseline simulation.
QFRESP	0.3	Schulze (2011) recommends 0.30 as being typical at the spatial scale of quinary catchments and is based on experimental evidence.
COFRU	0.009	A typical value is 0.009 (or 0.9%) for the quinary catchments (Schulze, 2011).

CHAPTER 8: MODEL DESCRIPTION AND INPUTS

Use of the ACRU agrohydrological model for assessment of potential SFRA has been accepted by DWS (Gush et al., 2002; Jewitt et al., 2009). The previous SFRA model output used in the SFRA Utility was produced with ACRU Fortran version 3.31. Since then, significant updates to the ACRU model have taken place. Of significant benefit to this project is the improvements made by Kunz et al. (2020) to ACRU to optimise the speed at which the model runs, as well as significant changes made to the print and statistics utilities to optimise their computational performance and output format which facilitated being able to undertake the different species runs. Since 2009, the ACRU model has been compiled into a Java version. A comparison of the differences in streamflow generated by the Fortran version of ACRU when compared to that from the Java version showed a difference in the way in which the two versions adjust the daily crop coefficient within the model. The Fortran version was programmed to reset the daily crop coefficient (K_c) value to that of the monthly input value at the beginning of every month. However, this monthly “resetting” procedure was removed in the Java version, thus allowing the daily K_c value to continue decreasing until recovery from stress begins when the soil water content rises above a threshold value. The Fortran version of the model was modified to mimic the Java version. ACRU version 3.52 was used in this project.

As the runoff simulated by the ACRU model is extremely sensitive to rainfall input, it cannot be over-emphasised that rainfall data used as input for ACRU must be as error-free as possible. Hence, the improved the quinary catchments climate database was used in this project. The improvements included changes to driver rainfall stations used, correction of extreme rainfalls and a change to the use of lapse rate adjusted observed temperatures (which replaced values derived from the 1'x1' gridded temperature database). A further addition to the climate database used is that daily reference evapotranspiration (ET_0 in mm) were

calculated using the FAO56 version of the Penman-Monteith equation, and then adjusted to be A-pan equivalent reference evaporation using the PenPan method developed by Kunz et al. (2015). Similarly, the K_c values derived for the forestry species were converted to A-pan equivalent values using the PenPan method.

CHAPTER 9: HYDROLOGICAL IMPACTS OF COMMERCIAL AFFORESTATION

This project produced updated data for inclusion in the SFRA Utility, by broadening the number of species included and making use of the revised climate and soils databases available, as well as undertaking the assessment against the CWRR clusters hydrological baseline.

The ACRU model was used to simulate mean monthly and annual runoff response for:

- baseline conditions (MAR_{BASE}), i.e., the runoff produced from a land cover of natural vegetation (the CWRR clusters), and
- each of the forestry scenarios (MAR_{FOR}), assuming a 100% change in land cover.

This was done using the updated quinary climate database and improved quinary soils database. The only variables that were altered between the model runs under the various tree species and the baseline were the vegetation related parameters.

The framework suggested Jewitt et al. (2009) that a 10% reduction in mean annual runoff (MAR) by a land use can be considered a significant reduction or that a 25% reduction of low flows can be considered significant was used. Maps showing simply the quinary catchments where the change in MAR, under the species considered, would be deemed a SFRA ($\geq 10\%$ reduction in MAR) were provided.

CHAPTER 10: SFRA UTILITY

The initial version of the SFRA Utility was developed in 2009 as part of the SFRA project (Jewitt et al., 2009) was modified by Kunz et al. (2015) to improve its performance and to facilitate the dissemination of ACRU output related to the water use of selected biofuel crops. A key improvement being the change to an XML file to avoid installation problems associated with the Microsoft Access database previously used. For this project, further improvements were made to the version of the SFRA Utility developed by Kunz et al. (2015). Core to the utility is the data simulated by the ACRU model. As these datasets grow through the addition of more scenarios, the decision was made to store the monthly time series data produced by ACRU's post-processing software, as opposed to the raw daily time series files outputted by ACRU. This required a complete restructuring of the data reading and aggregation processes within the utility. Further development has also been focused on restructuring and updating the code base from the original .NET Framework 2.0 technology, since it is becoming increasingly difficult to deploy software requiring these older technologies onto newer computing systems. The original map interface was dependant on this older framework and thus, was removed from the utility as it would only hamper the installation and was not deemed necessary to correctly use SFRA Utility.

CHAPTER 11: Genus Assessment Utility User Manual (Version 2.0.0.2)

The user manual providing information on installation and operation of the SFRA Utility.

CHAPTER 12: CONCLUSIONS & RECOMMENDATIONS

The project brought the simulations under commercial tree species into alignment with other national scale simulations for the impacts of biofuel crops, climate change impacts, bamboo impacts and those that will be used in the ongoing WRC project titled “Development of Datasets for Multi-Scale Water Resource Assessments towards a Water Secure South Africa” by undertaking the model runs with the latest version of the ACRU model as well as the revised quinary catchments climate database. A significant advancement in this project was the improvements made to the quinary soils database used as input to the ACRU model given the critical role soils play in the regulation and generation of catchment hydrological responses. Using the South African soils terrain unit database, substantial gain in spatial resolution was obtained over the previous use of only land type information.

The revised hydrological baseline, CWRR clusters, together with the associated vegetation water use parameters required as input by ACRU was used as the reference against which the impacts of commercial afforestation were assessed. This move away from the Acocks (1988) Veld Types as the baseline can be considered a step forward as the SANBI (2012) vegetation map, from which the clusters were derived, has become the accepted natural vegetation map for South Africa by other disciplines, and the biome concept as well as the typical vegetation structures within those, have become commonly understood and referred to. More importantly, the documented and repeatable method used to derive the vegetation water use parameters allows for alignment across water use parameters for other land cover and land use types.

Literature and the experiences gained in the field-based component of this project, illustrated the significant influence of site characteristics on the growth, rooting patterns and the water use of commercial tree species. Sites with shallow soils or those in rain shadows will have different growth characteristics to those on wetter slopes or more favourable soils. Further, the growth patterns may even vary across a compartment due to variations in slope and soils. For determining the impacts of commercial tree species on streamflow generation, a broad picture, representative of large portions of the area under that commercial tree species, is needed. Thus, field-based studies to understand water use and determine LAI pose significant challenges. Thus, a method for developing a LAI database and determining K_c values that were more broadly representative of trees within a large compartment was developed. The method chosen took advantage of the recent advancements in geospatial cloud-based computing platforms, most notably Google Earth Engine and machine learning and aligned with the methodology used to derive vegetation water use parameters for the CWRR clusters, where remotely sensed LAI is used to estimate K_c . The K_c values estimated from MODIS LAI using machine learning showed good correlation to K_c values calculated from observed data. However, similar to the challenges experienced in the baseline project, very few datasets of total evaporation were available over commercial trees to develop and validate the model for determining K_c from LAI. Data for only two species grown at the same site was available. However, like the baseline project, the method is documented, repeatable and is consistent across species. As more data becomes available, the water use parameters can be refined.

Through the project, the required ACRU input vegetation parameters for seven *Eucalyptus*, four *Pinus* and *Acacia mearnsii* were derived. All of the estimated monthly K_c values were above 1, and both the month-by-month variation in K_c values for a specific species and between species was low. Generally, the K_c values for sites in the WTM climate zone had the smallest variation in the monthly values. ACRU model simulations were undertaken with version 3.52 (enhanced performance), the updated South African TU database, revised quinary catchments climate database, using the derived vegetation water use parameters for the 11 species, hybrids and clones, as well as the vegetation water use parameters for the CWRR clusters. All model inputs were held constant between the runs, except for the vegetation water use parameters. A

comparison to the ACRU output in the previous SFRA utility developed in 2009 were not undertaken due to the extent of the changes made to the 1) ACRU model, 2) climate and soils databases used as input, 3) changes in the reference land cover, and 4) methodology used to derive water use parameters. Further, these database updates and the use of a consistent and repeatable methodology to determine the vegetation water use parameters across both the land use of impact and the reference, represent a step forward in the science that can be used to support the implementation of the declaration of land used for commercial afforestation as a SFRA.

The various approaches developed and implemented in this study are by no means considered “exhaustive”. Although much effort was spent on producing simulated output that is considered reliable and error-free, the following suggestions would further improve the accuracy of modelled results:

- The root zone storage concept showed potential and therefore warrants further investigation.
- More process-based research is needed to improve ACRU’s ability to simulate deep-rooted vegetation.
- The ACRU model should be modified to use FAO56 (i.e. Penman-Monteith) reference evapotranspiration.
- Expand the database used for the derivation of crop coefficients from LAI, additional compartment data and additional evapotranspiration data to strengthen the machine learning algorithms developed in this project.

Reflecting on the project as a whole, the following recommendations are made:

- There is a need for agreement on the best measure of forestry water use. Should the measurement be of just the water use of the trees (i.e. green water) or of the water productivity which includes soil water evaporation and intercepted water?
- Agreement on scale also needs to be reached. Measurement at the scale of a tree (or cluster of trees) is valuable in terms of tree level water use and process understanding. However, these site-specific findings are possibly not broadly applicable nor able to be incorporated into modelling that is undertaken at a quinary catchment scale with supporting databases of that resolution.
- Given the repeatable method derived in this project, it is suggested that 5-year updates that utilise any additionally available field-based datasets, additional LAI sites and any quinary database or model updates be undertaken, and this be aligned with similar updates to the baseline.

ACKNOWLEDGEMENTS

Reference Group	Affiliation
Mr W Nomquphu	Water Research Commission (Chairman)
Ms P Jaka	Water Research Commission
Ms N Fourie	Department of Water and Sanitation (DWS), Compliance Monitoring Afforestation
Ms N Muthraparsad	DWS Compliance Monitoring Afforestation (SFRA)
Ms D Maluleke	DWS Stream Flow Reduction
Ms A Madonsela	DWS Compliance Monitoring Afforestation
Mr J Bester	DAFF Scientific Services
Mr F Fourie	DWS Groundwater (Water Resources Planning Systems)
Dr I Thompson	(Retired DWS Planning official) Private
Mr B Mdluli	Department of Water and Sanitation
Prof BE Kelbe	University of Zululand/HRTS
Dr MB Demlie	University of KwaZulu-Natal
Mr JC Nel	TWK Agri
Dr RN Heath	Forestry South Africa
Dr AR Morris	Institute for Commercial Forestry Research
Dr S Dovey	SAPPI
Dr M Govender	South African Sugar Association
Dr DC Le Maitre	CSIR

Further acknowledgements:

- Mondi are acknowledged and thanked for allowing the project team to monitor in their forestry compartments. Allowing access to those sites, facilitation of access and the continued support of the project has been a significant contribution to the project by Mondi. Further, Mondi is acknowledged and thanked for their provision of data.
- The participants of the workshop held at the start of the project (25 April 2018) are thanked for their time and contributions that helped to guide the project at the outset.

CONTENTS

EXECUTIVE SUMMARY	iii
ACKNOWLEDGEMENTS	xvi
LIST OF FIGURES	xxi
LIST OF TABLES	xxv
ABBREVIATIONS, PARAMETERS AND VARIABLES	xxvii
REPOSITORY OF DATA	xxix

CHAPTER 1. INTRODUCTION 1

1.1	Introduction	1
1.2	Project aims	3
1.3	Scope and limitations	3
1.4	Structure of the Report	5

CHAPTER 2. MAPPING SOIL HYDROLOGICAL ATTRIBUTES AT TERRAIN UNIT SPATIAL RESOLUTION FOR THE SOUTH AFRICAN PRODUCTION FORESTRY INDUSTRY 6

2.1	Background	6
2.2	Introduction	6
2.3	Terrain units in a South African soils context	8
2.3.1	Background to Soils Terrain Units in South Africa	8
2.3.2	Soils Terrain Units Defined	8
2.4	The soils components of mapped terrain units and their derivation from soils land types	11
2.5	Definitions of key soil physical attributes and algorithms used	20
2.5.1	Determination of thicknesses of topsoil and subsoil horizons	20
2.5.2	Determination of soil water content at the soil's permanent wilting point	21
2.5.3	Determination of soil water content at the soil's drained upper limit	23
2.5.4	Determination of soil water content when soils are at total porosity, i.e. when the soil is totally saturated	24
2.5.5	Determination of saturated redistribution rates, or saturated drainage	26
2.6	Mapped outcomes and interpretations of results from a forestry perspective.	29
2.6.1	The plantation forestry study area	29
2.6.2	Thickness of the topsoil	30
2.6.3	Thickness of the subsoil	32
2.6.4	Thickness of the subsoil (m) mapped at TU resolution	33
2.6.5	Soil water content in the topsoil at Permanent Wilting Point	34
2.6.6	Soil water content in the subsoil at Permanent Wilting Point	35
2.6.7	Soil water content in the topsoil at the Drained Upper Limit	36
2.6.8	Soil water content in the subsoil at the Drained Upper Limit	37
2.6.9	Total profile plant available water	38
2.6.10	Soil water content in the topsoil at saturation	39
2.6.11	Soil water content in the subsoil at saturation	40
2.6.12	Drainage rates from the topsoil to the subsoil	41

2.6.13	Drainage rates out of the subsoil	42
2.7	Concluding Thoughts	43

CHAPTER 3. INVESTIGATION OF THE POTENTIAL USE OF THE ROOT ZONE STORAGE CONCEPT **44**

3.1	Introduction	44
3.2	Literature review of the root zone storage concept	44
3.2.1	Increased modelling uncertainty due to below ground parameter estimation and process parameterisation	45
3.2.2	Background and Introduction to the Root Zone Storage capacity concept	46
3.2.3	The Water Balance approach	48
3.2.4	Summary	50
3.3	Methodology	51
3.3.1	Site description	51
3.3.2	Data acquisition	52
3.3.3	Calibration of the ACRU model	53
3.3.4	The estimation of the root-zone storage capacity	53
3.4	Results	56
3.4.1	Comparison of observed and simulated streamflows and soil water	56
3.4.2	Observed and simulated actual evaporation	58
3.4.3	Root-zone storage capacity	60
3.4.4	Validation of the root-zone storage capacity in hydrological modelling	64
3.5	Discussion and conclusion	64

CHAPTER 4. THE CWRR CLUSTERS AS A HYDROLOGICAL BASELINE **69**

4.1	Background and introduction	69
4.2	The CWRR clusters	69
4.3	Hydrological Parameterisation of the CWRR Clusters	71
4.4	Hydrological Response under the CWRR Hydrological Baseline as Compared to Acocks (1988) Veld Types	72
4.5	Concluding thoughts	73

CHAPTER 5. ADDRESSING THE SHORTCOMINGS IN THE AVAILABILITY OF LEAF AREA INDEX INFORMATION FOR COMMERCIAL TREE SPECIES **74**

5.1	Background and introduction	74
5.2	Review of using Leaf Area Index to estimate evapotranspiration	74
5.3	Estimating evapotranspiration from leaf area index: A case study from Two Streams Catchment	80
5.4	Deriving moderate spatial resolution leaf area index estimates from coarser spatial resolution satellite products	82
5.4.1	Introduction	82
5.4.2	Materials and methods	84
5.4.2.1	Study Area	84
5.4.2.2	Data collection and processing	86
5.4.3	Results	89
5.4.3.1	Validation of machine learning-based models	89
5.4.3.2	Testing of machine learning-based models and deriving moderate spatial resolution LAI estimates using Landsat and Sentinel-2 data	90

5.4.4	Discussion	93
5.4.5	Conclusions	95
5.5	Conclusion, recommendations, and way forward	95

CHAPTER 6. DETERMINING CROP COEFFICIENTS FOR COMMERCIAL TREE SPECIES **96**

6.1	Introduction	96
6.2	Using leaf area index to derive a crop coefficient	97
6.3	Quantifying crop coefficients for commercial forests using a combination of field-based evapotranspiration measurements and satellite earth observation data	98
6.3.1	Introduction	98
6.3.2	Methodology	100
6.3.2.1	Study Area	100
6.3.2.2	Data collection and processing	100
6.3.3	Results	102
6.3.3.1	Validation of K_c and evapotranspiration estimates for <i>Acacia mearnsii</i>	102
6.3.3.2	Validation of K_c and evapotranspiration estimates for <i>Eucalyptus dunnii</i>	103
6.3.4	Discussion	105
6.3.5	Conclusion	106
6.4	Crop coefficients for various commercial tree species for use in The Acru agrohydrological model	107
6.4.1	Introduction	107
6.4.2	Methodology and Species included	108
6.4.3	Results and Discussion	110

CHAPTER 7. OTHER ACRU INPUT PARAMETERS **112**

7.1	Introduction	112
7.2	Canopy Interception Loss	113
7.2.1	Methodology	113
7.2.1.1	The Von Hoyningen-Huene Method	113
7.2.1.2	The variable storage Gash model	113
7.2.1.3	Estimation of VEGINT per quinary catchment	114
7.2.2	Results and Discussion	114
7.2.3	Conclusion	114
7.3	Root specific below ground parameters	117
7.4	Fraction of plant available water at which plant stress occurs	119
7.5	Coefficient of initial abstraction	119
7.6	Percentage surface cover	120
7.7	Streamflow response parameters	120
7.8	Summary	121

CHAPTER 8. MODEL DESCRIPTION AND INPUTS **122**

8.1	The ACRU agrohydrological model	122
8.2	Updated quinary catchment climate database	123
8.3	Rainfall adjustment	124
8.4	Adjusting to the crop coefficients to a-pan reference potential	124
8.5	Improved soils input	125

CHAPTER 9. HYDROLOGICAL IMPACTS OF COMMERCIAL AFFORESTATION	126
<hr/>	
9.1 Introduction	126
9.2 Methodology	126
9.3 Results: Quinaries where a more than 10% reduction in MAR occurs	127
9.4 Results: influence of the different LAI products	131
CHAPTER 10. SFRA UTILITY	133
<hr/>	
10.1 Background and introduction	133
10.2 Recent updates to the SFRA Utility	133
10.3 Recommendations	133
CHAPTER 11. GENUS ASSESSMENT UTILITY USER MANUAL (VERSION 2.0.0.2)	134
<hr/>	
11.1 Introduction	134
11.1.1 Installation	134
11.2 Using the Genus Assessment Utility	140
11.2.1 User Selection Controls	143
11.2.2 Display Option Tabs	146
11.2.2.1 Time series	146
11.2.2.2 Time series graphs	147
11.2.2.3 Stats tables	148
11.2.2.4 Stats graphs	152
11.2.3 Interpreting of results	153
11.2.3.1 Calculating annual reductions in stream flow	153
11.2.3.2 Calculating monthly reductions for low flow period	154
11.2.3.3 Percentile values and flow duration curve	155
11.2.3.4 Understanding differences	156
CHAPTER 12. CONCLUSIONS & RECOMMENDATIONS	157
<hr/>	
12.1 Conclusions	157
12.2 Recommendations	159
CHAPTER 13. REFERENCES	161
<hr/>	
APPENDIX A: Data storage	176
APPENDIX B: New knowledge creation report	178
APPENDIX C: Capacity building report	179

LIST OF FIGURES

Figure A:	Example of the spatial information gain when utilising terrain unit information (left) compared with detail when using area-averaged Land Type information (right map: Schulze and Horan, 2008)	iv
Figure B:	Maximum (top of line), minimum (bottom of line) and average (marker) K_c values estimated with the MODIS LAI (black), Landsat LAI (grey) and Sentinel LAI (blue)	x
Figure 2-1:	Soil profile characteristics of concern to the agro-hydrologist (Schulze et al., 1991)	7
Figure 2-2:	Idealised representation of terrain units from crest to scarp to midslope (here termed “middleslope”), footslope and valley bottom (SCWG, 1991)	9
Figure 2-3:	Idealised examples of single phase (top) and multi-phase (bottom) terrain types (after SIRI, 1989)	9
Figure 2-4:	Examples of terrain unit sequences from actual South African landscapes (SIRI, 1989)	10
Figure 2-5:	Diagnostic topsoil and subsoil classes in the Binomial system (After MacVicar et al., 1977)	12
Figure 2-6:	Examples of Soil Land Type maps, around Lake St Lucia (left) and Durban (right) in KwaZulu-Natal Province of South Africa (SIRI, 1989)	14
Figure 2-7:	Modelled soil water contents (in m/m) of the respective topsoils of three terrain units of a soils Land Type, illustrating the importance of identifying individual TUs within a soils Land Type in regards to hydrological	16
Figure 2-8:	Terrain units and Quinary Catchments west and north of Durban, South Africa	19
Figure 2-9:	Zooming in from the inset in Figure 8 to show more detail on soils Terrain Units in dark brown (crests), light brown (midslopes), green (footslopes) and dark blue (dark blue) within Quinary Catchments (black)	19
Figure 2-10:	Flowchart illustrating the working rules for the determination of the thicknesses of the topsoil (DEPAHO; m) and the subsoil (DEPBHO; m) when using information contained in the Terrain Unit Database	21
Figure 2-11:	Flowchart illustrating the working rules for the determination of soil water content at permanent wilting point when using information contained in the Terrain Unit Database	22
Figure 2-12:	Flowchart illustrating the working rules for the determination of soil water content at the drained upper limit when using information contained in the Terrain Unit Database	23
Figure 2-13:	Soil water content (m/m) for soil texture classes at porosity for topsoils (PO1) and subsoils (PO2)	25
Figure 2-14:	South African texture triangle (MacVicar et al., 1977)	25
Figure 2-15:	Flowchart illustrating the working rules of saturated redistribution of soil water from the topsoil into the subsoil	26
Figure 2-16:	Flowchart illustrating the working rules of saturated redistribution out of the subsoil	27
Figure 2-17:	Flowchart illustrating the working rules of saturated redistribution out of the subsoil	29
Figure 2-18:	The plantation forestry study area within South Africa (top) in relation to mean annual precipitation (bottom left) and (bottom right) its inter-annual coefficient of variation (Bottom maps: Schulze, 2008)	30
Figure 2-19:	Thickness of the topsoil (m) mapped at TU resolution	31
Figure 2-20:	Thickness of the subsoil (m) mapped at TU resolution	32

VOLUME 2: WATER USE ESTIMATION OF SFRA SPECIES

Figure 2-21:	Thickness of the entire soil profile (m) mapped at TU resolution	33
Figure 2-22:	Soil water content at permanent wilting point (m/m) of the topsoil mapped at TU resolution	34
Figure 2-23:	Soil water content at permanent wilting point (m/m) of the subsoil mapped at TU resolution	35
Figure 2-24:	Soil water content at drained upper limit (m/m) of the topsoil mapped at TU resolution	36
Figure 2-25:	Soil water content at drained upper limit (m/m) of the subsoil mapped at TU resolution	37
Figure 2-26:	Plant available water (mm) in the in the entire soil profile mapped at TU resolution	38
Figure 2-27:	Soil water content in the topsoil at saturation (m/m) mapped at TU resolution	39
Figure 2-28:	Soil water content in the subsoil at saturation (m/m) mapped at TU resolution	40
Figure 2-29:	Drainage rates (fraction of excess water per day) from the topsoil to the subsoil, mapped at a resolution of terrain units	41
Figure 2-30:	Drainage rates (fraction of excess water per day) out of the subsoil, mapped at a resolution of terrain units	42
Figure 2-31:	Example of the spatial information gain when utilising terrain unit information (left) compared with detail when using area-averaged Land Type information (right map: Schulze and Horan, 2008)	43
Figure 2-32:	Further example of spatial information gain when utilising spatial terrain unit soils information, from (left) a region/provincial to (right) a local perspective	43
Figure 3-1:	A basic conceptualisation of the root-zone storage within common hydrological models in wet and dry periods under grassland conditions	47
Figure 3-2:	The soil moisture deficit constructed from a time series of water inflow and outflow through the root-zone storage system (Wang-Erlandsson et al, 2014)	49
Figure 3-3:	Location of Two Streams and Cathedral Peak Catchment VI within South Africa.	52
Figure 3-4:	The daily simulated soil water (blue line) and the daily observed soil water (black line) in the A horizon plotted within the field capacity (purple dashed line) and the wilting point (blue dashed line) for the period of November 2011 until October 2013.	57
Figure 3-5:	The daily simulated soil water (blue line) and the daily observed soil water (black line) in the B horizon plotted within the field capacity (purple dashed line) and the wilting point (blue dashed line) for the period of November 2011 until October 2013	58
Figure 3-6:	The daily observed evaporation (purple line) and the daily actual evaporation estimated by the ACRU model (using the maximum and minimum temperatures) (black dashed line) at the Two Streams Catchment over the period of March 2007 until October 2013.	59
Figure 3-7:	The daily observed evaporation (red line) and the daily actual evaporation estimated by the ACRU model (black dashed line) at Cathedral Peak Catchment VI over the period of July 2014 until August 2018.	60
Figure 3-8:	Estimated daily root-zone storage capacity for the Nijzink (red line), Wang (blue line) and DiCaSM (dashed black line) methods and daily rainfall (black line) at the Two Streams catchment for March 2007 to October 2013.	61
Figure 3-9:	Daily root-zone storage capacity calculated using the Nijzink (purple line), Wang (green line) and DiCaSM (blue line) methods and the daily rainfall (black line) for the Cathedral Peak Catchment VI from July 2014 to August 2018.	63
Figure 3-10:	Daily estimated root-zone storage capacity using the Nijzink (grey line), Wang (pink line) and the DiCaSM (green line) methods with the observed soil water (blue line) and ACRU simulated soil water (black line) in the soil profile at Two Streams.	65

VOLUME 2: WATER USE ESTIMATION OF SFRA SPECIES

Figure 4-1:	CWRR Clusters derived from the statistically clustered hydrological profiles of the SANBI (2012) vegetation units	70
Figure 4-2:	Changes in the mean annual runoff in mm under the CWRR clusters using the derived LAI based equation relative to Acocks' (1988) Veld Types.	73
Figure 5-1:	Tree leaf area versus mean daily transpiration for a plantation growing on a saline groundwater gradient in South Australia (Hatton et al., 1998)	76
Figure 5-2:	Leaf area versus mean daily transpiration for the sampled mountain ash trees (Vertessy et al., 1995)	76
Figure 5-3:	The relationship between leaf area (m ²) and diameter at breast height (DBH, mm), for (a) all genera and (b) eucalypts only. The inset in (b) shows a close-up of trees with DBH to 250 mm (Zeppel, 2013).	77
Figure 5-4:	The relationship between sapwood area (m ²) and diameter at breast height (DBH; mm), for (a) all genera and (b) eucalypts only. The inset in (b) shows a close-up of trees with DBH to 250 mm (Zeppel, 2013).	78
Figure 5-5:	The relationship between leaf area (m ²) and tree water use (L day ⁻¹), for (a) all genera and (b) eucalypts only. The inset in (b) shows a close-up of trees with leaf area to 150 m ² (Zeppel, 2013).	78
Figure 5-6:	Relationship between Leaf Area Index and transpiration for different ages of <i>Jatropha curcas</i> trees (Gush and Moodley, 2007)	79
Figure 5-7:	Plot of in-situ monthly LAI against monthly evapotranspiration (mm) for the Two Streams catchment (periodic data from 2008-2017)	81
Figure 5-8:	Plot of remotely sensed mean monthly LAI against monthly evapotranspiration (mm) for the Two Streams catchment (periodic data from 2008-2017)	82
Figure 5-9:	Geographic distribution of the study sites with respect to a) Africa, b) South Africa and the c) Inkomati-Usuthu and d) Pongola-uMzimkhulu WMAs (DWA, 2020)	85
Figure 5-10:	A graphical representation of the procedure that was applied to generate LAI _{MR}	87
Figure 5-11:	An illustration of the spatial resolution characteristics of the VIs acquired over a commercial forestry compartment situated within the Pongola-uMzimkhulu WMA	88
Figure 5-12:	Box and whisker diagram comparing the distribution of MODIS LAI reserved for validation and LAI estimated from MODIS VIs using the best performing MLBM	90
Figure 5-13:	Box and whisker diagram comparing the distribution of MODIS LAI against Landsat-based LAI	91
Figure 5-14:	Box and whisker diagram comparing the distribution of MODIS LAI against Sentinel-based LAI	92
Figure 5-15:	A comparison of average monthly LAI _{MR} estimates derived at the original a) Landsat (7 and 8) and b) Sentinel-2 spatial resolutions	93
Figure 6-1:	A comparison of the measured and estimated monthly K _c for <i>Acacia mearnsii</i> , where Sim1 is the conventional and Sim 2 is the machine learning based approach	102
Figure 6-2:	A comparison of the measured and estimated ET of <i>Acacia mearnsii</i> , where Sim1 and Sim 2 represents ET estimated using conventionally and EMLM derived monthly K _c estimates, respectively	103
Figure 6-3:	A comparison of the measured and estimated monthly K _c for <i>Eucalyptus dunnii</i> , where Sim1 is the conventional and Sim 2 is the machine learning based approach	104
Figure 6-4:	A comparison of the measured and estimated ET of <i>Eucalyptus dunnii</i> , where Sim1 and Sim 2 represents ET estimated using monthly K _c derived from the conventional and EMLM approaches respectively	105

VOLUME 2: WATER USE ESTIMATION OF SFRA SPECIES

Figure 6-5:	Maximum (top of line), minimum (bottom of line) and average (marker) K_c values estimated with the MODIS LAI (black), Landsat LAI (grey) and Sentinel LAI (blue)	111
Figure 7-1:	Mean monthly interception loss in January for (a) <i>E. grandis</i> , (b) <i>P. patula</i> and (c) <i>A. mearnsii</i> , derived using the Von Hoyningen-Huene (VHH) method and variable storage Gash (VSG) model	115
Figure 7-2:	Mean monthly interception loss in July for (a) <i>E. grandis</i> , (b) <i>P. patula</i> and (c) <i>A. mearnsii</i> , derived using the Von Hoyningen-Huene (VHH) method and variable storage Gash (VSG) model	116
Figure 7-3:	Cumulative distribution of (A) fine root intersects (diameter less than 1 mm) and (B) medium root intersects (diameter 1-3 mm) down to a depth of 10 m, from observations on 2-6 soil profiles at each <i>E. grandis</i> stand (Laclau et al., 2013).	118
Figure 8-1:	Structure of the ACRU agro-hydrological modelling system (Schulze, 1995)	122
Figure 9-1:	Quinary catchments where the change in MAR under <i>Pinus</i> species may be deemed a SFRA ($\geq 10\%$ reduction in MAR)	128
Figure 9-2:	Quinary catchments where the change in MAR under <i>Eucalyptus</i> species may be deemed a SFRA ($\geq 10\%$ reduction in MAR)	130
Figure 9-3:	Quinary catchments where the change in MAR under <i>Acacia mearnsii</i> may be deemed a SFRA ($\geq 10\%$ reduction in MAR)	131
Figure 9-4:	Percentage of quinary catchments per primary basin where the change in MAR estimated using K_c values derived with either MODIS or Landsat under <i>P. patula</i> , <i>P. exc</i> and <i>E. grandis</i> may be deemed a SFRA ($\geq 10\%$ reduction in MAR)	132
Figure 11-1:	Genus Assessment Utility's User Interface	141
Figure 11-2:	Genus Assessment Utility's User Selection Controls	141
Figure 11-3:	Assessment Utility's <i>Display Option Tabs</i>	142
Figure 11-4:	Genus Assessment Utility's (a) 'Current' Land Use, and (b) Proposed Land Use selectin options under User Selection Control	143
Figure 11-5:	Genus Assessment Utility's variable selection from User Selection Control	144
Figure 11-6:	Sub-Catchment (a) User Selection Control, and (b) search feature	145
Figure 11-7:	Genus Assessment Utility's <i>Time Series</i> tab (data for illustration purposes only)	146
Figure 11-8:	Genus Assessment Utility's <i>Time Series Graphs</i> tab (data for illustration purposes only)	148
Figure 11-9:	<i>Stats Tables</i> tab ('Current' Land Use, data for illustration purposes only)	149
Figure 11-10:	<i>Stats Tables</i> tab (Proposed Land Use, data for illustration purposes only)	150
Figure 11-11:	<i>Stats Tables</i> tab ('Current' Land Use – Proposed Land Use, data for illustration purposes only)	151
Figure 11-12:	<i>Stats Tables</i> tab ('Current' Land Use – Proposed Land Use (as %), data for illustration purposes only)	152
Figure 11-13:	<i>Stats Graphs</i> tab ('Current' Land Use, data for illustration purposes only)	153
Figure 11-14:	Calculation of the relative reduction in low flow totals of monthly runoff for quinary A10A1 (0001) for a proposed land use change from natural vegetation to <i>A. mearnsii</i>	155

LIST OF TABLES

Table A:	Vegetation input parameters and streamflow response variables	xi
Table 2-1:	Extract from the Terrain Unit Database showing selected attributes of the Terrain Unit Database up to soil series level information (original source: Beukes, 2018)	17
Table 2-2:	Further extract from the Terrain Unit Database showing soil profile depths (mm) per soil series in a TU in the last eight columns (Original source: Beukes, 2018)	17
Table 2-3:	Another extract from the Terrain Unit Database showing (top table) clay percentages in the topsoil and (bottom table) in the subsoil per soil series in a TU in the respective last eight columns (Original source: Beukes, 2018)	18
Table 3-1:	The overall and seasonal streamflow goodness of fit statistics for the Two Streams (TS) and Cathedral Peak Catchment VI (CP6) calculated using the daily streamflow values	56
Table 3-2:	The overall and seasonal actual evaporation goodness of fit statistics for the Two Streams (TS) and Cathedral Peak Catchment VI (CP6) calculated using the daily observed and simulated actual evaporation values	58
Table 3-3:	Statistics of the root-zone storage capacities estimated using the Nijzink, Wang and DiCaSM methods at Two Streams.	61
Table 3-4:	Statistics of the root-zone storage capacities estimated using the Nijzink, Wang and DiCaSM methods with observed evaporation (OET) and simulated actual evaporation (SET) for the Two Streams catchment.	62
Table 3-5:	Statistics of the root-zone storage capacity estimated using the Nijzink, Wang and DiCaSM methods at Cathedral Peak catchment VI over the period July 2014 to August 2018.	62
Table 3-6:	Statistics describing the root zone storage capacity estimated using the Nijzink, Wang and DiCaSM methods with observed evaporation (OET) and simulated actual evaporation (SET) for the Cathedral Peak catchment VI.	63
Table 3-7:	Statistics and goodness of fit measures describing the root zone storage capacity estimated using the Nijzink, Wang and DiCaSM methods and the ACRU simulated soil water at Two Streams.	64
Table 5-1:	Performance statistics for the comparisons between the MODIS LAI reserved for validation and LAI estimated from MODIS VIs using the best performing MLBM,* denotes detection of multicollinearity	90
Table 5-2:	Performance statistics for the comparisons between the MODIS LAI and LAI estimated by the MLBMs using upscaled Landsat-derived VIs as inputs	91
Table 5-3:	Performance statistics for the comparisons between MODIS LAI and LAI estimated by the MLBMs using Sentinel-derived VIs as inputs	92
Table 6-1:	A comparison of the performance metrics for ET estimates of <i>Acacia mearnsii</i> derived using monthly K_c estimates from the conventional (Sim1) and EMLM (Sim 2) approaches	103
Table 6-2:	A comparison of the performance metrics for water use estimates of <i>Eucalyptus dunnii</i> derived using monthly K_c estimates from the conventional (Sim1) and EMLM (Sim 2) approaches	105
Table 6-3:	Planted areas of eucalypt and pine for the large scale growers (Source: ICFR, 2018)	107
Table 6-4:	Planted areas classified according to the ICFR defined climate zones (Source: ICFR, 2018)	108
Table 6-5:	Planted areas according to ICFR Climate zone and species only shown for those that account for more than 1% of the growth area (Source: ICFR, 2018)	109

VOLUME 2: WATER USE ESTIMATION OF SFRA SPECIES

Table 6-6:	The commercial forestry species and the ICFR climate zone of the sites for which crop coefficients were estimated	109
Table 6-7:	The monthly averaged K_c values derived using the MLBM and the MODIS LAI inputs for the 15 sites	110
Table 6-8:	The monthly averaged K_c values derived using the MLBM and the Landsat LAI inputs for the 15 sites	110
Table 6-9:	The monthly averaged K_c values derived using the MLBM and the Sentinel-2 LAI inputs for the 15 sites	111
Table 11-1:	Description of each User Selection Control	142
Table 11-2:	Description of each <i>Display Option Tab</i>	142
Table 11-3:	Description (and units) of each output variable	144

ABBREVIATIONS, PARAMETERS AND VARIABLES

ACRU	Agricultural Catchments Research Unit
CAY	Crop coefficient
COFRU	Baseflow recession constant
COIAM	Coefficient of initial abstraction
COLON	Root colonisation of the B-horizon
CONST	Fraction of PAW at which plant water stress occurs
CORPPT	Correction factor for rainfall
CSIR	Council for Scientific and Industrial Research
CTM	Cool temperature moist
CWRR	Centre for Water Resources Research
DUL	Drained upper limit
DWS	Department of Water and Sanitation
EFRDEP	Effective rooting depth
ET _c	Actual evapotranspiration
ET _o	Reference potential evaporation
EVI	Enhanced vegetation index
FC	Field capacity
FSA	Forestry South Africa
GEE	Google Earth Engine
GIS	Geographic information system
K _c	Crop coefficient
KGE	Kling-Gupta Efficiency
LAI	Leaf area index
MAR	Mean annual runoff
MLBMs	Machine learning based models
NDVI	Normalized difference vegetation index
NSE	Nash-Sutcliffe Efficiency
PAW	Plant available water
PCSUCO	Percentage surface cover by vegetation or mulch/litter
PO	Total porosity
PWP	Permanent wilting point
Θ	Soil water content
QFRESP	Stormflow response fraction
RMSE	Root Mean Squared Error
ROOTA	Fraction of effective roots in the topsoil horizon
SAWS	South African Weather Service
SCWG	Soil classification working group
SEBS	Surface energy balance system
SFRA	Streamflow reduction activity

VOLUME 2: WATER USE ESTIMATION OF SFRA SPECIES

SIRI	Soil and Irrigation Institute
SMDDEP	Soil moisture deficit depth
TU	Terrain unit
TUDB	Terrain unit database
VEGINT	Vegetation interception losses
VI	vegetation indices
WTD	Warm temperate dry
WTM	Warm temperate moist

REPOSITORY OF DATA

For details related to the project's data, please contact:

Richard Kunz (Researcher)
Centre for Water Resources Research
School of Agricultural, Earth and Environmental Sciences
University of KwaZulu-Natal
Private Bag X01, Scottsville 3209
Pietermaritzburg, South Africa
Email: kunzr@ukzn.ac.za

This page was intentionally left blank

CHAPTER 1. INTRODUCTION

1.1 Introduction

Concerns over catchment-scale hydrological impacts of forest plantations in South Africa were already being expressed by 1915, with research on this subject starting in 1935 and still continuing today as there remain questions around the water use of the different commercial forestry species, clones and hybrids. Since the introduction of the Afforestation Permit System in 1972 using the Nänni curves, the method and tools used to assess the impacts of commercial afforestation have been continuously updated. With the declaration of commercial afforestation as a streamflow reduction activity (SFRA) in 1999, these tools and methods became more important. Gush et al. (2002) produced tables of reductions in mean, median and low flows in an average year relative to a baseline flow derived from modelled results using the ACRU model. More recently, Jewitt et al. (2009) developed the SFRA Assessment Utility to assist in water use licensing, which provided estimates of reductions at a finer scaler and an improved consideration of low flows. However, as the regulation of afforestation needs to be achieved within an environment that is continually changing and evolving with regard to legal, social and biophysical characteristics. Therefore, an update to the SFRA Assessment Utility was required with an inclusion of improved knowledge to address the current questions.

The current SFRA Assessment Utility (Jewitt et al., 2009) estimates the streamflow reductions of commercial forestry based on the water use of three species, namely *Pinus patula*, *Eucalyptus grandis* and *Acacia mearnsii*. However, the forestry industry currently uses 17 *Pinus*, 26 *Eucalyptus* and 3 *Acacia* species, hybrids and clones. Thus, there is a pressing need to expand the knowledge on the water use of the different species, clones and hybrids used by the forestry industry. This need has become more important with the ongoing disputes surrounding genus exchange. Due to changes in the demands for the various forestry products, and to a lesser extent pests and diseases, there has been a shift towards eucalypts over pines, particularly in KwaZulu-Natal (FSA, 2016). Thus, in some forestry compartments, a genus exchange has occurred or is planned. The Department of Water and Sanitation (DWS) issued a notice in October, 2015 for the draft of Regulations on Afforestation Genus Exchanges in Terms of the National Water Act, 1998 (Act No.36 of 1998). The draft Genus Exchange Regulations state that any existing afforestation water user that wishes to exchange the genus of their plantation or part thereof, is required to apply to the responsible authority for authorisation to implement the proposed exchange (DWS, 2015). In terms of assessing and evaluating the conditions associated with genus exchanges, the following aspects are considered by DWS:

- (a) the exchange ratio must be determined by using the best information available on the water use of the different genera at quinary or quaternary catchment level;
- (b) the genus exchange must not cause an increase in the existing lawful water use of the property, where the DWS regulations only allow an exchange in the authorised genus of an equal area or a reduced area of the existing lawful afforestation area based on the differences in the water use of the different genera. Therefore, an exchange to a genus with a higher water use than the existing lawful genus will lead to the amendment of the original authorisation, resulting in a proportionally smaller area to be planted. Alternatively, an exchange to a genus with a lower water use than the existing lawful genus will not necessarily result in an increased size of the planted area, unless authorised in a water use licence;
- (c) Reductions in both total flows and low flows must be accounted for the determination of the amendment to be made to the planted area.

These regulations were contested by Forestry South Africa (FSA) using a commissioned report (Gush, 2016) which claimed that DWS had overstated the reductions in areas required when switching from pines to eucalypts. DWS took the decision to suspend the Genus Exchange Regulations pending a review. This project addresses the knowledge gaps surrounding the influences of genus exchange on water use.

Beyond the above concerns two additional knowledge gaps have been highlighted by DWS, Gush (2016) and Jewitt et al. (2009). The first knowledge gap is around determining the most representative tree age for rotation length water use. In the initial growth phases, water use is low, but is followed by rapid increases associated with high leaf area indices (LAI) and canopy closure (Scott and Smith, 1997; Dye and Bosch, 2000; Clulow et al., 2011), thereafter water use flattens out as the trees reach maturity. With the genetic selection towards faster growth rates, canopy closure and a higher LAI are reached earlier, changing the water use curve of the trees. Linked to this, the rotation lengths have decreased, particularly for eucalypts and thus, the water use of the trees is predicted to be higher in the initial growth phases but the length of time they use water is reduced. This trade-off between faster growth rates resulting in greater initial water use, with shorter rotation lengths needs to be better understood. With improved knowledge on the water use of the various species, hybrids and clones through the proposed project, this question will be also be addressed. The water-use of tree stands with different planting densities (espacement) are a further confounding aspect that needs to be considered together with the representative tree age for rotation length. Due to mechanical harvesting and silviculture, stand densities may be decreased from 1667 spha (3 x 2 m spacing) to 1333 spha (3 x 2.5 m spacing). However, for biomass production the stand densities may be increased to 2222 spha (3 x 1.5 m). How these changes in stand density will affect water use remains unclear, and needs to be addressed through field-based observations and research.

The second knowledge gap concerns the baseline vegetation against which the water use of the commercial tree species is compared. At the outset of this project, DWS supported the use of natural vegetation in the form of the Acocks (1988) Veld Types as the reasonable standard or reference land cover against which to assess land use impacts (Schulze, 2004; Jewitt et al., 2009). However, concerns about the use of Acocks (1988) Veld Types had been raised by Jewitt et al. (2009). These concerns centred on the country-wide scale resolution of the Acocks (1988) maps with relatively little local scale detail and that the water use parameters of each veld type were derived using expert knowledge. The detailed SANBI (2012) maps of natural vegetation, together with a larger database of natural vegetation water use, allowed for a revised hydrological baseline (together with associated water use parameters) to be developed through WRC project K5/2437 (Toucher et al., 2020). Linked to this, is the continual need to ensure that the hydrological model results used in the assessment of SFRA are based on the best available data. Furthermore, the climate and soils information that produced the model results used in the SFRA Assessment Utility (Jewitt et al., 2009) has been superseded by recent work done within the Centre for Water Resources Research (CWRR). Thus, the opportunity exists for a revised estimation of the water use of commercial trees to be made against this updated baseline, an updated quinary catchments climate and soils database, thereby addressing current shortcomings. This will lead to an update of the SFRA Assessment Utility produced by Jewitt et al. (2009), both in terms of the data/information included in the utility and the functionality of the utility.

1.2 Project aims

The following were the aims of the project:

1. To expand the knowledge of the estimates of water use of different clones and hybrids of eucalypt, wattle and pine species (e.g. clones/hybrids most commonly used, clones/hybrids planted in optimal sites).
2. To address shortcomings in the availability of leaf area index information for different SFRA species, clones and hybrids.
3. To improve existing tools used for the estimation of the impacts of SFRA through the inclusion of improved soils data and baseline land cover data, as well as the inclusion of the latest process results related to water use (i.e. evapotranspiration) of SFRA clones, hybrids and species.

The outcomes, findings and products of the project are comprised of two final reports. This document details the research that contributes to the SFRA Utility to address Aims 3 and 4, while the other deliverable speaks to Aim 1, which focuses on the improved water use estimation of SFRA species. Initially the project included an aim 'to expand the knowledge on the water use of different stand densities', however, it was recommended at a stakeholder workshop, and support by the reference group, that this aim was beyond the reach of the project and should not be a focus of the project.

1.3 Scope and limitations

The impacts of commercial trees on South Africa's water resources is a topic of significant concern to many from varying points of view, from policy and decision makers, to the forestry industry and stakeholder concerned about the impacts at their local scale. In particular, the ongoing disputes surrounding genus exchange has resulted in increased conflict. From the project's inception workshop held in April 2018, it was clear that the project was not going to be able to answer the numerous questions surrounding forestry and water use. However, a detailed "bigger picture" that could answer some of the questions can only be built from a number of detailed pictures of smaller areas. At the same workshop, concerns were raised about the intended use of the research in policy. As was noted at the workshop, this project was a scientific research project not a policy research project. The project aimed to expand the scientific understanding and evidence base related to the water use of afforestation and to improve the existing tools that could be used to estimate the impacts. For each of the project aims, the scope of the work undertaken and the limitations are detailed.

Aim 1: To expand the knowledge of the estimates of water use of different clones and hybrids of eucalypt, wattle and pine species (e.g. clones/hybrids most commonly used, clones/hybrids planted in optimal sites).

The research activities undertaken related to this aim are detailed in Deliverable 8 that accompanied this final report. To address this aim, field-based studies were undertaken at selected sites. The number of sites that could be instrumented was constrained by budget. The species investigated were those commonly grown in South Africa for which no water use data existed. Site selection was influenced by logistical constraints and the desire to pair sites of different genera. The project has met this aim and expanded the knowledge on water use estimates of different species, but also provided further evidence of the influence of site characteristics on tree water use.

Aim 2: To expand the knowledge on the water use of different stand densities.

At the inception workshop, there was much discussion surrounding this aim of the project. The suggestions were that considering stand density should not be prioritised, but rather the focus should be on collecting field-based data on aspects that could be adequately addressed, given the restricted number of sites that could be instrumented. As only four sites were instrumented, field-based investigations into stand density could not be undertaken as this would limit the advancement of the understanding of tree water use for a greater number of species. Therefore, developing a relationship between LAI and stand density using remote sensing was the path considered to address this.

Aim 3: To address shortcomings in the availability of leaf area index information for different SFRA species, clones and hybrids.

The initial approach to expand leaf area index (LAI) information was through field based activities. The challenges related to obtaining accurate estimates of LAI in field, and the logistical challenges around the field-based activities, meant a different approach was followed. This approach took advantage of the recent advancements in geospatial cloud-based computing platforms, by using Google Earth Engine (GEE) and machine learning packages that are available to analyse and utilise the available LAI remotely sensed products. Further to this, a methodology was developed to enhance the spatial resolution of coarse spatial resolution LAI products through the use of vegetation indices (VIs) derived from finer spatial resolution satellite datasets. This aspect of the study has been written up as a journal article and is currently under review.

Aim 4: To improve existing tools used for the estimation of the impacts of SFRA through the inclusion of improved soils data and baseline land cover data, as well as the inclusion of the latest process results related to water use (i.e. evapotranspiration) of SFRA clones, hybrids and species.

The scope of work undertaken to address this aim has been considerable. As noted under Aim 3, a method to derive crop coefficients from remotely sensed LAI values was developed using GEE and machine learning. The method produced acceptable crop coefficients when compared to values derived using the limited observed data available. The other ACURU parameters and variables related to vegetation water use were also estimated using an approach that is deemed consistent and repeatable.

The quinary catchments climate database was revised using observed temperature data, which accounted for the altitude difference between the temperature station selected to represent each quinary and the quinary's average altitude. A revised quinary catchments soils database at the terrain unit (TU) scale with associated attributes required for input to the ACURU model was developed. Mapping the soils at the TU scale represented a significant gain in spatial detail. Hence, these updated databases were used to estimate streamflow generated from the baseline vegetation layer, as defined by the CWRR clusters, and that from commercial tree species. This ensured consistency between the methods used to simulate the reference and impact land use. The outputs from these simulations were then included in an improved SFRA Utility to provide a tool for the assessment of the impacts of commercial afforestation on downstream water availability. Another avenue that was investigated to improve existing tools, was consideration of the root zone storage concept and the potential of using it within the ACURU modelling framework, in order to further improve root water uptake as well as overcome the paucity of available rooting information.

1.4 Structure of the Report

Chapter 2 describes the improved quinary catchments soils database that was developed by ascribing soil physical attributes to the mapped terrain units. To supplement and potentially advance knowledge, the question of whether the root zone storage concept could be used to determine the root zone storage capacity and thus, the soil depth under commercial tree species is addressed in Chapter 3. Although the study was limited in scope, the results suggested that the root zone storage concept showed potential and warranted further investigation. Chapter 4 provides a short summary of the revised hydrological baseline that was developed by Toucher et al. (2020) that was used in this project.

Chapter 5 describes the activities undertaken to address the shortcomings in the available LAI from the field-based studies to the revised approach which utilised GEE and machine learning. This chapter underpins the methodology used to estimate crop coefficients as described in Chapter 6. Building from this, the estimation and derivation of other required ACRU inputs are detailed in Chapter 7. A brief description of the ACRU model and the quinary databases is given in Chapter 8, with the hydrological impacts of commercial afforestation being assessed in Chapter 9. The SFRA Utility and improvements made are described in Chapter 10, followed by conclusions and recommendations in Chapter 11.

CHAPTER 2. MAPPING SOIL HYDROLOGICAL ATTRIBUTES AT TERRAIN UNIT SPATIAL RESOLUTION FOR THE SOUTH AFRICAN PRODUCTION FORESTRY INDUSTRY

R.E. Schulze¹ and S. Schütte¹

¹ Centre for Water Resources Research, University of KwaZulu-Natal, Pietermaritzburg

2.1 Background

The soils used in the quinary catchments database, which is used in the ACRU model runs to provide input to the SFRA Utility developed by Jewitt et al. (2009), are based on the Agricultural Research Council (ARC) and Institute for Soil-Climate-Water (ISCW) division of the country at 1 in 250 000 scale into zones of similar broad soil categories with a particular focus on agriculture. These divisions are referred to as land types and are based on broad categorisations, but include detail as to the predominant soil forms and series of an area and their texture classes. Any particular land type is made up of many different (although similar) soil series, and with the committee-based knowledge of the water holding capacities of the individual soils within a land type, through a process of area weighting, land type specific values of the hydrological parameters were derived. A computerized set of algorithms, designed by Pike and Schulze (2004) called autosoils was created to do this.

With the advent of GIS and finer resolution digital elevation models, coupled with the improvement of computing power and GIS functionality, it has become possible to subdivide landscapes in catenal sequences using elevation, slope, aspect and surface curvature. It is possible to identify spatially with a high level of precision the positions of crests, scarps, mid slopes, foot slopes and valley floors. Fortuitously, when the ARC published the Land Types, it not only included the breakdown of land types as a whole by ratio of soil series, but also the percentages of each catenal sequence in the land type, as well as the soil series percentages for each catenal stage. Based on this it is possible to identify with more detail, both spatially and from a soils mix perspective, the soil series per sequence, and then by extension, the location of each sequence. Using this, the country can be divided into small homogeneous areas of, for example, crests, mid slopes, with their associated soil mixes. This Chapter describes the methodology which has been followed to achieve this.

2.2 Introduction

Marked spatial differences in the rates of, and lags in, forest hydrological processes occur both within a plantation and a catchment, as well as between different plantations and different catchments as a consequence of responses associated with different soil properties. In essence, forest growth and hydrological responses, be they evaporation, surface/near surface runoff or baseflow, differ as a result of the vertical sequences of soil properties because these regulate

- entry into,
- storage and retention in, and
- redistribution within, and out of, the soil profile.

Some forest (and other crop) hydrologically important vertical sequence scenarios are sketched in the seven self-explanatory soil profiles making up Figure 2-1. This figure illustrates that the forester and hydrologist have to be concerned with

- respective thicknesses of various soil horizons;
- surface properties of the soil (e.g. crusting, sealing, cracking, site preparation) which affect the soil's infiltrability, i.e. the rate of water entry into the soil;
- the sequence of soil horizons in regards, for example, to
 - the distributions of clay, sand and silt percentages within the soil profile as they relate to the redistribution rates of water (permeability, hydraulic conductivity); or
 - impeding layers within the soil profile, either natural or man-made, which may cause drainage/waterlogging problems or induce interflow to occur;

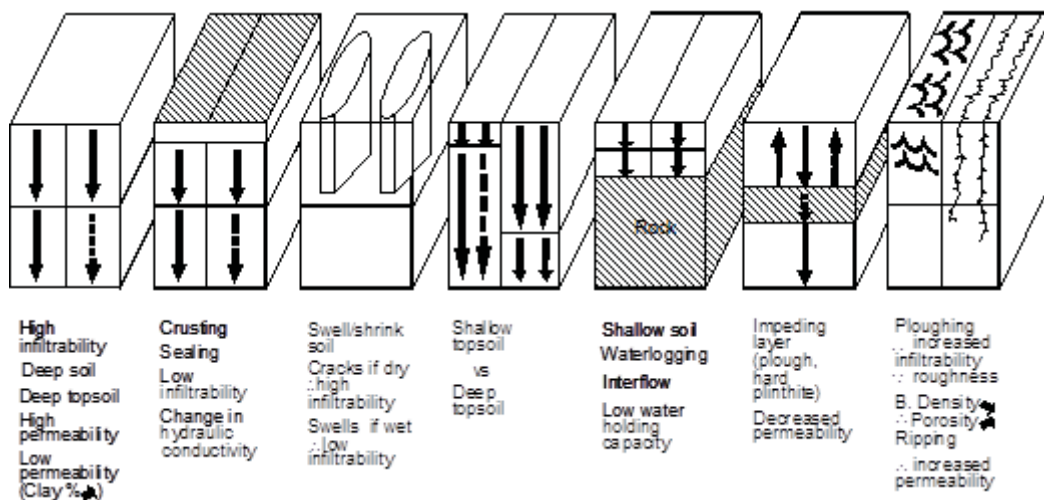


Figure 2-1: Soil profile characteristics of concern to the agro-hydrologist (Schulze et al., 1991)

furthermore

- the water holding capability of the soil, which (other than being related to soil depth) finds expression, inter alia, through
 - its textural composition into percentages of clay, silt and sand, and
 - the amount of water a soil of a given texture retains at specified/critical soil water conditions, viz. at the soil's
- permanent wilting point (i.e. the soil water content constituting the lower limit of soil water available to the plant; see later), at its
- drained upper limit (previously also termed field capacity, i.e. the soil water content held by capillary forces that are great enough to resist gravity after natural percolation from the soil has ceased; see later), and when the soil water content is at
- total porosity, i.e. at saturation (when all pore spaces are filled with water; see later), and under which condition water retention may be increased when the soil's bulk density is decreased, e.g. by tillage practices;

furthermore, with

- soil properties may influence the depth and density of the plant root system, since these roots have a major effect on soil water extraction patterns; or with
- drainage rates of water above threshold wetnesses of the soil, occurring between soil horizons within the plant's root zone and out of the root zone.

Other factors, not considered in this document, may also operate, for example,

- the inherent erodibility of the soil and how that might be altered by pre- and post-harvest management practices, or
- the capillary fringe just above the water table into which, in certain landscapes, tree roots may penetrate and utilise that water for growth.

With soil physical attributes playing such a key role in the water use by, the growth of, and runoff responses from, plantation forests, these attributes need to be ascertained and mapped at a high spatial resolution. On a national scale, within those areas which are climatically suitable for plantation tree growth, this spatial resolution is the so-called soils terrain unit.

This Chapter will thus address

- the concept of terrain units within a South African soils context,
- the soils components of mapped terrain units and their derivation from South Africa's Soils Land Types,
- properties of a South African soils terrain unit database,
- definitions of the key soils physical attributes to be mapped, together with the algorithms used to map those attributes at TU resolution, and
- the mapped outcomes, including interpretations of results from a forestry perspective.

2.3 Terrain units in a South African soils context

2.3.1 Background to Soils Terrain Units in South Africa

The background to identifying, defining and delineating soils terrain units (TUs) in South Africa is based on a method devised by Kruger (1973) when researching concepts, techniques and procedures for a global natural resource survey. Kruger, in turn, made use of ideas by Hammond (1964) on the analysis of properties of land form mapping and those of King (1953) on landscape evolution.

2.3.2 Soils Terrain Units Defined

As defined in SIRI (1989), a terrain unit (TU) is any part of the land surface with homogeneous slope and form (e.g. a convex or a concave slope or a near-vertical cliff). Terrain can be thought of as being made up of all, or some, of the following kinds of TUs, viz.

- a crest
- scarp
- midslope
- footslope and the
- valley bottom.

An idealised representation of terrain units is illustrated in Figure 2-2.

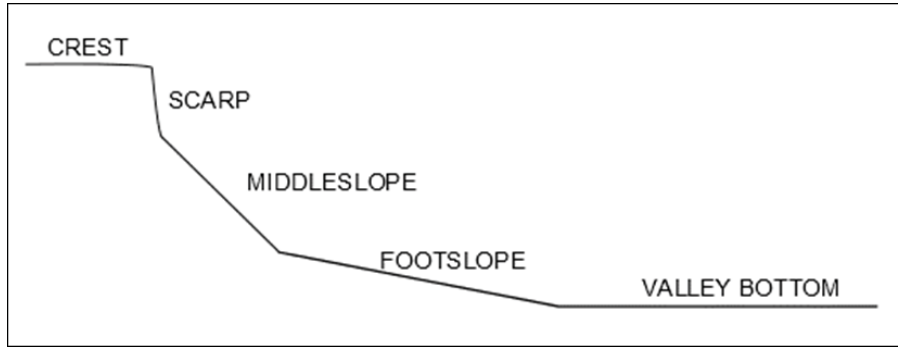


Figure 2-2: Idealised representation of terrain units from crest to scarp to middleslope (here termed "middleslope"), footslope and valley bottom (SCWG, 1991)

A terrain type in the above context denotes an area of land over which there is a marked uniformity of surface form and which, at the same time, in the South African soil mapping context, could be shown easily on a map at a scale of 1:250 000. Land shown on a map as belonging in a terrain type may cover only a single terrain type (e.g. a floodplain), or it may cover a single crest-valley bottom sequence, or it may cover a large number of crest to valley bottom sequences that repeat themselves three-dimensionally (e.g. a large area of rolling hills). Although a terrain type is not without genetic implication (e.g. influenced by geology or large-scale landscape upliftment), it is the morphology and not genesis that is the basis for its delineation and description.

In Figure 2-3, a '1' represents a crest, '3' a middslope, '4' a footslope and '5' a valley bottom. A '2', which would represent a scarp, is not shown in this diagram. Terrain types can either be single phase, as in the top diagram of Figure 2-3, or they can be multi-phase, as in the bottom diagram, where the symbol 3⁽¹⁾ indicates a second phase middslope and 3⁽²⁾ a third phase middslope.

Whether a TU is a footslope or a middslope depends

- on its position in the landscape (with a middslope lying immediately below a crest or scarp) and, to an extent,
- on the steepness of the slope, whereby in contrast to a middslope, a scarp is steeper than 100% (i.e. 45°) and usually steeper than 70°.

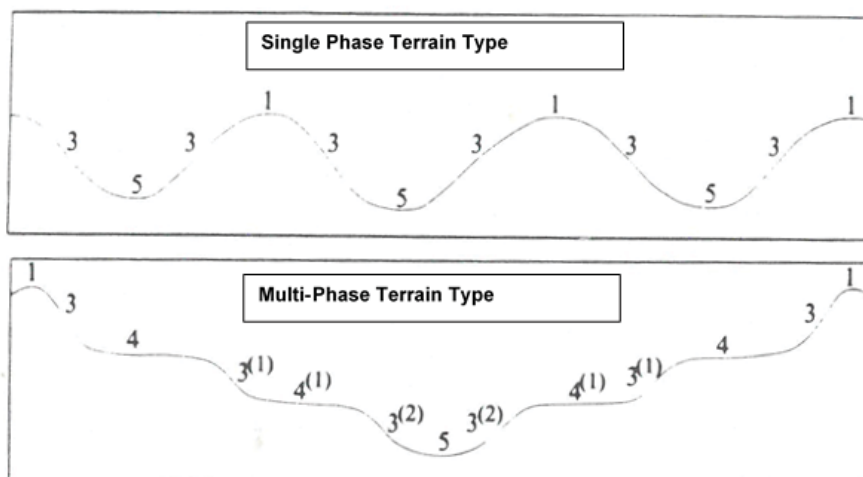


Figure 2-3: Idealised examples of single phase (top) and multi-phase (bottom) terrain types (after SIRI, 1989)

In actual South African landscapes, TUs take on many combinations of sequences of crest, scarp, midslope, footslope and valley bottom, as the examples in Figure 2-4, taken from the “Land Types of the Maps 2330 Tzaneen and 2430 Pilgrim’s Rest” (SIRI, 1989), illustrate.

Terrain unit surveys were originally undertaken with the use of 1:50 000 and 1:250 000 with boundaries drawn in the office and then field-checked, with the chief criteria for delimitation having been the pattern and density of the drainage system, relief and slope, profile and extent of each of the TUs, and with the TU inventories made after the Land Type boundaries had been finalised.

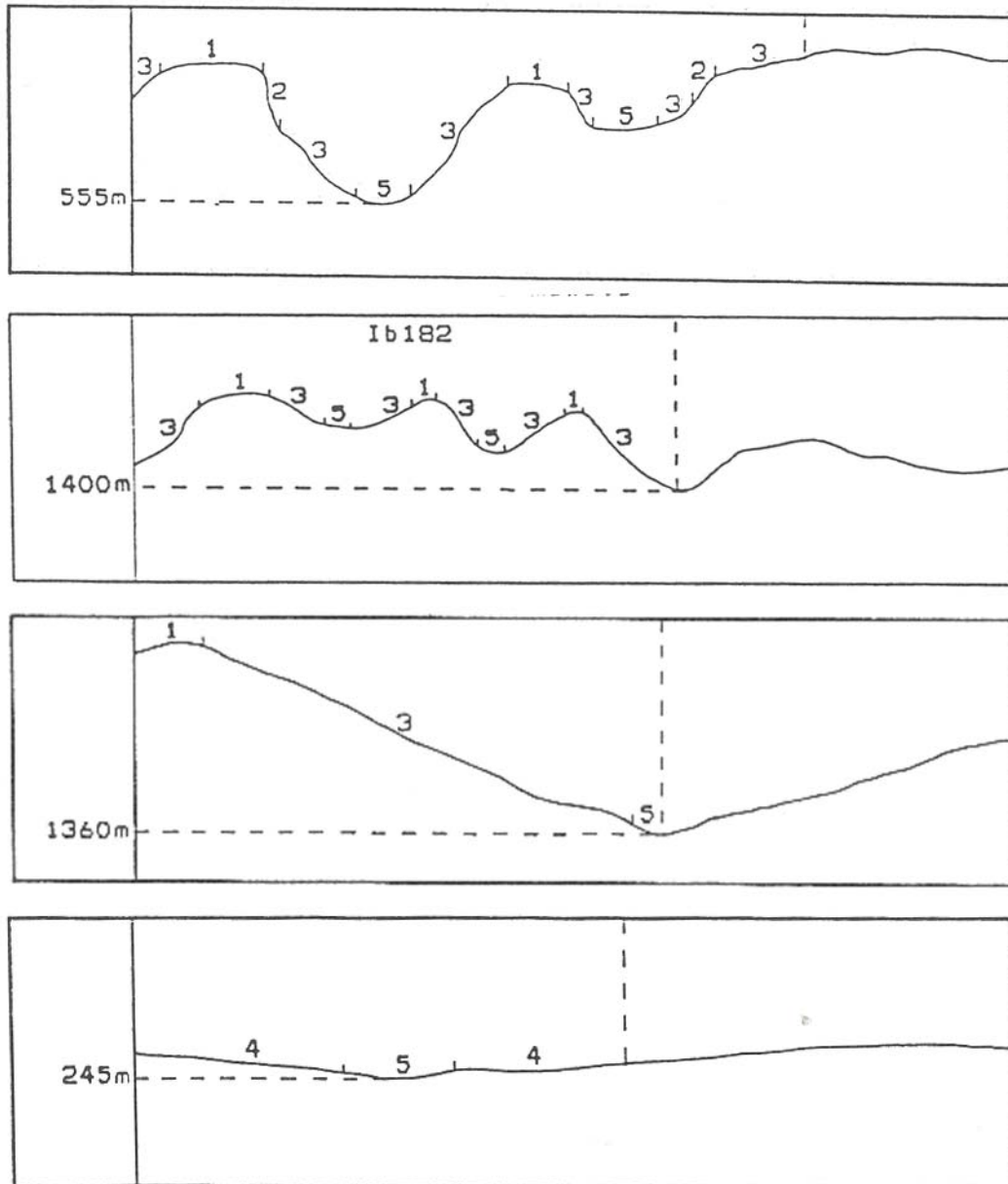


Figure 2-4: Examples of terrain unit sequences from actual South African landscapes (SIRI, 1989)

2.4 The soils components of mapped terrain units and their derivation from soils land types

While a soils terrain unit is considered to be a relatively homogeneous topographic/landscape entity, each TU is nevertheless made up of different (albeit generally related) soil groupings, each with different (albeit generally related) soil physical attributes. These soil groupings are termed “soil series”, with a TU made up of several soil series. This section provides, in a series of steps, some background to the derivations and definitions of soil series from a perspective of the specific soil classification system that was used to map soils across South Africa, viz. the Binomial classification system, and which provided the basic information on the soil series making up the TUs.

Point of Departure 1: The Binomial Soil Classification System into Soils Land Types

Background

The two seminal publications to date on classification systems for South African soils are the Taxonomic Classification by the Soil Classification Working Group, SCWG (1991) in their so-called Blue Book, and its precursor, the Binomial Classification by MacVicar et al. (1977), i.e. the so-called Red Book, with an updated classification in the process of being complete.

At the heart of being able to map hydrological attributes of soils at TU resolution over South Africa, however, are the detailed and readily available soil maps, now also available digitally, based on the Binomial Classification by MacVicar et al. (1977), together with their associated soils inventories from which soil groups were deduced. Elements of the Binomial classification system which are relevant to the objectives of mapping hydrological attributes of soil across South Africa are therefore described briefly below.

Master and Diagnostic Soil Horizons and Their Relevance to Mapping Hydrological Soils Attributes at Terrain Unit Level

Soil as a medium in which hydrological processes occur has a heterogeneous character by virtue of its horization, which controls rates of water uptake, storage and redistribution, both vertically and laterally. Horizons formed under given genetic conditions tend to be reproduced over and over again, with their organisation resulting in a small number of vertically stratified, usually easily identifiable and generalised master horizons (MacVicar et al., 1977).

The specific properties of master horizons led to the recognition by MacVicar et al. (1977) of fairly rigorously defined topsoil and subsoil diagnostic horizons, in which a vertical grouping of pedological features, which may be identifiable (i.e. diagnosed) in the field, is recognised. These diagnostic horizons of the Binomial classification system are shown in Figure 2-5, classed into 5 diagnostic topsoil and 15 diagnostic subsoil horizons, each with unique soil characteristics.

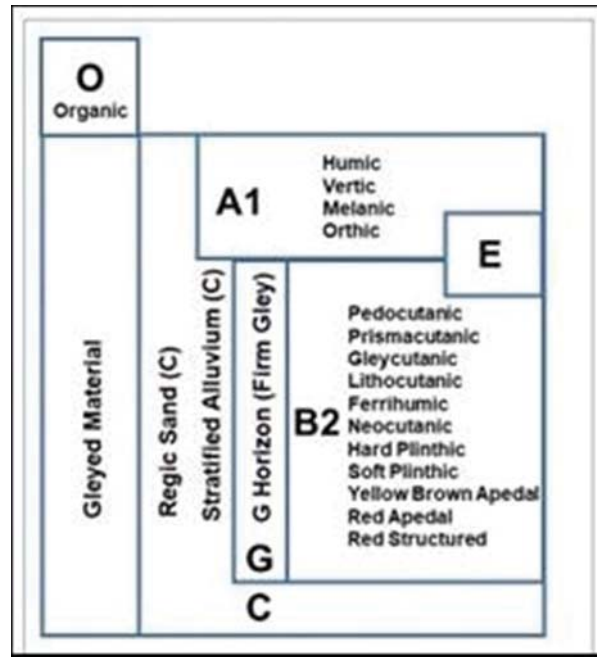


Figure 2-5: Diagnostic topsoil and subsoil classes in the Binomial system (After MacVicar et al., 1977)

While defined according to many genetic and other criteria, in regards to the hydrological soil mapping at TU level, the following diagnostic horizons in Figure 2-5 are identified as important as they were used explicitly in the working rules developed for calculations of

- soil water content at permanent wilting point
 - saturated redistribution of soil water from the top- to the subsoil, and
 - saturated redistribution of soil water out of the subsoil,
- viz. the
- vertic topsoil horizon – with high clay contents (hence low hydraulic conductivities) as well as shrink/swell properties, which imply high infiltrability (macropore flow) when the soil is dry and low infiltrability when it is wet;
- and in the subsoil, the
- G horizon – which is strongly gleyed and characterised by waterlogging for the greater part of the year;
 - soft plinthic horizon – containing manganese oxides and hydrates, but not hard as a result of only periodic (rather than more permanent) saturation;
 - hard plinthic horizon, or ironpan – consisting of a hard indurated zone and indicating very poor drainage and a potential for waterlogging;
 - prisma-cutanic horizon – displaying abrupt increases in clay content and firmness with depth, with associated decreases in hydraulic conductivity/permeability;
 - gley-cutanic horizon – with marked evidence of gleying and a well-developed structure;
 - neo-cutanic horizon – formed in recent sediments/unconsolidated material with some aggregation of soil particles and a clay increase with depth;
 - ferri-humic horizon – often on sandy material under fynbos in the winter/all year rainfall region, and quite variable in hardness;
 - pedo-cutanic horizon – which is clay-enriched and sometimes displays an abrupt textural transition, but is not as wet as a G-horizon;
 - litho-cutanic horizon – which has characteristics largely attributable to material in various stages of alteration between hard rock and homogenized soil;

- regic sand – usually coarse-textured sand to sandy loam, unstructured with generally loose consistency, found in dry regions; and while not a diagnostic horizon, also
- hard rock – which has no or only a minimal soil cover and is impermeable.

This does not imply that the remaining four diagnostic topsoil horizons, viz. the organic, humic, orthic and melanic horizons, nor the remaining subsoil horizons, viz. the yellow brown apedal, red apedal and red structured horizons are not of importance in mapping hydrological attributes of soils at TU level – they just do not feature in explicit equations in the working rules which are based on information contained in the Terrain Unit Database.

From Diagnostic Soil Horizons to the Soil Forms and Soil Series Used in Terrain Unit Analyses

Groupings of soils within a TU are by soil form and soil series.

From the diagnostic soil horizons described above, the concepts of soil forms and soil series are now described from a perspective of mapping soil hydrological attributes at TU resolution.

Soils are organised combinations of horizons and the grouping of specific kinds of diagnostic horizons in specific sequences has resulted in the concept of broadly defined soil forms, of which 41 were identified in South Africa in the Binomial classification system (MacVicar et al., 1977) and more than 70 in subsequent classifications.

Each soil form is, in turn, subdivided into soil series. These are defined, inter alia, for the purpose of enabling non-soil scientists such as hydrologists to describe soils more specifically according to criteria influencing a soil's response, e.g. in regards to hydrological responses. The concept of a soil form divided into a number of series is akin to the plant Kingdoms classification into genera and species. A number of soil physical and chemical criteria are used in the identification of soil series. Criteria important to hydrological responses include

- soil texture properties – with a soil's clay content (which influences soil water retention and redistribution) being divided into five classes, also with abrupt textural discontinuities being indicative of interflow potential and/or hydraulic conductivity changes and sand being graded into coarse, medium and fine, with these textural properties being the prime criteria used in the working rules of hydrological attributes in conjunction with the TU Database;
- degree of leaching – classed into highly (dystrophic), intermediate (mesotrophic) and minimally (eutrophic) leached categories, these being indicative of the soil's permeability and the ease to which saturated drainage (percolation) can take place, and with the degrees of leaching being related to the level of aridity of the soil water regime;
- calcareousness – the degree of which is again associated with levels of permeability and aridity of the soil water regime;
- surface crusting tendencies – which would influence infiltrability;
- cutan formation – associated with the degree of illuviation and/or the soil's shrink/swell potential, i.e. swelling when wet and shrinking when dry; and the
- degree of wetness – usually associated with bottomland soils which may be hydrologically more responsive in stormflow generation as a result of lateral flow accumulation in the bottomlands and, under certain conditions, groundwater ridging.

Soil Forms and Soil Series as the Key Criteria to the Land Type Inventories as the Basis for Mapping Soil Hydrological Attributes

The most detailed mapping unit for the entire country to which hydrological soil attributes could be linked is the soils Land Type. Soils Land Type maps, together with the soils inventories linked / associated with them, were produced by the Agricultural Research Council's Institute for Soil, Climate and Water (ISCW)

and its predecessor, the Soil and Irrigation Research Institute (SIRI), with mapping originally in hard copy, but subsequently available digitally. Some background on that approach, relevant to the present study, is provided below.

A Land Type (MacVicar et al., 1974) is a class of land over which macroclimate, terrain form and soil patterns each display a marked degree of uniformity. This uniformity is such that with insights and technologies available in the 1980s it was originally believed that there would be little advantage in mapping, on a countrywide basis, smaller and more uniform landscape entities for the purpose of, for example, hydrological modelling. The ISCW, in having an agricultural rather than a hydrological mandate, also endeavoured to capture those natural factors that determine agricultural, rather than hydrological, responses. The Institute thus initiated the Land Type surveys with the aims of

- delineating soils Land Types, with fieldwork at a scale of 1:50 000, but eventual mapping at 1:250 000 resolution,
- defining each Land Type, and
- analysing, in-depth, the soil profiles within Land Types (SIRI, 1987).

The Land Type maps were compiled by superimposing detailed climate maps for the region over a pedosystem map and then identifying unique Land Type units. Examples of soils Land Type maps based on the Binomial Classification system are shown in Figure 2-6.

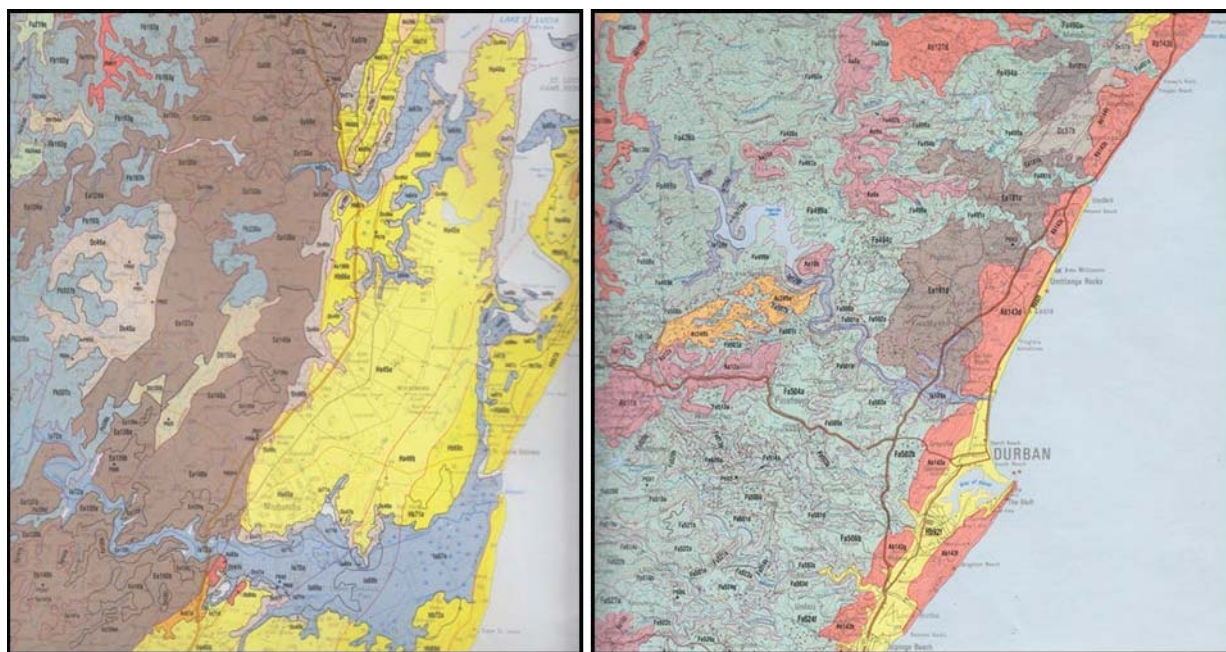


Figure 2-6: Examples of Soil Land Type maps, around Lake St Lucia (left) and Durban (right) in KwaZulu-Natal Province of South Africa (SIRI, 1989)

Land Types over South Africa were grouped into nine broad soil patterns, A, B, C... which were then further sub-divided into map units coded Aa, Ab, Ac... Ai etc., with a mapping unit representing soils of a certain uniformity in regards, inter alia, to colour, base status, depth range and other factors. With reference to those sub-divisions, numbered Land Types were then identified in South Africa with, for example, Ae23 being the 23rd Land Type, with specific local soil properties, of the broader mapping unit Ae. In total some 6 000 Land Types were delineated over South Africa.

Point of Departure 2: From Inventories of Information Associated with Each Soils Land Type to Terrain Unit Information

Land Type Inventory Information Relevant to Terrain Unit Delineation

The delineated and mapped Land Types, of which there are over 6 000, are accompanied by detailed tabulated inventories of information on each Land Type. These Land Type inventories were compiled using data collected during the terrain, soil and climate survey phases. Each Land Type is made up of a number of soil series.

The inventory of each Land Type contains information regarding, inter alia,

- the percentage, by area, of the individual soil series making up that Land Type, and
- for each soil series within a Land Type contains information on soil physical properties such as clay content, soil texture class, soil profile thickness and soil depth limiting material.

More importantly in the inventory (but not mapped with the Land Types) of each of the 6 000+ Land Types is information on the soil series which are found in up to 5 terrain units (TUs) making up a Land Type. These TUs, which had been identified in the field (cf. previous section), are mentioned here again, being

- the crest, termed TU1, which is defined as being convex shaped,
- the scarp, or TU2, which is akin to a cliff,
- the midslope, TU3, which is concave in shape,
- the footslope, TU4, also concave in shape, and
- the valley bottom, or TU5, often also known a wet area adjunct to a stream.

A key question arising at this juncture is whether there is significant hydrological information gain by mapping from Land Type resolution to TU resolution. This is addressed in the next sub-section by way of a sensitivity analysis.

Sensitivity of Hydrological Responses to Terrain Unit Information within a Soils Land Type

Intuitively, because each TU within a Land Type is comprised of different (but usually related) individual soil series, each with different soil thicknesses and hydrological properties, it stands to reason that each TU within a single mapped Land Type should have a different hydrological response. That this is so, is illustrated in Figure 2-7 in which the different soil water contents of the topsoil of the crest (TU1), of the footslope (TU4) and the topsoil of the valley bottom (TU5) of Land Type Ac207, all modelled with the ACRU daily time-step and process-based model (Schulze, 1995 and updates), are shown for an identical climate time series and the same land use.

From Figure 2-7 there is significant hydrological information gain in going from the Land Type to the TU resolution.

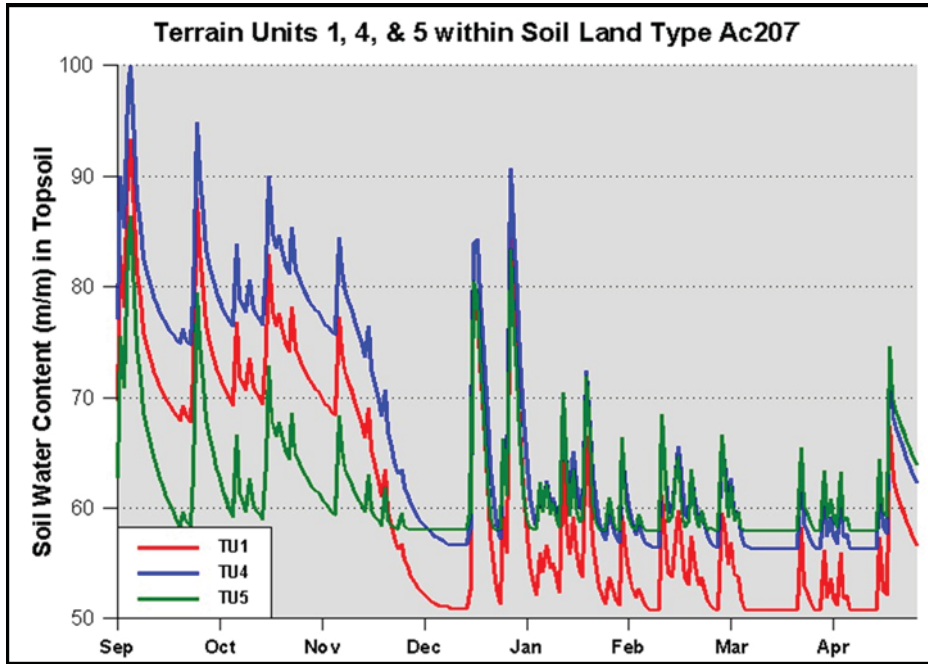


Figure 2-7: Modelled soil water contents (in m/m) of the respective topsoils of three terrain units of a soils Land Type, illustrating the importance of identifying individual TUs within a soils Land Type in regards to hydrological

Point of Departure 3: Delineation of Terrain Units within Soils Land Types

Beukes’ Technique

While still employed at the Agricultural Research Council (ARC) of South Africa, Beukes (2018, pers. com.; now retired) superimposed a Digital Elevation Model (DEM) with a 90 m resolution (pixel) over each mapped soils Land Type which had been identified in South Africa, and then used Neighbourhood Analysis to compute the slope to the North, East, South and West pixel from the pixel of interest in order to determine convexity or concavity to the neighbouring pixels (Beukes, 2018; pers. com.). On the premise that that the crest was convex shaped, but that the midslope was concave in shape, he then applied Zonal Statistics to delineate / map the individual TUs within a Land Type. Following that procedure, he superimposed satellite imagery at a 30 m resolution over the map of TUs to refine the delineations of the TUs, especially the valley bottoms in hilly areas, as a 90 m DEM, while being at a satisfactory spatial resolution in flattish terrain, was found to be too coarse where it was hilly.

The TU Database

From Beukes’ ARC Database of Terrain Units per Soils Land Type, based on the refined 90 m DEM, 27 491 spatially defined TUs across South Africa were identified by the techniques described above, with

- 6 793 of those TUs being convex-shaped crests,
- 6 586 TUs being concave midslopes,
- 7 046 TUs identified as footslopes and
- 7 066 TUs being valley bottoms.

For each TU in this Terrain Unit Database (TUDB)

- the Land Type is identified (e.g. Ia155, Fb143 and Db218 in Table 2-1),
- the TU numbers within the Land Type are listed (e.g. TU1, TU3, TU4 and TU5 within Land Type Fb143 in Table 2-1),

VOLUME 2: WATER USE ESTIMATION OF SFRA SPECIES

- the percentages of each TU in a Land Type are given (e.g. in Table 2-1 TU5 makes up 20% of Land Type Fb143, TU4 30%, TU3 30% and TU1 the remaining 20%),
- the spatial extent of each TU is given by the number of 90 x 90 m pixels making it up (e.g. Table 2-1 shows TU5 of Land Type la155 to be made up of 1 560 pixels and TU4 of 14 180 pixels),
- the soil series constituting a TU are then listed, with up to 15 soil series in the original TUDb, but with only up to 8 series shown in the example of Table 2-1, where it is seen that TU5 of Land Type la155 is made up of soil series Ar10, Va40, Oa46, Va10 and Oa13), and
- the individual areas, as percentages, of each soil series within a TU are then listed (e.g. in Table 2-1, for TU5 in Land Type la155 soil series Ar10 makes up 50% of the TU, Va40 20%...).

Table 2-1: Extract from the Terrain Unit Database showing selected attributes of the Terrain Unit Database up to soil series level information (original source: Beukes, 2018)

LAND TYPE	TERRAIN UNIT	% OF TU IN LAND TYPE	PIXELS PER TU	SOIL SERIES 1	SOIL SERIES 2	SOIL SERIES 3	SOIL SERIES 4	SOIL SERIES 5	SOIL SERIES 6	SOIL SERIES 7	SOIL SERIES 8	% SOIL SERIES 1	% SOIL SERIES 2	% SOIL SERIES 3	% SOIL SERIES 4	% SOIL SERIES 5	% SOIL SERIES 6	% SOIL SERIES 7	% SOIL SERIES 8
la155	5	10	1560	Ar10	Va40	Oa46	Va10	Oa13				50	20	20	5	5	0	0	0
la155	4	90	14180	Oa26	Oa33	Oa13	Oa46	Va10	Hu36			35	30	15	10	5	5	0	0
Fb143	5	20	7949	Oa16	Ms22	Hu36	Cv46	Cv36	R			30	25	20	15	5	5	0	0
Fb143	4	30	6871	Hu36	Ms22	Hu36	Ms10	R	Oa16	Cv46	Cv36	30	25	10	10	10	5	5	5
Fb143	3	30	9225	Ms10	Ms22	Cv36	Hu36	Hu36	R			30	20	15	15	10	10	0	0
Fb143	1	20	7884	Ms10	R	Hu36						50	30	20	0	0	0	0	0
Db218	5	30	17505	Va30	Ar10	Oa46	Du10	Oa17	S	Sw20		30	20	20	10	10	5	5	0
Db218	4	60	37958	Va30	Oa26	Va10	Sw20	Oa17	Hu36	Oa46		40	20	15	10	5	5	5	0
Db218	1	10	5165	Sw10	Hu35	Ms10	R					40	30	20	10	0	0	0	0

Further to that, in Table 2-2,

- soil profile depths for each soil series in a TU are given in mm, with a set of working rules shown later in Figure 2-10 which are applied to determine respective thicknesses of the topsoil and subsoil for each soil series in the TU,

while in Table 2-3

- clay percentages for each soil series in a TU are given for the topsoil (in the upper table) and for the subsoil (in the lower table), with this information used with a set of working rules shown later for the determination of the permanent wilting point and the drained upper limit for the top- and subsoils.

Table 2-2: Further extract from the Terrain Unit Database showing soil profile depths (mm) per soil series in a TU in the last eight columns (Original source: Beukes, 2018)

LAND TYPE	TERRAIN UNIT	% OF TU IN LAND TYPE	PIXELS PER TU	SOIL SERIES 1	SOIL SERIES 2	SOIL SERIES 3	SOIL SERIES 4	SOIL SERIES 5	SOIL SERIES 6	SOIL SERIES 7	SOIL SERIES 8	PROFILE DEPTH 1	PROFILE DEPTH 2	PROFILE DEPTH 3	PROFILE DEPTH 4	PROFILE DEPTH 5	PROFILE DEPTH 6	PROFILE DEPTH 7	PROFILE DEPTH 8
la155	5	10	1560	Ar10	Va40	Oa46	Va10	Oa13				1200	1200	900	1050	1200	0	0	0
la155	4	90	14180	Oa26	Oa33	Oa13	Oa46	Va10	Hu36			1000	1200	1200	900	1050	600	0	0
Fb143	5	20	7949	Oa16	Ms22	Hu36	Cv46	Cv36	R			1200	200	650	400	650	0	0	0
Fb143	4	30	6871	Hu36	Ms22	Hu36	Ms10	R	Oa16	Cv46	Cv36	650	200	400	200	0	1200	400	650
Fb143	3	30	9225	Ms10	Ms22	Cv36	Hu36	Hu36	R			200	200	650	650	400	0	0	0
Fb143	1	20	7884	Ms10	R	Hu36						200	0	400	0	0	0	0	0
Db218	5	30	17505	Va30	Ar10	Oa46	Du10	Oa17	S	Sw20		1050	1050	1200	1200	1200	0	650	0
Db218	4	60	37958	Va30	Oa26	Va10	Sw20	Oa17	Hu36	Oa46		1050	975	1050	650	1200	600	1200	0
Db218	1	10	5165	Sw10	Hu35	Ms10	R					450	300	200	0	0	0	0	0

VOLUME 2: WATER USE ESTIMATION OF SFRA SPECIES

Table 2-3: Another extract from the Terrain Unit Database showing (top table) clay percentages in the topsoil and (bottom table) in the subsoil per soil series in a TU in the respective last eight columns (Original source: Beukes, 2018)

LAND TYPE	TERRAIN UNIT	% OF TU IN LAND TYPE	PIXELS PER TU	SOIL SERIES 1	SOIL SERIES 2	SOIL SERIES 3	SOIL SERIES 4	SOIL SERIES 5	SOIL SERIES 6	SOIL SERIES 7	SOIL SERIES 8	CLAY TOP 1	CLAY TOP 2	CLAY TOP 3	CLAY TOP 4	CLAY TOP 5	CLAY TOP 6	CLAY TOP 7	CLAY TOP 8
la155	5	10	1560	Ar10	Va40	Oa46	Va10	Oa13				50	30	9	20	12	0	0	0
la155	4	90	14180	Oa26	Oa33	Oa13	Oa46	Va10	Hu36			20	10	12	9	20	13	0	0
Fb143	5	20	7949	Oa16	Ms22	Hu36	Cv46	Cv36	R			18	18	15	17	14	0	0	0
Fb143	4	30	6871	Hu36	Ms22	Hu36	Ms10	R	Oa16	Cv46	Cv36	15	18	14	18	0	18	17	14
Fb143	3	30	9225	Ms10	Ms22	Cv36	Hu36	Hu36	R			18	18	14	15	14	0	0	0
Fb143	1	20	7884	Ms10	R	Hu36						18	0	14	0	0	0	0	0
Db218	5	30	17505	Va30	Ar10	Oa46	Du10	Oa17	S	Sw20		25	40	25	11	25	0	18	0
Db218	4	60	37958	Va30	Oa26	Va10	Sw20	Oa17	Hu36	Oa46		25	15	20	18	25	10	25	0
Db218	1	10	5165	Sw10	Hu35	Ms10	R					18	8	13	0	0	0	0	0

LAND TYPE	TERRAIN UNIT	% OF TU IN LAND TYPE	PIXELS PER TU	SOIL SERIES 1	SOIL SERIES 2	SOIL SERIES 3	SOIL SERIES 4	SOIL SERIES 5	SOIL SERIES 6	SOIL SERIES 7	SOIL SERIES 8	CLAY SUB 1	CLAY SUB 2	CLAY SUB 3	CLAY SUB 4	CLAY SUB 5	CLAY SUB 6	CLAY SUB 7	CLAY SUB 8
la155	5	10	1560	Ar10	Va40	Oa46	Va10	Oa13				0	40	15	25	13	0	0	0
la155	4	90	14180	Oa26	Oa33	Oa13	Oa46	Va10	Hu36			23	10	13	15	25	18	0	0
Fb143	5	20	7949	Oa16	Ms22	Hu36	Cv46	Cv36	R			20	0	15	20	16	0	0	0
Fb143	4	30	6871	Hu36	Ms22	Hu36	Ms10	R	Oa16	Cv46	Cv36	15	0	19	0	0	20	20	16
Fb143	3	30	9225	Ms10	Ms22	Cv36	Hu36	Hu36	R			0	0	16	15	19	0	0	0
Fb143	1	20	7884	Ms10	R	Hu36						0	0	19	0	0	0	0	0
Db218	5	30	17505	Va30	Ar10	Oa46	Du10	Oa17	S	Sw20		38	40	28	0	35	0	33	0
Db218	4	60	37958	Va30	Oa26	Va10	Sw20	Oa17	Hu36	Oa46		38	21	30	33	35	25	28	0
Db218	1	10	5165	Sw10	Hu35	Ms10	R					28	12	0	0	0	0	0	0

The full TUDB from which the above extracts were made contains a wide range of other attributes of the constituent soil series in a TU which are unrelated to mapping hydrological soils attributes.

Illustration of the Spatial Detail of Terrain Unit Mapping

To illustrate the spatial detail from mapping South Africa’s soils at the TU level, an area to the north and west of Durban in KwaZulu-Natal was selected (Figure 2-8). The figure shows the delineated crests in dark brown, midslopes in light brown, footslopes in green and the valley bottoms in dark blue (Figure 2-8). Scarps, taken to be vertical to near-vertical, are assumed to have no spatial extent when mapped in plan view. The black polygons on the map are Quinary Catchments delineations, i.e. the hydrologically and agriculturally relatively homogeneous spatial unit now widely used in South Africa in water resources and climate change studies and for which currently area-averaged soils attributes are a modelling input. Within a Quinary Catchment the large number of TUs, each with their own hydrological attributes, are seen clearly. When the rectangular inset in Figure 2-8 is zoomed in upon in Figure 2-9, the degree of detail of the TU delineations is even more amply evident, with individual pixels of a specific TU visible in places. It is at this level of spatial detail that the hydrological attributes of soils were mapped.

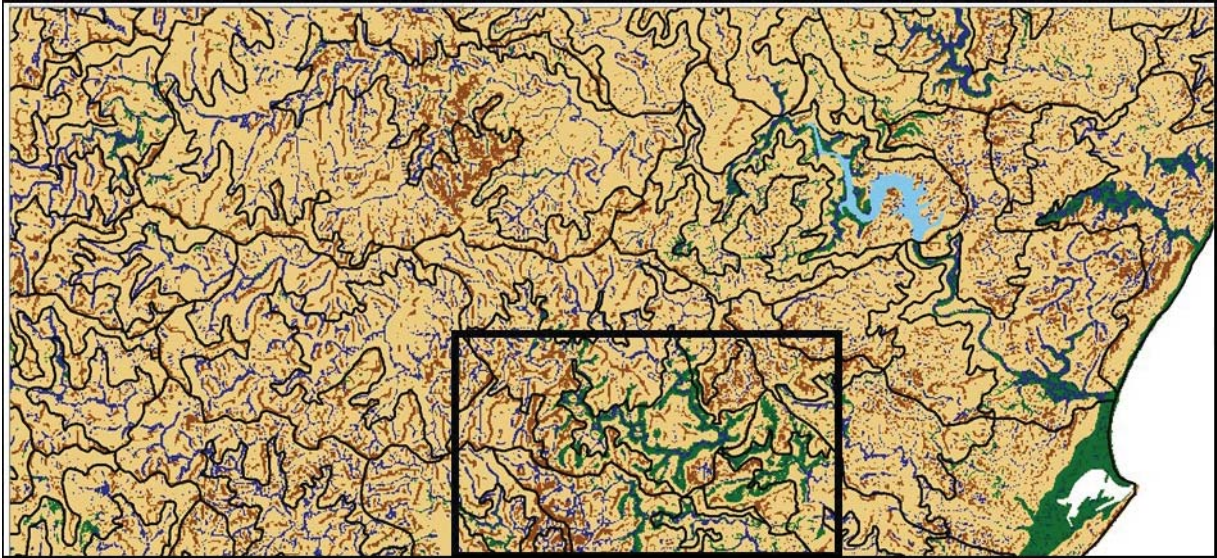


Figure 2-8: Terrain units and Quinary Catchments west and north of Durban, South Africa

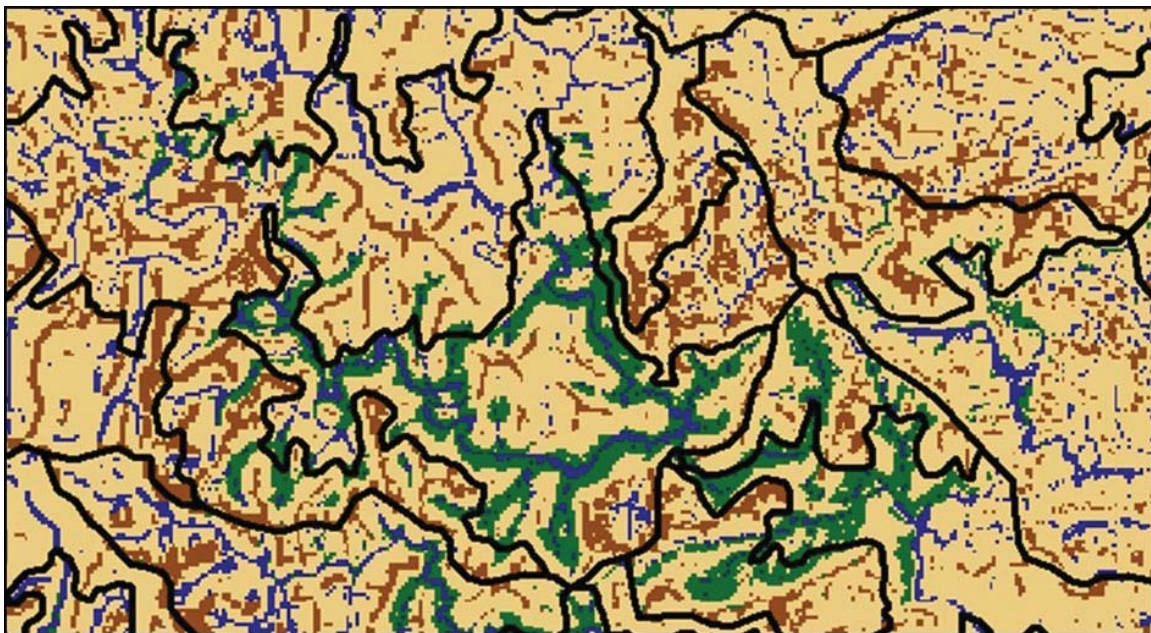


Figure 2-9: Zooming in from the inset in Figure 8 to show more detail on soils Terrain Units in dark brown (crests), light brown (midslopes), green (footslopes) and dark blue (dark blue) within Quinary Catchments (black)

2.5 Definitions of key soil physical attributes and algorithms used

2.5.1 Determination of thicknesses of topsoil and subsoil horizons

Importance in Hydrology of the Thickness of the Topsoil Horizon

The topsoil is the “action” horizon in both forestry and in hydrology, as it is the horizon

- into which rainfall infiltrates,
- which contains most of the plant’s roots,
- out of which most transpiration and soil water evaporation occurs,
- which may be disturbed by forest management practices such as site preparation,
- the soil water content of which largely controls stormflow responses to rainfall, and
- which can display cracks in shrink-swell type clay soils.

Importance in Hydrology of the Thickness of the Subsoil Horizon

The subsoil horizon, on the other hand,

- is the “moisture storage” horizon, which
- largely determines plant available water,
- controls recharge into the vadose/ groundwater zones, and
- is the contact horizon overlying either unconsolidated material or parent material which, in a wetland/bottomland, can also be a gleyed horizon).

Determining Respective Horizon Thicknesses

The Terrain Unit Database, based on information from the Land Type inventories, provides a total depth, or thickness, of the soil profile for each of the soil series within a TU, as shown in the example in Table 2-2. The active root depth of plantation forests is taken to be the total soil profile depth as given in the TUDB, with a maximum depth of 1 500 mm assumed for modelling purposes when that depth is exceeded. Experience-based working rules, initially developed by Angus and Schulze (1990) and Schulze et al. (1991), and then modified by Schulze and Horan (2005) and again by Schulze (2018; for the present study), have been developed and are used to

- modify the total soil profile depth given in the TUDB for use in modelling, and to then
- partition the total depth into respective thicknesses of top- and subsoil horizons.

These working rules are summarised by the flowchart shown in Figure 2-10, where THICK is the soil profile thickness (mm), as given in the TUDB and shown by way of example in Table 2-2.

The working rules are essentially self-explanatory. However, key features are that the maximum soil thickness is assumed to be 1 500 mm, as indicated above, and that where the total active root depth is deeper than 500 mm the topsoil is assumed to be 0.30 m thick, while when below 500 mm the topsoil horizon is assigned a thickness of 60% of the total profile thickness and a special case is made for rocks, which are assigned an arbitrary “soil” thickness of 10 mm.

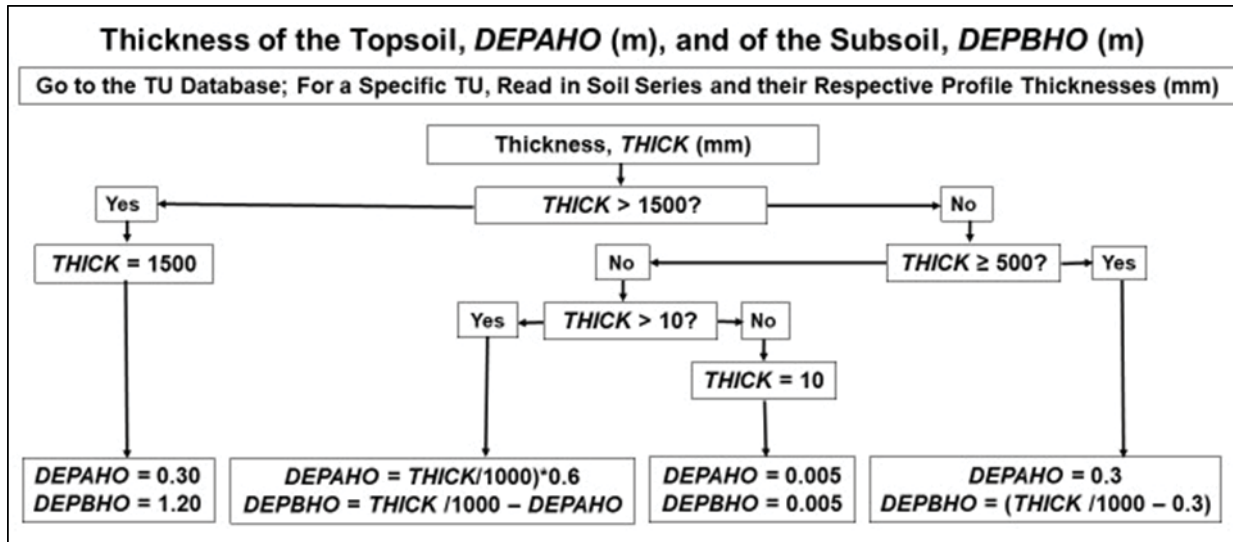


Figure 2-10: Flowchart illustrating the working rules for the determination of the thicknesses of the topsoil (*DEPAHO*; m) and the subsoil (*DEPBHO*; m) when using information contained in the Terrain Unit Database

2.5.2 Determination of soil water content at the soil’s permanent wilting point

The Concept of the Permanent Wilting Point

Permanent Wilting Point (PWP) is taken here as the dry (i.e. lower) limit of soil water available to plants. At the stage of permanent wilting point, the hydraulic conductivity is so low that water cannot move to the roots fast enough, even over short distances, and no water is available for transpiration. As such the soil water content at PWP, viz. Θ_{PWP} , is usually assumed to be a soil characteristic with a matric potential assumed to be fixed at -1 500 kPa.

This is not strictly so, however, as it depends also on the plant as well as on the depth, intensity and ramification of the root system at the different depths in the soil profile at which the plant is attempting to extract soil water.

Overall, values of soil water content at permanent wilting point for top- and sub-soil horizons of the soil profile will depend, inter alia, on the

- soil texture, i.e. dependent on the particle size distribution of the soil into percentages of clay, silt and sand, where particularly the percentage of the fine clay is important, as well as the
- percentage organic matter, the soil’s
- bulk density,
- instability of the soil in regard to swell/shrink properties found in vertic topsoils and prisma- and pedo- as well as certain gleycutanic subsoils, and the
- change of clay content with depth.

Not every one of the above variables is contained, either explicitly or by implication, in the Land Type inventories on which the TUDB is based, and certain simplified rules thus had to be applied, as explained below.

Soil Water Content at Permanent Wilting Point

Soil water content, Θ in m/m, largely reflects the texture class of the soil and especially its clay percentage. The flowchart making up Figure 2-11 has thus been derived from Hutson’s (1984) equations when using clay content as the only variable, based on over 3 000 soil analyses.

As may be gleaned from Figure 2-11, the Θ_{PWP} also depends largely on Hutson’s (1984) findings that values are affected by whether the soils are stable or unstable and, if unstable with shrink-swell characteristics, whether the diagnostic horizons are vertic and, if not, whether or not they are either prismatic, or gleycutanic, or pedocutanic soils, in which case the soil water content is different to that of stable soils not displaying those characteristics.

It should be stressed that in many soil series in South Africa clay content increases with depth as a result of the translocation of finer clay particles down the soil profile, mainly in higher rainfall areas. This is illustrated for Land Type Db218 in Table 2-3. For that reason alone, the Θ_{PWP} of a subsoil will frequently be higher than that of its topsoil.

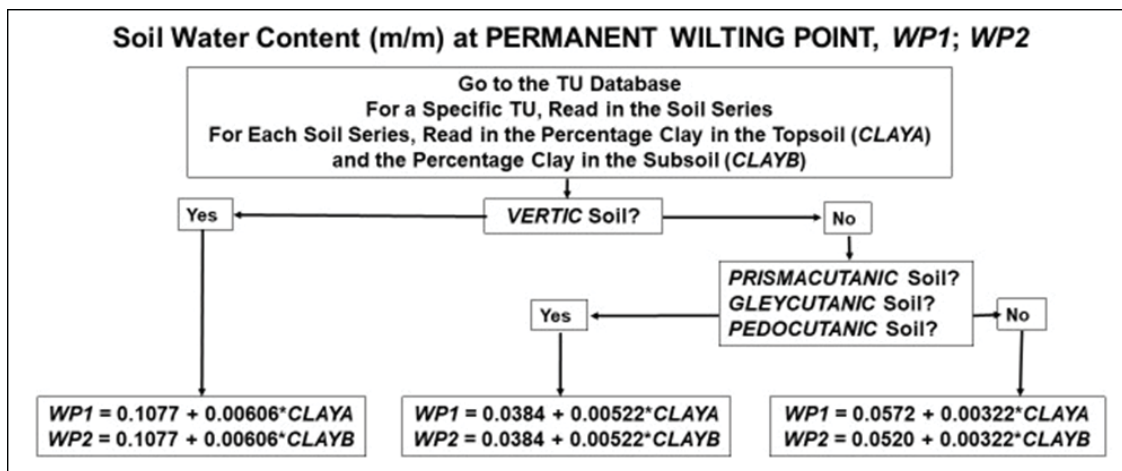


Figure 2-11: Flowchart illustrating the working rules for the determination of soil water content at permanent wilting point when using information contained in the Terrain Unit Database

With reference to the soil forms with unstable soils which are given in Figure 2-11, some key hydrological properties of which were described in the section on “Master and Diagnostic Soil Horizons and Their Relevance to Mapping Hydrological Soils Attributes at Terrain Unit Level” they are as follows:

Vertic soils are all soil series of the following soil forms:	Rensburg	Rg
	Arcadia	Ar
Prismacutanic soils are all soil series of the following soil forms	Estcourt	Es
	Sterkspruit	Ss
Pedocutanic soils are all soil series of the following soil forms:	Bonheim	Bo
	Swartland	Sw
	Valsrivier	Va
Gleycutanic soils are all soil series of the following soil forms:	Kroonstad	Kd
	Pinedene	Pn
Lithocutanic soils are all soil series of the following soil forms:	Cartref	Cf
	Glenrosa	Gs
	Mayo	My
	Nomanci	No

2.5.3 Determination of soil water content at the soil's drained upper limit

The Concept of the Drained Upper Limit

Drained Upper Limit (DUL) is the soil water condition reached when water has been allowed to percolate naturally from the soil until drainage ceases and the water remaining is held by capillary forces that are great enough to resist gravity. The soil water content at DUL, Θ_{DUL} , is often described as being the wet limit of the soil water available freely to plants. This theoretical definition has drawbacks when applied to soils in a natural environment and Θ_{DUL} can be described as the soil water content below which the hydraulic conductivity is sufficiently small for redistribution of moisture due to hydraulic head to be ignored. A definition in terms of matric potential is difficult owing to the fact that Θ_{DUL} may vary with texture, but it is conventionally taken to fall somewhere between -5 and -33 kPa. In this document a value of -10 kPa is used as the matric potential representing Θ_{DUL} .

Soil Water Content at the Soil's Drained Upper Limit

From Hutson's (1984) analyses of over 3 000 soil samples, values of soil water content at the DUL for top- and sub-soil horizons of the soil profile will depend, inter alia, on the

- percentage of clay
- percentage of silt, the
- bulk density, and the
- change of clay content with depth.

Applying Hutson's simplified equations using only clay content as a variable, as that is what is available in the TUDB, and in recognition that for many soils the clay content increases with depth (see Table 2-3), his equations for soil water content at DUL are given in Figure 2-12.

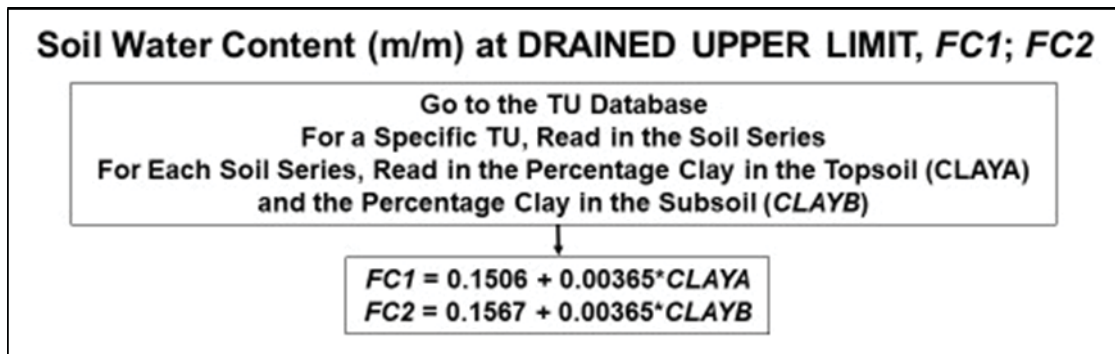


Figure 2-12: Flowchart illustrating the working rules for the determination of soil water content at the drained upper limit when using information contained in the Terrain Unit Database

Profile Plant Available Water

Profile Plant Available Water (PAW, in mm) is assumed to be the water in the soil profile which is readily available to plants. Conventionally,

$$PAW = \Theta_{DUL} - \Theta_{PWP}$$

The concept of PAW is not without flaws, however, as plants can extract soil water at levels $> \Theta_{DUL}$, albeit at a reduced rate (Schulze, 1995). Furthermore, at a given fraction of PAW between Θ_{DUL} and Θ_{PWP} plant stress sets in, implying again a reduced rate of a plant's ability to extract soil water. This fraction of PAW is often fixed at around 0.5 (i.e. 50% PAW), especially for agricultural crops, but under natural conditions it

varies according to soil texture (fraction is higher in clays, lower in sandy soils) as well as varying on a day-by-day basis with different crops, depending on atmospheric demand (the hotter the day, the higher the fraction because plants close their stomata) and the plant's critical leaf water potential (i.e. some plants are inherently more resilient to stress than others).

In the case of plantation species, the fraction of PAW at which stress sets in varies by genus, it being assumed in modelling of *Pinus* species to commence at 0.3PAW already since pines are conservers of soil water, while for *Eucalyptus* species it is set at 0.2PAW as eucalypts use soil water freely until there is very little available water remaining before stress sets in.

Because PAW represents a store of water available, it will depend on

- soil texture, with different textures having different water holding capacities (e.g. loam can hold more water than clay or sand) and
- soil profile depth, where depth here refers to the profile's depth to which plant roots are active.

Profile PAW may be expressed as

$$PAW = ([DEPAHO * 1000 * DUL1] - [DEPAHO * 1000 * WP1]) + [DEPBHO * 1000 * DUL2] - [DEPBHO * 1000 * WP2]$$

2.5.4 Determination of soil water content when soils are at total porosity, i.e. when the soil is totally saturated

Some Background on Soil Water Content at Porosity

Total porosity (PO in m/m) is the percentage soil volume occupied by voids, and as such contains the maximum possible soil water storage, with all pore spaces filled with water. At total porosity the soil is therefore saturated with water. The matric potential at saturation is 0 kPa.

Hydrologically the soil water content at saturation attains significance because it is the difference between PO of a critical soil depth and the actual soil water content for the same depth which defines the soil water deficit, S (mm) – a crucial variable used in the computation of stormflows in the ACRU model (Schulze, 1995 and updates).

In the maps which follow on soil water content at saturation for the topsoil (Θ_{PO1}), the soil is assumed not to be tilled. It should be noted that, depending on the soil's texture class, a freshly tilled topsoil's Θ_{PO1} can increase by between 11% and 34% (average: 20%) because of a change in bulk density with ploughing, with this increase gradually declining to between 2% and 25% (average: 12%) by the end of the growing season as the soil compacts again.

Estimation of Soil Water Content at Total Porosity under Various Conditions

The amount of water held by a soil when all pore spaces are filled at saturation, is used in computations of soil water redistribution and stormflow generation. Total porosity will depend largely on the soils

- texture class, which reflects its percentages of the sand, silt and clay fractions, its
- bulk density, which generally varies with clay content and depth, and its
- state of tillage, through which bulk density of the tilled layer is changed.

For this study soil texture class is the only variable used (Figure 2-13). Note that soil water content at total porosity is highly variable within a given soil texture class (Hutson, 1984). The South African database on total porosity values is, furthermore, not extensive. Hence, literature derived values of total porosity, by soil texture class, are used. These are given in Figure 2-13.

In Figure 2-13 reference is made to the ACRU model's Soils Database (Smithers and Schulze, 1995 and updates). If that is not readily accessible, the percentage clay given in the Terrain Unit Database (Table 2-3)

can be used in conjunction with the South African texture triangle (Figure 2-14) to determine the soil texture class, especially since a silt content around 10% may be assumed as a general value for most of South African soils (Hutson, 1984).

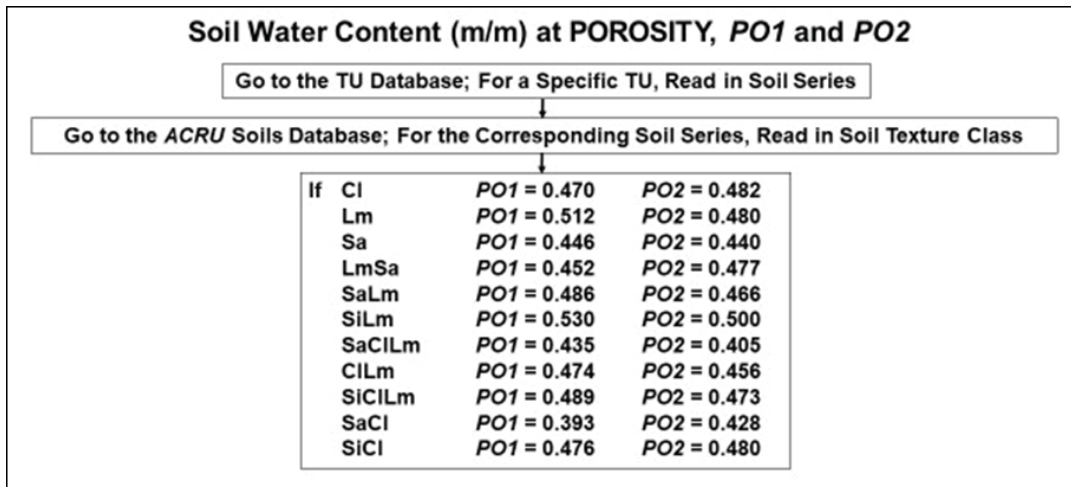


Figure 2-13: Soil water content (m/m) for soil texture classes at porosity for topsoils (PO1) and subsoils (PO2)

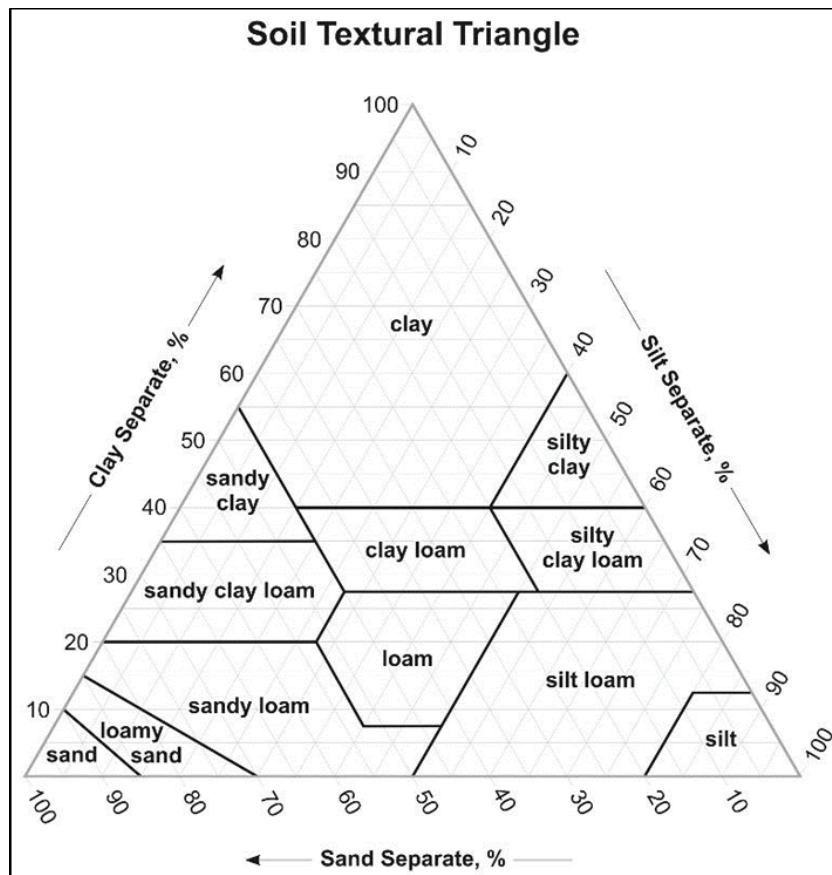


Figure 2-14: South African texture triangle (MacVicar et al., 1977)

2.5.5 Determination of saturated redistribution rates, or saturated drainage

Some Background on Saturated Redistribution Rates

Saturated drainage occurs when soil water content exceeds the soil water content at drained upper limit, Θ_{DUL} . The daily amounts of drainage are dependent on a fraction of that excess water (i.e. the soil water content exceeding Θ_{DUL}) which, in a soil with two horizons, would drain

- from the topsoil to the subsoil horizon when the topsoil’s DUL is exceeded, and
- from the subsoil out of the active root zone when the subsoil’s DUL is exceeded.

Redistribution Rates from Topsoil to Subsoil

The redistribution fraction of the “excess” water per day from top- to subsoil is dependent, as a point of departure, on soil texture, with clays draining slowly and sands rapidly, and with this initial rate then modified, as illustrated in Figure 2-14.

These redistribution fractions depend largely (but not solely) on soil textural conditions. However, South African soils are hydrologically complex, and are characterised by hydraulic discontinuities because of their heterogeneous horization. Where gradual or abrupt changes toward finer textures take place between the top-and subsoil horizons the redistribution rate is reduced. Similarly, where impervious stonelines, clay- or other hardpan horizons occur in the subsoil of a soil profile, rates are reduced, as illustrated in Figure 2-15.

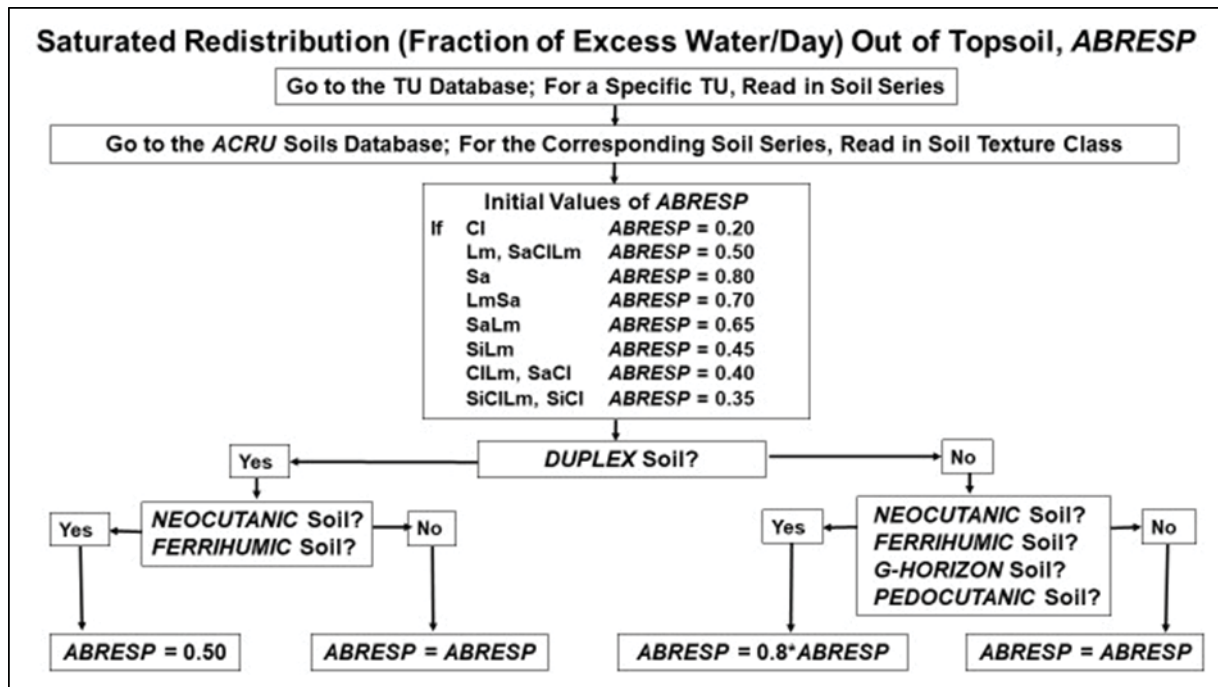


Figure 2-15: Flowchart illustrating the working rules of saturated redistribution of soil water from the topsoil into the subsoil

With reference to the soil attributes shown in Figure 2-15 which modify saturated redistribution of soil water from the topsoil into the subsoil, some key hydrological properties of which were described in the section on “Master and Diagnostic Soil Horizons and Their Relevance to Mapping Hydrological Soils Attributes at Terrain Unit Level”, they are as follows:

Duplex soils are all soil series of the following soil forms:	Cartref Constantia Estcourt Houwhoek Kroonstad Lamotte Longlands Shepstone Vilafontes Wasbank	Cf Ct Es Hh Kd Lt Lo Sp Vf Wa
Pedocutanic soils are all soil series of the following soil forms:	Bonheim Swartland Valsrivier	Bo Sw Va
Neocutanic soils are all soil series of the following soil forms:	Inhoek Oakleaf Vilafontes	Ik Oa Vf
Ferrihumic soils are all soil series of the following soil forms	Houwhoek Lamotte	Hh Lt
G-Horizon soils are all soil series of the following soil forms:	Katspruit Rensburg Willowbrook	Ka Rg Wo

Redistribution Rates out of the Subsoil

As illustrated in Figure 2-16, the initial texture-based redistribution rates out of the subsoil are modified by a different set of conditions.

With reference to the soil attributes shown in Figure 2-16 which modify saturated redistribution of soil water out of the subsoil, some key hydrological properties of which were described in the section on “Master and Diagnostic Soil Horizons and Their Relevance to Mapping Hydrological Soils Attributes at Terrain Unit Level”, they are as follows:

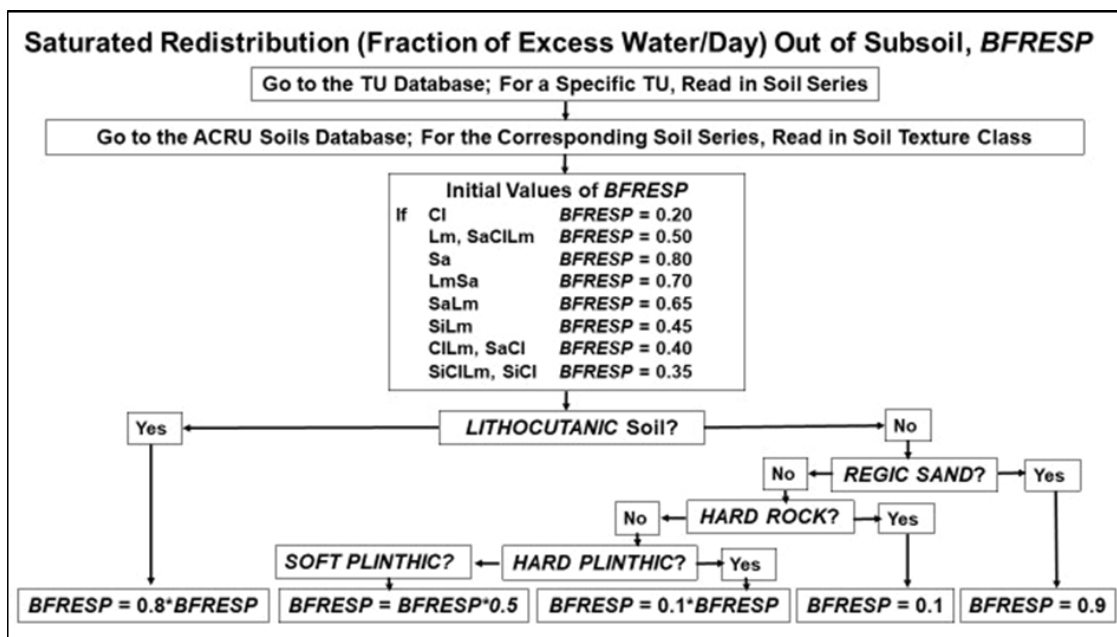


Figure 2-16: Flowchart illustrating the working rules of saturated redistribution out of the subsoil

VOLUME 2: WATER USE ESTIMATION OF SFRA SPECIES

With reference to the soil attributes shown in Figure 2-16 which modify saturated redistribution of soil water from the topsoil into the subsoil, some key hydrological properties of which were described in the section on “Master and Diagnostic Soil Horizons and Their Relevance to Mapping Hydrological Soils Attributes at Terrain Unit Level”, they are as follows:

Duplex soils are all soil series of the following soil forms:	Cartref Constantia Estcourt Houwhoek Kroonstad Lamotte Longlands Shepstone Vilafontes Wasbank	Cf Ct Es Hh Kd Lt Lo Sp Vf Wa
Pedocutanic soils are all soil series of the following soil forms:	Bonheim Swartland Valsrivier	Bo Sw Va
Neocutanic soils are all soil series of the following soil forms:	Inhoek Oakleaf Vilafontes	Ik Oa Vf
Ferrihumic soils are all soil series of the following soil forms:	Houwhoek Lamotte	Hh Lt
G-Horizon soils are all soil series of the following soil forms:	Katspruit Rensburg Willowbrook	Ka Rg Wo

Redistribution Rates out of the Subsoil

As illustrated in Figure 2-17, the initial texture-based redistribution rates out of the subsoil are modified by a different set of conditions.

With reference to the soil attributes shown in Figure 2-17 which modify saturated redistribution of soil water out of the subsoil, some key hydrological properties of which were described in the section on “Master and Diagnostic Soil Horizons and Their Relevance to Mapping Hydrological Soils Attributes at Terrain Unit Level”, they are as follows:

Lithocutanic soils are all soil series of the following soil forms:	Cartref Glenrosa Mayo Nomanci	Cf Gs My No
Regic Sand soils are all soil series of the following soil forms:	Fernwood	Fw
Hard Rock soils are all soil series of the following soil forms:	Milkwood Mispah	Mw Ms
Hard Plinthic soils are all soil series of the following soil forms:	Glencoe Wasbank	Gc Wa
Soft Plinthic soils are all soil series of the following soil forms	Avalon Bainsvlei Longlands Tambamkulu Westleigh	Av Bv Lo Tk We

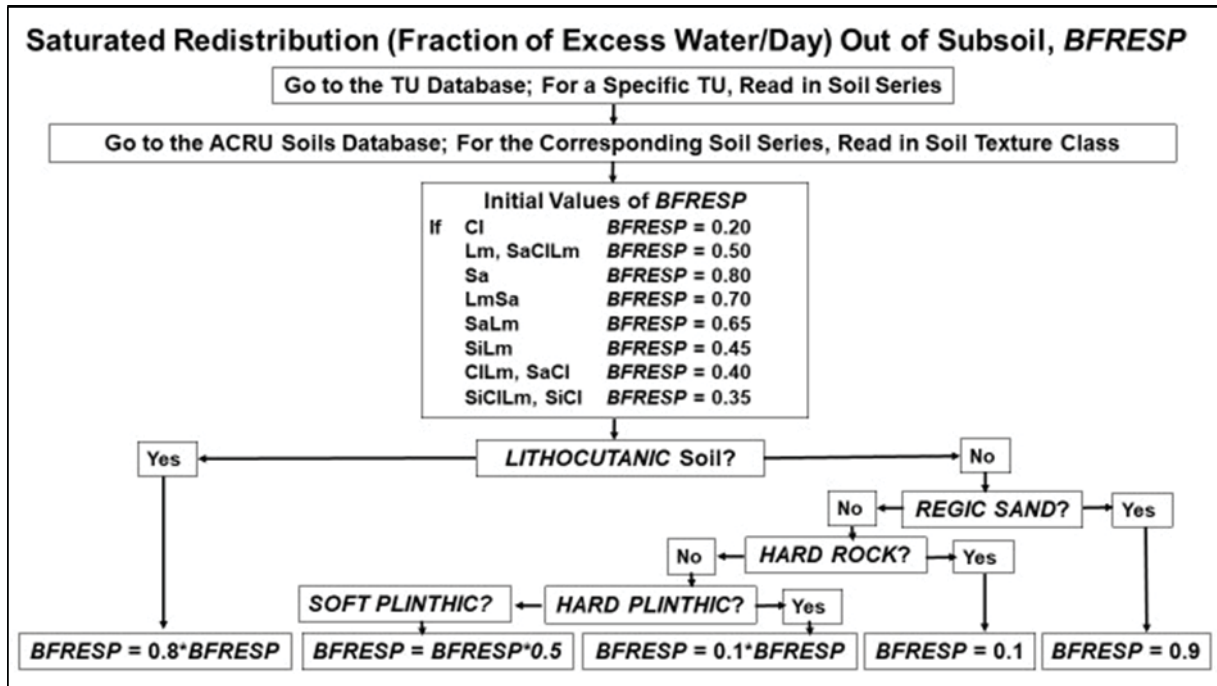


Figure 2-17: Flowchart illustrating the working rules of saturated redistribution out of the subsoil

2.6 Mapped outcomes and interpretations of results from a forestry perspective.

In the sub-sections to follow the forestry plantation study area is first defined, followed by displays of maps of the various soils parameters assessed, initially at a South Africa-wide level and then zoomed in to an area around Durban in KwaZulu-Natal to illustrate the spatial detail that can be attained when mapping at Terrain Unit resolution.

2.6.1 The plantation forestry study area

The plantation forestry study area within South Africa is shown in Figure 2-18 (top) in relation to mean annual precipitation (Figure 2-18 bottom left) and its inter-annual coefficient of variation (Figure 2-18 bottom right). It has been defined as essentially areas with MAP in excess of 600 mm which simultaneously display a relatively low inter-annual CV of rainfall, by South African criteria, at < 30%.

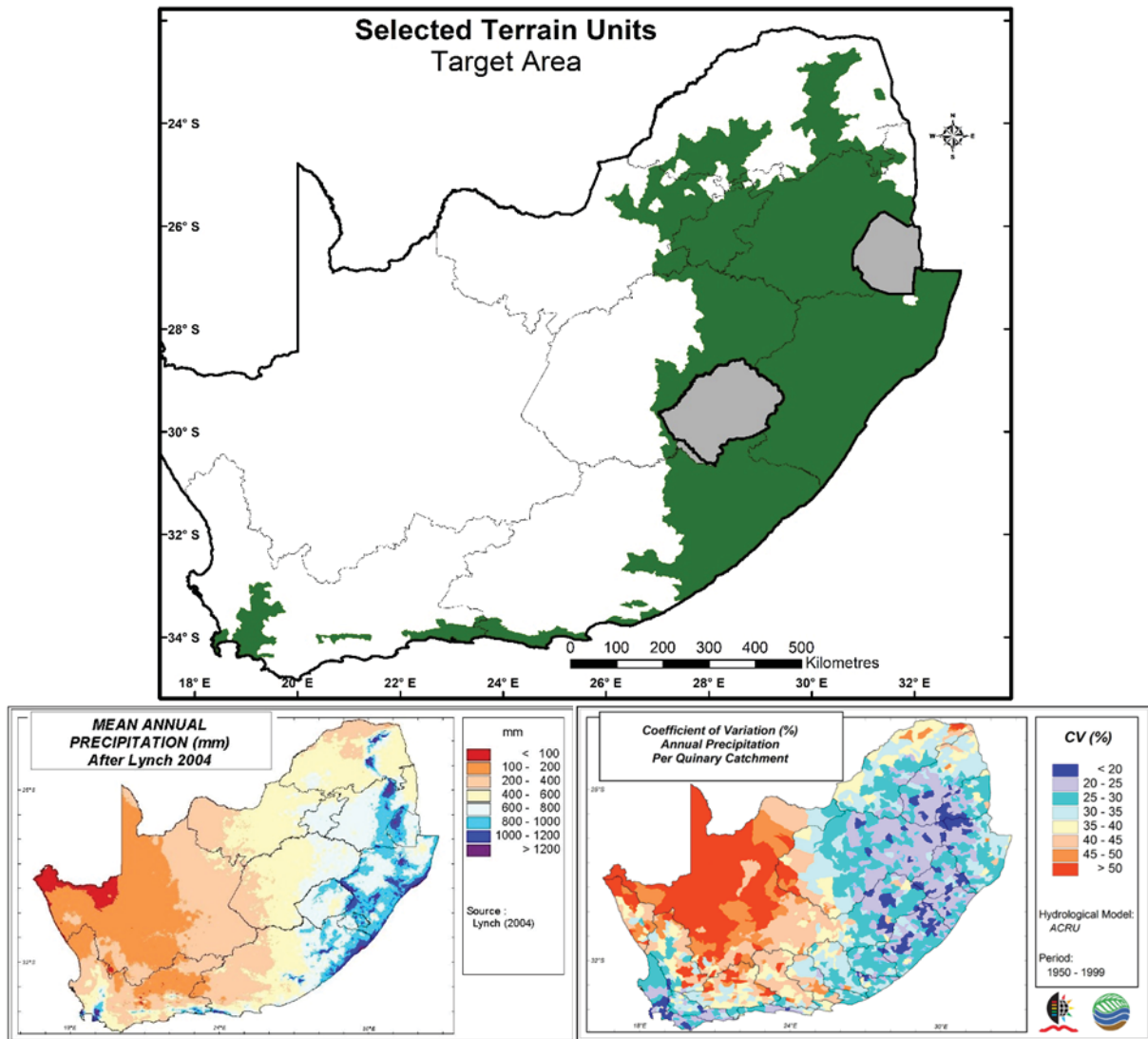


Figure 2-18: The plantation forestry study area within South Africa (top) in relation to mean annual precipitation (bottom left) and (bottom right) its inter-annual coefficient of variation (Bottom maps: Schulze, 2008)

2.6.2 Thickness of the topsoil

Topsoil thickness in the areas potentially afforestable in South Africa are shown in Figure 2-19 (top) to range from < 0.10 m to 0.3 m, the maximum thickness to which topsoils have been defaulted in this study. Many areas display topsoil thicknesses below what could be considered an optimum at 0.3 m, given that most tree roots reside in the topsoil. The zoomed-in map shows that topsoil thickness can vary widely across very short spaces.

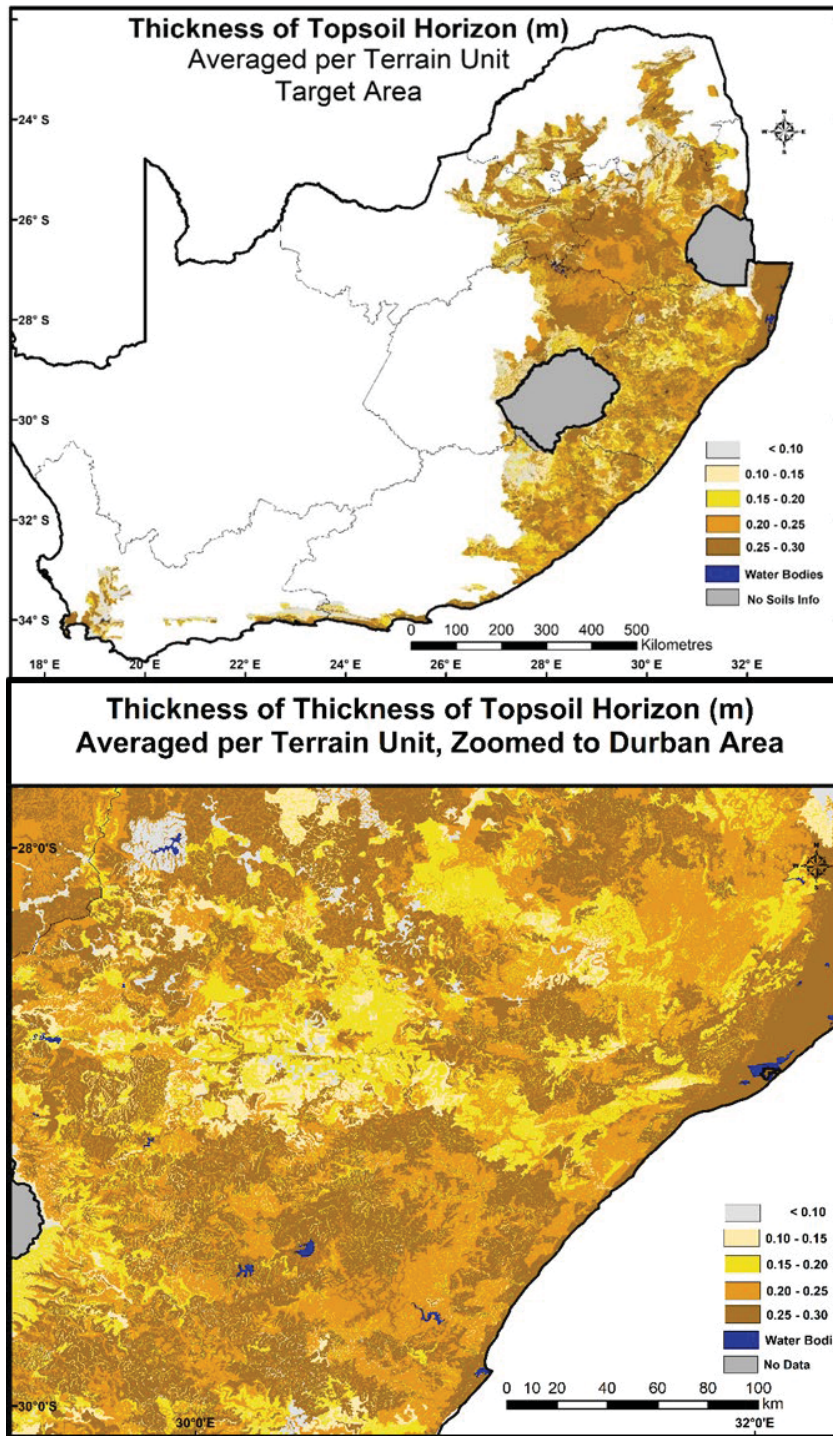


Figure 2-19: Thickness of the topsoil (m) mapped at TU resolution

2.6.3 Thickness of the subsoil

The thickness of the subsoil in the potential forest areas of South Africa ranges from < 0.1 m to > 0.8 m, with most subsoil thicknesses in the range of 0.2 to 0.4 m – not particularly thick (Figure 2-20 top). The zoomed-in map does, however, show that in many areas actually under plantation forestry in the midlands of KwaZulu-Natal at present the subsoils are in the range of 0.3 to 0.5 m thick (Figure 2-20 bottom), but as in the case of topsoils, showing a wide range of thicknesses over short distances.

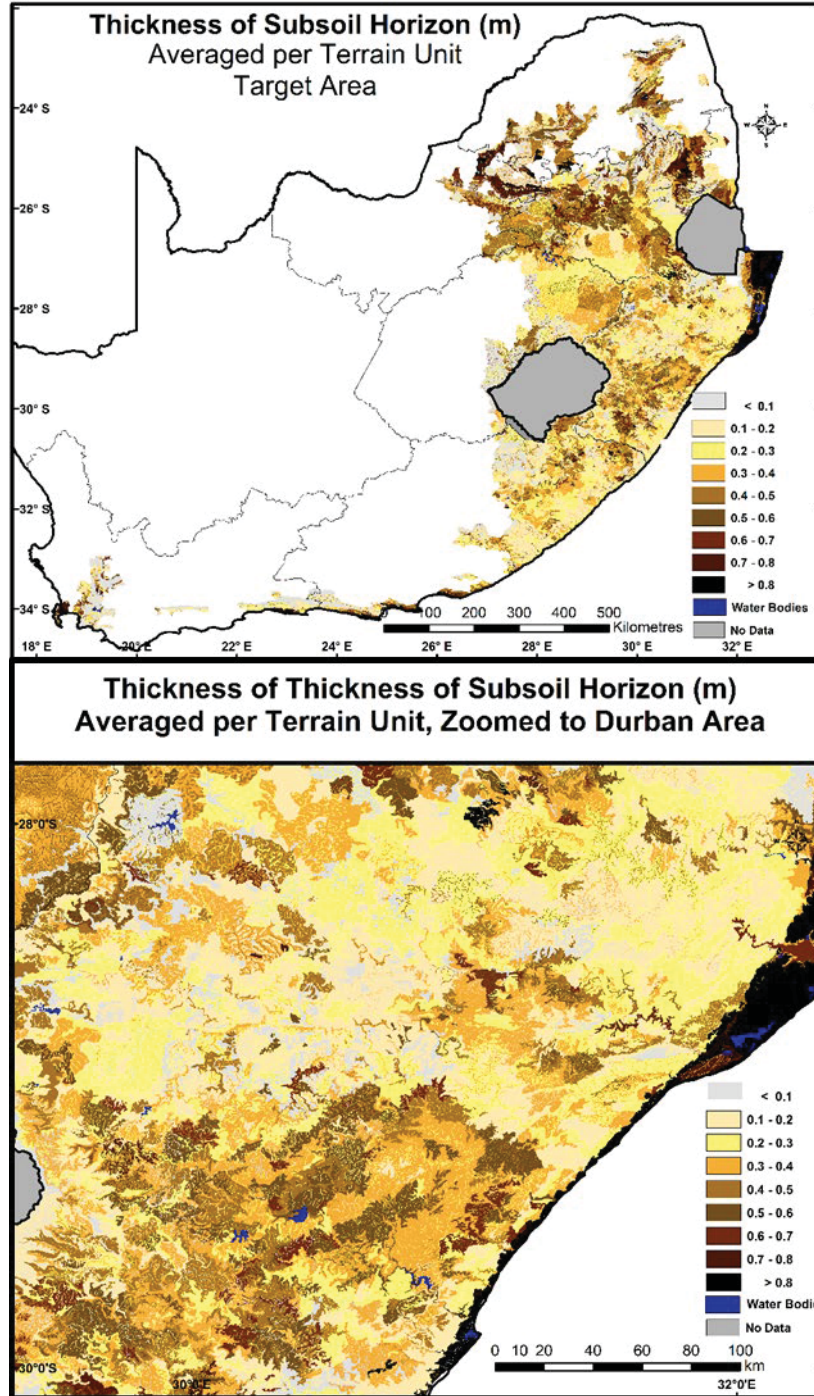


Figure 2-20: Thickness of the subsoil (m) mapped at TU resolution

2.6.4 Thickness of the subsoil (m) mapped at TU resolution

The entire soil profile thickness in the South African areas potentially afforestable from a climatic perspective range from <0.1 m to > 0.8 m (Figure 2-21 top), with many soils where plantation forestry is actually practised in the range of 0.4 to 0.8 m thick, as shown in the zoomed-in map within KwaZulu-Natal in Figure 2-21 (bottom). It may even be argued that plantation forestry utilises among the best agricultural soils in the east of South Africa.

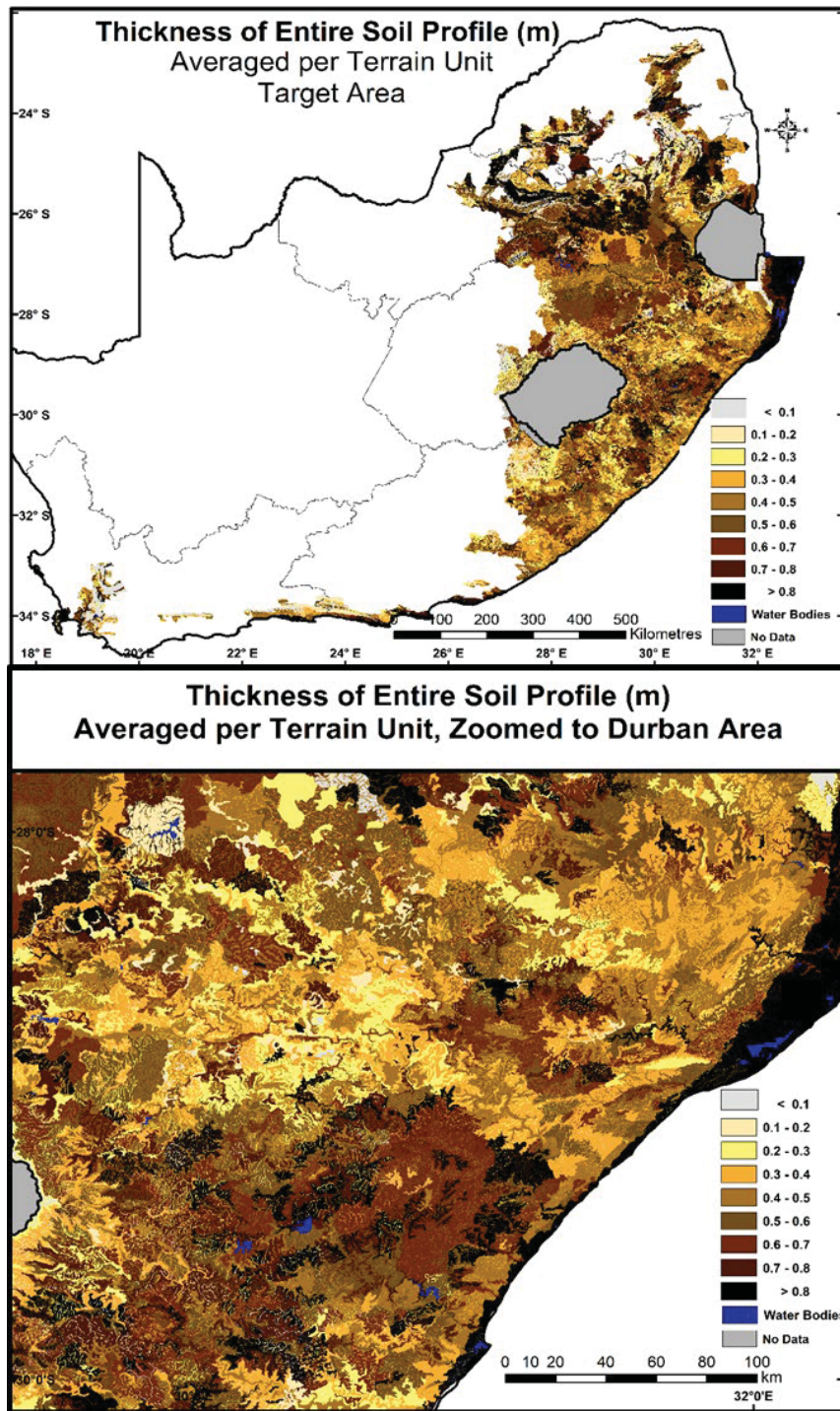


Figure 2-21: Thickness of the entire soil profile (m) mapped at TU resolution

2.6.5 Soil water content in the topsoil at Permanent Wilting Point

Soil water content at the permanent wilting point (PWP) is the lowest amount of water a soil can hold under field conditions, and for the topsoil this is shown in Figure 2-22 (top) to range from < 0.08 m per m thickness of soil to > 0.30 m/m, but mostly from 0.12 to 0.20 m/m in the actual “forestry belt”. As with other soil hydrological parameters, PWP of the topsoil can vary quite markedly over short distances as the zoomed-in map of Figure 2-22 (bottom) shows.

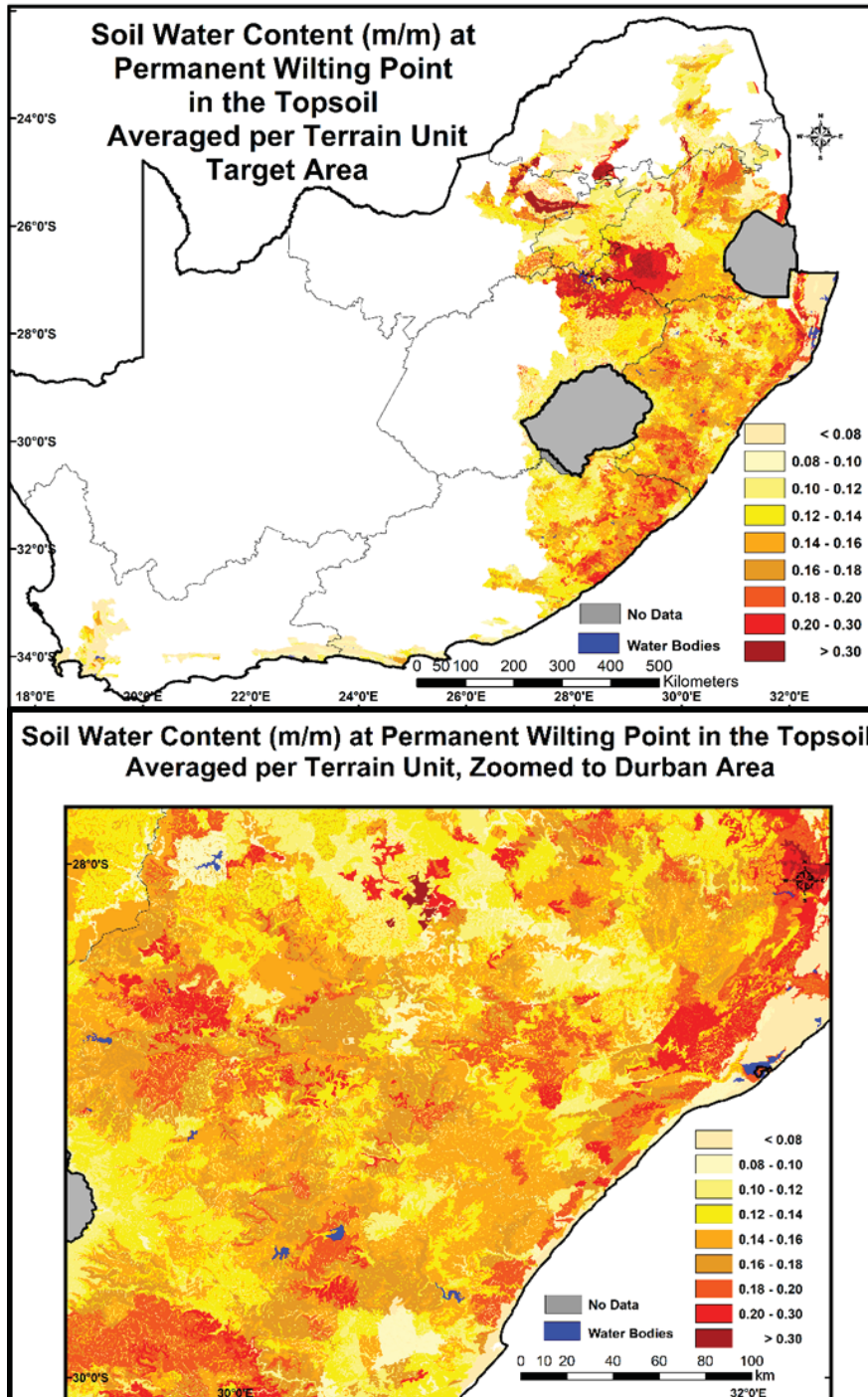


Figure 2-22: Soil water content at permanent wilting point (m/m) of the topsoil mapped at TU resolution

2.6.6 Soil water content in the subsoil at Permanent Wilting Point

As for the topsoil, the PWP of the subsoil in the potential plantation forest areas of South Africa varies from < 0.08 m/m to > 0.30 m/m (Figure 2-23), with a tendency for the subsoil's PWP to be slightly less than that of the topsoil.

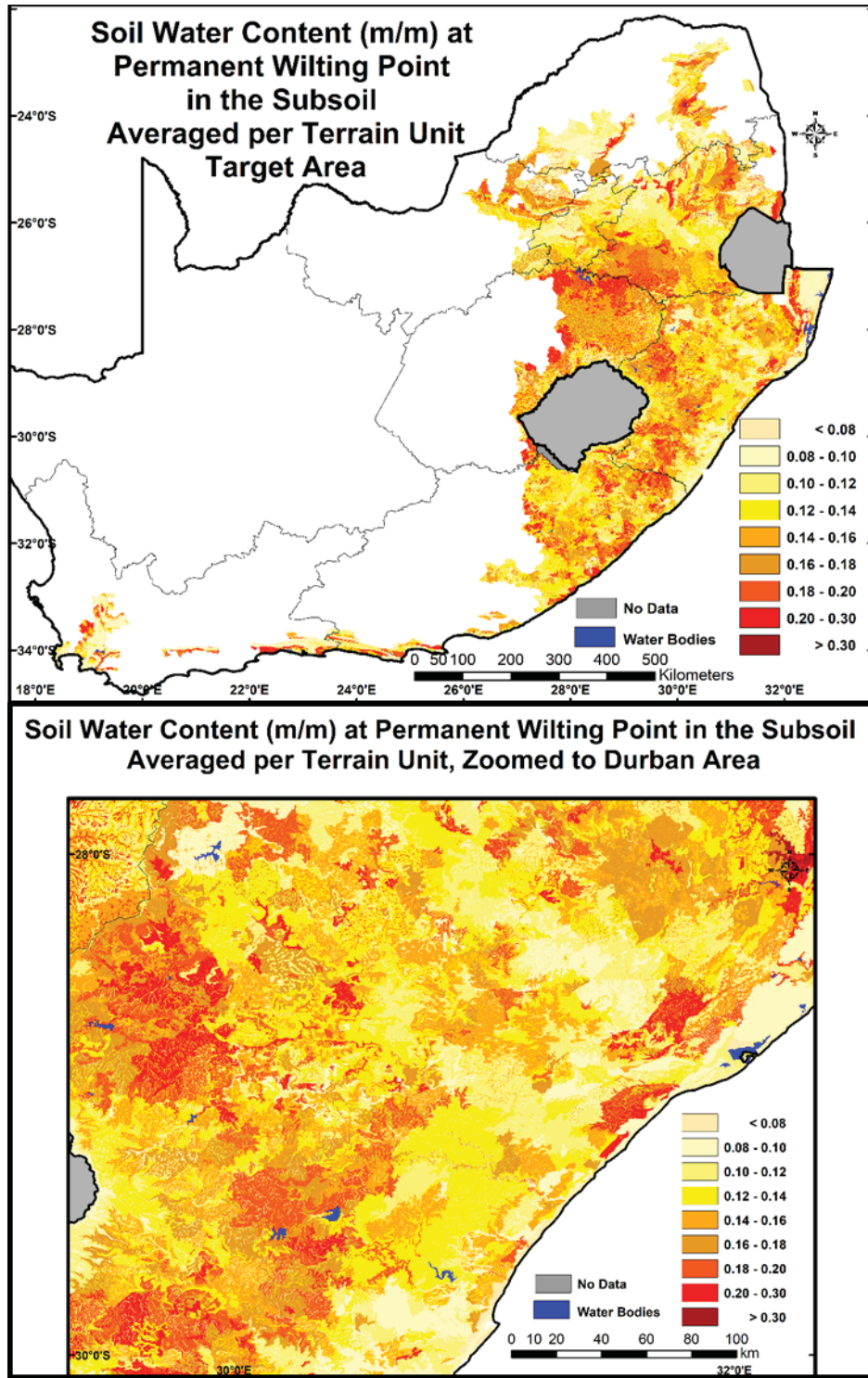


Figure 2-23: Soil water content at permanent wilting point (m/m) of the subsoil mapped at TU resolution

2.6.7 Soil water content in the topsoil at the Drained Upper Limit

As a rule of thumb, soils hold approximately 0.1 m/m more water at DUL than they do at PWP. Patterns of soil water content of the topsoil at the drained upper limit show values in the range of 0.18-0.32 m/m (Figure 2-24) and in the main forestry areas generally between 0.24 and 0.30 m/m, depending on the clay fraction in the soil. The low topsoil DUL values along the east coast are indicative of the sandy soils there.

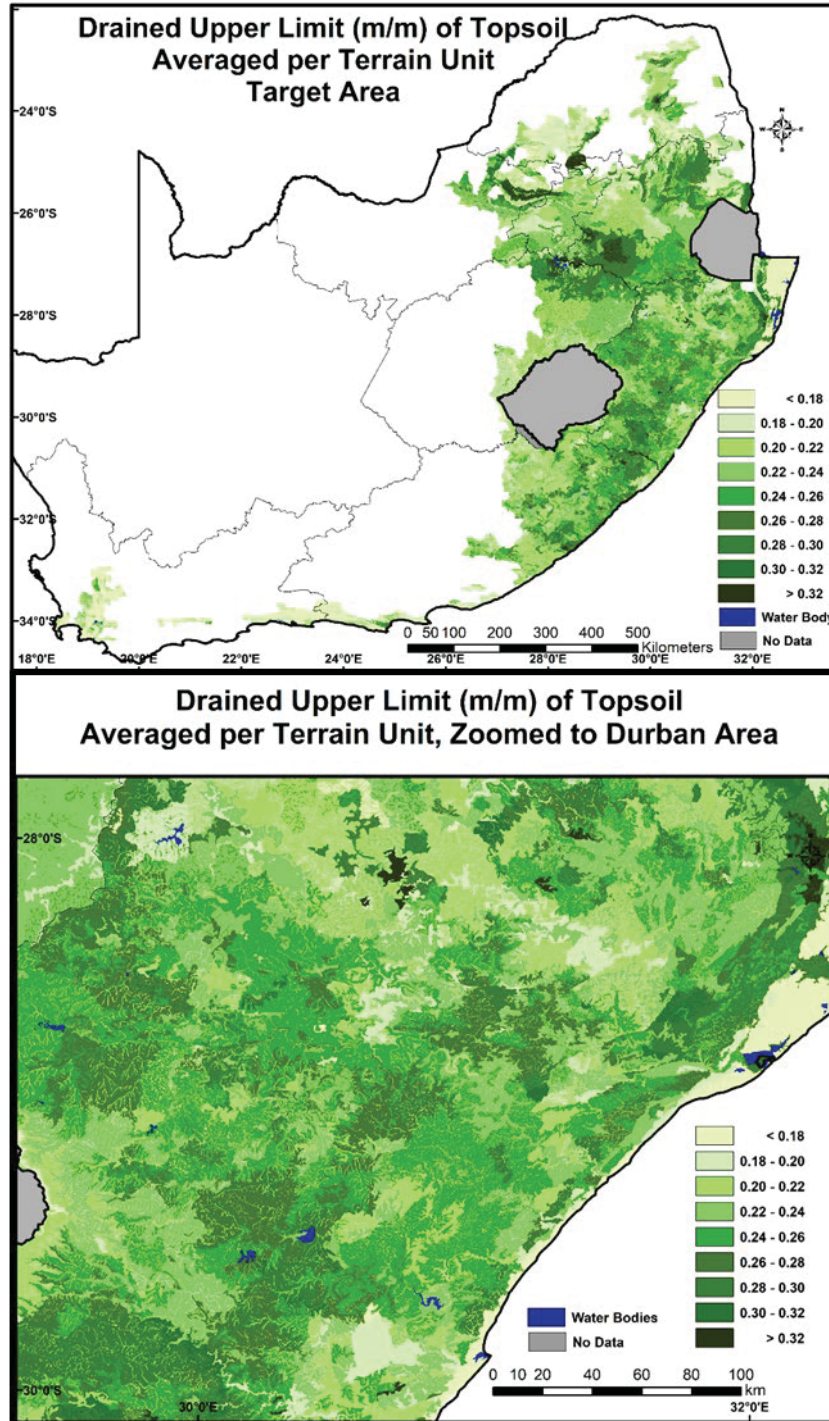


Figure 2-24: Soil water content at drained upper limit (m/m) of the topsoil mapped at TU resolution

2.6.8 Soil water content in the subsoil at the Drained Upper Limit

A slightly more coherent picture emerges in the map of the forestry areas of South Africa of the soil water content of the subsoil at the drained upper limit compared with that of the topsoil (cf. Figure 2-25 vs Figure 2-24). Translocation of clay particles into the subsoil results in higher values in the subsoil by approximately 0.02 m/m (i.e. 20 mm/m), with these increasing by up to 0.06 m/m (60 mm/m) where soils with a high clay fraction predominate, which is mainly in the wetter eastern forest potential regions of South Africa.

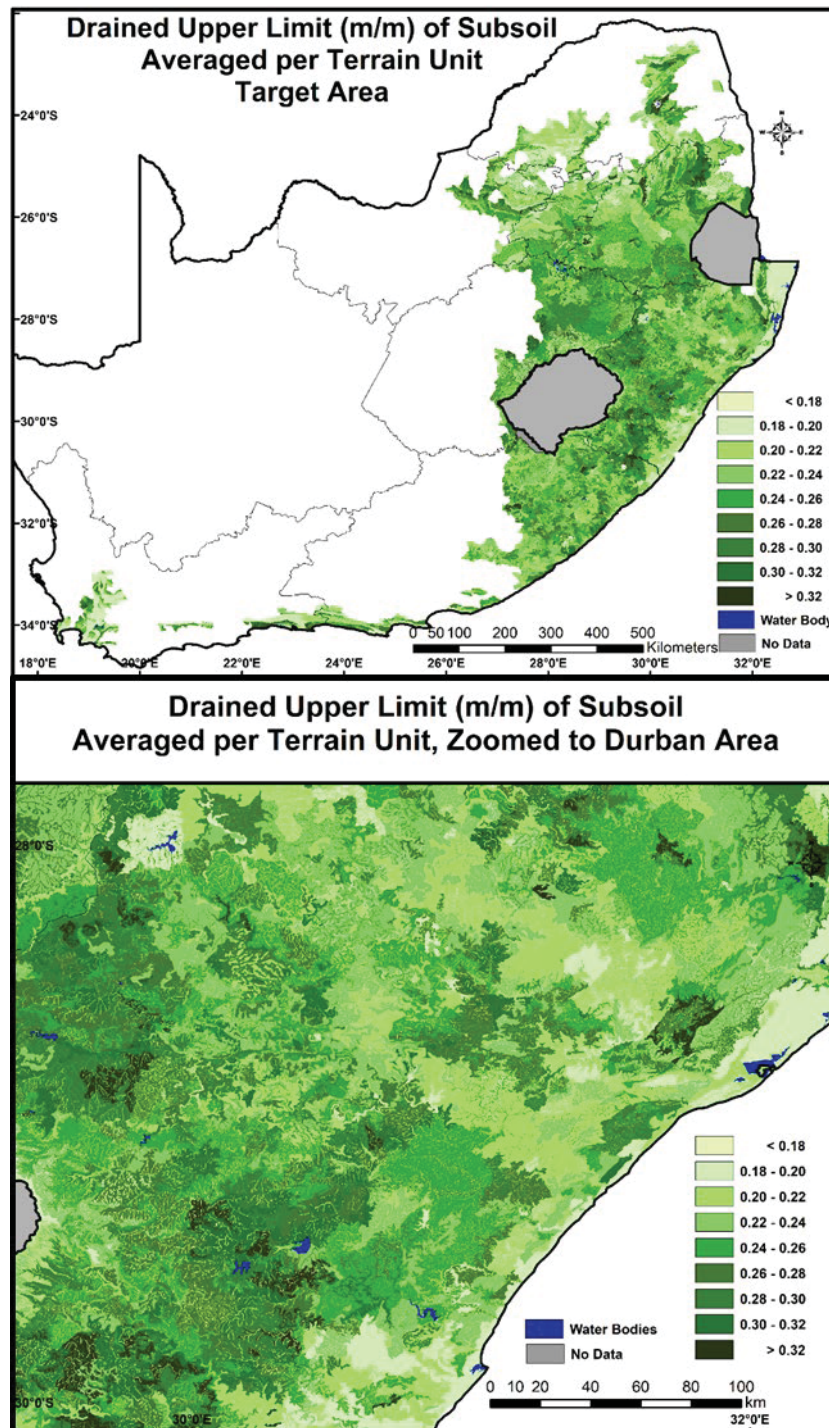


Figure 2-25: Soil water content at drained upper limit (m/m) of the subsoil mapped at TU resolution

2.6.9 Total profile plant available water

With PAW of the total soil profile representing a store of water available, it depends on both soil texture (with different textures having different water holding capacities) and on the total soil profile thickness (i.e. the combined thicknesses of the top- and subsoils), assuming that plant roots are active throughout the entire profile. Values in the forestry areas of South Africa range from < 20 mm to > 100 mm (Figure 2-26), with the higher values reflecting either deep soils (e.g. the east coast of KwaZulu-Natal) or high clay contents. High values of PAW are beneficial to the forest industry as trees develop deep root systems from which water may be extracted.

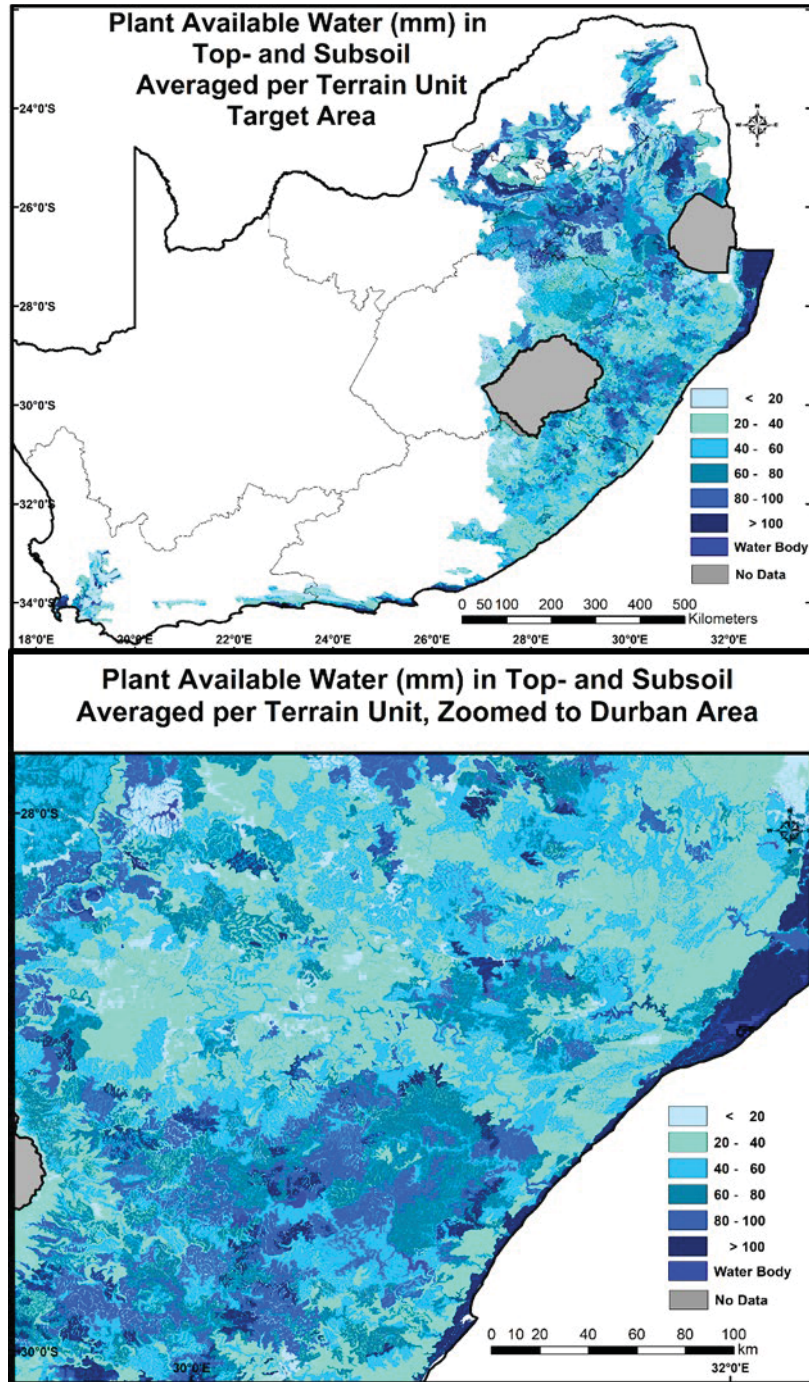


Figure 2-26: Plant available water (mm) in the in the entire soil profile mapped at TU resolution

2.6.10 Soil water content in the topsoil at saturation

Mapped values of soil water content at saturation in the topsoil, when all the soil's pore spaces are filled with water, display a narrow range in the potential plantation forestry areas of South Africa, from < 0.42 to > 0.48 m/m, with most of the higher values in the eastern coastal areas (Figure 2-27).

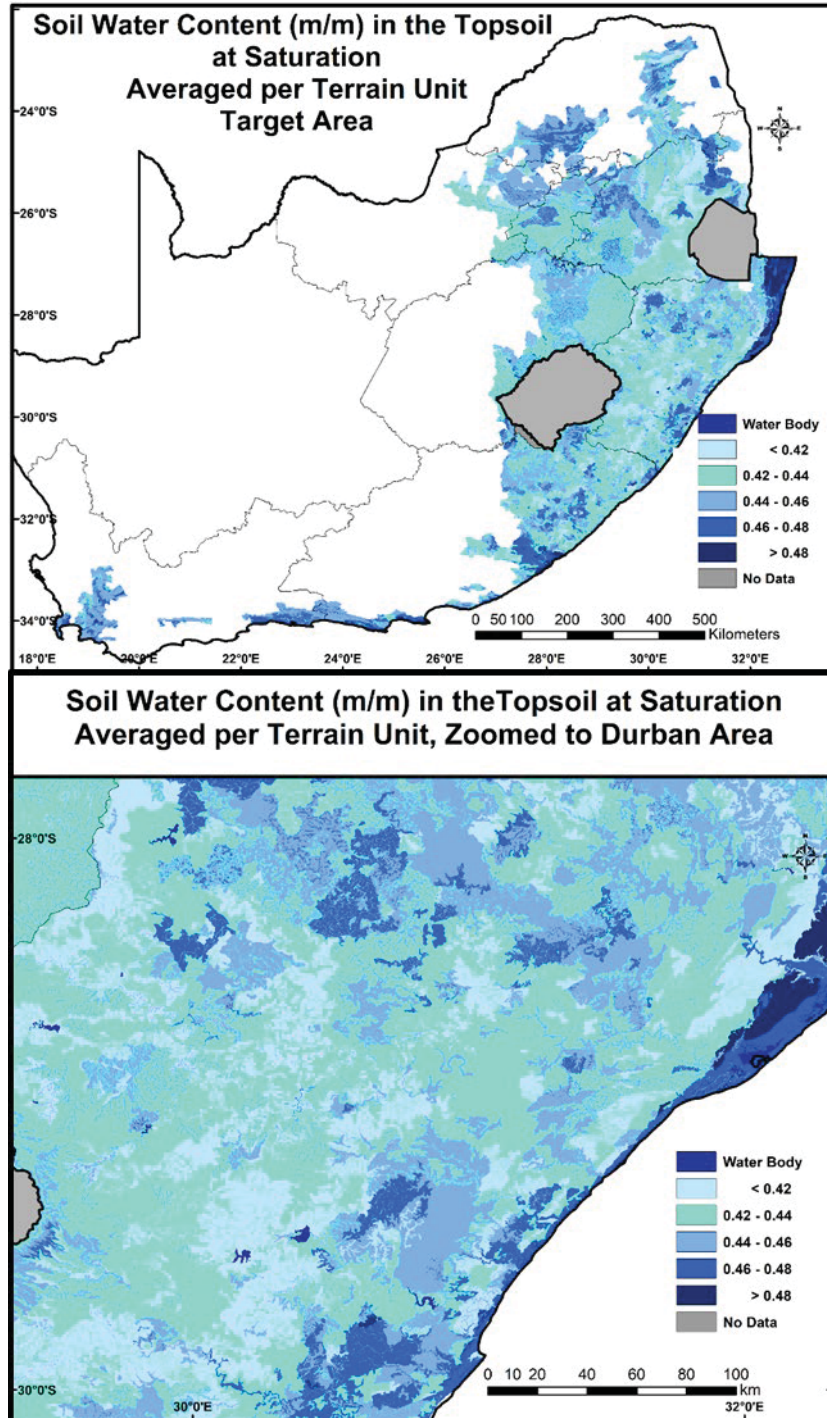


Figure 2-27: Soil water content in the topsoil at saturation (m/m) mapped at TU resolution

2.6.11 Soil water content in the subsoil at saturation

As was the case with soil water content at saturation in the topsoil, for the subsoil a very narrow range of values is evident in the forestry belt of South Africa, with values most commonly in the range of 0.42 to 0.44 m/m (Figure 2-28), the exception again being the deep sandy east coast zone.

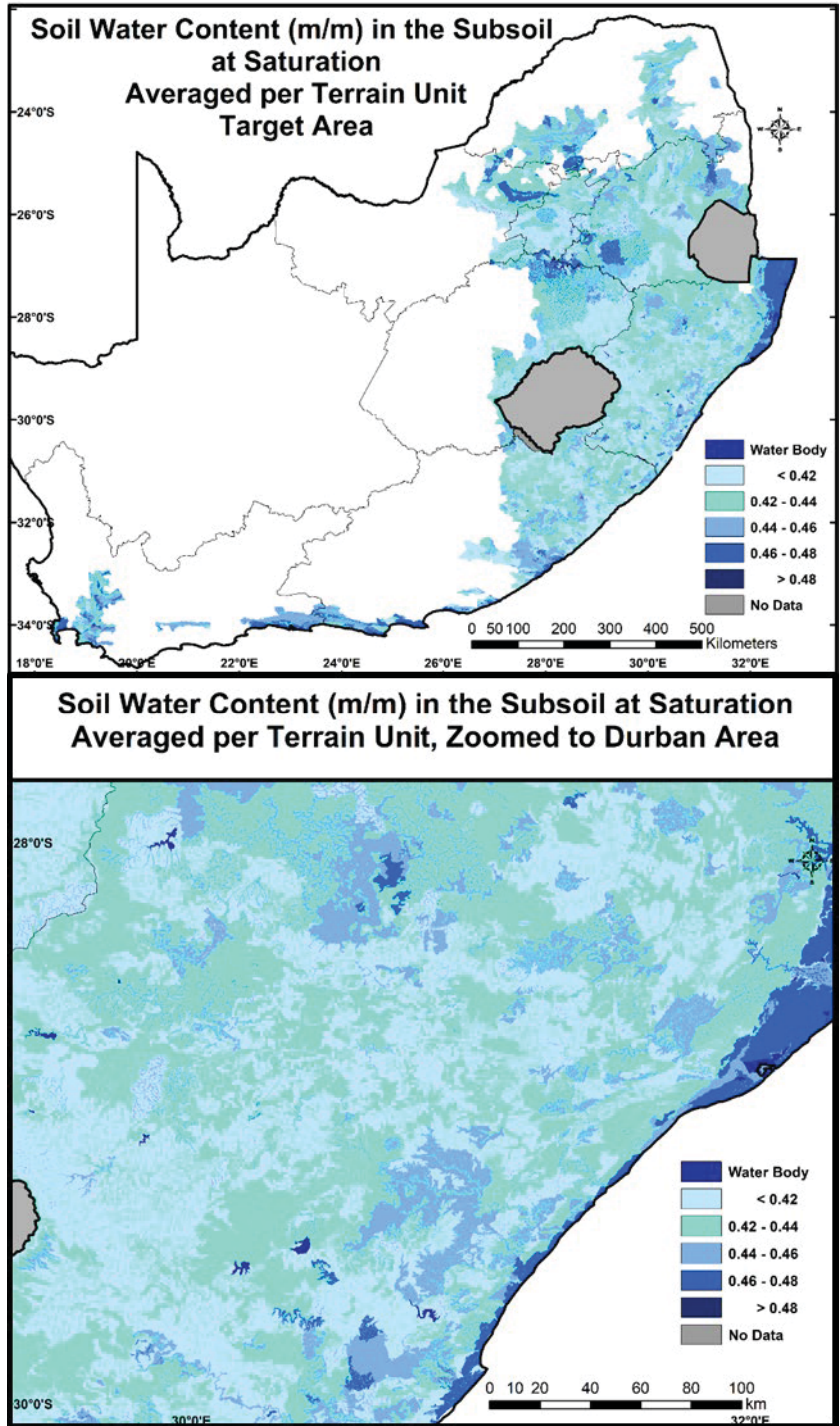


Figure 2-28: Soil water content in the subsoil at saturation (m/m) mapped at TU resolution

2.6.12 Drainage rates from the topsoil to the subsoil

Drainage rates indicate the fraction per day of excess soil water, i.e. soil water content above the drained upper limit, which drains from an upper to a lower soil horizon. Drainage rates from the top- to the subsoil in the climatically suitable plantation forestry areas of South Africa display a wide range from < 0.2 to > 0.8 of the excess soil water draining down per day (Figure 2-29), but mostly in the range of 0.3 to 0.5.

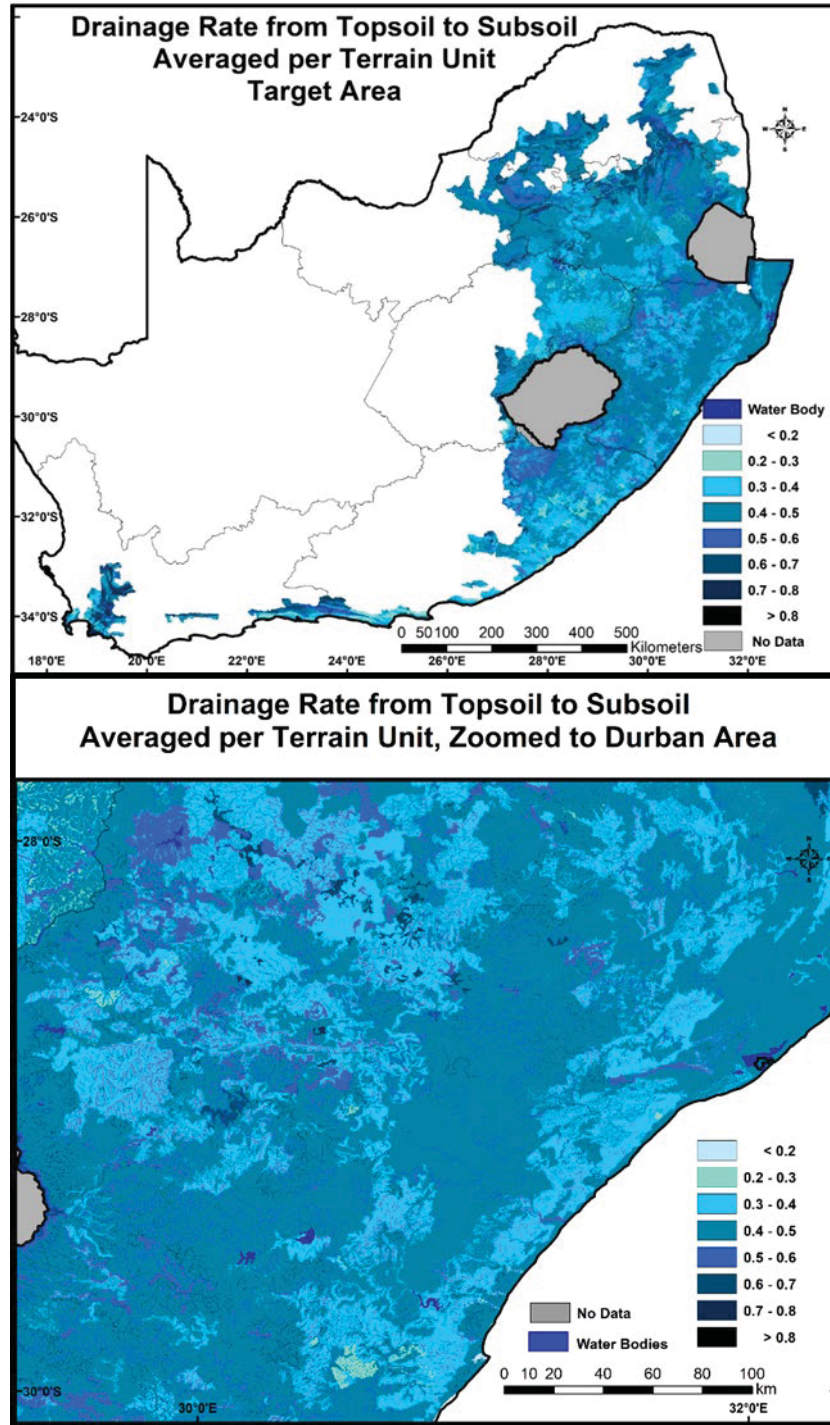


Figure 2-29: Drainage rates (fraction of excess water per day) from the topsoil to the subsoil, mapped at a resolution of terrain units

2.6.13 Drainage rates out of the subsoil

Drainage rates out of the subsoil display much more spatial heterogeneity than those from the top- to the subsoil because they are influenced not only by soil texture, but also by a range of impeding layers below the active root zone of a soil. The relatively high drainage rates along the northeastern coastline of KwaZulu-Natal (> 0.60/day; Figure 2-30), are indicative of the sandy nature of the soil there while similarly the Mpumalanga-Free State axis of low drainage rate values (0.20-0.30/day) reflect the relatively high clay contents of soils there.

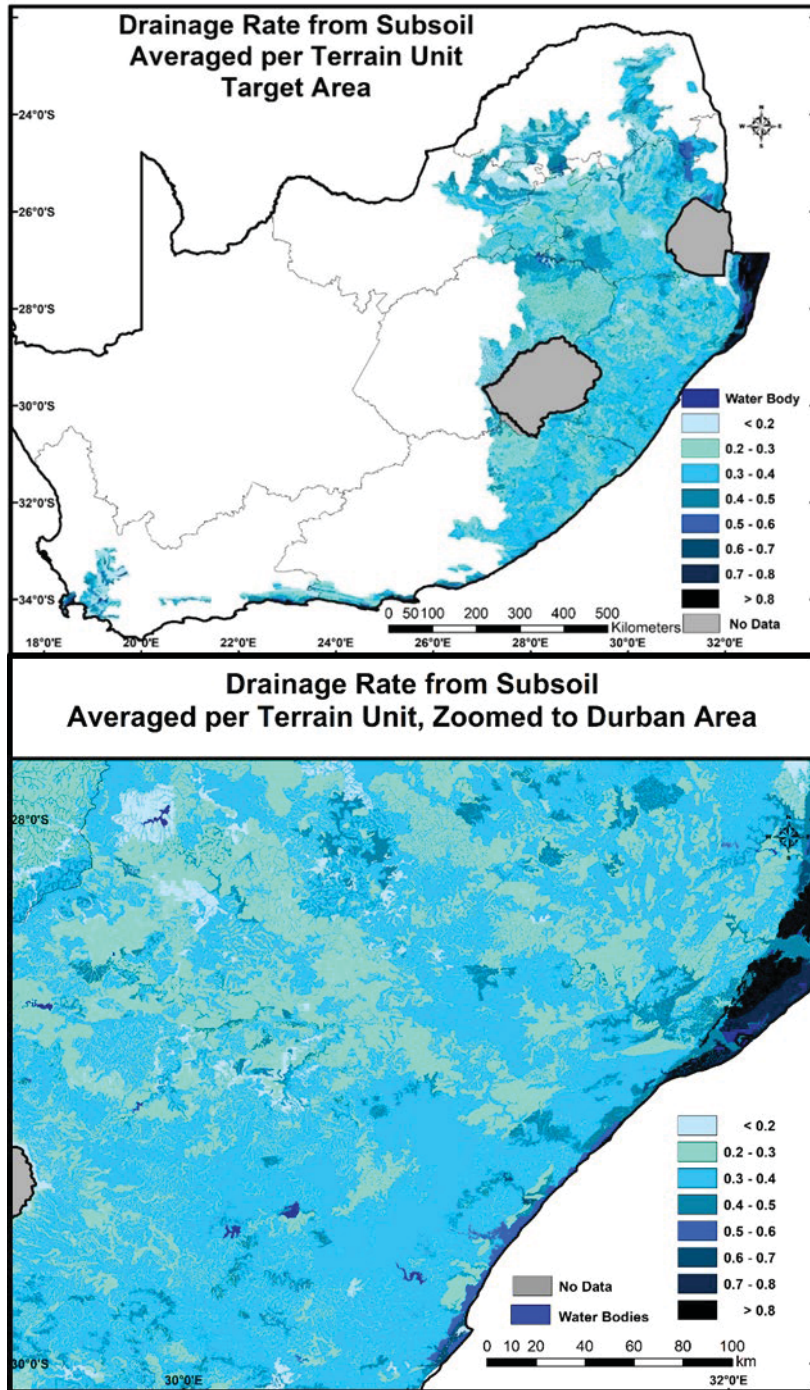


Figure 2-30: Drainage rates (fraction of excess water per day) out of the subsoil, mapped at a resolution of terrain units

2.7 Concluding Thoughts

There is significant spatial information gain when using TU level information compared with the use of Land Type information, which has aggregated and, as such, has area-averaged much the detail available on the soils of South Africa. This is illustrated in Figure 2-31, which shows the spatial detail of the thickness of the topsoil horizon mapped from TUs (left map) versus that mapped from Land Type information (right map), using the identical thickness classes in the legend.

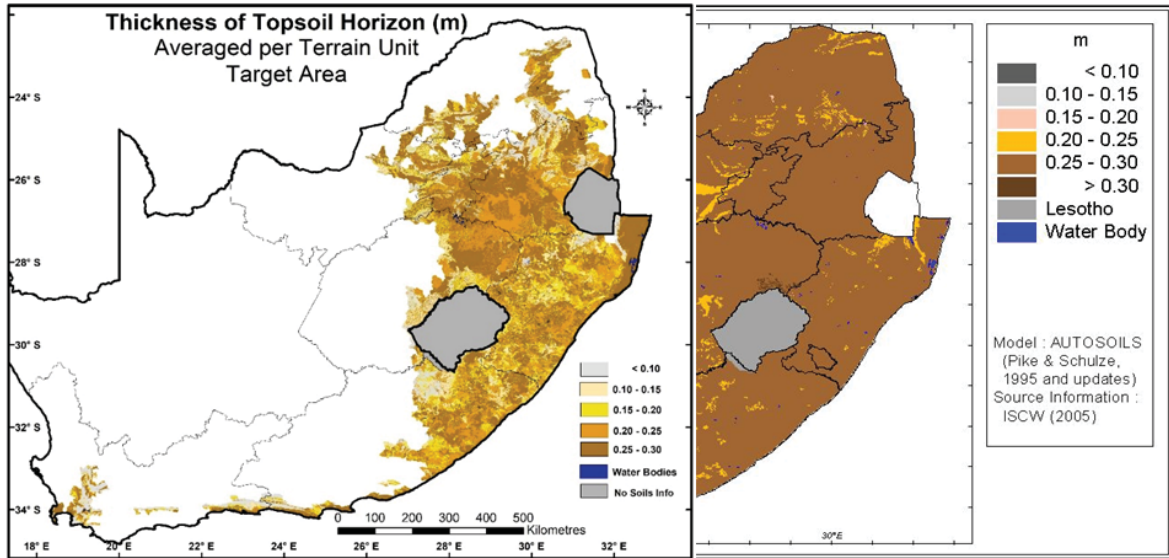


Figure 2-31: Example of the spatial information gain when utilising terrain unit information (left) compared with detail when using area-averaged Land Type information (right map: Schulze and Horan, 2008)

The gain in spatial information becomes even more evident when the area blocked off in white in the already zoomed in map of the thickness of the entire soil profile of Figure 2-32 (left) is Figure 2-31 enlarged even more to that of the right-hand map of Figure 2-32. Soil hydrological characteristics mapped at the spatial resolution of terrain units, as shown in this document, have important potential applications which go beyond those of the forest industry and will be utilised as the soils data in the Quinary catchments database.

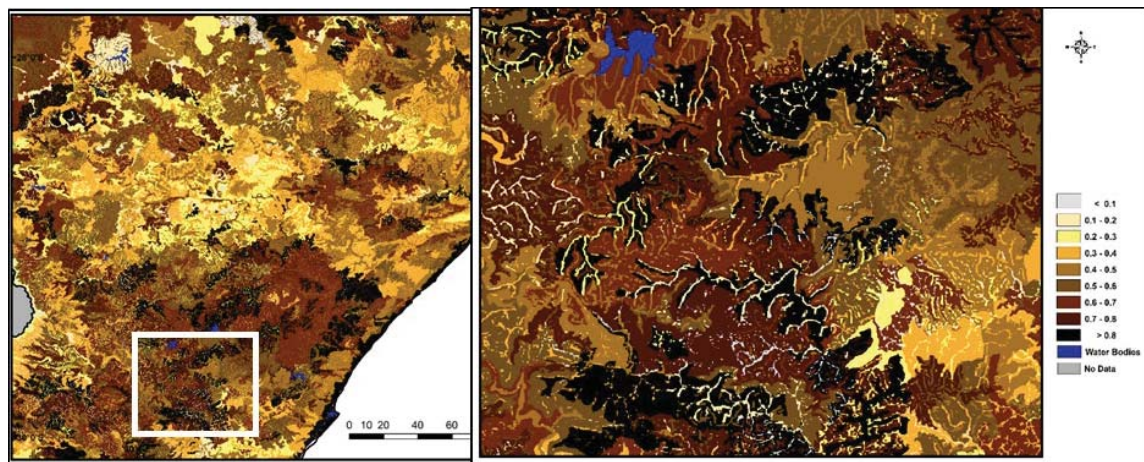


Figure 2-32: Further example of spatial information gain when utilising spatial terrain unit soils information, from (left) a region/provincial to (right) a local perspective

CHAPTER 3. INVESTIGATION OF THE POTENTIAL USE OF THE ROOT ZONE STORAGE CONCEPT

R. Horan¹ and M.L. Toucher^{1,2}

¹ Centre for Water Resources Research, University of KwaZulu-Natal, Pietermaritzburg

² South African Environmental Observation Network

3.1 Introduction

The improved soils information presented in Chapter 2 was used in quinary catchments database and the refined SFRA runs produced in this project. However, to supplement and potentially advance knowledge, a further question related to the soils information was addressed during the course of the project. The question is:

“Can the root zone storage concept be used to determine the root zone storage capacity and thus the soil depth under commercial tree species?”

Hydrological modelling, in particular the ACRU model, has become the accepted method of assessing the impact of commercial afforestation on water resources (Jewitt and Schulze, 1999). However, hydrological models require detailed catchment scale soils data to generate satisfactory results as soils play a critical role in the regulation and generation of catchment hydrological responses (Schulze and Pike, 2004). As no universal soils map for South Africa exists, as described in Chapter 2, the Land Type maps are used with hydrological parameters assigned to the TU for the purpose of hydrological modelling. A further problem, however, is the lack of detailed root depth estimates and understanding of their establishment over time to input into hydrological models. Typically, coarsely averaged values from literature are used along with the assumption that porosity drives the root zone storage capacity.

A possible alternative to intensive soils mapping is the use or requiring detailed rooting information, is the incorporation of the root zone storage concept into hydrological modelling. Successful studies have been performed in Asia, Europe and the United States of America using this concept but not as yet in South African conditions. For example, Nijzink et al. (2016), detected the change in root zone storage with deforestation but little work has been performed on the root zone storage capacity under afforestation. The utilization of the root zone storage capacity under commercial afforestation could potentially be useful in the improvement of modelling for SFRA purposes.

3.2 Literature review of the root zone storage concept

The hydrological regime and the partitioning of water fluxes within a catchment is altered by the continuous adaption of vegetation to change in the biosphere (Black, 1997; Wagener et al., 2007; Nijzink et al., 2016). Vegetation survives by extracting plant available water between the field capacity and wilting point of their immediate soil (Vietz, 1972). Within their sphere of influence, vegetative roots create a moisture storage volume known as the root-zone storage capacity (Moore and Heilman, 2011). The root-zone storage capacity exists in the unsaturated soil and is a vital component of the hydrological regime (Rodriguez-Iturbe et al., 2007 and Nijzink et al., 2016). The role of the soils in the hydrological cycle and how they are

represented in ACRU is, to an extent, covered in Chapter 2. Therefore, the uncertainties introduced in modelling due to below ground parameter estimation are reviewed prior to the root zone storage concept.

3.2.1 Increased modelling uncertainty due to below ground parameter estimation and process parameterisation

The root profile distribution acts as the primary control of water uptake through the soil horizons. In current modelling methods, the root depth and root vertical profile, are pivotal in determining the movement of water through the soil-vegetation-atmosphere continuum (Gu et al., 2007). The depth and structure of the root system determines the maximum amount of soil water that can potentially be taken up by the plant xylem and transpired by the vegetation (Tron et al., 2015). The ability to uptake water is critically important during the dry season and prolonged drought (Lobet et al., 2014). Root growth and the process of root water uptake is spatially and temporally dynamic and reacts to the availability of water within the soil profile (Bleby et al., 2010; Jung and McCouch, 2013).

Models considering below-ground vegetation began to emerge in the early 1970s. These models were based on mathematical representations of root depth distribution in soil. Over the last two decades, more complex architectural models have been developed and the use of more computer-intensive methods have been utilised (Dupuy et al., 2010). Most catchment-scale models are originally developed to address stationary scenarios and are not well equipped to deal with predicting the variance in hydrological parameters due to change (Nijzink et al., 2016). Although modelling studies have been performed with the attempt to incorporate temporal change, most or all of the changes to the hydrological parameters have been assumed or estimated (Legesse et al., 2003; Mahe et al., 2005; Fenicia et al., 2009). More systematic approaches have only recently gained momentum, with the incorporation of temporal change into the model formulation (Nijzink et al., 2016; Zhang et al., 2016).

In most hydrological models, two plants of the same species growing in two different soils would be considered to have the same average rooting depth. This would subsequently mean that the plants have access to different volumes of water because of the difference in the porosity of the two soils. Research by Milly (1994); Schymanski et al. (2008) and Troch et al. (2009), has shown that this is not the case and that plants design their root systems to access similar volumes of water and limit unnecessary carbon investment in root growth. Recently this consideration has been supported by De Boer-Euser et al. (2016), who showed that in most environments the water balance-derived estimates for the root-zone storage capacity are as accurate as the soil-derived estimates and concluded that the maximum rooting depth controls the transpiration of the plants and the soil drainage.

Soil and rooting depth are key parameters in hydrological and land-surface modelling (Fan et al., 2017). The global distribution of soil and rooting depths are largely unknown due to the difficulties in measurement and the high variance between soil type, plant species and combinations thereof within modelling units (Yang et al., 2016). A common trait amongst many plant species is a deep complex rooting system. The rooting systems are essential in the determination of the soil pedogenesis, soil water partitioning and soil chemistry processes (Pierret et al., 2016). Current research efforts are focussed towards shallow root systems whilst the study of deep root systems remain disproportionate, due to challenging procedures to observe and measure deep systems.

The rooting depth of a plant directly affects their resilience to environmental stresses (Maeght et al., 2013). Deep roots enhance many functions such as bedrock weathering, determination of the soil water and regulation of chemical cycles. However, little is known about the limits to which roots grow and the factors that determine this limit (Beerling and Berner, 2005). A study by Fan et al. (2017), showed that in well-

drained uplands, the rooting depth followed the infiltration depth to the capillary fringe. In waterlogged lowlands, the roots remained shallow to avoid anaerobic respiration conditions. These results suggest that the variation in rooting depths observed under the same climate for the same species is due to different topographic positions.

Large portions of continental landmasses are characterised by shallow soils overlying weathered bedrock and cemented soil layers (Schwinning, 2010; Zhao et al., 2017). Studies show that the majority of the soils are deeper than 1.2 metres and many plants grow beyond this depth. However, the depth of 1.2 metres is often considered as the maximum soil depth in literature and hydrological modelling (Richter and Markewitz, 1995; FAO, 2006). The drivers of deep root growth remain poorly understood (Maeght et al., 2013). Deep rooting could be a more prevalent and a more important trait due to the overall distribution of root biomass through the deeper layers (da Silva et al., 2011). The misrepresentation of soil and root depths in hydrological models causes uncertainty in hydrological prediction and land-surface modelling (Schwinning, 2010 and Vrettas and Fung, 2017). Schwinning (2010) suggested that further research is necessary to improve the characterization of dynamic water recharge and depletion throughout the root-zone.

3.2.2 Background and Introduction to the Root Zone Storage capacity concept

Root-zone storage capacity can be considered as a volume of water per unit area within the range of plant roots and available for transpiration (Zhu et al., 2008; De Boer-Euser et al., 2016; Mao and Liu, 2019). Vegetation survives by extracting plant available water between the field capacity and wilting point of their immediate soil (Coppin and Richards, 1990; Irmak and Djaman, 2016). Within their sphere of influence, vegetative roots create a moisture storage volume known as the root-zone storage capacity (Schenk and Jackson, 2002). It is a vital component of the hydrological regime (Nijzink et al., 2016).

Vegetation has a significant influence on the hydrological cycle (Bates, 1921; Zegre, 2008). The vegetative roots structurally adapt to establish an equilibrium resulting in the avoidance of water shortage within the ecosystem (Eagleson, 1982). Research suggests that root systems are designed for the most efficient extraction of water from the soil to meet the transpiration demands of the canopy while minimising the root growth necessary to sustain these demands (Milly, 1994). Studies, for example by Reynolds et al. (2000); Laio et al. (2001); Schenk and Jackson (2002), show that climate has a strong influence on the hydrologically active root-zone, whilst periods of drought and flood are critical situations that affect the establishment of the root-zone.

The root-zone storage capacity currently cannot be physically measured in the field (Gao et al., 2014). Within hydrological models, if the root-zone is considered, it is normally treated as a calibration parameter or a range of soil parameters estimated on assumed knowledge about the in-situ soil characteristics and estimates of the rooting depth (Liu et al., 2006). Generally, this parameter is conceptually considered to change with season but not over the growth cycle of the plant (Figure 3-1). This does not reflect the real-world processes accurately and could be a potential source of error when modelling non-stationary conditions (Blasone et al., 2008). Models account for the seasonal change in effective rooting depth and the colonisation of each horizon but do not account for the change in the root collar diameter or volume of roots (Figure 3-1).

Recently there have been an increased number of studies focussed on determining the root-zone storage capacity. Summarising available literature, six methods of estimating the root-zone storage capacity have been identified for application in hydrological modelling.

The first of these approaches is the field observation approach (Wang-Erlandsson, 2014). This approach estimates the rooting depth using the rooting depth measurements taken by removing vegetation from the soil profile and measuring the length of the longest rooting structure (Zeng, 2001). This method is advantageous as it relies on actual observations and measurements of vertical root distributions, but is handicapped by data scarcity, location bias, vegetation and soil heterogeneity and the assumption that water uptake is from a set portion of the soil profile.

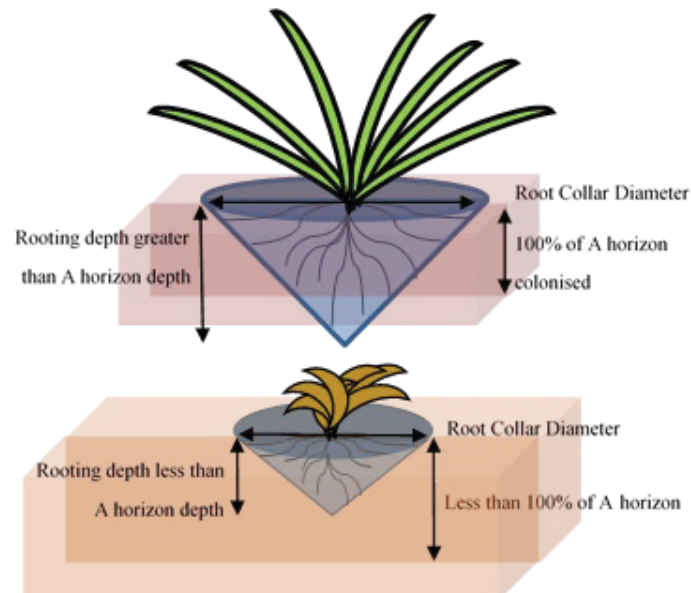


Figure 3-1: A basic conceptualisation of the root-zone storage within common hydrological models in wet and dry periods under grassland conditions

The Lookup Table approach, where mean biome rooting depths and soil texture are determined from literature (Wang-Erlandsson et al., 2014), is favoured in hydrological modelling to parameterise the root-zone storage capacity. Although this approach is useful in land-use change studies, it has a significant downfall in that it assumes that the root-zone storage is solely based on vegetation and soil type, with no climatic consideration other than those indirectly expressed through vegetation and soil characteristics (Collins and Bras, 2007; Wang-Erlandsson et al., 2014).

Two approaches that have proven valuable are the Optimisation approach and the inverse modelling approach. The Optimisation approach predicts the rooting depth based on existing soil, vegetation and climate variables, including but not limited to soil hydraulic properties and root distribution. This method can incorporate complex algorithms, complicated eco-hydrological modelling and analytical modelling (Collins and Bras, 2007). The Inverse Modelling approach makes use of satellite data to estimate the rooting depth using either absorbed photosynthetically active radiation or total terrestrial evaporation along with different rooting depth parameterisations (Kleidon, 2004). This approach is highly dependent on ground-truthed soil information and accurate evaporation estimations. The value of both with further development could be enhanced.

The Calibration approach, a commonly used approach, is whereby a hydrological model is calibrated on the root-zone storage capacity using records of precipitation, runoff and evaporation and for use only at a catchment scale. However, these parameters are strictly tied to the model used and not transferable between models as they compensate for uncertainties in the model structure. Further, the calibration

becomes more uncertain when only discharge data is available as the parameterisation absorbs the uncertainty in data (Pappenberger and Beven, 2006). The approach of interest in this study is the water balance approach, and this is reviewed in more detail.

3.2.3 The Water Balance approach

The root-zone storage capacity is strongly related to climate variables utilised in the estimation (Kleidon and Heimann, 1998; Gentile et al., 2012; Gimbel et al., 2015), thus as an alternative approach to parameterization of the root-zone storage capacity and to allow for temporal variability, a water balance approach is considered (De Boer-Euser et al., 2016; Gao et al., 2014; Wang-Erlandsson et al., 2016, Nijzink et al., 2016). This approach is climate-driven and thus incorporates climatic and vegetation conditions in a dynamic hydrological parameter (De Boer-Euser et al., 2019). It should be noted that this method estimates a catchment representative root-zone storage capacity, which reflects the root-zone storage capacity for all the combinations of vegetation that exist in a catchment (De Boer-Euser et al., 2019). The currently published studies are discussed in chronological order below.

The first published paper was that of Zhu et al. (2008) who performed one of the first root-zone storage studies. This study considered the temporal variation of the root-zone storage capacity under natural undershrub in China. The root-zone storage capacity was modelled using a two-layer soil water balance model. This model comprised of a shallow surface layer and a root-zone layer. Model results from this study were found to simulate the observed data sufficiently well.

Following the work of Zhu et al. (2008), at the Centre for Ecology and Hydrology, a simple root-zone storage routine was developed and integrated into the in-house Distributed Catchment Scale Model (DiCaSM). The model utilises a routine based on a root-zone water balance to determine the storage. Precipitation, streamflow and interception are used to calculate the infiltration into the root-zone. The total evaporation and recharge are calculated as water fluxes out of the root-zone and the remaining water is considered to be storage. Although there are no studies that have specifically isolated the root-zone storage routine, there are many studies that have used the DiCaSM model successfully as a whole entity, these include D'Agostino et al. (2010), Montenegro and Ragab (2010), Montenegro and Ragab (2012), Ragab (2012) and Afzal et al. (2018).

Wang-Erlandsson et al. (2014) calculated the root-zone storage capacity by estimating the soil moisture deficit constructed from a time series of water inflow and outflow through the root-zone storage system (Figure 3-2). A simple method using remotely sensed data, which can be adapted for in-situ observed data, was developed for the estimation of the root-zone storage capacity. It is assumed that the vegetation optimises the root-zone storage capacity and does not require any vegetation and soils data. The method is additionally model-independent. The advantages of the Wang-Erlandsson et al. (2014) technique over field-based studies is that it can be utilised with remotely sensed data. Remotely sensed data can reduce the dependence on human and financial capital, limit the need for intrusive measuring techniques, compliment modelling methods that make use of indirect observation data and contribute to the understanding of areas with limited direct observational studies. The Wang-Erlandsson et al. (2014) technique allows for the inclusion of irrigation and additional variables if they are available to adjust the root-zone storage.

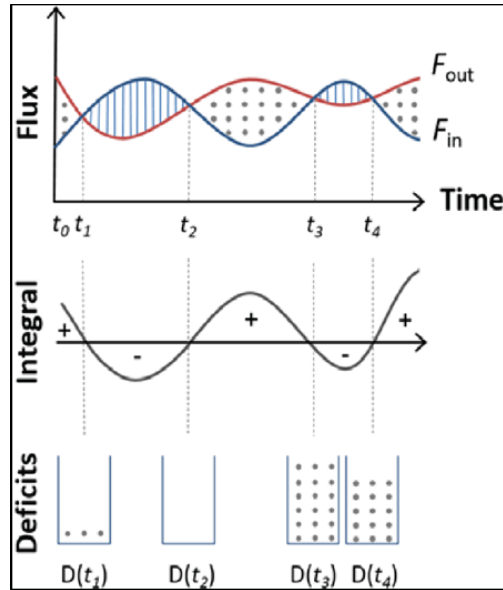


Figure 3-2: The soil moisture deficit constructed from a time series of water inflow and outflow through the root-zone storage system (Wang Erlandsson et al, 2014)

Building on the work of Wang-Erlandsson et al. (2014), Gao et al. (2014) tested a theory of treating the root-zone as a reservoir. The mass curve technique, an engineering method for reservoir design, was applied to over 300 catchments and was used to estimate catchment-scale root-zone storage capacity from effective rainfall and plant transpiration. It was found that the mass curve technique derived root-zone storage capacities reflected the model-derived estimates well. The estimates of root-zone storage capacity derived by Gao et al. (2014) could be used to constrain hydrological models. Furthermore, they concluded that root systems are controlled by climate and that ecosystems can potentially dynamically design their root systems to combat periods of drought.

Zhao et al. (2016) improved the mass curve technique for the root-zone of Gao et al. (2014) by incorporating a snowmelt module. Zhao et al. (2016) found the root-zone storage capacity estimates to vary greatly with changes in climatic conditions and soil characteristics whilst being most sensitive to changes in the transpiration of ecosystems. The adjusted mass curve technique proved to be a simple but effective tool for the root-zone storage capacity estimation in different climatic regions of China, however, the inclusion of additional climatic regions will improve knowledge on the variability of the storage capacity.

De Boer-Euser et al. (2016) undertook a study to investigate the nature of vegetative adaption to the root-zone storage capacity, especially under drought conditions. Precipitation and evaporative demand data were used in this methodology. The climate-based calculations were compared with a proportion of soil water measurements and modelled data within 32 catchments in New Zealand. It was found that the range of values between the catchments was greater for the climate-based calculations compared with those of the soil derived data in humid climates but was similar in arid climates. Using a model, it was shown that the climate-derived root-zone storage capacity better reproduced the hydrological regime signatures for humid catchments. However, in arid climates, the model produced similar results. De Boer-Euser et al. (2016) concluded that the climate-based root-zone storage capacity is a valuable addition in the process of understanding the root-zone storage capacity and reducing hydrological model uncertainty.

Nijzink et al. (2016) introduced a catchment-scale root-zone storage capacity estimation method using climatic data to reproduce the temporal evolution of root-zone storage capacity over the growth cycles and

multiple seasons. This method considers the maximum deficit between daily precipitation and transpiration as a proxy for root-zone storage capacity. The calculated values from this method were validated against model results from four different hydrological models over a two-year period. The calculated water-balance root-zone storage capacities were found to be similar to the values obtained from the hydrological models and proved a promising method to reflect the time-dynamic behaviour of a catchment.

De Boer-Euser et al. (2019) extended on the De Boer-Euser et al. (2016) study using a water balance-based method to estimate the root-zone storage capacity in Boreal forests. The study investigated the relationship between catchment and vegetation characteristics and the root-zone storage capacity. The intention was to further understand the physical meaning of the root-zone storage capacity parameter. A climate-derived root-zone storage capacity parameter was compared with climate variables and vegetation characteristics. It was concluded that the dynamic root-zone storage capacity gives additional information about the hydrological characteristics as of a catchment and represents climatic and vegetation conditions in a single dynamic hydrological parameter. This could be valuable in the assessment of changing conditions.

Lastly, Mao and Liu (2019) developed a hydrological model to simulate the root-zone storage capacity on a global scale. They claimed that most root-zone storage studies are focussed on the soil water at a certain depth rather than the water stored within the rooting system. The root-zone storage capacity was integrated into a well-validated lumped model to reflect the natural spatial heterogeneity of the plant rooting system across the globe. The model mimicked the observed root-zone storage capacity in most regions well, however, the regions of high latitudes were not considered and thus results from these regions cannot be justified.

3.2.4 Summary

A possible alternative to intensive soils mapping is the use or incorporation of the root-zone storage concept into hydrological modelling. This concept will overcome the problems associated with the lack of or inaccurate rooting and soil depths and the uncertainty of vegetative growth curves. Successful studies have been performed internationally using this concept but not as yet in South African conditions. There are several ways to estimate the root-zone storage capacity. Currently, the most accurate and popular method is using the water balance principle. The root-zone storage capacity is a core component in determining a dynamic hydrological response and could be a valuable concept in improving the development of dynamic models. The concept of root-zone storage in hydrological modelling would need to be treated as a dynamically evolving parameter as a function of vegetation and climate. A number of successful studies using the various variations of the water balance approach have recently been published. The strength of this approach is that the dynamic nature of the climate and vegetation temporally and across a catchment can be represented in a single parameter. The input data can be remotely sensed data or in-situ measurements of commonly measured climate variable and limited below ground information is necessary. The approach has been proven successful across a range of climate zones however, performs better in humid environments. At the time of this study, there were no published results from high altitude catchments.

Of the eight current studies using the water balance method, the methods by Nijzink et al. (2016), Wang-Erlandsson et al. (2014) and the DiCaSM routine are the most appropriate under South African conditions and for the potential use in ACRU. The Nijzink et al. (2016) method was tested under commercial afforestation in New Zealand thus it is the best choice of method to test under South African commercial forestry. Wang-Erlandsson et al. (2014) was developed for grassland conditions and thus it is a strong choice for comparison between grassland and afforestation conditions in South Africa. Although this method was developed for remotely sensed data, the nature of the fundamental equations allows for the input of

in-situ point observations. The DiCaSM method provides a strong opportunity to test an existing routine in a small scale catchment model that is similar to ACRU in its functioning. The utilization of the root-zone storage capacity could not only improve modelling in regions of limited below ground data but additionally, under commercial afforestation, it could potentially be useful in the improvement of modelling for SFRA purposes.

3.3 Methodology

Two well monitored catchments (Two Streams and Cathedral Peak Catchment VI) with sufficient length data were used. It must be noted that the ACRU model was set up and calibrated for both catchment using data that is readily available (i.e. maximum and minimum temperature, precipitation and streamflow) to identify the weaknesses within a common modelling environment. As the purpose was to use commonly available information as a way of determining the model adequacy under typical conditions, the observed evaporation and soil moisture data that was available in this case was used solely for the purpose of validation and not in the model calibration. A summary of the steps followed in the methodology, with a detailed explanation, is provided below.

1. The ACRU model was run using daily observed precipitation and maximum and minimum temperatures. Hargreaves and Samani daily was used internally to estimate the potential evaporation. The daily observed streamflow was used in the calibration of the model.
2. As observed actual evaporation and soil moisture are not commonly available, these were not used in the calibration of the model. In the calibration process, only parameters that were known or could be estimated with use of the ACRU manual were adjusted.
3. The calibration statistics were calculated on the best fit of streamflow obtained only from commonly available input data and parameters. Once all the parameters and information that would be commonly available for South African catchments were adjusted, the calibration process ceased.
4. The simulated actual evaporation and soil water was validated against observed data.
5. The root zone storage calculations were undertaken with both the observed and the simulated actual evaporation, observed precipitation, interception and observed streamflow. This was to test the robustness of the methodology to data scarcity.
6. The observed gravimetric water content, permanent wilting point and field capacity were converted to a depth of water using the soil depth before being compared to the root-zone storage capacity. To validate the root-zone storage capacity estimations, the estimations needed to be adjusted to reflect a water content within the soil profile using the permanent wilting point as the lower limit of the water in the root zone.

3.3.1 Site description

Both the Cathedral Peak Catchment VI and the Two Streams Catchment are located in KwaZulu-Natal, South Africa (Figure 3-3) and are intensely monitored by the South African Environmental Observation Network (SAEON) and University of KwaZulu-Natal, respectively.

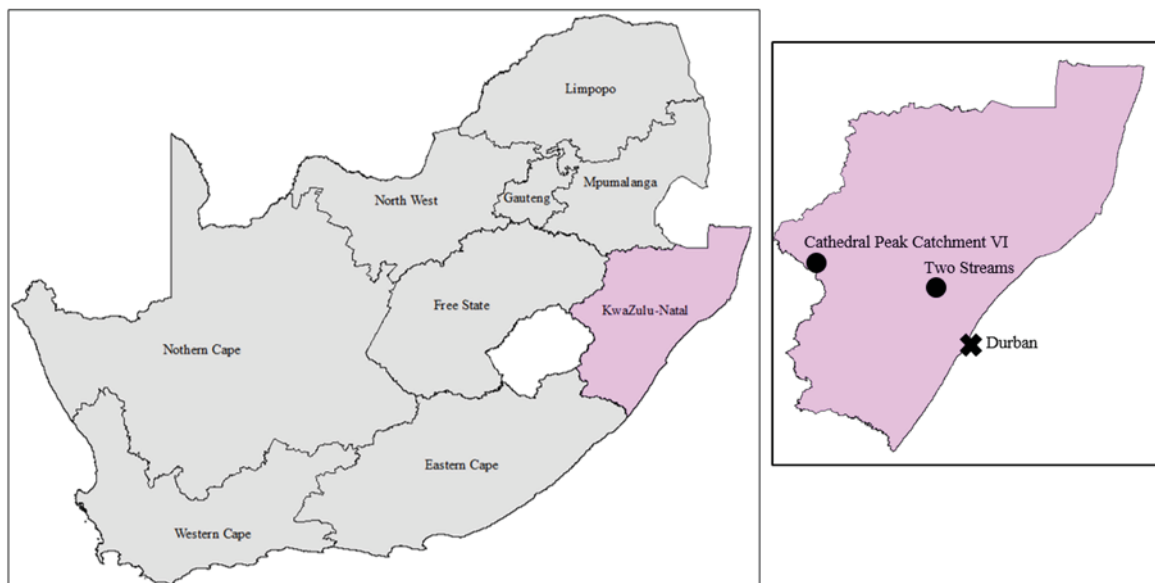


Figure 3-3: Location of Two Streams and Cathedral Peak Catchment VI within South Africa.

The Two Streams Research Catchment (0.65 km²) is in the ‘midlands mistbelt grassland’ bioregion (Clulow, 2011). The area experiences a humid climate with predominantly summer rainfall. The annual rainfall ranges from 659 to 1139 mm (Everson et al., 2018). The dominant soil forms are apedal and plinthic with dolerite dykes and sills present in the area. The Two Streams Catchment forms part of the Mistle-Canema Estate belonging to Mondi Forestry and was afforested with *Acacia meurnsii* until November 2017 (Everson et al., 2018). Rainfall, relative humidity, temperature and wind are monitored. The evaporation is estimated using an eddy covariance tower situated within the stand. The streamflow has been monitored continuously since 1999 using a 457.2 mm 90° V-notch weir, logger (CR200X, Campbell Scientific) and pressure transducer (CS451, Campbell Scientific) (Clulow, 2011). Groundwater is monitored at four boreholes located in the centre, western, northern and eastern corners of the plantation. Soil water is monitored using time-domain reflectance probes to a depth of 2.4 m in the centre of the plantation.

The Cathedral Peak research catchment IV is situated within the uKhahlamba Drakensberg Park. The vegetation is fire-maintained grasslands. The majority of the rainfall (85%) falls within the summer months, October to March (Morris et al., 2016). An estimated 50% of the rain originates from thunderstorms whilst some less intense longer events can last for several days. The MAP is 1400 mm (Morris et al., 2016). The catchment comprises of Drakensberg Basalt Group which intermittently overlies the Clarens Formation Sandstone. The sampled soils are moderately weathered and can be considered immature. The profiles are at least 1.5 m deep and have an average pH of 5.5 in the surface horizon and 6.6 in partly decomposed rock. The dominant soil forms are Hutton and Griffin (Kuenene et al., 2009).

3.3.2 Data acquisition

The physical characteristics of the catchments were obtained from various sources and used in the modelling exercises whilst the observed and estimated climate data, interception and recharge estimations and streamflow measurements, were assembled into a time series for each catchment extending from March 2007 until October 2013 and from July 2014 until August 2018 for both the Two Streams and Cathedral Peak catchment VI, respectively. The model input data used is extensively detailed in Horan (2020).

3.3.3 Calibration of the ACRU model

The ACRU model setups were not calibrated to their full potential but to the full extent possible with commonly available data as mentioned previously. The ACRU model setups were previously calibrated for Two Stream by Clulow et al. (2011) and for Cathedral Peak Catchment VI by Horan (2017) for different time periods. The model configurations were run for both catchments using the new climate forcing data and were calibrated further where possible under the set-out data constraints for the new time period.

For Cathedral Peak Catchment VI, the model under-simulated the low flows and over-simulated the magnitude of the high flows as not enough water was retained during the receding limb of the hydrograph. Parameters were adjusted systematically to improve the simulation. The soil depths for the A and/or B horizons were altered, and it was decided that an A horizon depth of 0.34 m and B horizon of 1.4 m provided the best simulation of streamflow. The model was run using the altered soil depths and the simulation was much improved. The SMDDEP was altered to various depths. A SMDDEP of 0.3 m yielded the best result when compared to the observed data.

For Two Streams, the model simulated the low flows well but the magnitude of the high flows were significantly under simulated whilst the duration of high flow is over-simulated. Parameters were adjusted systematically to improve the simulation. The soil depths for the A and/or B horizons were altered and it was decided that an A horizon depth of 0.2 m and B horizon of 0.57 m provided the best simulation of streamflow. The model was run using the altered soil depths and the simulation was much improved. The SMDDEP was altered to various depths. A SMDDEP of 0.2 m yield the best result when compared to the observed data.

3.3.4 The estimation of the root-zone storage capacity

Three methods were used to estimate the root-zone storage capacity for both catchments. For each catchment, identical datasets are used between the three methods to allow for comparison of results. Each dataset consisted of precipitation, actual evaporation, interception and streamflow at a daily time step. For the validation of the calculated root-zone storage capacity, the root-zone storage capacity needed to be adjusted to reflect a water content within the soil profile. The root-zone storage is the water available for plant uptake and thus can be defined as the water content above the permanent wilting point. The permanent wilting point was added to the root-zone storage content estimations to reflect the water content in the soil profile.

The different methods used in the estimation of the root-zone storage capacity are described below.

Nijzink Method

The change in interception storage over time was calculated by subtracting the actual evaporation and effective precipitation from the gross precipitation (Eq 3.1).

$$\frac{dI}{dt} = P_g - E_t - P_e \quad (3.1)$$

where:

- I = Interception (mm)
- t = time (days)
- P_g = Gross Precipitation (mm)
- E_t = Actual evaporation (mm)
- P_e = Effective Precipitation (mm)

The maximum root-zone storage capacity was calculated using the integral of the subtraction of the effective precipitation from the evapotranspiration over the time period (Eq 3.3).

$$RZSC = \max \int_{t_0}^{t_1} (E_t - P_e) dt \quad (3.2)$$

$$RZSC = ([E_t - P_e]_1 - [E_t - P_e]_0) \quad (3.3)$$

where:

RZSC = Root-zone storage (mm)
 E_t = Actual evaporation (mm)
 P_e = Effective Precipitation (mm)

The absolute values of the root-zone storage were calculated for each time period, the maximum value was determined for the time series and assumed to be the maximum root-zone storage capacity of the catchment.

Wang Method

Although the Wang method was derived for use with remote sensing datasets, in this study the fundamental equations from Wang-Erlandsson et al. (2014) were applied to in-situ point climate data. As the first step, the inflow (Eq 3.4) and the outflow (Eq 3.5). of the system were calculated using daily datasets of precipitation, actual evaporation and interception.

$$F_{out} = E = E_t + I \quad (3.4)$$

where:

F_{out} = Flow out of the system (mm)
 E_t = Actual Evaporation (mm)
 I = Interception (mm)

$$F_{in} = P_g + F_{irr} \quad (3.5)$$

where:

F_{in} = inflow to the system (mm)
 P_g = Precipitation (mm)
 F_{irr} = Irrigation applied within the system (mm)

The difference between the inflow and the outflow was calculated for each time step and the accumulated difference (A) was defined as follows (Eq 3.7).

$$A = \int_{t_n}^{t_{n-1}} F_{out} - F_{in} . dt \quad (3.6)$$

$$A = [F_{out} - F_{in}]_{t_{n-1}} - [F_{out} - F_{in}]_{t_n} \quad (3.7)$$

where:

t_n = final time interval
 t_{n-1} = initial time interval

The soil moisture deficit is calculated. The soil moisture deficit, by definition, cannot be negative as it is to be considered as a running estimate of the root-zone storage capacity. Thus the following is assumed (Eq 3.8):

$$D_{(tn)} = F_{out} - F_{in} \quad (3.8)$$

where:

$D_{(tn)}$ = Soil moisture deficit (mm)

If $D_{(tn)} < 0$ then $D_{(tn)}$ becomes 0

If $D_{(tn)} > 0$ then remains the initial value

The soil moisture deficit for the previous time interval is calculated as follows (Eq 3.9 and Eq 3.10):

When $D_{(tn)} < 0$

$$D_{(tn-1)} = (0 + A) \quad (3.9)$$

And when $D_{(tn)} > 0$:

$$D_{(tn-1)} = (D_{(tn)} + A) \quad (3.10)$$

As the final step, the root-zone storage capacity is calculated (Eq 3.11):

$$RZSC = (D(t_1), D(t_2), D(t_3) \dots D(t_{end})) \quad (3.11)$$

DiCaSM Routine

The DiCaSM model runs a simple routine to calculate the root-zone storage capacity. This routine requires the groundwater recharge per time interval, which was not available as an observed measurement.

The method used to estimate the groundwater recharge is an empirical relationship developed by Kumar (1977) for use in cases where recharge observation measurements are limited. The empirical relationship is defined as (Eq 3.12):

$$G = 0.63 \times P_e^{0.76} \quad (3.12)$$

where:

G = Groundwater recharge (mm)

P_e = Effective precipitation (mm)

With groundwater recharge estimates, the root-zone storage capacity method within the DiCaSM model (Ragab, 2010) could be applied. The root-zone storage capacity was calculated using (Eq 3.13):

$$RZSC = P_e - G - E_t \quad (3.13)$$

where:

RZSC = change in root-zone storage capacity (mm)

E_t = Actual Evaporation (mm)

3.4 Results

3.4.1 Comparison of observed and simulated streamflows and soil water

The streamflow at the outlets of the Two Streams catchment and Cathedral Peak catchment VI were simulated using the ACRU model. The streamflow was simulated for the Two Streams catchment from March 2007 until October 2013, and from July 2014 to April 2017 for Cathedral Peak. The performance of the model to simulate the streamflow was assessed using Nash-Sutcliff Efficiency (NSE), Kling-Gupta Efficiency (KGE), Root Mean Squared Error (RMSE), R² and percent bias.

In comparison to the observed streamflow, the model produced a poor simulation of streamflow at Two Streams as evident from the negative NSE and KGE values (Table 3-1). ACRU under-simulates the magnitude of the high flows but over-simulates the duration of high flow and over-simulates of the low flows resulting in an over-simulation of the total streamflow by 125% over the time period. The summer months were simulated better than the winter months (Table 3-1). Based on the suggestions in Smithers and Schulze (1995), the poor simulation could be attributed to errors in the soil parameters used or the actual evaporation. For Cathedral Peak catchment VI, in comparison to the observed streamflow, the model produced a fair simulation of streamflow with NSE and KGE values between 0.45 and 0.55 (Table 3-1). ACRU is over-simulating the magnitude of the high flow but receding too quickly and under-simulating the low flows resulting in a 12% under-simulation of the total discharge over the time period. The winter months were better simulated than the summer months (Table 3-1). The simulated hydrograph receded too rapidly, and the low flows were not maintained well. Based on the suggestions in Smithers and Schulze (1995), the concerns in the simulated streamflow could be attributed to errors in the soil parameters used or the actual evaporation.

Table 3-1: The overall and seasonal streamflow goodness of fit statistics for the Two Streams (TS) and Cathedral Peak Catchment VI (CP6) calculated using the daily streamflow values

Catchment	TS	CP6
NSE	-0.28	0.45
KGE	-0.64	0.52
RMSE	0.44	1.48
R ²	0.03	0.65
Bias (%)	125	-12
Summer NSE	-0.21	0.46
Winter NSE	-1.88	0.51

Due to data availability, the verifications using observed soil water could only be undertaken for the Two Streams catchment from November 2011 until October 2013. The observed data was obtained from Time Domain Reflectometer (TDR) soil water probes at 0.4 m intervals through the soil profile to a depth of 2.4 m. The soil water storage for the A and B horizons was selected as an output from the ACRU model simulation for the Two Streams catchment. The simulated soil water storage was compared to the observed data for the relevant horizons (Figure 3-4 and Figure 3-5). In the A horizon, the observed and simulated soil water fluctuated within the range of plant available water, the fluctuations have a visibly fair correlation and good seasonal trend (Figure 3-4) but statistically the simulation is poor with an NSE of -0.29, and R² of 0.17. The simulated soil water is more responsive to rainfall than the observed soil water causing the temporal correlation of the peaks to be weak and 23% over simulation. The simulated soil water reduced to the permanent wilting point in the dry season whereas the observed soil water did not. In the B horizon, the model produced a poor simulation with an NSE of -0.47 and R² of 0.27. The ACRU model over-simulated the magnitude and flux of the soil water (Figure 3-5). The observed data formed a smooth curve with a

single peak within the bounds of the plant available water whilst the simulated soil water was far more responsive.

There is not always a response to rainfall in the A soil horizon. This could be due to multiple factors such as low rainfall intensity, high levels of canopy interception, litter interception, immediate water uptake by water stressed trees and possibly surface sealing of the soil below the canopy which affects the infiltration. The simulated soil water in the B horizon fluctuated to a greater extent than the observed soil water. The B horizon is much deeper than the A horizon and therefore the response to rainfall events is lagged. Soil water in the B horizon tends to be taken up immediately by the trees as there is evidence that they are continuously stressed.

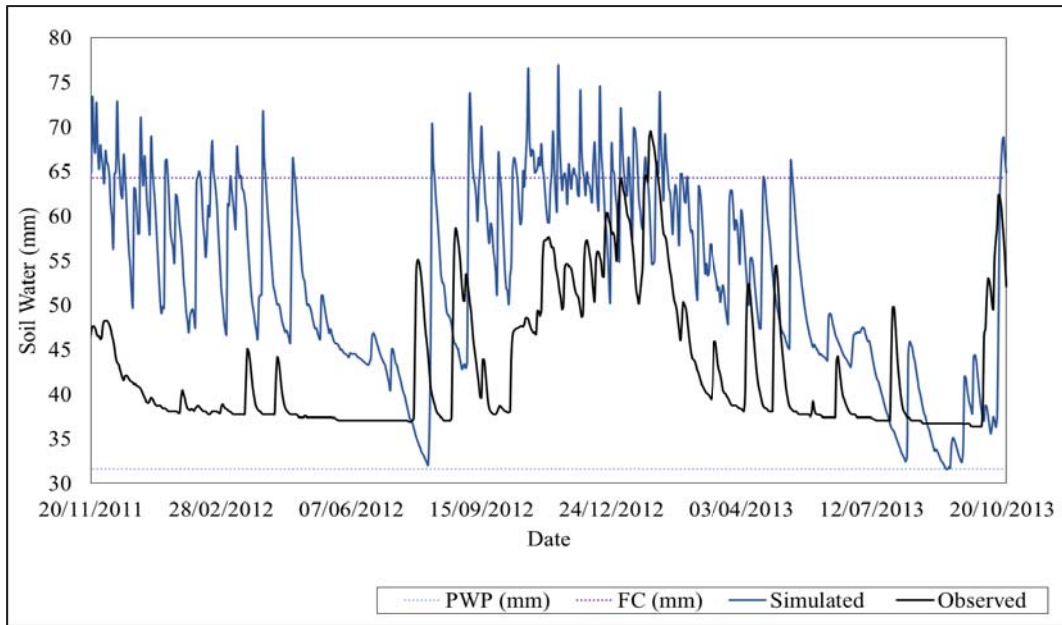


Figure 3-4: The daily simulated soil water (blue line) and the daily observed soil water (black line) in the A horizon plotted within the field capacity (purple dashed line) and the wilting point (blue dashed line) for the period of November 2011 until October 2013.

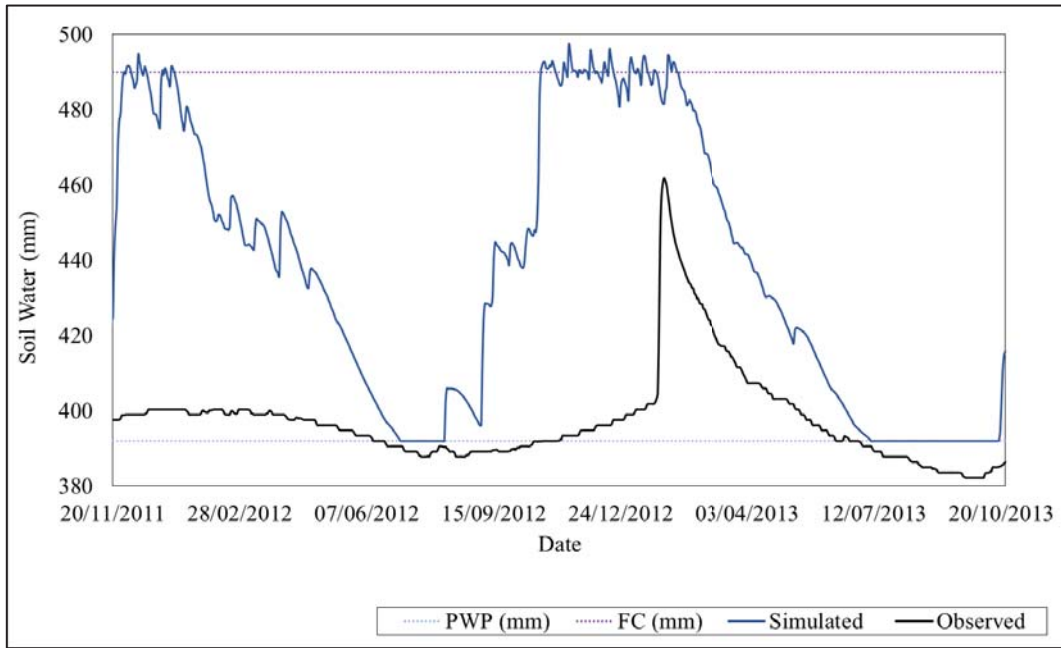


Figure 3-5: The daily simulated soil water (blue line) and the daily observed soil water (black line) in the B horizon plotted within the field capacity (purple dashed line) and the wilting point (blue dashed line) for the period of November 2011 until October 2013

3.4.2 Observed and simulated actual evaporation

The actual evaporation was simulated by the ACRU model (using the maximum and minimum temperatures) was compared to the observed records for the respective catchments from March 2007 until October 2013. The actual evaporation simulated by the model was used to determine the accuracy of the partitioning of water into the components of the water balance in the ACRU model. The overall and seasonal performance of the model to simulate the actual evaporation was assessed using NSE, KGE, RMSE, R² and percent bias (Table 3-2). The model produced a very poor simulation of the actual evaporation resulting in negative NSE and KGE values and a large RMSE for both catchments (Table 3-2). At Two Streams, the actual evaporation was under simulated by 50% over the time period (Table 3-2) and this was particularly evident in the daily time series (Figure 3-6). The seasonal NSE suggests that the winter months are simulated slightly better than the summer months (Table 3-2), however, the under-simulations in the dry season are more evident than in the wet season (Figure 3-6). The model reduced the actual evaporation to zero in periods of the dry season because of the soil water drying out. This is not realistic as the catchment was afforested with evergreen *Acacia mearnsii* that continues to transpire throughout the year as confirmed by the observed evaporation (Figure 3-6).

Table 3-2: The overall and seasonal actual evaporation goodness of fit statistics for the Two Streams (TS) and Cathedral Peak Catchment VI (CP6) calculated using the daily observed and simulated actual evaporation values

Catchment	TS	CP6
NSE	-0.06	-0.19
KGE	-0.17	0.165
RMSE	2.3	1.9
R ²	0.17	0.10
Bias (%)	-50	-33
Summer NSE	-0.17	-0.44
Winter NSE	-0.04	0.15

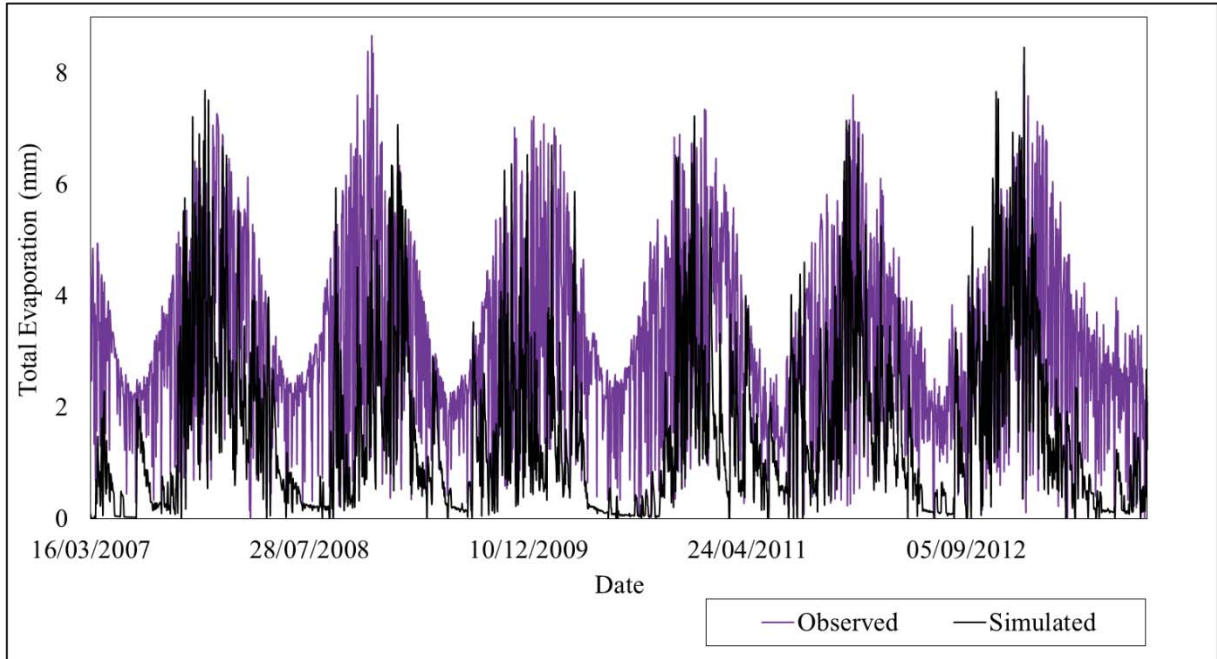


Figure 3-6: The daily observed evaporation (purple line) and the daily actual evaporation estimated by the ACRU model (using the maximum and minimum temperatures) (black dashed line) at the Two Streams Catchment over the period of March 2007 until October 2013.

The actual evaporation was simulated by ACRU (using the minimum and maximum temperatures) at Cathedral Peak Catchment VI from July 2014 until August 2018. In comparison to the observed evaporation records, the model poorly simulated the actual evaporation as evidenced by low NSE and KGE values, a large RMSE and a negative bias of 33% over the time period (Table 3-2). The seasonal NSE suggests that the winter months were simulated better than the summer months (Table 3-2), however, from the daily time series the under-simulations in the dry, winter season were more evident (Figure 3-7). The poor temporal simulation in comparison to the observed data is evident from the daily time series (Figure 3-7), for example, due to late rains in (April) 2016 and the re-sprouting of the vegetation following initial senesce, the observed evaporation was at a maximum for a longer time than the simulated evaporation. ACRU was unable to account for the re-sprouting of senescing vegetation (due to intra-annual variation of rainfall) within the modelling period as stationary monthly crop coefficients are input, thus the model simulates the same transpiration trend every year.

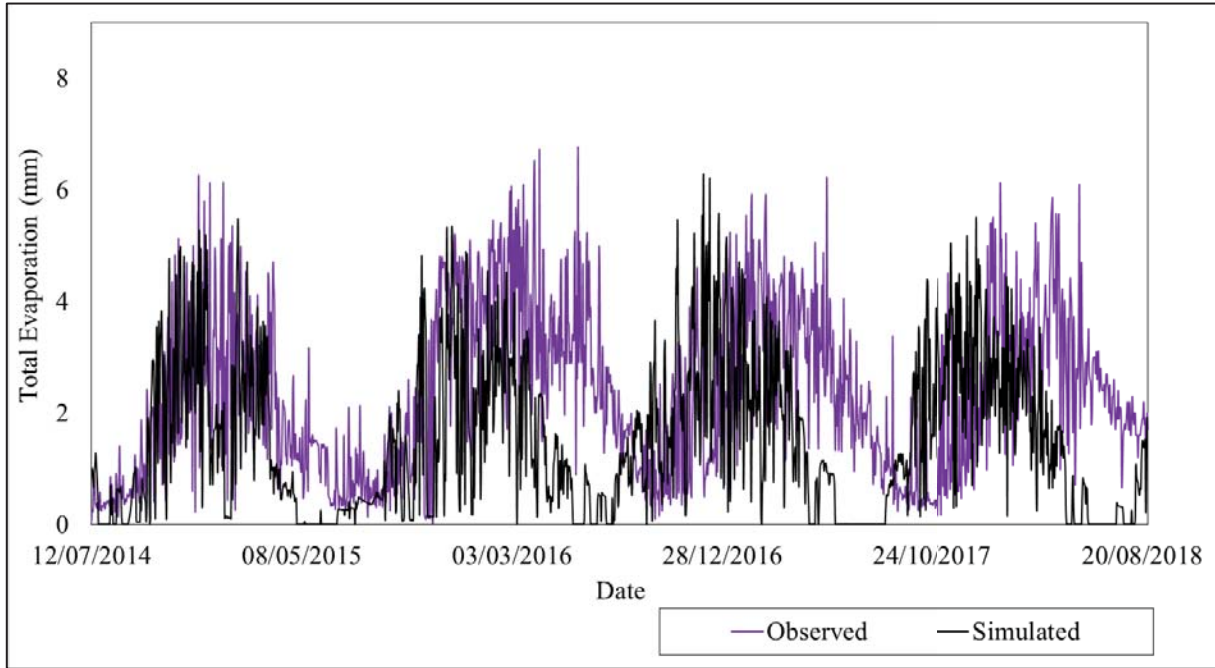


Figure 3-7: The daily observed evaporation (red line) and the daily actual evaporation estimated by the ACRU model (black dashed line) at Cathedral Peak Catchment VI over the period of July 2014 until August 2018.

The ACRU model performed poorly at Cathedral Peak VI and more so at Two Streams. The streamflow simulations at Cathedral Peak Catchment VI were fair however the actual evaporation and soil water simulations were poor. At Two Streams the simulation of the streamflow, actual evaporation and soil water were all poor. McNamara (2018) illustrated that the ACRU model output is highly sensitive to the crop coefficient parameter. Thus, the conceptualisation of and uncertainty with the use of the crop coefficient (Allen et al., 2005 and Kunz et al., 2015) in the estimation of actual evaporation in the ACRU model could be contributing to the poor simulations of actual evaporation and consequently the soil water. In South Africa, there is a lack of site-specific crop coefficient data and thus estimations from FAO and other sources are commonly used. Added to this, the lack of adequate root depth and distribution information, and poor soils data further compounds the poor estimation of the soil water. The use of the root-zone storage capacity concept could potentially be used in addressing the uncertainties with the crop coefficient and the data deficits. It incorporates both climatic and vegetation conditions into a single dynamic hydrological parameter and represents all the combinations of the vegetation in a catchment (De Boer-Euser et al., 2019) and thus removing the reliance on the crop coefficient, rooting and soils data.

3.4.3 Root-zone storage capacity

Three methods were used to estimate the root-zone storage capacity for each of the catchments. The first, the Nijzink et al. (2016) method is based on a complex long-term water balance principle which supersedes the second method developed by Wang-Erlandsson et al. (2014). The final method is adapted from the DiCaSM model root-zone storage routine, which requires a groundwater recharge calculation, and for the purposes of this study, the method developed by Kumar (1977) was used. The results from the three methods are presented for each catchment.

Two Streams Catchment

All three methods produced root-zone storage capacities that displayed strong seasonal trends throughout the study period with sporadic high peaks in the summer months in response to large rainfall events in the catchment (Figure 3-8). The median root-zone storage capacity (Table 3-3) and the daily root-zone storage time series (Figure 3-8) show that the Nijzink method estimates the greatest root-zone storage capacities and the Wang method estimates the lowest root-zone storage capacities. The Nijzink method results have the greatest variability in the calculated root-zone storage capacities and were very responsive to rainfall events. The root-zone storage capacities calculated using the DiCaSM method were the least variable. The DiCaSM method produced a root-zone storage capacity similar to that of the Nijzink method (Table 3-3) but did not produce sporadic peaks in response to the rainfall events evident from the range and the time series plot.

Table 3-3: Statistics of the root-zone storage capacities estimated using the Nijzink, Wang and DiCaSM methods at Two Streams.

	Nijzink	Wang	DiCaSM
Mean (mm)	6.1	4.0	6.04
Median (mm)	5.3	3.1	5.6
Variance (mm)	17.6	14.4	7.8
Range (mm)	39.7	29.8	16.7

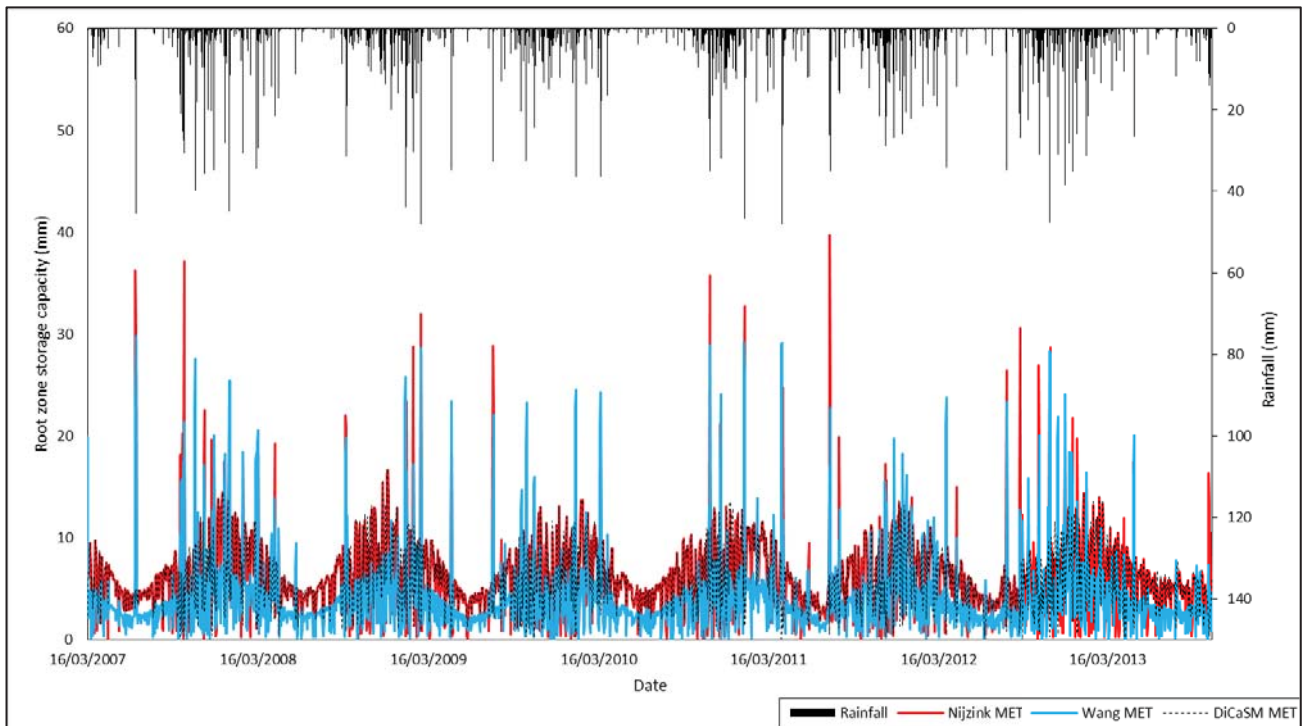


Figure 3-8: Estimated daily root-zone storage capacity for the Nijzink (red line), Wang (blue line) and DiCaSM (dashed black line) methods and daily rainfall (black line) at the Two Streams catchment for March 2007 to October 2013.

The root-zone storage capacities were re-calculated using the same methodologies (Nijzink, Wang and DiCaSM) however, the observed evaporation was replaced with the simulated actual evaporation using the to determine the sensitivity to the actual evaporation input in the root-zone storage capacity and to investigate the robustness of this method to data scarcity.

Using the simulated actual evaporation in the Nijzink method decreased the mean root-zone storage capacity however, it increased the variance and the range over the time period (Table 3-4). Higher peaks in the root-zone storage were calculated using the simulated actual evaporation although the mean and median were lower than those derived using the observed evaporation. Using the simulated actual evaporation in the Wang method decreased the mean root-zone storage capacity and slightly increased the variance and the range over the time period (Table 3-4). A significant decrease in the root-zone storage capacity using the simulated actual evaporation was seen in the dry season when the simulated actual evaporation was significantly under-simulated. Using the simulated actual evaporation in the DiCaSM method decreased the mean root-zone storage capacity, the variance and the range over the time period (Table 3-4). Throughout the time period, the root-zone storage capacity estimated using the simulated actual evaporation was significantly lower than when using the observed evaporation. The DiCaSM method was highly sensitive to the evaporation component but less sensitive to the precipitation than the Nijzink and Wang methods.

Table 3-4: Statistics of the root-zone storage capacities estimated using the Nijzink, Wang and DiCaSM methods with observed evaporation (OET) and simulated actual evaporation (SET) for the Two Streams catchment.

	Nijzink		Wang		DiCaSM	
	OET	SET	OET	SET	OET	SET
Mean (mm)	6.1	4.1	4.0	2.9	6.04	2.7
Median (mm)	5.3	2.6	3.1	1.6	5.6	2.1
Variance (mm)	17.6	23.0	14.4	159	7.8	5.2
Range (mm)	39.7	40.2	29.8	30.8	16.7	11.6

Cathedral Peak Catchment VI

The Nijzink, Wang and DiCaSM methods produced very similar root-zone storage capacities for Cathedral Peak catchment VI that displayed strong seasonal trends throughout the study period with sporadic high peaks in the summer months in response to rainfall events in the catchment (Figure 3-9). The median root-zone storage capacity (Table 3-5) and the daily root-zone storage time series (Figure 3-9) show that the Nijzink and DiCaSM methods estimated the greatest root-zone storage capacities and the Wang method estimated the lowest root-zone storage capacities. The Nijzink method resulted in the greatest variability within the calculated root-zone storage capacities and was highly responsive to rainfall events. The root-zone storage capacities calculated using the DiCaSM method were the least variable and did not respond rapidly to rainfall.

Table 3-5: Statistics of the root-zone storage capacity estimated using the Nijzink, Wang and DiCaSM methods at Cathedral Peak catchment VI over the period July 2014 to August 2018.

	Nijzink	Wang	DiCaSM
Mean (mm)	8.4	6.8	8.6
Median (mm)	7.0	5.5	8.0
Variance (mm)	61.3	33.2	23.0
Range (mm)	110.5	83.0	77.7

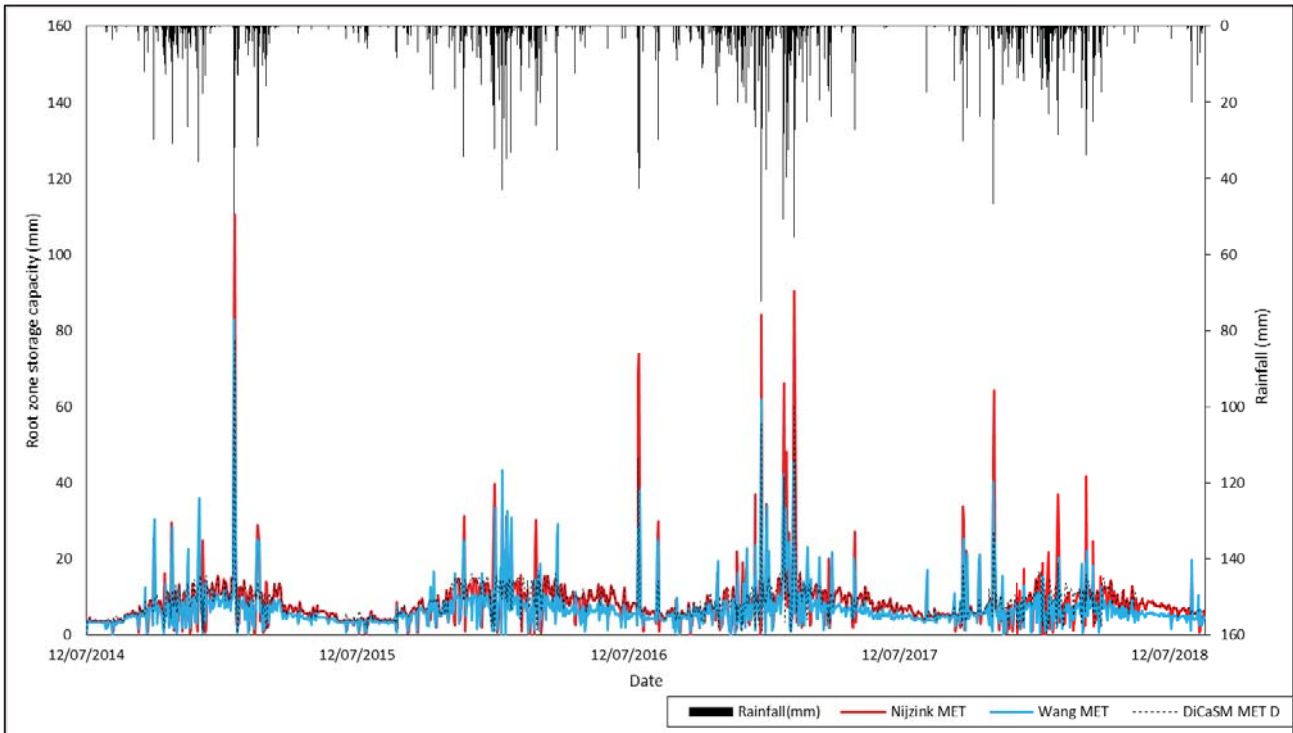


Figure 3-9: Daily root-zone storage capacity calculated using the Nijzink (purple line), Wang (green line) and DiCaSM (blue line) methods and the daily rainfall (black line) for the Cathedral Peak Catchment VI from July 2014 to August 2018.

The root-zone storage capacities were re-calculated using the same methodologies (Nijzink, Wang and DiCaSM) however, the observed evaporation was replaced with the simulated actual evaporation to determine the sensitivity to the actual evaporation input in the root-zone storage capacity and to investigate the robustness of this method to data scarcity.

Using the simulated actual evaporation in the Nijzink method decreased the mean root-zone storage capacity and more markedly decreased the median, as well as slightly increasing the variance and range over the time period (Table 3-6). Using the simulated actual evaporation in the Wang method resulted in little difference in the mean root-zone storage capacity, variance or range (Table 3-6). Using the simulated actual evaporation in the DiCaSM method decreased the mean root-zone storage capacity and increased the variance and the range over the time period (Table 3-6). Following the calculations and understanding of the sensitivities of the three root-zone storage capacity methods, it was necessary to validate the calculated root-zone storage capacities with the observed soil water measurements.

Table 3-6: Statistics describing the root-zone storage capacity estimated using the Nijzink, Wang and DiCaSM methods with observed evaporation (OET) and simulated actual evaporation (SET) for the Cathedral Peak catchment VI.

	Nijzink		Wang		DiCaSM	
	OET	SET	OET	SET	OET	SET
Mean (mm)	8.4	7.5	6.8	6.3	8.6	7.48
Median (mm)	7.0	5.2	5.5	4.7	8.0	6.3
Variance (mm)	61.3	71.8	33.2	34.7	23.0	28.7
Range (mm)	110.5	113.6	83.0	84.7	77.7	80.7

3.4.4 Validation of the root-zone storage capacity in hydrological modelling

The validation of the calculated root-zone storage capacity with observed soil water data was only undertaken at Two Streams as there is no soil water data available for Cathedral Peak Catchment VI. The root-zone storage capacity was defined as the water in the root-zone available to the plant and thus the calculated root-zone storage capacities were adjusted using the permanent wilting point for the profile. The observed soil water and the ACRU simulated soil water were produced as a soil water content value (metres per metre). The water content for each horizon was weighted by the depth of the soil horizon to produce a depth of water in millimetres. To account for the soil water throughout the extent of the soil profile the depth of soil water in the A and B horizons were summed.

Across the soil profile, the root-zone storage capacity methods produced better simulation of the soil water than the ACRU model at the Two Streams catchment. The goodness of fit statistics showed a poor simulation for all the root-zone storage capacity methods and the ACRU simulation compared to the observed data (Table 3-7). However, the estimated root-zone storage capacity methods produced better statistics compared to the ACRU simulation. The estimated root-zone storage capacity methods all produce an accurate bias, which indicates that the volume of water within the soil profile was comparable to observed values but the root-zone storage capacities were substantially more reactive to the rainfall compared to the observed data (Figure 3-10). The goodness of fit statistics suggest that the DiCaSM method produced the best simulation of the observed soil water although all three methods produced less variance than the observed data.

Table 3-7: Statistics and goodness of fit measures describing the root-zone storage capacity estimated using the Nijzink, Wang and DiCaSM methods and the ACRU simulated soil water at Two Streams.

	Observed	Simulated	Nijzink	Wang	DiCaSM
Mean (mm)	440.69	480.97	435.77	437.75	445.80
Median (mm)	437.87	476.81	434.23	435.23	443.86
Range (mm)	109.50	150.58	79.47	88.53	68.34
KGE	-	-0.47	0.047	0.142	0.235
NSE	-	-0.39	-0.02	-0.10	0.11
Bias (%)	-	10	-1.5	-0.64	1.09

3.5 Discussion and conclusion

The limited calibration of the ACRU model at Two Streams, utilising data commonly available in South Africa, yielded a poor simulation of the streamflow and additionally through an independent validation of the actual evaporation and soil water it was found that these were simulated poorly. The model under-simulates the high flows and actual evaporation whilst over-estimating the low flows and soil water. The model is retaining too much water in the soil profile resulting in the magnitude of high flows being reduced and lag time being extended in the summer. Both soil layers store excess soil water in the wet season and dry out in the dry season. The over-estimation of the soil water in B horizon maintains the water available in the intermediate zone. The baseflow is generated as a function of water available in the intermediate zone. Baseflow occurs year around which maintains the low flows in the stream through the winter. In reality the soils would retain less water and the baseflow would cease in the winter. The model reduces the transpiration minimum in the winter months as the soil water in the B horizon is at PWP. In reality the trees would continue to transpire through the deep rooting system during the winter. The inaccuracies in the simulations could be occurring for the conceptualisations of the soil profile and baseflow generation in the model.

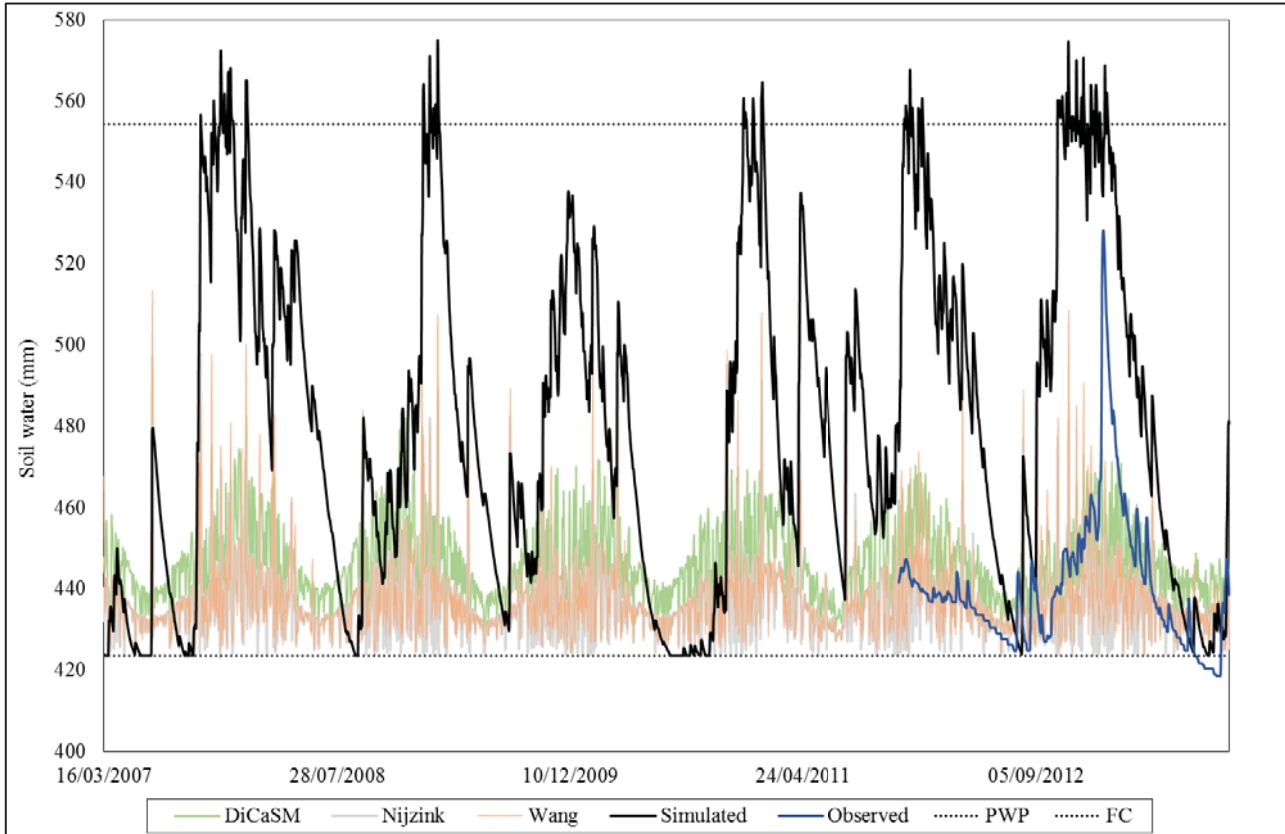


Figure 3-10: Daily estimated root-zone storage capacity using the Nijzink (grey line), Wang (pink line) and the DiCaSM (green line) methods with the observed soil water (blue line) and ACRU simulated soil water (black line) in the soil profile at Two Streams.

The limited calibration of the ACRU model at Cathedral Peak Catchment VI, utilising data commonly available in South Africa, yielded a fair simulation of the streamflow and additionally through an independent validation of the actual evaporation it was found that it was simulated poorly. The model over-simulates the high flows whilst under-estimating the low flows and actual evaporation. The model does not retain the receding limb of the hydrograph as in reality. Due to the conceptualisation of the soil profiles and rooting structure in the model it was found that there were periods in the winter where the soil water flatlines in the B horizon. This is due to all the roots retreating to the A horizon and thus no water can evaporate/transpire from the B horizon and because the soil water is far below DUL it cannot drain to the intermediate zone (The ACRU assumption is that drainage only occurs downwards and then only when the soil is above or some value close to DUL), so it remains stationary at this level until big rains or roots return to the B horizon. The model can only release baseflow through the intermediate zone. If this zone is dry no baseflow will occur. The catchment seems to have a large storage that is released (probably laterally through bank discharge or shallow groundwater uprising) in the winter but ACRU struggles to simulate this and thus cannot replicate the low flows well. For the Cathedral Peak Catchment VI, the model simulation of the actual evaporation followed a seasonal pattern as the monthly crop coefficients for the grassland repeated consistently through the years. However, late April rains resulted in the grass continuing to transpire into winter. This transpiration in April and May was not accounted for when estimating the actual evaporation using the potential evaporation and crop coefficients. It would be recommended to utilise observed evaporation, where available, to account for varying climatic conditions and abnormalities which the inter-annual stationarity of the monthly crop coefficient values does not. However, for most sites in South Africa no observed records of actual evaporation are readily available.

The uncertainty in the conceptualisation of the soils routine within ACRU and the limited availability of soils and rooting data provided an opportunity to investigate the root-zone storage capacity concept. Literature suggests that the root zone storage capacity is independent of the soil depth, the number of horizons in the soil profile and the vegetation rooting depth. Three methods were used to calculate the root-zone storage with both observed and calculated actual evaporation. The variation between the root-zone storages produced using the three different methods with the same input data were significant. These variations increased when using the simulated actual evaporation. The Nijzink and DiCaSM methods produced the highest root-zone storage capacities at both the Two Streams catchment and Cathedral Peak Catchment VI. The Nijzink method had the greatest variance and was highly responsive to rainfall events. The DiCaSM method had the least variance. The Nijzink and Wang methods were shown to be sensitive to evaporation in the wet and dry season but more sensitive to the precipitation in the wet season. The Wang method was less sensitive to evaporation in the winter than the Nijzink method. The DiCaSM method was highly sensitive to the evaporation component but did not produce as many high peaks as the Nijzink and Wang methods, thus suggesting less sensitivity to precipitation.

The Nijzink method and the Wang method estimated a mean root-zone storage capacity of approximately 430 mm at Two Streams. This is in strong agreement with the work of Nijzink et al (2016) in the HJ Andrews catchment under a coniferous canopy and with Wang-Erlandsson et al. (2014) under deciduous forest and less of an agreement with De Boer-Euser et al. (2019) where a root-zone storage capacity of approximately 410 mm, 395 mm and 325 mm respectively were estimated. The agreement with the work of Nijzink et al (2016) and Wang-Erlandsson et al. (2014) proves promising for the potential use of the root-zone storage concept in South Africa as it suggests that the both these methods are capturing the simplified forest hydrological processes, critical in the development of these internationally recognised methods, at Two Streams relatively accurately. The study area of De Boer-Euser et al. (2019) was vastly climatically different. Based on the conclusion of Wang-Erlandsson et al. (2014) that the vegetation had less effect on the root-zone storage capacity than the variation in climate, this could account for the lower root-zone storage capacity in the De Boer-Euser et al. (2019) study.

The Wang method estimated a mean root-zone storage capacity of approximately 130 mm at Cathedral Peak Catchment VI. This falls within the range of root-zone storage capacity (100-150 mm) determined by Wang-Erlandsson et al. (2014) for grassland vegetation. The strong correlation of the Wang method at both Two Streams and Cathedral Peak Catchment VI with the results of Wang-Erlandsson et al. (2014) highlights the strength of the concept in being independent of vegetation within the catchment. This finding could demonstrate that one method can be utilised for a multiple vegetation types. The results for the three methods are relatively similar and thus it could be said with caution that the three methods could be used under various vegetation types. It would be recommended that additional studies in more climatically, vegetative and spatially diverse catchments are necessary to confirm this finding.

Although soil depth at Cathedral Peak Catchment VI (0.77 m) is substantially shallower than at Two Streams (1.74 m), the mean calculated root-zone storage across the three methods was greater at Cathedral Peak Catchment VI than that at Two Streams. This could suggest that the root-zone storage capacity reflects the catchment climate and vegetative conditions rather than the soil depth. This is consistent with the work of Srinivasan et al. (2015) who describes that commercial plantations create unsaturated conditions in the root-zone and therefore reduce the immediate root-zone storage capacity even though the roots may be deeper. The work of Laio (2006) who found that plants distribute their roots in soil depth-independent fashion to achieve soil moisture uniformity throughout the root-zone. At a local scale, it is likely that root development is not limited to climatic variation alone but also site conditions. However, studies such as Schenk and Jackson (2002) and Feddes et al. (2001) found that rooting depths very closely correlated with climatic factors such as MAP and potential evaporation.

The increase in effective rainfall and decrease in actual evaporation of grassland environments could be additional contributing factors. Wang-Erlandsson et al. (2014) recorded that the global mean root-zone storage capacity of a grassland ranges between 10 mm greater and 50 mm smaller than a deciduous forest, when using a variety of models and input datasets, and concluded that the vegetation had less effect on the root-zone storage capacity than the variation in climate. Additionally, De Boer-Euser et al. (2019) found that vegetation characteristics did not strongly correlate with the patterns of the estimated root-zone storage capacities. In consideration of the studies mentioned above, the difference in root-zone storage capacities at Two Streams and Cathedral Peak Catchment VI could be attributed to varying climate conditions between the two catchments rather than the soil depth or vegetation. The two catchments have a high variance in climatic conditions as well as elevation. Two Streams has an elevation of 1 000 m.a.s.l. and a MAP of 964 mm whilst Cathedral Peak Catchment VI has a greater elevation and MAP of 1 952 m.a.s.l. and 1 135 mm, respectively. The water balance approach to the root-zone storage estimation assumes a classical water balance approach and a non-leaky catchment for it to be successful along with accurate observed climate data.

At Two Streams the soil water contents estimated using the root-zone storage capacities provided a better simulation of the observed soil water than the ACRU model did. The results from the Two Streams catchment indicate that the calculated root-zone storage capacity could provide a viable alternative method of soil water estimation. The performance of ACRU and the root-zone storage capacity concept were evaluated on a daily timestep. This might not be the most appropriate and representative timestep for assessing soil water simulations as the long term or seasonal fluctuations could be of more significance. The model fit could improve when using a longer timestep as the fluctuations would be less impactful. The calculated root-zone storage capacity is independent of soil and rooting characteristics. Boer-Euser et al. (2016) determined that a climate derived root-zone storage capacity better reproduced soil water signatures than the traditional soil parameter derived root-zone storage capacity. Federer et al. (2003) stated that when utilising the BROOK90 and WBM models, increasing the number of soil layers conceptualised in the models and the inclusion of the rooting depth parameters had an insignificant effect on the monthly soil water estimates compared with using a single soil layer without the rooting depth parameter. The study undertaken by Robock et al. (1994) showed no evidence that a complicated biosphere model better simulated the soil water compared to a simple bucket-type hydrological model. Similarly, Baroni et al. (2010) concluded that the soil water simulated using the simple ALHymus model had a smaller normalised root mean squared error and mean error than the soil water simulated by a more complex SWAP model. In agreement with these studies, Orth et al. (2015) determined that two complex models HBV and PREVAH performed better than the simple water balance model (SWBM) in the simulation of streamflow but not for the soil water component. SWBM had approximately 0.8 correlation with the observed soil water compared with an approximate 0.6 for the HBV and PREVAH models. The above-mentioned studies and the root-zone storage validation illustrate that a simple, one layer, climate-driven, water balance soils routine may provide a better representation of the soil water than a highly complex, multi-layered, parameter-based alternative. Overly complex models can suffer from over-parameterization in the simulation of soil water.

Intensive soils data and measured rooting depths were used in the modelling of both catchments however, the soil water results yielded, were poor. This highlights the possibility that although there are uncertainties with the use of soils data and rooting characteristics in hydrological modelling, the model conceptualisation could be an equally significant source of error. The root-zone storage concept could provide an alternative method to decrease modelling uncertainty where limited soils data and rooting depths are available.

The use of the root-zone storage concept within the ACRU model could limit the model uncertainty. The method could allow areas of limited soils and rooting data to be modelled more accurately and the implication of afforestation be fully understood. There is opportunity for the concept to be used with future climate data to provide predictions of the root-zone storage for the future. The study was limited to two small catchments, over a period of six and four years, respectively. The soil water data used in the validation was only representative of a two-year period under mature commercial forestry. A more spatially and temporally explicit study would improve the understanding and confidence in the methodology and concept. Although this study has its limitations, it's a step forward in the modelling of soil water in South Africa.

CHAPTER 4. THE CWRR CLUSTERS AS A HYDROLOGICAL BASELINE

M.L. Toucher^{1,2}

¹ Centre for Water Resources Research, University of KwaZulu-Natal, Pietermaritzburg

² South African Environmental Observation Network

4.1 Background and introduction

The second knowledge gap, as noted in the introduction, concerns the baseline vegetation against which the water use of the commercial tree species is compared. Currently, DWS supports and accepts the use of natural vegetation in the form of the Acocks (1988) Veld Types as the reasonable standard or reference land cover against which to assess land use impacts (Schulze, 2004; Jewitt et al., 2009). However, concerns about the use of Acocks (1988) Veld Types were raised by Jewitt et al. (2009). These concerns centred on the country-wide scale resolution of the Acocks (1988) maps with relatively little local scale detail and that the water use parameters were derived using expert knowledge. The detailed SANBI (2012) maps of natural vegetation, together with a larger database of natural vegetation water use, has allowed for a revised hydrological baseline (together with associated water use parameters) to be developed through WRC project K5/2437 (Toucher et al., 2020).

The recommendations of WRC K5/2437 is that the CWRR clusters, a hydrological grouping of the SANBI (2012) vegetation map, be considered as the new hydrological baseline against which assessments are made. Through this project, the CWRR clusters will be used as the hydrological baseline against which the impacts of commercial afforestation on flows are assessed. A summary of the key aspects of WRC K5/2437 is provided here given that this new baseline will be adopted by this project. The full details are provided in Toucher et al. (2020).

4.2 The CWRR clusters

The Acocks' (1953, 1988) Veld Types were agriculturally based, with a veld type defined as "an agro-ecological unit of vegetation whose range of variation is small enough to permit the whole of it to have the same farming potentialities" (Acocks, 1953). Whereas the SANBI vegetation map was developed with the aim of producing a "sound theoretical classification of the vegetation of South Africa" that describes and maps the vegetation diversity across South Africa, based on the current knowledge of vegetation structure and biogeographical patterns, producing a baseline vegetation map and associated descriptions which can be used by various specialist and disciplines (Mucina and Rutherford, 2006). The fine scale at which the SANBI (2012) vegetation map is drawn and more importantly the methodology used to produce it, have led to it being largely adopted by other disciplines as a good representation of natural vegetation.

The SANBI (2012) vegetation map defines 453 vegetation units. The vegetation unit is defined as "a complex of plant communities ecologically and historically (both in spatial and temporal terms) occupying habitat complexes at the landscape scale" (Mucina and Rutherford, 2006). The vegetation complexes within a vegetation unit share similar general ecological properties, e.g. position on ecological gradient and nutrient levels, and appear similar in vegetation structure, particularly floristic composition. Often the division of a vegetation unit is more floristic than based on vegetation structure. For hydrological modelling purposes it

was not feasible nor practical to adopt the 453 vegetation units as the baseline. Thus, the SANBI (2012) vegetation units were grouped into clusters of vegetation units that respond hydrologically similar, known as the CWRR clusters. The clustering was undertaken by developing hydrological profiles for each of the vegetation units and was then hierarchical clustered using Euclidean distances and Ward method to produce robust and compact clusters. After which expert opinion was sought. This process resulted in 128 CWRR clusters being defined (Figure 4-1).

Due to the finer scale at which the SANBI (2012) vegetation map was drawn, the CWRR clusters provide a finer spatial resolution map of natural vegetation for use as a hydrological baseline vegetation than the Acocks' (1988) Veld Types. Although the number of vegetation units may not appear to be greatly more for the CWRR clusters, it is the more detailed mapping which is advantageous. The CWRR clusters align better to the altitude and underlying geology than the Acocks' (1988) Veld Types. This implies that with the CWRR clusters, different clusters will be mapped on the different topographic formations across the landscape, i.e. the flat valley bottoms will have a different cluster to the valley slopes. Previously with the Acocks' (1988) Veld Types different topographic formations may have had the same veld type given the resolution of mapping. As the impacts of a land use are assessed against the natural vegetation it replaces, this improvement in resolution may significantly affect the assessed land use impact in certain locations. Beyond this, the SANBI (2012) vegetation maps have gained acceptance in the ecological community, as well as with practitioners concerned with land management. This together with the SANBI vegetation units aligning with the biomes for which a common understanding of the vegetation structure exists, provides a convincing argument for the change to the CWRR clusters as the baseline vegetation to use in determining the hydrological baseline.

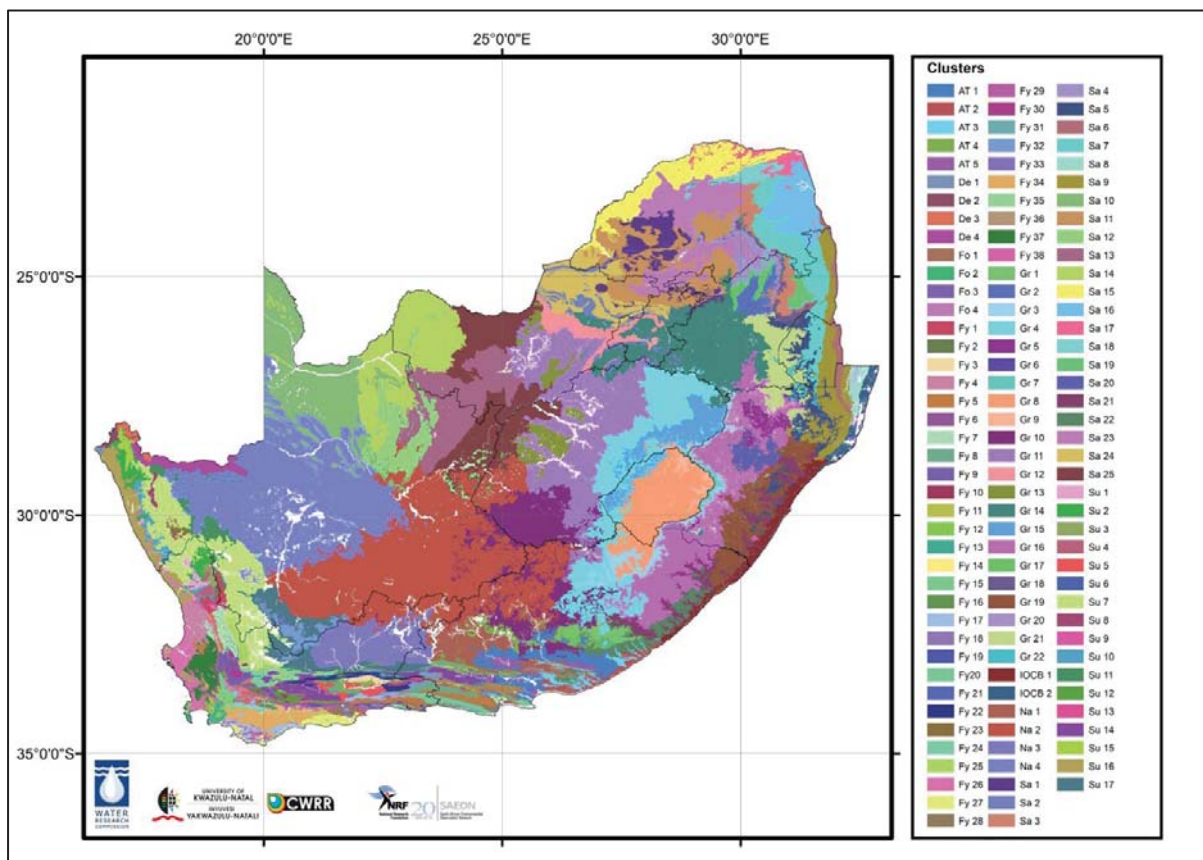


Figure 4-1: CWRR Clusters derived from the statistically clustered hydrological profiles of the SANBI (2012) vegetation units

To be able to adopt the CWRR clusters as the hydrological baseline, the vegetation and water use parameters required by the ACRU agrohydrological model (Schulze, 1995) needed to be derived for each cluster. WRC project K5/2437 developed repeatable, scientifically defensible methodologies for the estimation of all the required vegetation and water use input parameters.

4.3 Hydrological Parameterisation of the CWRR Clusters

The vegetation water parameters required as input for the hydrological model that were derived for the CWRR clusters include,

- crop coefficient (K_c)
- vegetation interception losses (VEGINT)
- the effective rooting depth (EFRDEP)
- the fraction of effective roots in the topsoil horizon (ROOTA)
- the root colonisation of the B-horizon (COLON)
- the coefficient of initial abstraction (COIAM)
- the percentage surface cover by vegetation or mulch/litter (PCSUCO)

The approach adopted by WRC project K5/2437 for each of these variables was to use observed or remotely sensed data and a documented approach that could be repeated. A brief summary of the method used to produce each variable is provided below.

Of the required ACRU model input parameters to describe the vegetation, the model output is most sensitive to K_c . K_c provides a means for estimating the land covers potential evapotranspiration rate, relative to the evapotranspiration from a reference crop, expressed as

$$K_c = \frac{ET_c}{ET_o} \quad (4.1)$$

Where,

- K_c = the crop coefficient (dimensionless)
- ET_c = crop (or vegetation) evapotranspiration (mm.d^{-1} or mm.month^{-1})
- ET_o = reference crop evapotranspiration (mm.d^{-1} or mm.month^{-1})

Therefore, to derive K_c , an estimate of the actual vegetation evapotranspiration was required as well as the reference crop evapotranspiration which was derived using climate data and the FAO Penman-Monteith equation. The proposed and first approach taken to estimate the actual evapotranspiration of the CWRR clusters used remote sensed LandsAT 4/5 images and the Surface Energy Balance System (SEBS) model. A validation study was undertaken as the initial step to determine the viability of the approach. The evapotranspiration estimated using the SEBS model was compared to in-situ observed evapotranspiration values at sites located in seven of the South African biomes. The results of the validation study were considered acceptable, despite the SEBS model tending to overestimate the evapotranspiration of natural vegetation. The methodology was then scaled up to estimate the water use of each of the CWRR clusters through using a representative Quinary assigned to each cluster. The results obtained and produce evapotranspiration estimates which did not correspond to the expected seasonal trends of evapotranspiration for vegetation types nor the expected pattern of evapotranspiration across the biomes. The contributors to this included several temporal and spatial resolution issues. Compared to the expected number of LANDSAT images based on an 8-day resolution over a ten-year period, few images were considered acceptable due to cloud cover. To the extent that for some clusters no images were acceptable over the ten-year period. This implied that a soil water stress factor could not be used as it would have

further decreased the number of acceptable images. The lack of observed evapotranspiration data for natural vegetation limited the corrections which could be applied. Thus, alternatives for determining the K_c values had to be explored.

Literature supported the use of leaf area index (LAI) to determine K_c for natural vegetation and the estimates of LAI obtained from the remotely sensed MODIS product proved to be consistent, both seasonally and across the biomes as well as in alignment with in-situ observations. Methods to estimate the K_c values using LAI were verified. None of the methods performed well, thus an equation was fitted between the K_c values produced for sites where evapotranspiration was observed over natural vegetation and the remotely sensed LAI these sites. The derived relationship explained 75% of the variation in K_c using LAI. Fair confidence existed in the long-term monthly K_c values produced for the CWRR clusters using this equation. Further, the methodology used was repeatable, transparent and standardised with the possibility of being revisited to produce revised K_c values as more data becomes available. The vegetation interception was estimated using the MODIS LAI product and both the Von Hoyningen-Huene (VHH) Method and the variable storage Gash model. The rooting parameters (EFRDEP, ROOTA and COLON) were developed using historical root measurements and observations from previous studies and linking these to the physical properties of the vegetation clusters. The COIAM values were derived using the working rules defined by Schulze (2004). The PCSUCO values were estimated using the LAI derived K_c values for each cluster and the working rules derived by Schulze (2004). A full database of vegetation water use parameters for each of the clusters for the different methods investigated accompanied the report.

4.4 Hydrological Response under the CWRR Hydrological Baseline as Compared to Acocks (1988) Veld Types

The hydrological response under the CWRR clusters were simulated with the ACRU agrohydrological model configured using input data from the Quinary catchments database (following the methodology of Jewitt et al., 2009) and the following vegetation water use parameters derived by Toucher et al. (2020) for the clusters

- K_c (Derived Eq)
- VEGINT (VHH)
- ROOTA
- COIAM
- PCSUCO (Derived Eq)
- COLON was set to 100 and CONST to 0.4

and compared to the hydrological response simulated under the Acocks (1988) Veld Types baseline (Figure 4-2). A higher runoff under the CWRR clusters was evident along the east coast of the South Africa relative to the runoff produced under the Acocks' (1988) Veld Types. Whereas lower runoffs were generally produced for areas in the Free State and Eastern Cape provinces under the CWRR clusters relative to Acocks' (1988) Veld Types. The generally higher crop coefficients in winter months for the CWRR clusters for these areas were the cause behind the decreased flows; whereas the increased flows corresponded to areas where the crop coefficients of the CWRR clusters were generally lower. To note, these simulations were undertaken using the original soils data and climate.

4.5 Concluding thoughts

The methodology used by Toucher et al. (2020) was clearly documented and repeatable. Using LAI to derive the K_c was supported in the literature, and through investigation in the project using LAI derived from MODIS satellite estimates to determine K_c proved to be consistent with vegetation structure across the biomes. In terms of the vegetation water use parameters, the simulated streamflow output from the ACRU model is most sensitive to changes in the crop coefficient and following this the percentage surface cover which is related to the crop coefficient. Thus, a recommendation from the project was to improve the vegetation water use parameters for all current and potential future SFRA, to allow streamflow reductions to be simulated accurately relative to the CWRR clusters baseline streamflow. The use of the methodology for estimating K_c from LAI should be investigated for the commercial forestry crops and other land uses for consistency.

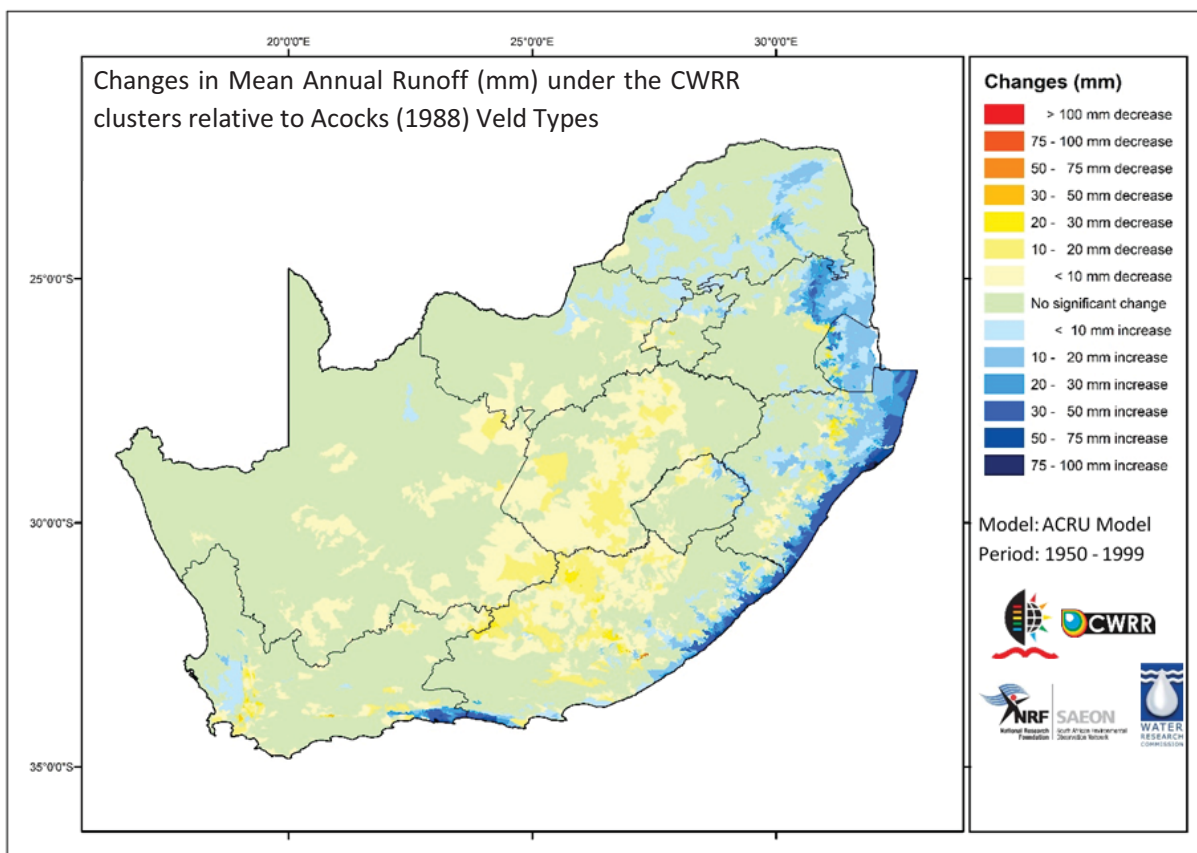


Figure 4-2: Changes in the mean annual runoff in mm under the CWRR clusters using the derived LAI based equation relative to Acocks' (1988) Veld Types.

CHAPTER 5. ADDRESSING THE SHORTCOMINGS IN THE AVAILABILITY OF LEAF AREA INDEX INFORMATION FOR COMMERCIAL TREE SPECIES

S. Gokool¹, R.P. Kunz¹ and M.L. Toucher^{1,2}

¹ Centre for Water Resources Research, University of KwaZulu-Natal, Pietermaritzburg

² South African Environmental Observation Network

5.1 Background and introduction

It is not practical to measure the water use of the various species, clones and hybrids used by the forestry industry, particularly as new clones are continuously being developed. Added to this, is that the measurements would need to be undertaken across a range of tree ages and different stand densities. Thus, a more easily obtainable surrogate measure is required. The surrogate that has been proposed is the Leaf Area Index (LAI). Thus, an identified aim of the project (Aim 3) is “To address the shortcomings in the availability of leaf area index information for different SFRA species, clones and hybrids”.

LAI, defined as the one-sided leaf area (m^2) per unit ground surface area (m^2) (Wang *et al.*, 2017), is a key canopy structural parameter, which controls the exchange of energy, carbon and water between the canopy and the atmosphere (Wang *et al.*, 2017; Chen *et al.*, 2018). LAI varies over the development of the trees and with the forestry management practices, as well as with tree species, tree density, seasonality, and site conditions (Jonkheere *et al.*, 2004). Together with leaf biomass, LAI has a strong relationship to productivity (Peduzzi *et al.*, 2012). Thus, LAI is a critical input variable to process models that estimate the growth and water use of forests (Liu *et al.*, 2015). Advances in the estimation of LAI from remotely sensed data mean that high resolution LAI estimates that can be used as input to modelling are more readily available. Through this project a methodology to derive moderate spatial resolution LAI estimates from coarser spatial resolution satellite products has been developed. The methodology was written as a journal paper and submitted to Remote Sensing Applications Society and Environment, and is under review. The paper is included in this chapter as it was submitted. However, prior a review of the use of to estimate tree water use is provided.

To note, field-based measurements of LAI were attempted during the course of the project. Representative sites that covered the dominant species and climate zones were selected. With three compartments selected per dominant species and climate zone to represent young, intermediate and mature trees. A LiCor LAI 2200 plant canopy analyser was to obtain the infield estimates of LAI. A significant constraint of the LAI 2200 is that the optimal conditions for accurate measurements are diffuse lighting, i.e. early morning or late afternoon with no cloud cover. This requirement significantly hampered the field campaigns to the extent that it was determined that the only feasible path forward was to use satellite-based estimations of LAI.

5.2 Review of using Leaf Area Index to estimate evapotranspiration

As stated above, a strong relationship exists between tree productivity and leaf area (Peduzzi *et al.*, 2012). Several studies have demonstrated relationships between LAI and evapotranspiration. For example, Al-Kaisi

et al. (1989) found that 90-95% of the variation in transpiration could be described using LAI. Bian et al. (2018) showed a high correlation between evapotranspiration and LAI for the Poyang Lake watershed, China. Considering trees specifically, tree transpiration has been linked to LAI by several researchers (e.g. Vertessy et al., 1995; Hatton et al., 1998; Kelley et al., 2007; Whitley et al., 2008, 2009, 2013; Zeppel, 2013). These studies are reviewed below.

Whitley et al. (2008; 2009; 2013) reported promising findings and described the development of relatively simple, but robust methods to assess stand transpiration using only solar radiation, vapour pressure deficit and soil moisture content, plus LAI as inputs. In essence, the approach they took was to modify the Jarvis-Stewart method to allow for the estimation of tree transpiration directly, rather than a two-step approach of estimating canopy conductance with the Jarvis-Smith equation and then using this to estimate transpiration using the Penman-Monteith equation. In some cases, these models have been shown to outperform the more complex Penman-Monteith equation, especially under high transpiration conditions and have the advantage of fewer input requirements. The approach taken was based on the understanding that tree stand water use (E_c) can be calculated from canopy conductance (G_c) and vapour pressure deficit (D), since

$$E_c = G_c \times D \text{ and } G_c = LAI \times G_s \quad (5.1)$$

Where G_s is stomatal conductance and is a function of its driving environmental variables. Therefore, canopy water use can be calculated from:

$$E_c = LAI G_s (R_s, D, \vartheta) D \quad (5.2)$$

This equation holds for well coupled forests (Whitley et al. 2008; 2009; 2013) and, although functionally equivalent to the Penman-Monteith equation, requires fewer measurements and is simpler to fit. Whitley et al. (2008) concluded that the modified Jarvis-Stewart functions adequately described the response of open woodland stand water use to variation in solar radiation, vapour pressure deficit and soil moisture content.

Building on earlier work that established an empirical relationship between LAI and available soil water for tree growth at regional scales (Grier and Running, 1977; Gholz, 1982; Nemani and Running 1989; Pierce et al., 1993), Hatton et al. (1998) investigated whether leaf efficiency varied among eucalypt species grown at the same site with seasonal water limitations. The findings indicated that the leaf efficiency of different eucalypts species grown at the same site is similar regardless (Figure 5-1). These findings supported those of Vertessy et al. (1995) who demonstrated a linear relationship between LAI and tree transpiration (Figure 5-2) for a 15-year-old mountain ash forest in Australia. Similarly, Kelley et al. (2007) found a close relationship between LAI and tree water use for a eucalypt stand with two species in northern Australia. O'Grady et al. (1999) investigated how transpiration patterns vary across the seasons for an open forest in Australia and the findings of a tight relationship between transpiration and leaf area or DBH for both dominant eucalypt species lead them to conclude that the major determinants of spatial variability in stand water use are basal area and LAI.

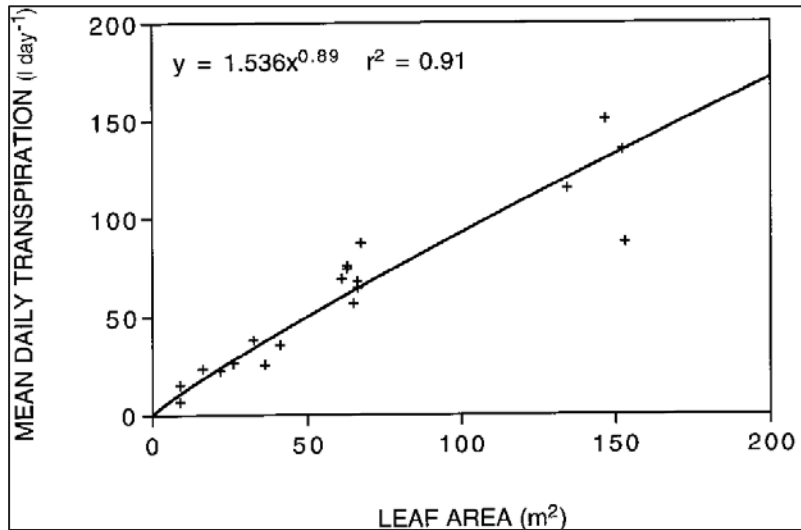


Figure 5-1: Tree leaf area versus mean daily transpiration for a plantation growing on a saline groundwater gradient in South Australia (Hatton et al., 1998)

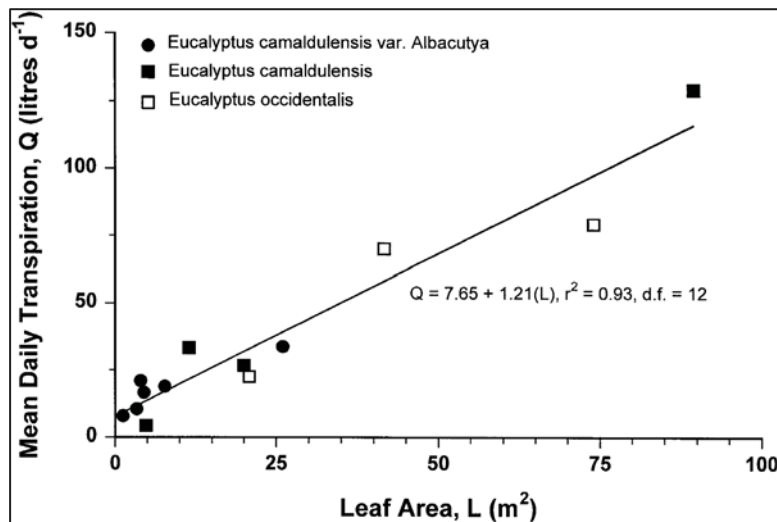


Figure 5-2: Leaf area versus mean daily transpiration for the sampled mountain ash trees (Vertessy et al., 1995)

Due to the increasing need to be able to model tree water use to allow for an improved understanding of water budgets under global change, Zeppel (2013) undertook a quantitative review to investigate whether functional convergence occurs in the relationships between tree size, leaf area, sapwood area and water use in evergreen trees across sites under water limited conditions. Functional convergence is defined as different species having similar relationships between two different physiological properties. Zeppel (2013) considered a wide range of species across multiple genera, varying tree sizes and diverse ecosystems, incorporating differences in microclimates and most importantly water availability.

Zeppel (2013) compiled data from a number of previous studies where diameter at breast height (DBH), sapwood area (SA), leaf area and tree water use was determined. This data was then tested for homogeneity of variances, after which slopes and intercepts were compared for all species using analysis of covariance. Only species with three or more data points were included. The results showed that there were different relationships between the species for leaf area and DBH (Figure 5-3); SA and DBH

(Figure 5-4) and leaf area and tree water use (Figure 5-4). Similarly, no functional convergence within the eucalypt genera was evident for the relationships between leaf area and DBH (Figure 5-3); SA and DBH (Figure 5-4). However, and most notable in the context of this study, is that the slope of leaf area and tree water use within the eucalypt genera did not differ significantly across the species (Figure 5-5). The intercept did vary between species. Zeppel (2013) suggests that the differences in the intercepts may be due to nutrient and water availability at the site rather than inherent genetically based differences; and goes on to state that the relationship may require canopy closure to be reached to hold. The eucalypt trees included in the study by Zeppel (2013) spanned a 100-fold difference in size across a range of sites. The similar slope across the species implies, that for a given leaf area, all eucalypts use the same volume of water. This finding has particular relevance for this study, together with the convergence of hydraulic traits in eucalypt species by O’Grady et al. (1999). These results imply that through the development of a relationship between leaf area and tree water use data for eucalypt species, the relationship could be up scaled and would be applicable across the genera to species where the water use has not been monitored, provided leaf area was available.

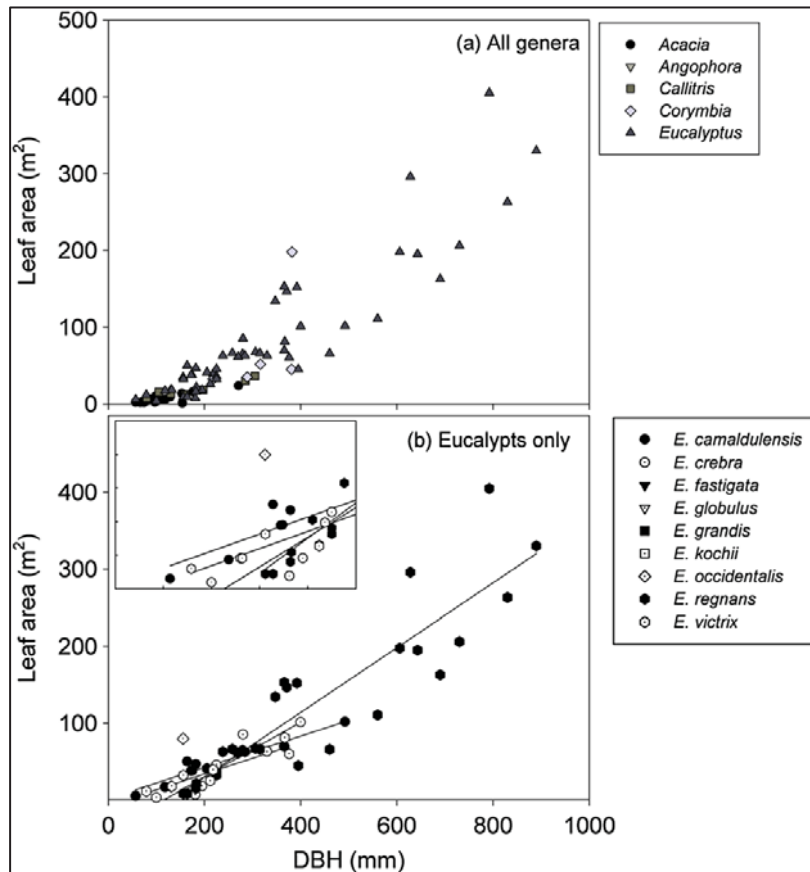


Figure 5-3: The relationship between leaf area (m^2) and diameter at breast height (DBH, mm), for (a) all genera and (b) eucalypts only. The inset in (b) shows a close-up of trees with DBH to 250 mm (Zeppel, 2013).

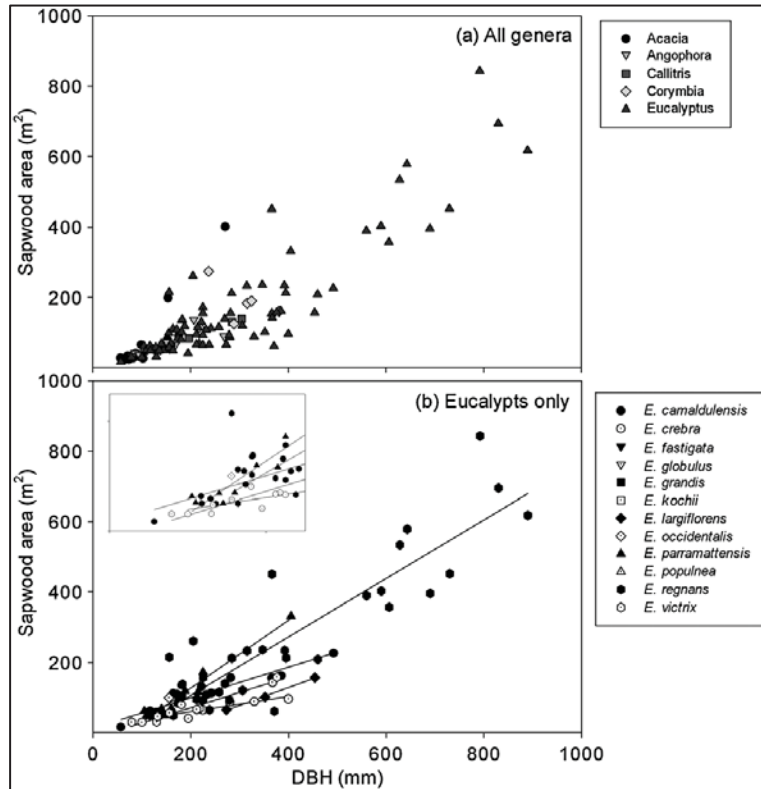


Figure 5-4: The relationship between sapwood area (m^2) and diameter at breast height (DBH; mm), for (a) all genera and (b) eucalypts only. The inset in (b) shows a close-up of trees with DBH to 250 mm (Zeppel, 2013).

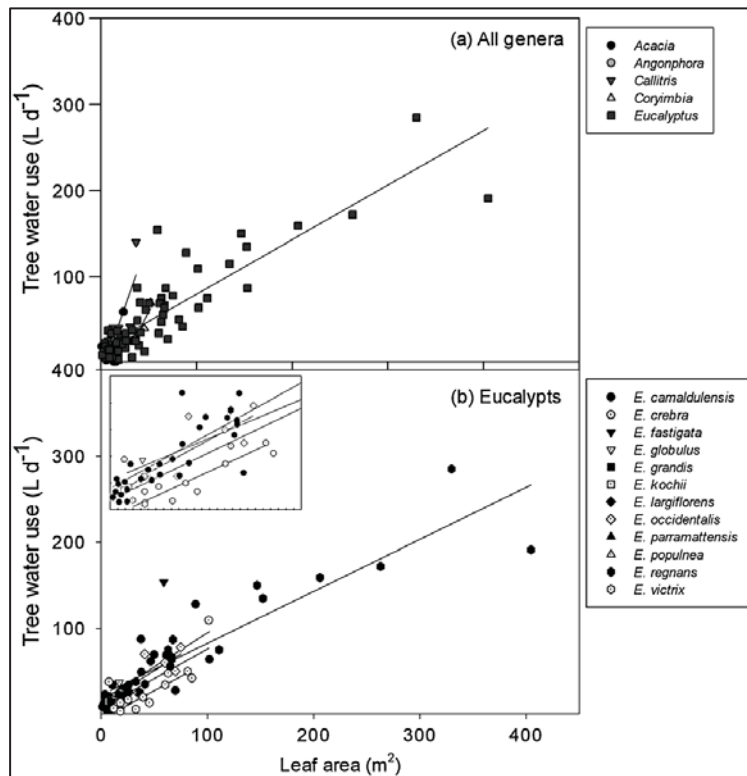


Figure 5-5: The relationship between leaf area (m^2) and tree water use ($L day^{-1}$), for (a) all genera and (b) eucalypts only. The inset in (b) shows a close-up of trees with leaf area to $150 m^2$ (Zeppel, 2013).

From the literature reviewed, there appears to be support for a strong relationship between LAI and tree water use of eucalypts that is similar across all species. However, this is under the following conditions

- Canopy closure
- Water limited conditions, at least for a part of the year
- Leaf areas are in equilibrium with rainfall; and
- Where tree water use is defined solely as the transpiration component of evapotranspiration.

In South Africa, with soil water limited conditions, soil water is recognised as primary factor influencing the growth of commercial plantations. In the South African environment, can soil water be sufficiently recharged where LAI (and thus water use) remain high throughout the rotation (Albaugh et al., 2013)? O’Grady et al. (2011), based on findings that vegetation which can access groundwater has a higher LAI, suggested that the use of the difference between LAI and the LAI attainable for that climate wetness index could be used to estimate groundwater discharge. Accounting for the use of groundwater under commercial tree stands in South Africa has been a long-standing area of concern in forestry water use estimations. Using LAI in the manner suggested by O’Grady et al. (2011) may have the potential to address this concern.

A South African study which has considered the relationship between LAI and transpiration for a tree crop is that by Gush and Moodley (2007). Although not a commercial tree plantation, Gush and Moodley (2007), as an alternative to modelling, demonstrated that the transpiration of *Jatropha curcas* could be determined from the LAI values (Figure 5-6). By fitting a third order polynomial equation through the LAI and transpiration (mm) measurements, Gush and Moodley (2007) derived an equation that could be used to determine transpiration (mm) from a LAI value. Building from this, the available LAI and evapotranspiration data from the Two Streams catchment was considered as a case study to investigate whether LAI could be used to explain evapotranspiration.

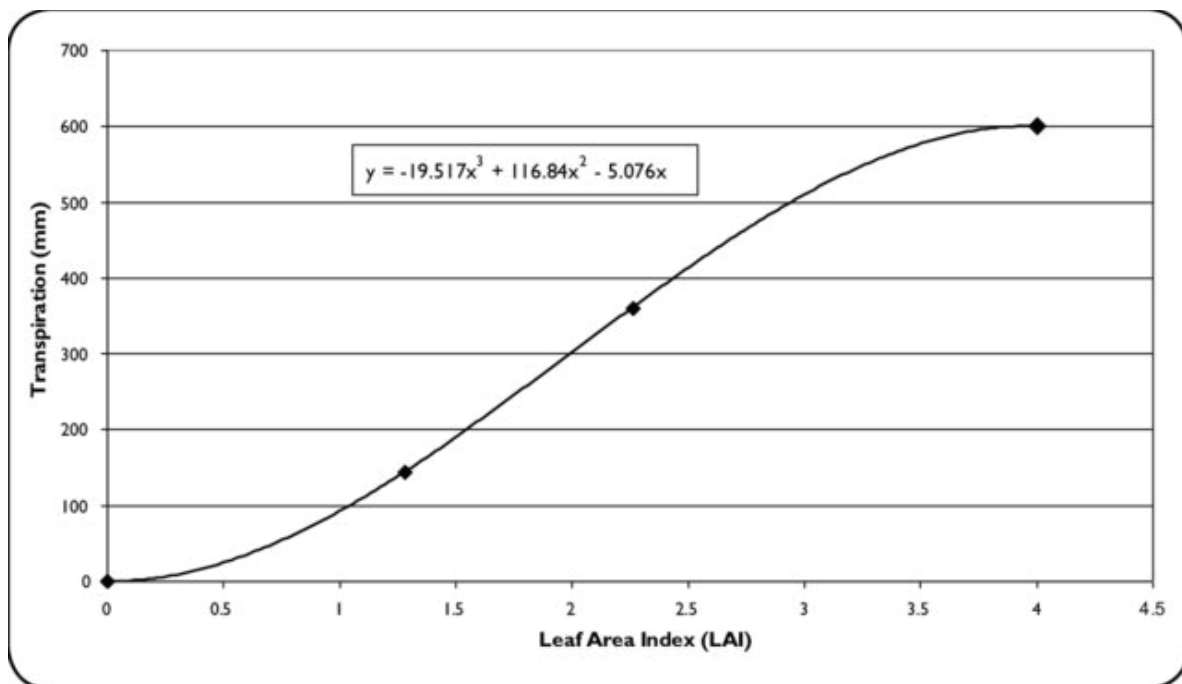


Figure 5-6: Relationship between Leaf Area Index and transpiration for different ages of *Jatropha curcas* trees (Gush and Moodley, 2007)

5.3 Estimating evapotranspiration from leaf area index: A case study from Two Streams Catchment

The Two Streams catchment experiments have been used over the past 17 years to study the impact of commercial trees on hydrological processes (Everson et al., 2008) with detailed observations and hydrological modelling. The observations from the catchment have provided a good opportunity to extend the understanding of hydrological processes such as low flows and deeper soil water dynamics under commercial tree plantations as well how hydrological models perform. Streamflow gauging was started in 1999 in a mature stand of wattle trees (*Acacia mearnsii*). Following a short calibration period, all the trees in the riparian zone were cleared in July 2000. The trees in the remainder of the catchment were removed in 2004/2005 and the catchment was replanted with wattle in August 2006. In 2014, a study was concluded on the impacts of the newly planted *A. mearnsii* rotation on the water balance of the catchment (WRC K5/2022). In November 2017 the trees were clear felled and a short WRC funded project (K5/2780) was undertaken to main monitoring leading up to the clear felling as well as determining the impacts of mature *A. mearnsii* on the water balance.

The Two Streams catchment is situated 70 km from Pietermaritzburg near Seven Oaks on the Greytown road. It is located in the summer rainfall 'midlands mistbelt grassland' Bioregion, with a mean annual precipitation that ranges from 659 to 1139 mm. The components of the hydrological cycle and variables are observed through the catchment include

- Streamflow which is monitored at a V-notch weir using a pressure transducer.
- Climatological variables at two Automatic Weather Station (AWS)
- Soil water contents
- Groundwater monitored in four boreholes were drilled in 2001 and 2007.
- Total evaporation monitored using an Eddy Covariance system mounted on a lattice mast erected close to the centre of the Wattle stand (6 ha). Transpiration has been measured for short periods of time.

Beyond this, the tree growth parameters have been monitored. The full records for these variables are presented in Everson et al. (2018). The in-situ data from the Two Streams catchment was used to investigate whether a relationship between LAI and evapotranspiration was evident.

Given the limited transpiration data available for the Two Streams catchment, the relationship between evapotranspiration and in-situ LAI was investigated (Figure 5-7). The assumption made is that once canopy closure of a commercial forest stand is reached, the soil water evaporation component of total evapotranspiration is minimal and transpiration is dominant. The data included in the analysis is from 2008 following canopy closure. Unfortunately, the number of LAI measurements taken were limited, only 16 of the 42 months for which evapotranspiration data existed had in-situ LAI measurements. The points inside the red circle on Figure 5-7 are the wetter summer months. No strong relationship between evapotranspiration and in-situ LAI was evident from the limited data included. Given the sparsity of the in-situ LAI measurements, remotely sensed LAI values obtained from the MODIS satellite were considered.

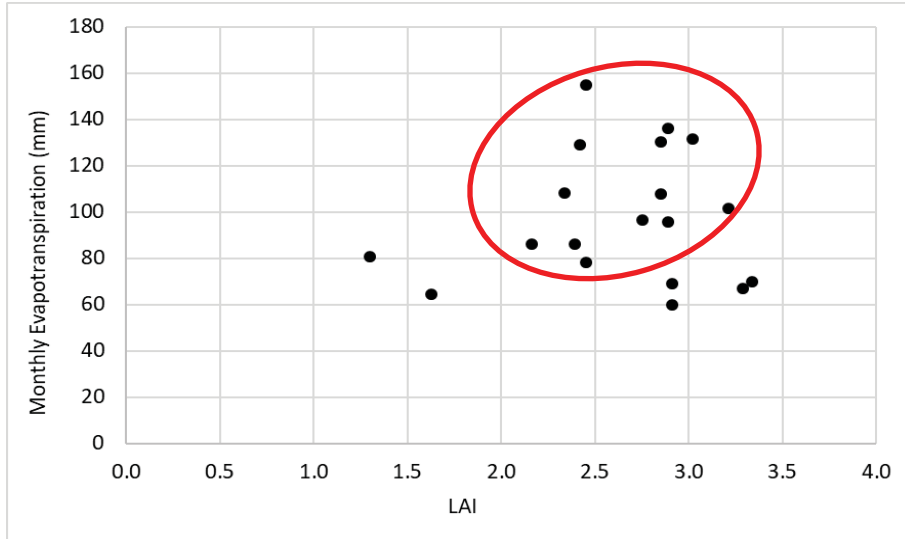


Figure 5-7: Plot of in-situ monthly LAI against monthly evapotranspiration (mm) for the Two Streams catchment (periodic data from 2008-2017)

The mean monthly MODIS LAI values for the Two Stream catchment were obtained for the months that in-situ evapotranspiration data were available. The mean monthly remotely sensed LAI was plotted against the 42 monthly evapotranspiration values (Figure 5-8). A linear relationship between LAI and evapotranspiration was evident, however, it was not strong with only 60% of the variation in evapotranspiration being explained by the mean monthly LAI values. A possible contributor to the weak relationship would be the resolution of the MODIS images as the pixels extended beyond the catchment. The preference would be to investigate the Sentinel-2 LAI data, unfortunately this data is only available from 2015 onwards which would only provide 5 points to test on. Referring back to the literature review, for the relationship between LAI and tree water use to hold canopy closure is needed. The tree species was *A. mearnsii*, and it was considered to have reached canopy closure by the end of 2007. However, the canopy is not as dense as eucalypt species and it was noted that towards the end of the rotation (2017) several trees had already died, possibly contributing to the weak relationship. Without canopy closure, the measured evapotranspiration used was not solely transpiration as there would have been soil water evaporation. Thus, the criteria that tree water use be solely transpiration for the relationship to be held was not met. Additionally, the criteria identified from the literature that the LAI be in equilibrium with the rainfall was not met. Although there is a response of the LAI values to the drier, winter months the response appears to be lagged.

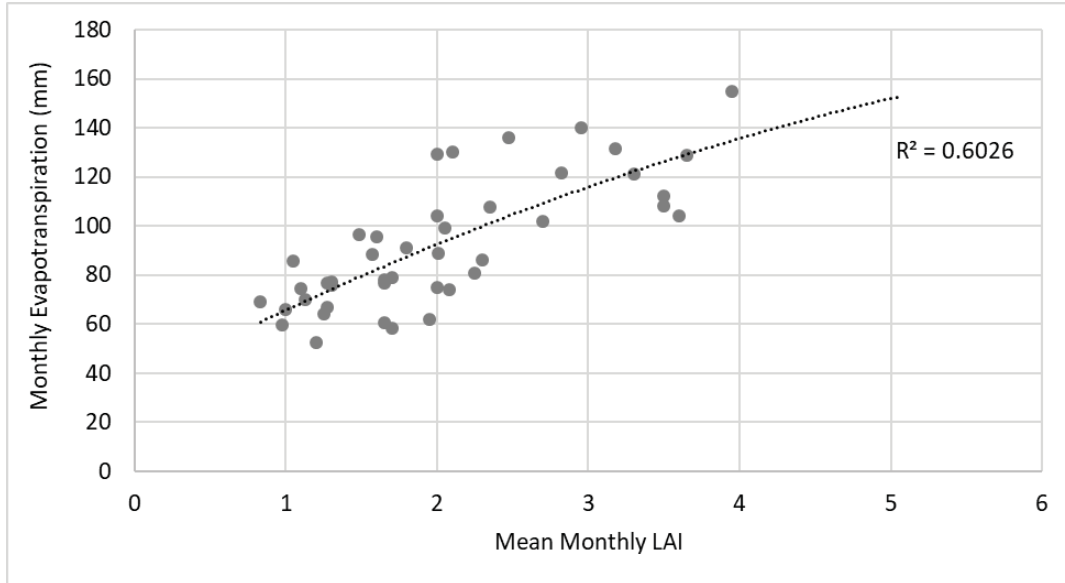


Figure 5-8: Plot of remotely sensed mean monthly LAI against monthly evapotranspiration (mm) for the Two Streams catchment (periodic data from 2008-2017)

Despite this, however, there does appear to be a relationship between LAI and evapotranspiration which needs to be further explored as more data becomes available and, together with the strong evidence from the literature of a relationship between LAI and tree water use, there is justification for using LAI to describe water use. The first step towards achieving this was to determine if finer resolution remotely sensed LAI values for a long time period could be obtained.

5.4 Deriving moderate spatial resolution leaf area index estimates from coarser spatial resolution satellite products¹

5.4.1 Introduction

Commercial afforestation in South Africa (SA) is a major contributor to employment and the country's GDP, however, there exists a long history of concern regarding its impacts on water resources. Extensive research has been undertaken within SA which has contributed to commercial afforestation being declared a streamflow reduction activity (SFRA) in the National Water Act of South Africa (1998). Consequently, this industry is now highly regulated, with water use licenses being required for the growth of commercial trees (Nänni, 1970; Van der Zel, 1995; Scott et al., 1998; Gush et al., 2002; Dye and Versfeld, 2007; Jewitt et al., 2009).

The research which the regulations governing commercial afforestation activities were based on, centred around the impacts of three species (*Pinus patula*, *Eucalyptus grandis* and *Acacia mearnsii*) on streamflow. However, the forestry industry currently uses 17 *Pinus*, 26 *Eucalyptus* and 3 *Acacia* species, hybrids and clones (Toucher and Everson, 2018). Furthermore, in some plantations there has been a shift towards utilizing certain species over others (for e.g. replacing *Pinus spp.* with *Eucalyptus spp.*) due to current timber

¹ This sub-chapter is a paper that has been submitted to Remote Sensing Applications Society and Environment. The paper is currently under review. The text as it stands here is the same as that submitted to the journal with the authors of Chapter 5 as the authors of the paper.

demands. This has become quite a contentious issue and has raised a number of concerns regarding the impact of this practice on water resources.

Subsequently, there is an urgent need for further research to better understand the biophysical characteristics and hydrological impact of these species, hybrids and clones so that the tools which are used as decision support systems to issue water use licences, can be updated and adapted accordingly (Toucher and Everson, 2018). For such purposes, the accurate quantification of Leaf Area Index (LAI) can play an important role as it is a key parameter used to characterize vegetation biophysical characteristics and is an essential component which influences exchanges in energy, water and CO₂ between terrestrial environments and the atmosphere (Bonan, 1993; GCOS, 2011). LAI is defined as the total single-sided leaf area per unit ground area (Myneni, 2002) and is often a critical data input to various evapotranspiration, hydrological and climatic models (Törnros and Menzel, 2014; Fang et al., 2019a; Pasqualotto et al., 2019; Zhai et al., 2020; Zhang et al., 2020).

Despite its importance, spatially and temporally explicit LAI data records are not always readily available in SA particularly for the various species, hybrids and clones used by the forestry industry. This situation is quite problematic as the tool used to guide and inform the issuing of water use licenses in SA relies on outputs from a hydrological model where LAI is an essential input variable. Subsequently, the ability to accurately quantify LAI can play a central role in updating and improving existing tools to better understand and quantify the hydrological impacts of commercial afforestation activities.

LAI data can be acquired from field-based measurements or from remotely sensed estimates. However, the acquisition of LAI via remote sensing (satellite-earth observation, aerial and un-manned aerial) platforms is generally more popular due to the laborious, costly and sometimes destructive nature of field-based approaches. Furthermore, remote sensing allows for longer term and larger scale estimation of LAI with minimal effort (Alexandridis et al., 2013; Clevers et al., 2017; Dube et al., 2019; Qiao et al., 2019). Remote sensing of LAI is based on the hypothesis that LAI increases with increased vegetation biomass, eliciting an increase in reflectance and absorption of light in the near infra-red and red regions of the electromagnetic spectrum, respectively (Knyazikhin et al., 1999).

Remote sensing of LAI can be broadly classified into two categories (Yin et al., 2015; Alexandridis et al., 2019): i) empirical methods which are based on the statistical relationship between vegetation indices (VIs) and LAI and ii) physically based approaches which rely on the inversion of radiative transfer models (RTMs). RTMs attempt to describe spectral variations in canopy reflectance as a function of vegetation and soil characteristics based on knowledge pertaining to physical processes governing photon transport within the vegetation canopy (Yin et al., 2015). Additionally, hybrid models have also been developed to create integrated LAI models which aim to combine the strengths of the aforementioned methods (Yin et al., 2015; Alexandridis et al., 2019). Global satellite-derived LAI products such as MODIS, GLASS, GEOV2, GLOBMAP, PROBA-V and VIIRS have become increasingly available and used over the past decade, playing a pivotal role in providing input to terrestrial-ecosystem and land-surface models (Fang et al., 2019b). The relatively high temporal resolution (4-10 days) and record length of these products makes them well-suited to monitor long-term trends, as well as intra- and inter-annual variations of LAI in response to climatic and phenological changes (Meyer et al., 2019).

However, their coarse spatial resolution (≥ 250 m) is not well suited for localised applications as pixel sizes may exceed the size of the area of interest, subsequently this has limited their use to predominantly global and regional studies (Ganguly et al., 2012; Ovakoglou et al., 2020; Pasqualotto et al., 2020; Zhang et al., 2020). More recently, it has become possible to generate LAI data at finer spatial resolutions (20 m) by processing Sentinel-2 imagery using tools available within the Sentinel Application Platform (SNAP).

However, the Sentinel-2 satellite has only been in orbit since 2015 and thus it is not possible to derive moderate spatial resolution LAI data prior to this date (Ovakoglou et al., 2020).

A common approach to address these limitations has been to use statistical approaches using vegetation indices (VIs) to estimate LAI (Alexandridis et al., 2019), since VIs can be generated fairly easily at various spatio-temporal resolutions using satellite-imagery and are often used in conjunction with or as an alternate to LAI to monitor and evaluate vegetation characteristics (Meyer et al., 2019; Ovakoglou et al., 2020). Although several studies have successfully demonstrated how satellite-derived VIs can be used for the estimation of LAI for global, regional and localised applications (Gao et al., 2012; Clevers et al., 2017; Alexandridis et al., 2019; Meyer et al., 2019; Padalia et al., 2019; Ovakoglou et al., 2020; Pasqualotto et al., 2020), data collection, storage and processing, particularly for long-term time series analyses may create barriers to many users that lack the computational power and technical abilities to effectively utilise these datasets (Gorelick et al., 2017; Robinson et al., 2017; Chen and Wang, 2018).

Recent advancements in geospatial cloud-based computing platforms, most notably Google Earth Engine (GEE) have removed many of these barriers allowing for a wider range of users to access, process and disseminate data (Frake et al., 2020). Furthermore, convenient machine learning packages are now becoming increasingly available which offer greater opportunities to more effectively analyse and utilise these information rich satellite earth observation datasets (Houborg and McCabe, 2018; Shao et al., 2021). Considering these advancements, we aim to explore and evaluate the potential of using GEE and machine learning to acquire moderate-spatial resolution estimates of LAI (LAI_{MR}) for various species, hybrids and clones used by the commercial forestry industry in SA.

The objective of this study is two-fold. Firstly, to establish whether the use of freely available satellite-earth observation data can be used to provide LAI_{MR} estimates in data limited circumstances for localised applications and then produce LAI_{MR} estimates for select commercial forest plantations situated within the KwaZulu-Natal and Mpumalanga provinces of SA.

5.4.2 Materials and methods

5.4.2.1 Study Area

The study sites are located within the eastern region of SA, with 10 of these situated in the KwaZulu-Natal (KZN) province and 5 situated in the Mpumalanga province (Figure 5-9). Altitude within KZN ranges from 0 to 3448 m.a.s.l along the eastern coastal and western escarpment regions, respectively (DWA, 2013). The topographical range has contributed to a varied climate, with warm sub-tropical conditions experienced along the coastal regions and progressively cooler conditions experienced further inland and towards the mountainous regions (DWA, 2013). KZN experiences relatively high rainfall, with mean annual precipitation ranging from 800-1500 mm. The majority of rainfall occurs during the summer months as thunderstorms (Kapangazwiri et al., 2017). Snowfall is also experienced occasionally in the high lying mountainous regions. Mean annual temperatures range from 25°C summer to 20°C in winter (Ndlovu and Demlie, 2020).

The 10 KZN study sites fall within the Pongola-uMzimkhulu water management area (WMA), which is quite a complex WMA to manage, as there is a high demand for water resources from various sectors such as agriculture, commercial afforestation, industry, mining, urban and domestic users. This WMA is a crucial contributor to SA's total water resources, accounting for approximately 40% of the total water availability (DWA, 2013). Furthermore, there are a number of rivers which flow through this WMA that share their catchments with neighbouring countries. Therefore, it is important that water resources within the

province are carefully managed to ensure that needs of all users are adequately met without threatening the sustainability of the resource.

The 5 Mpumalanga study sites are located within the south-eastern region of the Inkomati-Usutu WMA. Altitude within Inkomati-Usutu WMA ranges from 140 to above 2000 m.a.s.l (DWA, 2012). A majority of this WMA experiences a warm sub-tropical climate. Mean annual precipitation ranges from 400-1200 mm, with higher rainfall being received in the elevated western regions (DWA, 2012). Commercial afforestation is one of the largest consumers of water resources within the WMA, requiring approximately 13% of available water resources. According to DWA (2012), large portions of the WMA regularly experience water stress. Therefore, managing water resource allocations to the various competing users is a complex endeavour. This situation is further complicated by having to ensure that the water resources requirements of Mozambique and Swaziland are factored into management decisions (DWA, 2021).

Considering, the importance and complexity of managing the Pongola-uMzimkhulu and Inkomati-Usutu WMAs in concert with the impact of commercial afforestation on water resources, these study sites are ideally situated to test and evaluate the methodology proposed in this study as commercial forest plantations are a prominent feature within these provinces (Dye, 2013). The study sites were distributed between three climatically diverse zones and were selected based on the age of the commercial trees grown at each site, as well as the geographic extent of coverage. The rationale for this was to ensure that i) there was adequate representation of species, hybrids or clones within each climate zone ii) satellite-derived data covered different phenological growth stages and iii) the mixed-pixel effect would be potentially limited by allowing for data to be extracted from pure-pixels.

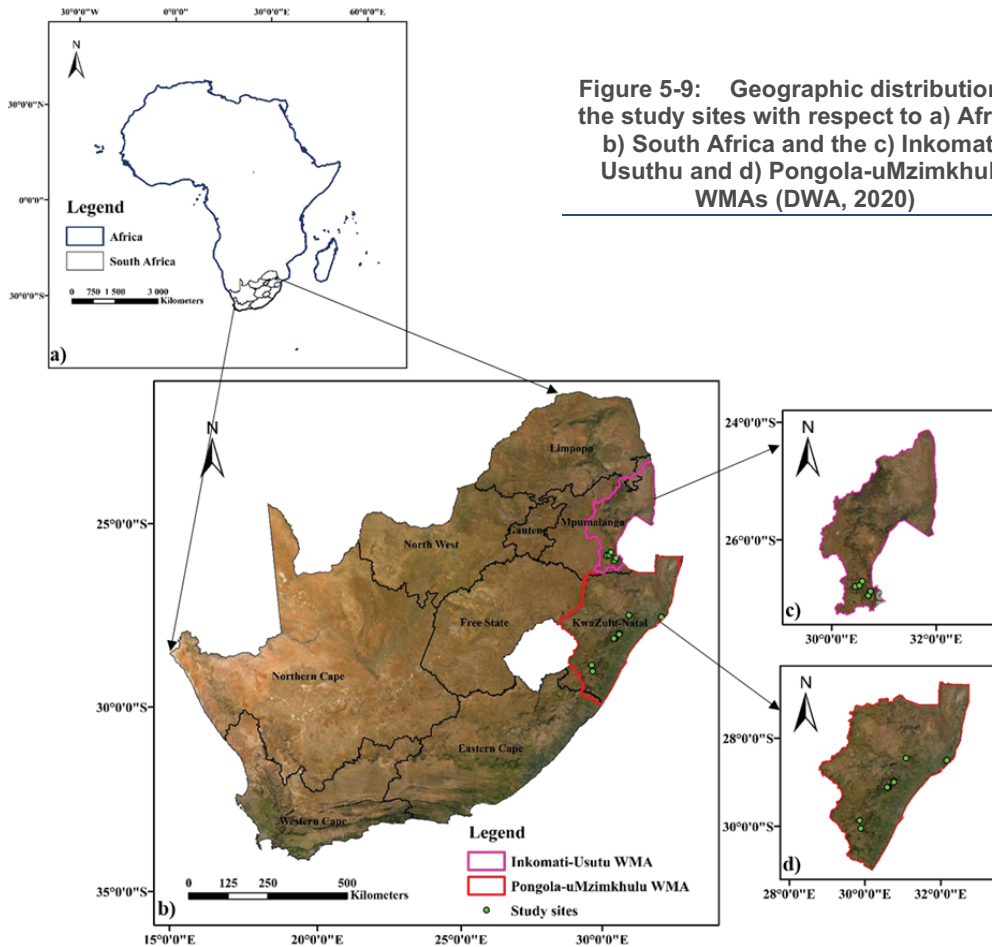


Figure 5-9: Geographic distribution of the study sites with respect to a) Africa, b) South Africa and the c) Inkomati-Usuthu and d) Pongola-uMzimkhulu WMAs (DWA, 2020)

5.4.2.2 Data collection and processing

Downscaling of coarse spatial resolution satellite-derived LAI products is often implemented to acquire higher spatial resolution LAI estimates, since spatially and temporally representative in-situ measurements of LAI are generally unavailable to develop and test algorithms. Downscaling of these LAI products usually involves the use of VIs that are derived at a finer spatial resolution to enhance the spatial information of the coarser resolution LAI product (Zhang et al., 2020).

The normalized difference vegetation index (NDVI) and enhanced vegetation index (EVI) have been most frequently used for this purpose. However, the use of EVI may be preferred due to the saturation of NDVI at medium to high LAI values (Wang et al., 2005; Alexandridis et al., 2019; Qiao et al., 2019; Ovakoglou et al., 2020). While several studies have successfully demonstrated how these VIs can be used to estimate LAI (Qiao et al., 2019), they typically use only one VI. Since both VIs are relatively easy to generate, we propose their combined application for LAI estimation in an attempt to maximize their respective strengths (Cohen et al., 2003; Middinti et al., 2017).

Satellite-earth observation datasets were accessed and processed using the GEE platform. GEE is a freely available, cloud computing platform which enables access to high-performance computing power for planetary-scale geospatial analysis (Gorelick et al., 2017). GEE provides users with easy access to a multi-petabyte curated catalogue of earth observation data sets, built-in algorithms for manipulating and analysing data, as well as a programming interface to create, customize and automatically run algorithms (Padarian et al., 2015; Gorelick et al., 2017; Sidhu et al., 2018). Additionally, users are able to ingest and process their own data using all of the aforementioned features available within the platform (Gorelick et al., 2017).

Figure 5-10 provides a schematic representation of the methodological process to better understand how the proposed methodology was executed. In order to generate LAI_{MR} estimates from coarse resolution products, ≈ 2350 MODIS LAI (MCD15A3H V6 level 4, 500 m spatial and 4-day temporal resolution) and Terra vegetation indices (MOD13A1 V6, 500 m spatial and 16-day temporal resolution) image collections were accessed and then filtered to select good quality images for each study site and for a particular date range (dependent on tree age within the period 2002-2021). Thereafter the mean LAI, NDVI and EVI for each image within the specified date range were then exported as a comma-separated values (CSV) file for further analysis.

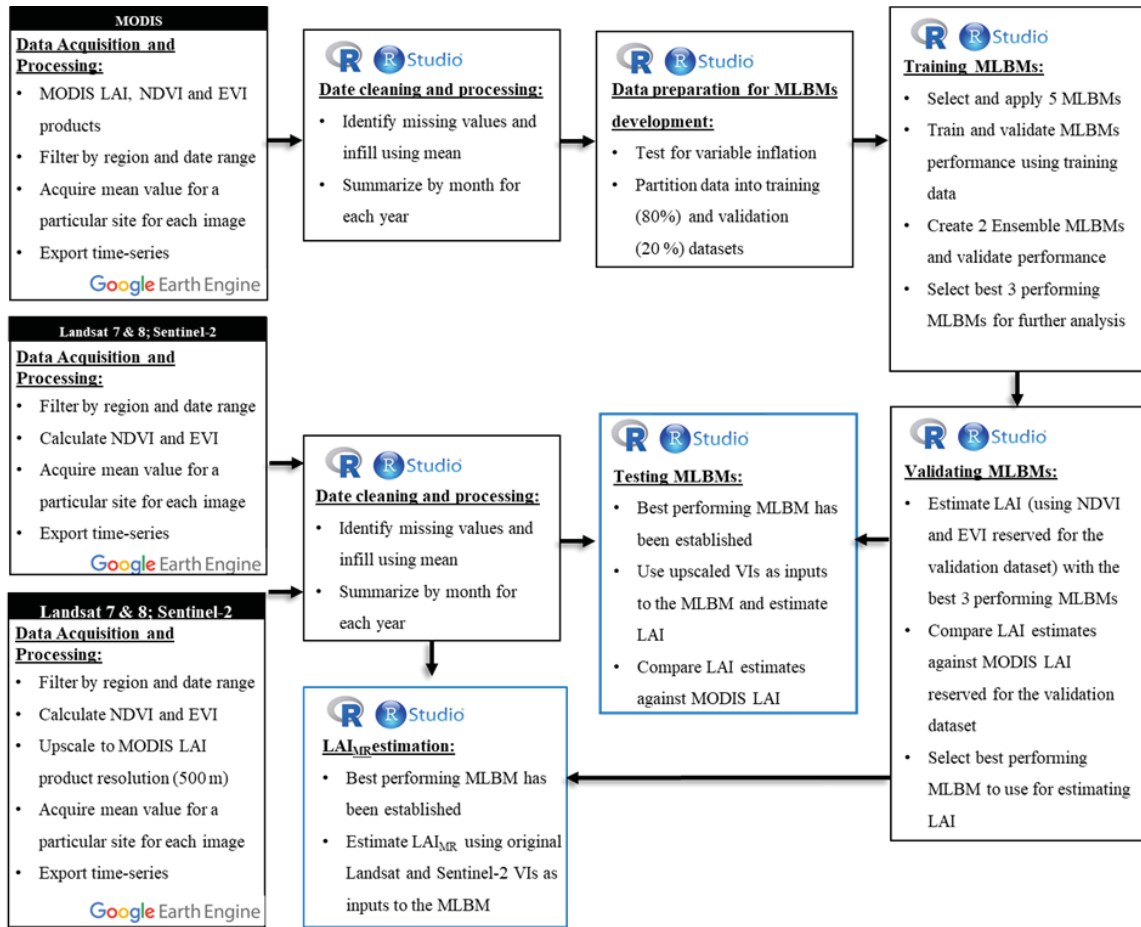


Figure 5-10: A graphical representation of the procedure that was applied to generate LAI_{MR}

Once the coarse spatial resolution data had been acquired, ≈ 1300 Landsat 7 and 8 (Collection 1 Tier 1 calibrated top-of-atmosphere reflectance, 30 m spatial and 16-day temporal resolution), as well as ≈ 840 Sentinel-2 (MultiSpectral Instrument, Level-1C, 10 m spatial and 5-day temporal resolution) collections were then respectively imported directly into GEE. A similar pre-processing process was followed, where NDVI and EVI was generated for both Landsat (7 and 8) and Sentinel-2 using the following equations:

$$NDVI = \frac{NIR - Red}{NIR + Red} \quad (5.3)$$

$$EVI = 2.5 \left[\frac{NIR - Red}{(NIR + 6Red - 7.5Blue + 1)} \right] \quad (5.4)$$

Where *NIR* (near-infrared) and *Red* and *Blue* are the atmospherically corrected surface reflectances. Figure 5-11 provides a comparison of the spatial resolution characteristics of the VIs derived from the satellite datasets.

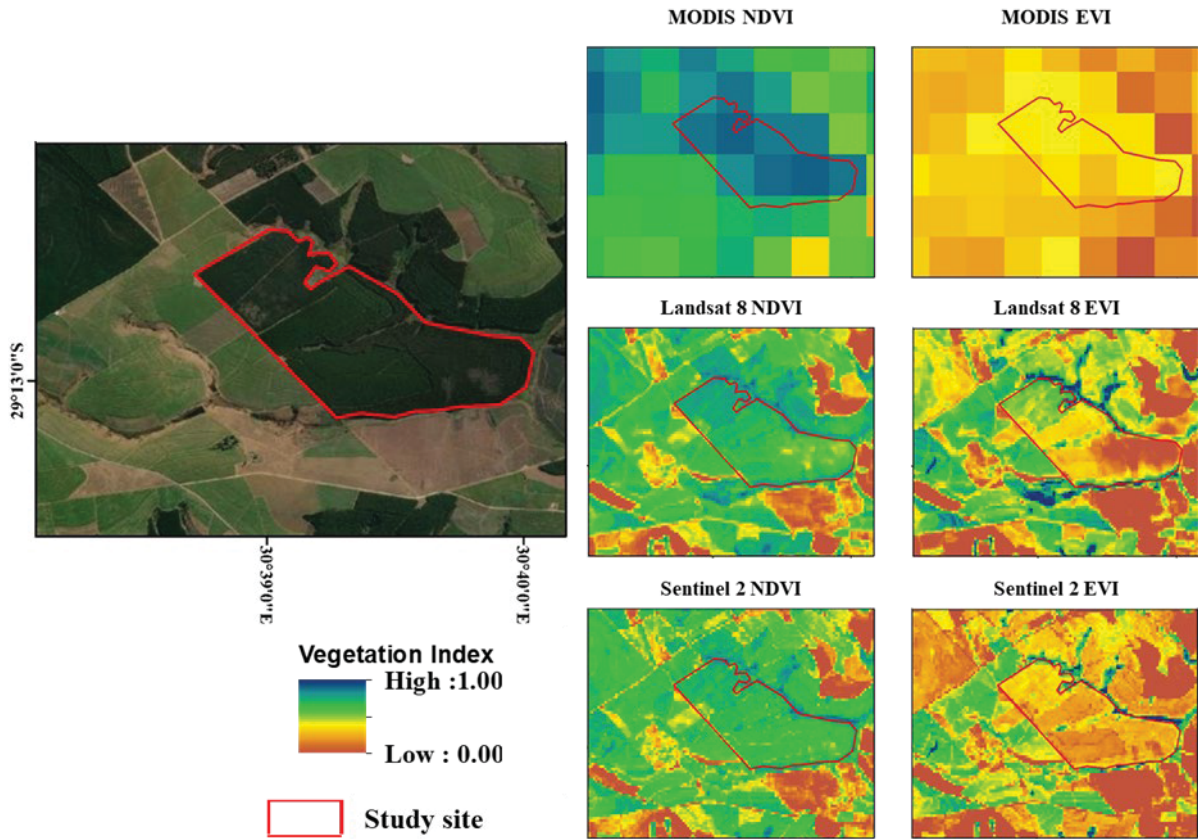


Figure 5-11: An illustration of the spatial resolution characteristics of the VIs acquired over a commercial forestry compartment situated within the Pongola-uMzimkhulu WMA

Once all the necessary satellite-derived data had been acquired, the data needed to be cleaned and processed further prior to the development of machine learning-based models (MLBMs) which were used to estimate LAI from NDVI and EVI.

For this purpose, R statistical software was used. The data was first checked to infill missing values with the mean value for a particular variable. Since there were differences in the temporal resolution of the variables within and between the MODIS, Landsat and Sentinel-2 datasets, they were summarized to create mean monthly values for each year within the collection period to allow for uniformity. Thereafter, the classification and regression training (Caret) (Kuhn, 2008) and caretEnsemble (Mayer, 2013) packages available as an add-in to R were used to develop and test the MLBMs. These machine learning packages facilitate the quick and efficient development and evaluation of machine learning algorithms, as it integrates all the tools necessary to perform both simple and complex machine learning tasks. The processed MODIS data was used within the machine learning packages to establish the relationship between LAI, NDVI and EVI and train the MLBMs to estimate LAI using NDVI and EVI estimates (Gao et al., 2012; Ovakoglou et al., 2020).

Prior to the training of the MLBMs, the EVI and NDVI were tested for the possibility of multicollinearity existing between them. A variable inflation score test was performed to establish how much the variance of a regression coefficient may be inflated due to multicollinearity in the MLA model. The results of this test indicated that multicollinearity between these variables was not an issue for 14 out of the 15 sites or for the combined dataset (values from all 15 sites). Following this test, the MODIS product data was split into

training (80%) and validation (20%) samples since we did not possess any long-term field-based measurements to validate or test the performance of the MLBMs against. Furthermore, by withholding some of the data from the MLBMs during the training phase, it was possible to get a better indication of how well these models will perform on unseen data.

During the training phase, a mix of simple and complex machine learning algorithms were selected from Caret for application, these included i) generalized linear model (GLM), ii) decision tree (CART), iii) k nearest neighbour (kNN), iv) random forest (RF) and v) support vector machine (SVM). In addition to these algorithms, two new MLBMs were created to find the best possible predictive model. For this purpose, the aforementioned MLBMs were considered as the base algorithms for the development of model ensembles. In order to determine which base algorithms should be used to develop the ensemble models we evaluated the performance of each MLBM, as well as analysed the correlation between the MLBMs. The two ensemble models were developed by stacking selected base algorithms and combining their predictions using a GLM and RF approach, respectively.

A 10-fold cross validation with 3 repeats was used to evaluate the performance of the original MLBMs and ensemble models based on the training data. The three best performing models were then selected and used for the validation phase. Estimations of LAI were made using NDVI and EVI values obtained from the validation dataset and these estimates were then evaluated against MODIS LAI product values. The best performing MLBM was then selected to estimate LAI using estimates of NDVI and EVI derived from Landsat and Sentinel-2 data. LAI was first estimated using the best performing MLBM with Landsat and Sentinel-2 derived estimates of NDVI and EVI that were upscaled (Ke et al., 2016; Zhang et al., 2020) in GEE to the MODIS LAI spatial resolution. The rationale for upscaling Landsat and Sentinel-2 derived VIs prior to the estimation of LAI was so that the estimated LAI could be evaluated against MODIS LAI product values, as these were the only long-term records available.

Following this process LAI_{MR} was estimated using the NDVI and EVI estimates derived at the original Landsat and Sentinel-2 spatial resolutions, respectively. It should be noted that the methodological approach described herein was undertaken for each study site, as well as for a combined dataset (all sites), subsequently allowing for both unique and a generalized MLBM to be developed, validated and tested. Evaluation of the MLBM performance was assessed using commonly applied machine learning performance metrics such as the correlation coefficient (r), root mean square error (RMSE), mean absolute error (MAE) and the non-parametric Kruskal-Wallis test (95% confidence interval). Acceptable target ranges for the performance evaluation and subsequent descriptions of the results are contextualized with respect to the findings presented in Ovakoglou et al. (2020) and Zhang et al. (2020).

5.4.3 Results

5.4.3.1 Validation of machine learning-based models

The results of the comparisons between the MODIS LAI product values and LAI estimates derived using MODIS VIs are presented in Table 5-1 and Figure 5-12 for each of the sites selected in the Cool Temperate Moist (CTM), Warm Temperate Dry (WTD) and Warm Temperate Moist (WTM) climatic zones. Correlation coefficients across all 15 sites were relatively high and ranged from 0.62 to 0.97, whereas the RMSE (0.13-0.71) and MAE (0.11-0.60) were low-moderate. Furthermore, there were no significant differences found between the MODIS LAI and estimated LAI for all 15 sites. A similar level of performance was observed for the generalized LAI model with a moderately high correlation coefficient of 0.78 and no significant differences found between the MODIS LAI and estimated LAI. However, there were marginal increases in the RMSE and MAE.

Table 5-1: Performance statistics for the comparisons between the MODIS LAI reserved for validation and LAI estimated from MODIS VIs using the best performing MLBM,* denotes detection of multicollinearity

Site	Species, Clone or Hybrid	Model	RMSE	r	MAE	Kruskal-Wallis p-value
All	All	Ensemble1	0.83	0.78	0.61	0.50
CTM 1	<i>E. benthamii</i>	Ensemble1	0.25	0.85	0.19	0.50
CTM 2	<i>E. grandis</i> x <i>E. nitens</i>	GLM	0.57	0.62	0.40	0.50
CTM 3	<i>E. macathurii</i>	SVM	0.20	0.87	0.15	0.50
CTM 4*	<i>E. nitens</i>	GLM	0.17	0.91	0.13	0.50
CTM 5	<i>P. patula</i>	Ensemble2	0.48	0.86	0.38	0.50
WTD1	<i>E. grandis</i>	Ensemble1	0.26	0.86	0.20	0.40
WTD2	<i>E. grandis</i> x <i>E. nitens</i>	kNN	0.59	0.95	0.40	0.40
WTD3	<i>A. mearnsii</i>	Ensemble 1	0.28	0.92	0.24	0.50
WTD4	<i>E. dunii</i>	RF	0.13	0.97	0.11	0.40
WTD5	<i>P. Elliottii</i>	Ensemble1	0.30	0.89	0.26	0.50
WTM1	<i>E. grandis</i>	GLM	0.50	0.83	0.41	0.50
WTM2	<i>E. grandis</i> x <i>E. urophylla</i>	GLM	0.45	0.86	0.34	0.50
WTM3	<i>P. elliotii</i> x <i>P. caribaea</i>	Ensemble1	0.71	0.69	0.60	0.50
WTM4	<i>P. patula</i>	kNN	0.27	0.87	0.20	0.40
WTM5	<i>P. taeda</i>	Ensemble1	0.28	0.94	0.23	0.50

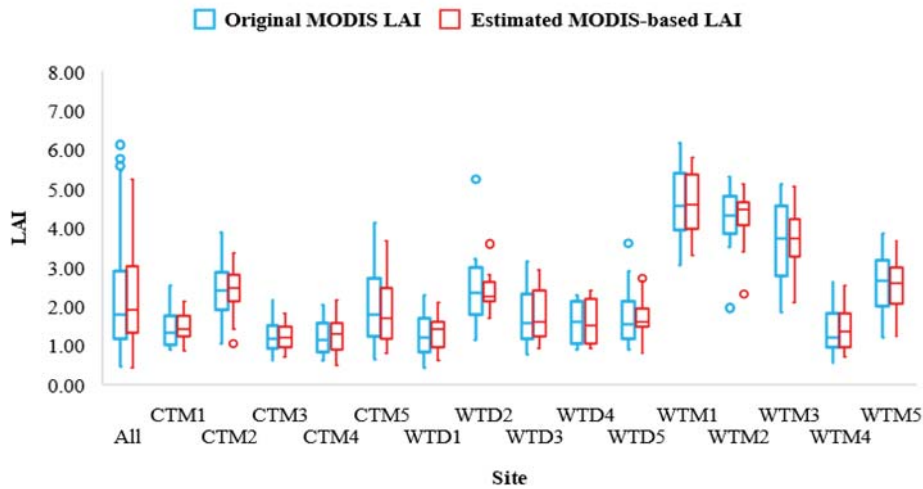


Figure 5-12: Box and whisker diagram comparing the distribution of MODIS LAI reserved for validation and LAI estimated from MODIS VIs using the best performing MLBM

5.4.3.2 Testing of machine learning-based models and deriving moderate spatial resolution LAI estimates using Landsat and Sentinel-2 data

The results of the comparisons between the MODIS LAI product values and estimated LAI demonstrated a satisfactory performance of the MLBMs that were driven by upscaled Landsat-derived VI inputs (Table 5-2 and Figure 5-13). In general, there were no significant differences between the MODIS LAI and estimated LAI. Correlation coefficients across all 15 sites remained moderate-high and ranged from 0.54 to 0.84. However, there was a noticeable increase in the range of RMSE (0.23-1.20) and MAE (0.17-1.07) relative to

the statistics obtained during the validation process. A similar level of performance was observed for the generalized LAI MLBM with a moderately high correlation coefficient of 0.68 and no significant differences found between the MODIS LAI and estimated LAI. In addition, both RMSE and MAE were relatively high.

Table 5-2: Performance statistics for the comparisons between the MODIS LAI and LAI estimated by the MLBMs using upscaled Landsat-derived VIs as inputs

Site	RMSE	r	MAE	Kruskal-Wallis <i>p</i> -value
All	1.09	0.68	0.90	0.20
CTM 1	0.34	0.78	0.29	0.50
CTM 2	0.42	0.75	0.31	0.50
CTM 3	0.35	0.75	0.31	0.50
CTM 4	0.23	0.84	0.17	0.50
CTM 5	1.04	0.54	0.91	0.50
WTD1	0.36	0.74	0.30	0.00
WTD2	0.76	0.57	0.52	0.00
WTD3	0.61	0.68	0.49	0.60
WTD4	0.57	0.78	0.39	0.10
WTD5	0.45	0.70	0.36	0.50
WTM1	1.20	0.68	1.04	0.50
WTM2	0.81	0.55	0.64	0.50
WTM3	0.92	0.76	0.75	0.30
WTM4	0.37	0.68	0.28	0.00
WTM5	0.48	0.76	0.39	0.40

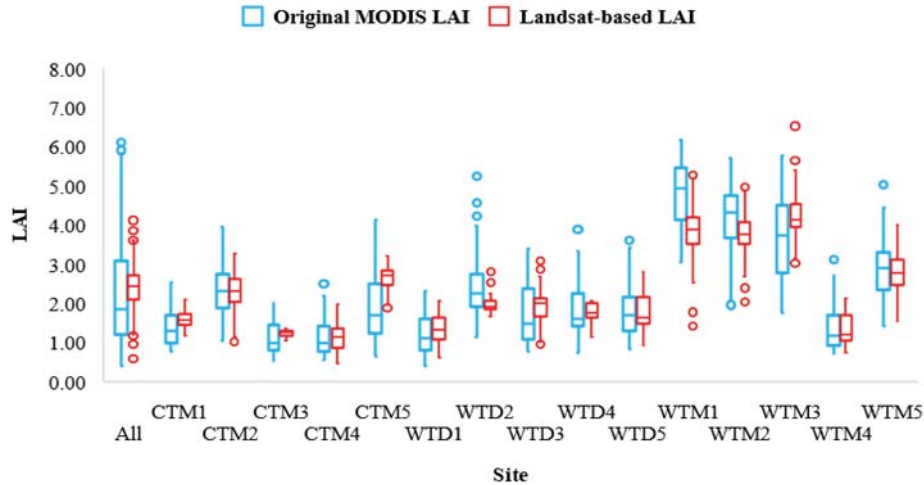


Figure 5-13: Box and whisker diagram comparing the distribution of MODIS LAI against Landsat-based LAI

A satisfactory performance was also observed for comparisons between the MODIS LAI and estimated LAI using upscaled Sentinel-derived VI inputs (Table 5-3 and Figure 5-14). In general, there were no significant differences between MODIS LAI and estimated LAI. Correlation coefficients ranged from 0.29-0.84, whereas the RMSE and MAE ranged from 0.25-1.20 and 0.19-1.06, respectively.

The use of the generalized LAI MLBM showed a similar level of performance, producing a moderately high correlation coefficient of 0.68 and relatively high RMSE and MAE.

Table 5-3: Performance statistics for the comparisons between MODIS LAI and LAI estimated by the MLBMs using Sentinel-derived VIs as inputs

Site	RMSE	r	MAE	Kruskal-Wallis <i>p</i> -value
All	1.07	0.68	0.79	0.20
CTM 1	0.25	0.79	0.19	0.50
CTM 2	0.52	0.76	0.39	0.50
CTM 3	0.36	0.63	0.30	0.40
CTM 4	0.31	0.58	0.25	0.50
CTM 5	0.64	0.71	0.55	0.40
WTD1	0.82	0.29	0.71	0.40
WTD2	0.77	0.78	0.55	0.00
WTD3	0.56	0.73	0.38	0.40
WTD4	0.64	0.77	0.43	0.50
WTD5	0.51	0.84	0.39	0.40
WTM1	1.20	0.70	1.06	0.40
WTM2	0.94	0.47	0.76	0.40
WTM3	0.57	0.84	0.49	0.40
WTM4	0.46	0.65	0.34	0.40
WTM5	0.75	0.66	0.58	0.40

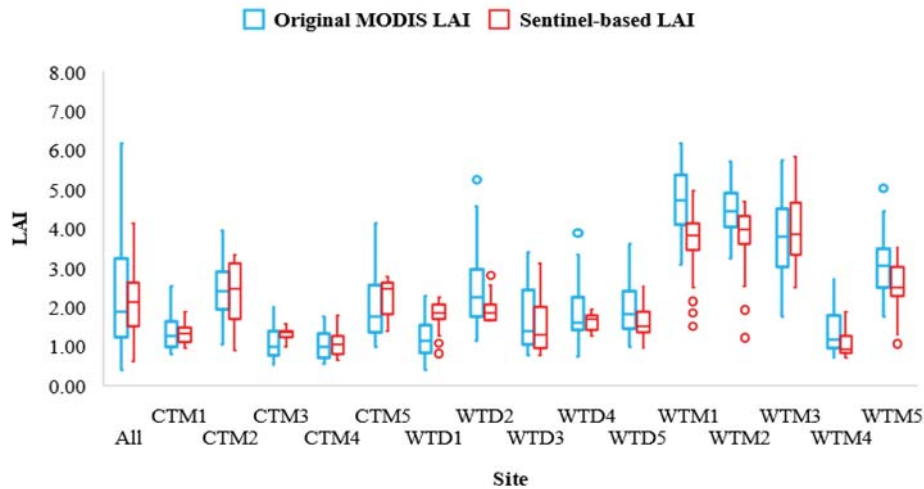


Figure 5-14: Box and whisker diagram comparing the distribution of MODIS LAI against Sentinel-based LAI

Monthly averages of Landsat, as well as Sentinel-2 LAI_{MR} estimates for each study site are presented in Figure 5-15. Monthly averages of Landsat LAI_{MR} ranged from 0.87-4.92, whereas Sentinel-2 LAI_{MR} ranged from 0.71-4.68. In general, the monthly averaged Landsat LAI_{MR} estimates were marginally higher than the Sentinel-2 LAI_{MR} estimates, however, the results of the Kruskal-Wallis test indicated that there were no significant differences between these data sets (*p*-value = 0.49).

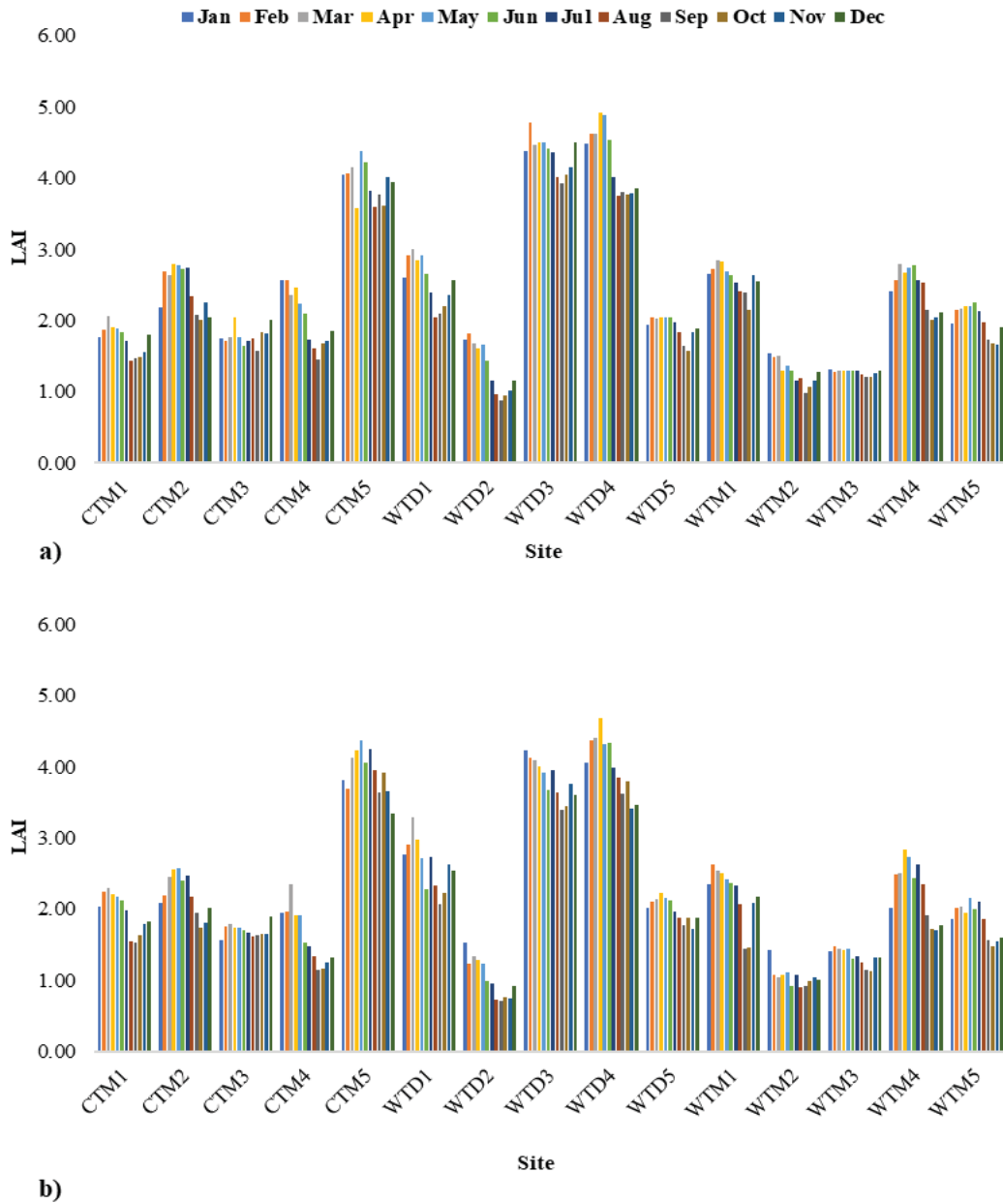


Figure 5-15: A comparison of average monthly LAI_{MIR} estimates derived at the original a) Landsat (7 and 8) and b) Sentinel-2 spatial resolutions

5.4.4 Discussion

Leaf Area Index (LAI) is a key parameter used to characterize vegetation biophysical properties and plays an important regulatory role in terrestrial-atmospheric exchanges. Despite the importance of LAI data for various environmental modelling applications, from a South African perspective, this data is often not available at spatio-temporal scales required to guide and inform management decisions for localised applications. In light of this situation, we proposed a methodology that can be implemented to acquire LAI_{MIR} estimates by making use of freely available satellite-earth observation data sets and data processing platforms. The rationale for this was to develop an approach that was both efficient and easily accessible to a wide range of users.

In general, the validation results demonstrated that LAI can be fairly accurately estimated by MLBMs that are driven by VIs and thus have the potential to enhance the spatial resolution of coarse resolution LAI products through the use of VIs derived from finer spatial resolution satellite datasets. This observation was reaffirmed by the performance of these models when driven by upscaled VIs derived from finer spatial resolution satellite datasets. The results of the comparisons from the validation and testing phases demonstrated satisfactory performance of the MLBMs, with no major bias being observed between MODIS LAI and estimated LAI across the different study sites and climate zones. The performance of the MLBMs driven by Landsat- and Sentinel-derived VIs were similar and satisfactory. According to Meyer et al. (2019) the similar performance of these MLBMs despite the use of VIs derived from data acquired from different sensors can be attributed to the compatibility of the bands between the sensors, as one of the key objectives of the Sentinel-2 mission was to provide data continuity for Landsat.

Although, the MLBMs were shown to perform satisfactorily during the various phases of the study, it should be noted that a major disadvantage of the proposed methodology is that the accuracy of the moderate spatial resolution estimates will ultimately be influenced by the accuracy of the coarse spatial resolution product (Ke et al., 2016). In addition to the aforementioned limitation, we found that there was a general decrease in the performance of the MLBMs when upscaled Landsat- and Sentinel-derived VIs were used as inputs to estimate LAI. This may be indicative of further limitations associated with the proposed methodology.

The poorer performance of the MLBMs when using upscaled Landsat- and Sentinel-derived VIs may be attributed to the combined effect of several factors (Ovakoglou et al., 2020). Due to the lack of long-term moderate-high spatial resolution LAI records, the LAI-VI relationship was developed using coarse spatial resolution data, assuming that these values were acquired from homogenous pixels (Zhang et al., 2020). However, there is a strong likelihood that this assumption did not always hold true and thus, the values associated with the Landsat- and Sentinel-derived VIs may have differed from the MODIS VIs used during the derivation of LAI-VI relationship at a particular site. This situation may have been compounded by missing data, as well as differences in the temporal resolution of the satellite-derived VIs.

The frequent occurrences of cloud-contamination and striping issues (Landsat 7), resulted in numerous occasions where it was not possible to derive VIs at the Landsat or Sentinel-2 spatial resolution. In these instances, data was infilled using the respective mean VI values. The infilling of missing data coupled with the differences in the temporal resolution of VI datasets may have resulted in situations whereby the coarser and finer resolution VIs were not describing vegetation conditions during the same period (Ovakoglou et al., 2020). Furthermore, the upscaling of the Landsat- and Sentinel-derived VIs prior to their use for LAI estimation may have also contributed to the discrepancies observed between the estimated LAI and the MODIS LAI product values (Zhang et al., 2020). The saturation of VIs at high biomass densities have also been shown to impact the estimation of LAI using VIs (Fensholt et al., 2004; Middinti et al., 2017), particularly when using coarse spatial resolution data to derive the LAI-VI relationship. This can be attributed to the effects of mixed pixels containing background radiative contributions (Myneni et al., 2002) which are not captured at finer spatial resolutions.

Notwithstanding the limitations of this study, the results presented herein are quite promising. Previous, studies have demonstrated the utility of adopting relatively simple regression and more advanced machine learning based approaches to acquire LAI_{MR} estimates for various vegetation types using VIs derived at finer spatial resolutions (Houborg and McCabe 2017; Middinti et al., 2017; Dube et al., 2019; Meyer et al., 2019; Hirigoyen et al., 2021). These approaches have used and generally benefitted from the availability of in-situ LAI measurements or moderate-high spatial resolution satellite-based LAI estimates for training the MLBMs and to evaluate the accuracy of their outputs.

However, in many instances this data may not be readily available. Subsequently, in such circumstances, the approach adopted in this study can be an extremely useful alternative as it provides a pragmatic approach to acquire LAI_{MR} estimates using freely available and easily accessible satellite datasets and data processing platforms.

5.4.5 Conclusions

The results of this study were encouraging and demonstrated that the proposed methodology can be a useful approach to enhance the spatial resolution of coarse spatial resolution LAI products through the use of VIs derived from finer spatial resolution satellite datasets. This in turn may aid in facilitating the acquisition of longer term spatially explicit estimates of LAI which are required for various applications but not always readily available. Although, it was shown that LAI_{MR} could be estimated with reasonable accuracy when compared against the MODIS LAI product, further testing of this approach across a diverse set of vegetation types and geographic regions is recommended. For this purpose, LAI derived from Sentinel-2 imagery processed in SNAP represents a promising source of data. Additionally, since this method is largely influenced by the accuracy of the coarse spatial resolution LAI product, caution should be exercised when applying this approach to derive LAI_{MR} estimates for various applications without first establishing the accuracy of the coarse spatial resolution LAI product or the downscaled output, at the intended scale of application. Notwithstanding the limitations of the study, the proposed methodology is flexible and robust and can be easily adapted to include alternate or additional VIs, as well as other environmental and climatic variables to generate LAI_{MR} for other vegetation types. While the focus of this study was centred around the estimation of LAI, the synergistic use of convenient machine learning packages as well as geospatial cloud computing platforms such as GEE provides users with powerful tools to make relatively quick and well-informed decisions which may facilitate improved water resources management in the future.

5.5 Conclusion, recommendations, and way forward

A method to determine moderate resolution LAI estimates from coarser spatial resolution satellite products was developed and shown to be reasonably accurate. However, as the method is influenced by the accuracy of the coarser spatial satellite products its use is cautioned. Therefore, the recommendation is for the MODIS LAI estimates to be primarily used further in this project. Similarly, MODIS LAI values were used for determining the vegetation water use parameters for the CWRR clusters (Toucher et al., 2020). The strong support in the literature for a relationship to exist between leaf area and tree water use, as well as the evident relationship between LAI and evapotranspiration of the Two Streams catchments case study despite conditions not being met, provides justification for the further investigation and use of LAI in estimating tree water use.

Commercial afforestation licenses are assessed based on the impact that a plantation will have on the streamflow of a specific catchment, not the evapotranspiration over the plantation or the transpiration of the tree. Thus, any relationship between evapotranspiration and LAI would need to be incorporated into a hydrological model to be able to determine the composite impact on streamflow. The ACRU agrohydrological model is currently the supported and accepted model used to determine streamflow flow reductions. Thus, any relationship between evapotranspiration and LAI would need to be related to ACRU model input parameter/s. Within the ACRU model, crop coefficients are used to provide a means for estimating the land covers potential evapotranspiration rate, relative to the evapotranspiration from a reference crop. Therefore, the crop coefficient would need to be derived from the relationship between evapotranspiration and LAI.

CHAPTER 6. DETERMINING CROP COEFFICIENTS FOR COMMERCIAL TREE SPECIES

S. Gokool¹, N. Kaptein¹, R.P. Kunz¹, A. Clulow¹, C. Everson¹ and M.L. Toucher^{1,2}

¹Centre for Water Resources Research, University of KwaZulu-Natal

²South African Environmental Observation Network (SAEON)

6.1 Introduction

Within ACRU total evaporation is driven by maximum potential evaporation (E_m) the forcing function of which is, in turn, a reference evaporation (E_r). The estimations of total evaporation in ACRU allow for the computation of the water balance, estimation of water availability and water requirements (crop water requirements). The daily American Class A-Pan equivalent is used as the reference total evaporation in ACRU. The ACRU model contains a number of equations that can be used to estimate reference potential total evaporation, or total evaporation can be estimated from A-pan data, depending on the information available (Schulze,1995). The evaporation from the soil surface and plant tissue within ACRU is computed using a meteorologically derived reference evaporation and a crop coefficient which represent the vegetation water use. Crop coefficients provide a means for estimating the land covers potential evapotranspiration rate, relative to the evapotranspiration from a reference crop, expressed as

$$K_c = \frac{ET_c}{ET_o} \quad (6.1)$$

Where,

K_c = the crop coefficient (dimensionless)

ET_c = crop (or vegetation) evapotranspiration (mm.d^{-1})

ET_o = reference crop evapotranspiration (mm.d^{-1})

ET_c refers to the crop evapotranspiration under non-stress conditions, where the crop is well managed and watered (referred to as standard conditions). ET_o refers to the evapotranspiration from a reference surface, which is a short grass (0.12 m), under non-stress conditions. By using a reference crop evapotranspiration, the evaporative demand can be determined independent of crop development and management and can be compared across locations. A reference surface also provides a benchmark against which the ET from other surfaces can be compared (Allen et al., 1998).

ET_o is only affected by climatic parameters, thus it can be calculated from meteorological data. The accepted and recommended method for determining ET_o is the FAO Penman-Monteith method (Allen et al., 1998). The reasons for this include, that the method closely approximates grass ET_o at the location evaluated, is physically based, and explicitly incorporates both physiological and aerodynamic parameters. The crop evapotranspiration differs from the ET_o , as the surface from which the evapotranspiration is occurring differs in terms of its ground cover, canopy properties and aerodynamic resistance. By using the K_c approach these differences between the reference surface and crop are accounted for.

ET_o , thus, represents the climatic demand, while K_c varies with vegetation characteristics and to a limited extent climate. This allows for the standard (those derived from non-stressed conditions) K_c values to be

transferable between locations (Liu and Luo, 2010; Kar et al., 2007). K_c can be considered a surrogate for the vegetation height, albedo, canopy resistance and the evaporation from the soil.

The only long-term dataset of actual evapotranspiration available for commercial tree species in South Africa is the datasets from the Two Streams research catchment, covering only two tree species. The lack of available actual evapotranspiration implies that, for commercial tree species, an alternative method to deriving K_c needs to be considered. Given the relationship between leaf area and tree water use (Chapter 5), deriving K_c from LAI was considered.

It needs to be noted, that in the ACRU agrohydrological model the reference is A-pan equivalent potential evaporation. Thus, the crop coefficients used in the model need to be relative to A-pan potential evaporation rather than FAO Penman-Monteith reference evaporation, or a correction factor needs to be applied.

6.2 Using leaf area index to derive a crop coefficient

Several authors have suggested that crop coefficients can be calculated as a function of LAI. This was first proposed by Monteith (1965) where he showed a strong relationship between transpiration and LAI. Following this, Ritchie and Burnett (1971) demonstrated a relationship between evapotranspiration and LAI for dryland cotton and grain sorghum,

$$\frac{ET_c}{ET_o} = -0.21 + 0.70LAI^{0.5} \quad (6.2)$$

Where

ET_c = actual crop evapotranspiration

ET_o = reference potential evapotranspiration

Ritchie (1972) further tested this relationship for grain sorghum and showed good correlation between the estimated evapotranspiration and the actual measured evapotranspiration. Providing additional evidence, Kristensen (1974) demonstrated a strong relationship between LAI and the ratio of actual to potential evapotranspiration for sugar beets, barley and rye grass. Using the data from Kristensen, Angus (1987) derived the following equation,

$$LAI = \frac{\ln(K_c - 1.0932)/-0.7947}{-0.6513} \quad (6.3)$$

Where

K_c is limited to values between 0.2 and 1.05.

The equation derived by Angus (1987) has been coded into ACRU to offer the option to determine K_c from LAI, if available. To determine K_c for the CWRR clusters, Toucher et al. (2020) used available evapotranspiration data at four validation sites to develop a relationship between LAI and K_c . The LAI values used were those obtained from the MODIS LAI product for the period 2012-2018, and then averaged to monthly values for the representative Quinary catchment. Using the monthly means of the 8-day MODIS LAI values and the monthly means of daily FAO Single crop coefficient adjusted to be representative of A-Pan equivalent reference evaporation, the following relationship was derived:

$$K_c = \frac{1.237}{(1 + 3.173e^{-0.657LAI})} \quad (6.4)$$

The standard error of the derived equation was 0.1, the correlation coefficient 0.87 and the coefficient of determination (R^2) 0.75. The R^2 of 0.75 indicates that 75% of the variation in K_c will be explained using this equation together with the LAI. As more evapotranspiration data for natural vegetation becomes available, the equation can be improved in its robustness through the inclusion of the additional data.

None of the studies demonstrating a relationship between LAI and K_c have tested the relationship for tall vegetation. However, Kristensen (1974) showed that the ratio of actual to potential evapotranspiration, or in other words K_c , approaches 1 when LAI approaches 3. While, according to USDA (2018), when the LAI is greater than 2.7, only atmospheric demand determines evapotranspiration, but when LAI is less than 2.7, atmospheric demand, LAI and the surface wetness of the soil determine evapotranspiration. Given this, an alternative approach using GEE and machine learning was developed.

6.3 Quantifying crop coefficients for commercial forests using a combination of field-based evapotranspiration measurements and satellite earth observation data²

6.3.1 Introduction

Commercial afforestation activities in South Africa have been shown to have a major impact on available water resources *viz.* streamflow and are thus highly regulated with water use licenses being required for their growth (Gush et al., 2002; Dye and Versfeld, 2007; Jewitt et al., 2009). The tool used to guide and inform the issuing of these licenses utilises outputs from the Agricultural Catchments Research Unit (ACRU) agrohydrological model which when configured is only able to represent the vegetation characteristics of three commercial plantation species *i.e.*, *Pinus patula*, *Eucalyptus grandis* and *Acacia mearnsii*. However, with the forestry industry presently using a far larger number of species, clones and hybrids to meet existing timber demands there is a pressing need to update these decision support tools so that water use licenses are issued in accordance with the hydrological impacts of a particular commercial plantation species, clone or hybrid (Toucher and Everson, 2018).

Evapotranspiration (ET) is a key input to hydrological models as it plays a prominent role in the hydrological cycle and energy balance. Subsequently, the accurate quantification of ET is crucial to effectively utilise these models to guide water resources management decisions (Allen et al., 2011; Zhao et al., 2013; Liu et al., 2016; Li et al., 2018; Li and Ma, 2019). Several field-based and remote sensing techniques exist which can potentially provide fairly accurate long-term estimates of ET. However, the Food and Agricultural Organization method (FAO-56) which is based on the reference evapotranspiration and crop coefficient (K_c) remains one of the most well established and extensively utilised approaches for the estimation of ET and is the method used in many hydrological models (Hunnik et al., 2017; Li et al., 2018; Pereira et al., 2021). This is due to the relative ease of application, strong physical conceptualization and universal applicability (Pereira et al., 2015).

The reference evapotranspiration represents the ET of a hypothetical reference surface such as grass (ET_o) or alfalfa (ET_r) and is computed from meteorological data. The K_c which encompasses all the biophysical

² This sub-chapter is a paper that has been submitted to xxx. The paper is currently under review. The text as it stands here is the same as that submitted to the journal with the authors of Chapter 5 as the authors of the paper.

characteristics of a particular crop is used as a multiplying factor to relate the reference ET rate to the potential ET rate of a particular crop (Allen et al., 1998; Pereira et al., 2021). K_c values for agricultural crops are well-defined and an extensive list of these has been developed and provided by Allen et al. (1998). Although the FAO-56 method has been widely utilised to estimate ET of agricultural crops, there has been relatively limited application of this approach for non-agricultural and natural vegetation (Descheemaeker et al., 2011; Glenn et al., 2011; Corbari et al., 2017; Liu et al., 2017).

This can be attributed to the lack of well-established K_c coefficients for these land-use land-cover classes (LULC) due to limited field-based measurements in these environments (Liu et al., 2017). While this does limit the utility of applying the FAO-56 method to estimate ET in non-agricultural and natural environments, Allen et al. (1998) outline procedures which can be implemented to derive K_c as a function of variables which directly influence it, such as fraction of ground cover, soil characteristics, plant height and leaf area index (Liu et al., 2017; Pereira et al., 2020). According to Beeri et al. (2017) the versatile nature of leaf area index (LAI) has contributed to a growing interest in its use with several studies demonstrating its potential in estimating K_c and vegetation water use (Feng et al., 2016; Liu et al., 2017; Park et al., 2017; Netzer et al., 2019; Chen et al., 2020; Ohana-Levi et al., 2020; Fan et al., 2021).

LAI is defined as the one-sided (green) leaf area per unit ground surface area (Myneni, 2002). Leaf area plays an important role in regulating the stomatal response to meteorological conditions, as the leaves provide a surface from which vegetation-atmospheric exchanges take place through processes such as photosynthesis, transpiration and respiration (Ohana-Levi et al., 2020; Shao et al., 2021). Since leaf area plays a major role in driving plant water consumption (Gao et al., 2008; Ohana-Levi et al., 2020), the ability to accurately quantify LAI across space and time can facilitate the improved estimation of water use in non-agricultural and natural environments using the FAO-56 method.

LAI data can be acquired through the use of optical in-situ instrumentation, direct sampling, Lidar technology and remote sensing (Fang et al., 2014; Clevers et al., 2017; Shao et al., 2021). However, the use of remote sensing methods is often preferred as it provides a pragmatic approach to acquire spatially and temporally explicit LAI data across large geographic extents (Alexandridis et al., 2019; Ovakoglou et al., 2020). Over the past decade, numerous global satellite-derived LAI data products have been made available and several methods have been developed to process satellite earth observation (SEO) data to estimate LAI at various spatial and temporal resolutions (Alexandridis et al., 2019; Fang et al., 2019; Ovakoglou et al., 2020). Furthermore, advances in geospatial cloud computing platforms such as Google Earth Engine (GEE) and the development of user-friendly machine learning programming packages have facilitated the seamless generation of long-term time-series data by providing a more powerful and efficient means of collecting, processing and storing SEO data (Gorelick et al., 2017; Ohana-Levi et al., 2020; Shao et al., 2021).

Since ACRU and many other hydrological models adopt the reference ET- K_c approach for ET estimation, it is vital to have well-defined K_c values that adequately represent a particular LULC class so that vegetation water consumption can be more accurately estimated. Considering the potential of utilizing satellite-derived estimates of LAI for the estimation of K_c in non-agricultural and natural environments, in this study we aimed to exploit the capabilities of GEE and machine learning techniques to derive K_c estimates for various commercial forest species, clones and hybrids in the eastern region of South Africa (SA). The specific objectives of this study were i) to derive K_c using a conventional and machine learning-based approach using satellite-derived estimates of LAI and ii) estimate ET using these K_c estimates and evaluate the accuracy of these ET estimates against in-situ measurements of ET.

6.3.2 Methodology

6.3.2.1 Study Area

The study area is situated within the Two Streams Research Catchment which is located approximately 70 km north-east from the city of Pietermaritzburg within the KwaZulu-Natal province of SA. This catchment is among the most extensively studied forested catchments in SA and possesses more than two-decades worth of detailed hydro-meteorological observational data (Vather et al., 2020). The altitude across the catchment ranges from 1080-1125 m.a.s.l. The study area experiences a warm sub-tropical climate with hot, humid summers and cooler, dry winters. Mean annual precipitation ranges from 659-1139 mm, a majority of which is received as rainfall during the summer, however, heavy mist is also a significant contributor to precipitation within the catchment. Furthermore, the study area experiences moderate occurrences of hail, frost and drought (Ngubo et al., 2020; Vather et al., 2020). The Two Streams Catchment lies within the Pongola-uMzimkhulu water management area (WMA) which is a major contributor to water resources within KZN and SA. Water resources management within this WMA is fairly complex due to the high local demand for water resources and international obligations that need to be factored into management decisions to ensure the equitable and sustainable use and supply of this critical resource (DWA, 2012; 2013). With commercial forestry featuring quite prominently in this region due to the favourable growing conditions (Vather et al., 2020), the ability to accurately estimate water use and quantify the hydrological impacts of these forests forms a crucial component of effective water resources management in this region.

6.3.2.2 Data collection and processing

The estimation of K_c as a function of satellite-derived LAI estimates was dependent on first quantifying K_c through in-situ measurements of ET and ET_0 to account for vegetation characteristics and weather conditions (Pereira et al., 2015). Meteorological data such as solar radiation, ambient air temperature, relative humidity, rainfall, wind speed and direction were acquired from a Campbell Scientific automatic weather station located within the study site. This data was then used to determine the daily ET_0 using the FAO-56 method. Additional sensors were also installed at the site to measure i) the components of the shortened energy balance and ii) ET of *Acacia mearnsii* and *Eucalyptus dunnii* stands using the Scintillometry and Eddy Covariance (EC) method, respectively. Further details regarding the instrumentation setup are provided in Clulow et al. (2011) and Everson et al. (2018).

A monthly time-series of K_c was derived using daily measurements of ET and ET_0 that were captured during the periods 2007-2013 for *Acacia mearnsii* and 2019-2021 for *Eucalyptus dunnii*. The daily ET and ET_0 were then scaled up to monthly totals and these values were used to create a monthly time series of K_c using Equation 6.5. During this process it was assumed that there was no limit on water availability and ET was occurring at potential rates:

$$K_{cObs} = \frac{ET}{ET_0} \quad (6.5)$$

Where,

ET is the measured cumulative ET (mm month⁻¹),

ET_0 is the cumulative grass reference evapotranspiration (mm month⁻¹), and

K_{cObs} is the monthly K_c derived from in-situ measurements.

The satellite-based LAI estimates used in this study were acquired from the MODIS LAI product as it is among the most widely used and extensively validated freely available satellite-based LAI products

(Myneni, 2002; Gao et al., 2012; Yan et al., 2016). The GEE platform was utilised to access and process the MODIS LAI product image collection (MCD15A3H V6 level 4, 500 m spatial and 4-day temporal resolution). This image collection was filtered to select good quality images that corresponded with the in-situ measurement period and the mean value for each of these images within the region of interest was then determined. These values were then exported as a time-series of comma-separated values (CSV). The 4-day MODIS LAI estimates were then summarized to create a time-series of average monthly values that was consistent with the K_{cObs} dataset.

In this study we adopted two approaches to estimate K_c as a function of LAI i.e., i) conventional and ii) machine learning-based approach. The conventional K_c estimation method described in Allen et al. (1998) was employed in this study and is given as:

$$K_c = K_{c_{min}} + (K_{c_{min}} + K_{c_{max}}) * (1 - e^{-0.7LAI}) \quad (6.6)$$

Where, $K_{c_{min}}$ and $K_{c_{max}}$ were determined from the monthly K_{cObs} time series for the *Acacia mearnsii* and *Eucalyptus dunnii* stands. However, it should be noted that in instances where K_{cObs} exceeded 1.3, a value of 1.3 was used as $K_{c_{max}}$. According to Allen et al. (2011), K_{cObs} values derived from using the grass reference surface should not exceed 1.2-1.3 in humid and sub-humid environments. Once the lower and upper limits of K_c were determined, the long-term average monthly LAI was used as inputs to Equation 6.6 to derive the long-term average monthly K_c .

For the estimation of K_c using a machine learning-based approach, the monthly K_{cObs} and MODIS LAI time-series were used to develop a K_c estimation model. For this purpose, we utilised the classification and regression training (Caret) (Kuhn, 2008) and caretEnsemble (Mayer, 2013) packages available as add-ins to R statistical software. Similar to the approach adopted in the Allen et al. (1998) method, monthly K_{cObs} values exceeding 1.3 were given a value of 1.3. However, instead of developing a unique machine learning based model (MLBM) model for the *Acacia mearnsii* and *Eucalyptus dunnii* stands, respectively, all the data was combined into a single dataset to develop a generic K_c -LAI model.

The rationale for this was to maximize the use of the available data for the development of a model that could be used to estimate K_c for various forestry species, hybrids and clones in the region when only LAI data is available. Due to the relatively small size of the datasets ($n = 94$), the data was not randomly split into a training and validation subset. Instead, we used a k-fold cross validation approach similar to Hirigoyen et al. (2021) to train and validate the machine learning based models (MLBMs). Model performance was then ascertained using metrics such as the correlation coefficient (r), root mean square error (RMSE) and mean absolute error (MAE). The machine learning algorithms that were selected for application included the; i) generalized linear model (GLM), ii) decision tree (CART), iii) k nearest neighbour (kNN), iv) random forest (RF) and v) support vector machine (SVM). These algorithms were selected as they are among the most frequently utilised for various applications and represent an eclectic mix of both simple and complex machine learning based approaches. Additionally, these algorithms were then used as base algorithms to develop a model ensemble that combines the strengths of each of the aforementioned algorithms into a single model. The model ensemble was developed by stacking the base algorithms and combining their predictions using a RF approach. The best performing model was then selected to estimate the average monthly K_c using the average monthly LAI for a specific region of interest.

Once the average monthly K_c was derived for each of the forestry stands using both the conventional and machine learning-based approaches, these values were used in conjunction with the daily ET_0 to estimate daily ET (assuming K_c remains constant within a given month). The daily ET estimates were then scaled up to monthly totals and these values along with the monthly K_c were then compared against the

corresponding values measured in-situ. The uncertainty in the K_c and ET estimates was then established using the aforementioned performance metrics and the Kruskal-Wallis significance test (95% confidence interval).

6.3.3 Results

6.3.3.1 Validation of K_c and evapotranspiration estimates for *Acacia mearnsii*

Monthly K_{cObs} ranged from 1.15 to 1.25, with an average value of 1.20 (± 0.03). Monthly K_c estimates derived using the conventional method ranged from 1.04 to 1.22, with an average value of 1.13 (± 0.07). The ensemble machine learning model (EMLM) performed the best of all the machine learning based approaches that were tested, producing RMSE, MAE and R^2 values of 0.07, 0.04 and 0.77, respectively. Monthly K_c estimates derived using the EMLM ranged from 1.06 to 1.25, with an average value of 1.18 (± 0.06). In general, both techniques were shown to perform fairly well with no significant differences found between the observed and estimated K_c values (p -value = 0.44). Both techniques, generally underestimated K_c when compared against K_{cObs} . However, the degree of underestimation was marginally higher for the conventional method (RMSE = 0.09) as compared to the EMLM (RMSE = 0.06). Overall, the results of the comparisons between the K_{cObs} and K_c estimated using the conventional and machine-learning based approaches showed that K_c could be fairly accurately estimated using satellite-derived estimates of LAI as shown in Figure 6-1.

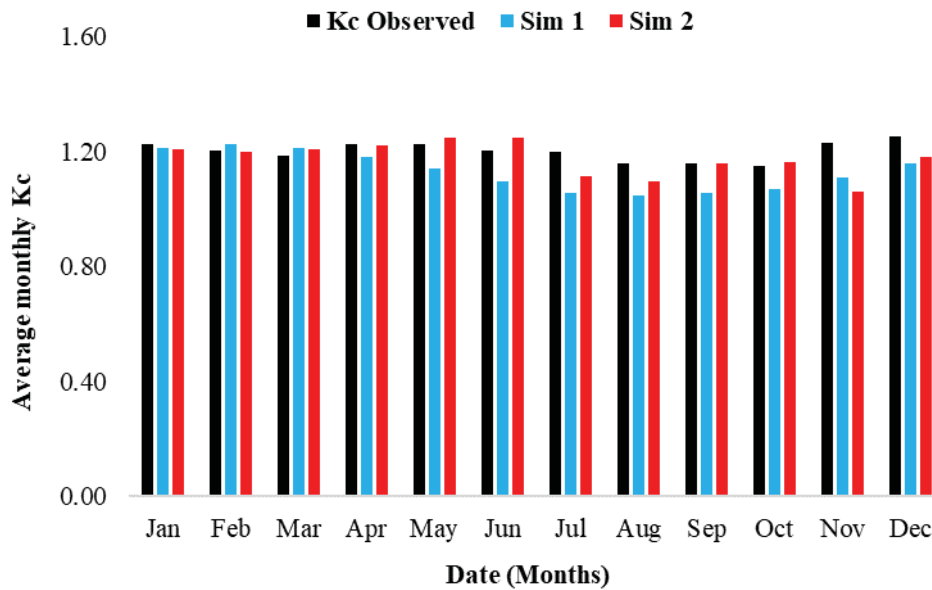


Figure 6-1: A comparison of the measured and estimated monthly K_c for *Acacia mearnsii*, where Sim1 is the conventional and Sim 2 is the machine learning based approach

The results of the comparisons between the estimated ET and measured ET of *Acacia mearnsii* are presented in Figure 6-2 and Table 6-1. In general, ET estimates derived using the conventional and EMLM derived monthly K_c compared favourably against in-situ measurements and showed similar levels of performance. Both approaches, were shown to generally underestimate ET with the degree of underestimation being higher for ET estimates derived using the conventionally derived monthly K_c . However, no significant differences were found between the measured and estimated ET for both techniques.

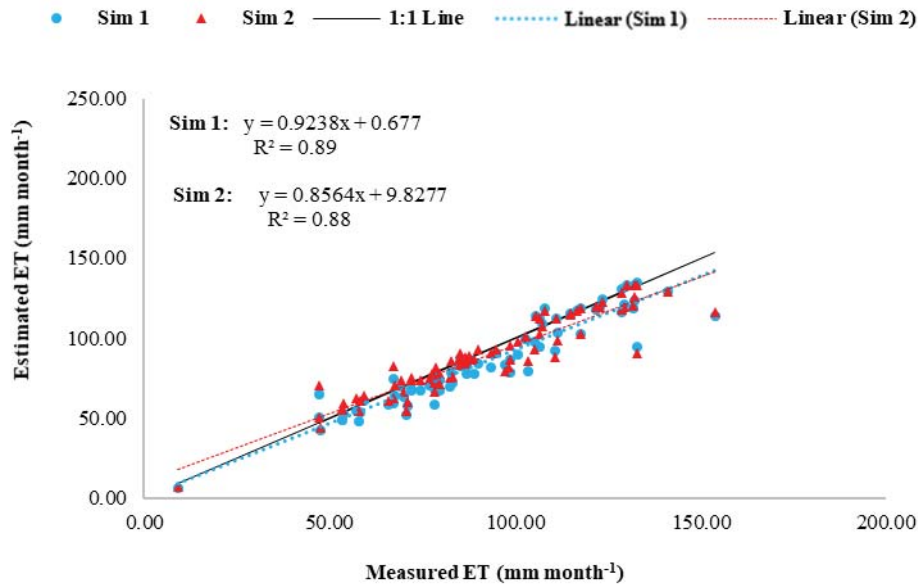


Figure 6-2: A comparison of the measured and estimated ET of *Acacia mearnsii*, where Sim1 and Sim 2 represents ET estimated using conventionally and EMLM derived monthly K_c estimates, respectively

Table 6-1: A comparison of the performance metrics for ET estimates of *Acacia mearnsii* derived using monthly K_c estimates from the conventional (Sim1) and EMLM (Sim 2) approaches

	Measured	Sim 1	Sim 2
Total (mm)	7341.07	6835.49	7072.90
Average (mm month ⁻¹)	91.76	85.44	88.41
RMSE (mm month ⁻¹)		11.02	10.03
MAE (mm month ⁻¹)		8.11	6.51
Correlation (r)		0.94	0.94
p-value		0.48	0.48

6.3.3.2 Validation of K_c and evapotranspiration estimates for *Eucalyptus dunnii*

Monthly K_{cObs} ranged from 0.68 to 1.30, with an average value of 1.08 (± 0.18). Monthly K_c estimates derived using the conventional method ranged from 1.04 to 1.20, with an average value of 1.12 (± 0.06). Monthly K_c estimates derived using the EMLM ranged from 1.09 to 1.24, with an average value of 1.19 (± 0.04). Overall, both techniques were shown to perform satisfactorily with no significant differences found between the observed and estimated K_c values (p -value = 0.44). Both techniques, generally overestimated K_c when compared against K_{cObs} . However, the degree of overestimation was marginally higher for the EMLM (RMSE = 0.20) as compared to the conventional method (RMSE = 0.15). Overall, the comparisons between the K_{cObs} and K_c estimated using the conventional and machine-learning based approaches showed that K_c could be satisfactorily estimated using satellite-derived estimates of LAI as shown in

Figure 6-3.

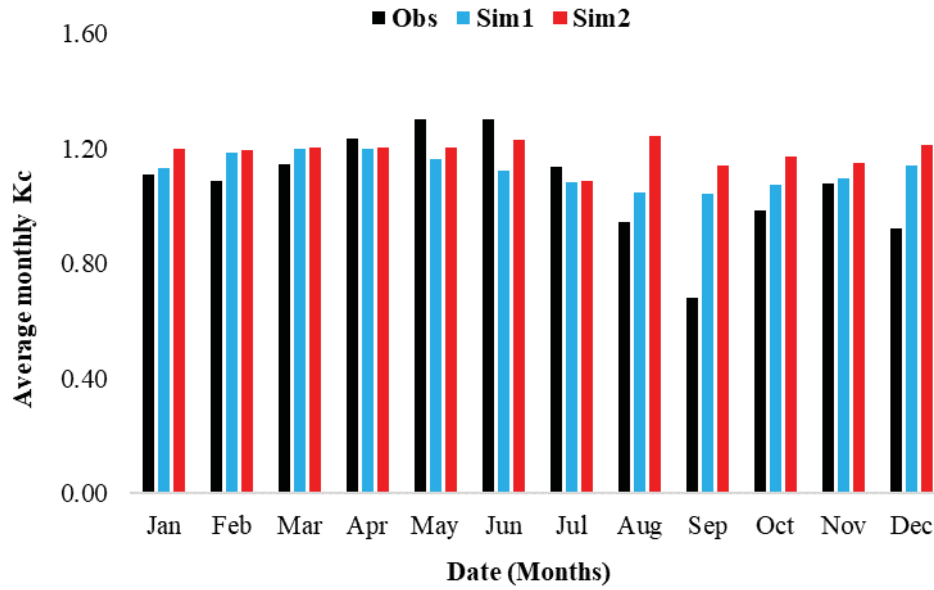


Figure 6-3: A comparison of the measured and estimated monthly K_c for *Eucalyptus dunnii*, where Sim1 is the conventional and Sim 2 is the machine learning based approach

The results of the comparisons between the estimated ET and measured ET of *Eucalyptus dunnii* are presented in Figure 6-4 and Table 6-2. In general, ET estimates derived using the conventional and EMLM derived monthly K_c estimates compared satisfactorily against in-situ measurements. However, in this instance ET estimated using monthly K_c estimates generated using the conventional approach were in better agreement with measured ET, whereas ET was generally overestimated using EMLM derived monthly K_c . Despite the poorer estimation of ET using the EMLM derived monthly K_c , no significant differences were found between the measured and estimated ET for both techniques.

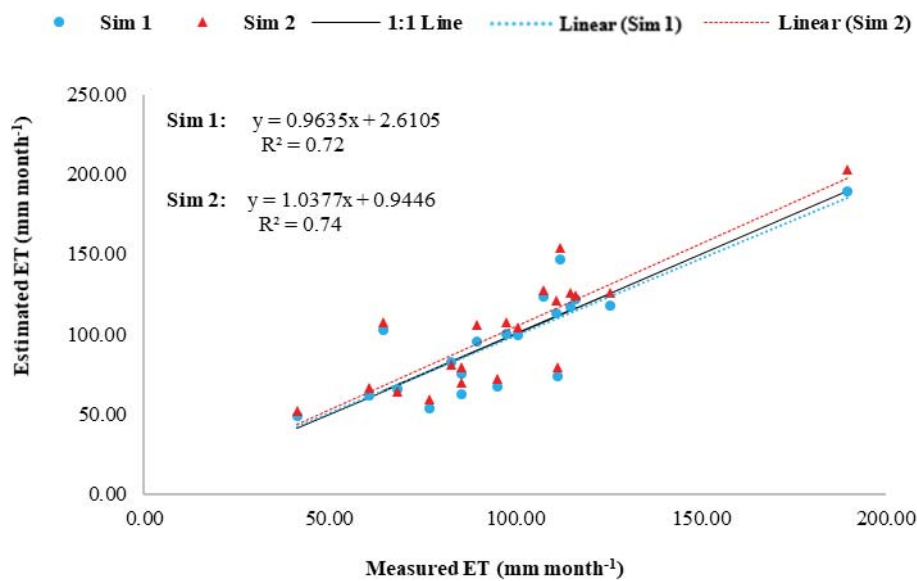


Figure 6-4: A comparison of the measured and estimated ET of *Eucalyptus dunnii*, where Sim1 and Sim 2 represents ET estimated using monthly K_c derived from the conventional and EMLM approaches respectively

Table 6-2: A comparison of the performance metrics for water use estimates of *Eucalyptus dunnii* derived using monthly K_c estimates from the conventional (Sim1) and EMLM (Sim 2) approaches

	Measured	Sim 1	Sim 2
Total (mm)	1937.72	1919.20	2029.69
Average (mm month ⁻¹)	96.89	95.96	101.48
RMSE (mm month ⁻¹)		1.11	18.97
MAE (mm month ⁻¹)		0.92	14.65
Correlation (r)		0.85	0.86
p-value		0.46	0.46

6.3.4 Discussion

The results of our investigations demonstrated that K_c could be estimated relatively accurately using satellite-derived LAI estimates as inputs to both a conventional and machine-learning based estimation approach. The range of the estimated K_c -RMSE values (0.06-0.20) when compared against K_{cObs} , are within the range of published values (0.04-0.30) highlighted in Beerli et al. (2020). It is also worth noting that both techniques were found to perform relatively well during the winter months (June-August) with the EMLM approach performing marginally better. During the drier periods forest species are likely to have greater impacts on available water resources, therefore, this is when it is particularly important to accurately estimate ET.

In general, the evaluation of ET estimates against measured ET, revealed that the water use of *Acacia mearnsii* and *Eucalyptus dunnii* could be fairly accurately estimated using the aforementioned K_c estimates. However, the relative accuracy of these estimates was higher for *Acacia mearnsii*. This may potentially be as a result of the shorter observed ET record for *Eucalyptus dunnii* which was also largely infilled ($\approx 50\%$). Subsequently, there may have been instances during which the estimated ET was being compared against a measured value that was higher or lower than what was actually taking place.

Considering the performance of the two K_c estimation approaches, it was found that the use of K_c estimates derived using both approaches was able to produce reasonable estimates of ET for *Acacia mearnsii* with both approaches showing similar levels of performance. While this level of performance was relatively maintained when using conventionally derived K_c estimates to estimate the ET of *Eucalyptus dunnii*, there was a marginal but noticeable decrease in performance when using the EMLM derived K_c estimates for ET estimation. This occurrence can be largely attributed to the intrinsic characteristics of the EMLM that was developed to estimate K_c . The development of this model was meant to serve as a generic K_c -LAI model, which could be used to estimate K_c for various forestry species, hybrids and clones in the region when only LAI data was available. Subsequently, the K_c -LAI regression relationship was determined using a combination of all the K_c and LAI data that was available for the *Acacia mearnsii* and *Eucalyptus dunnii* sites.

Since this combined dataset largely comprised of data for *Acacia mearnsii* ($\approx 80\%$), it can be expected that the estimated K_c and subsequent ET estimates derived using these values would be more accurate for *Acacia mearnsii*. However, despite the shorter data record that was available to more adequately represent the K_c -LAI regression relationship for *Eucalyptus dunnii*, the results presented herein suggest that this generic K_c -LAI model can potentially provide relatively accurate estimates of K_c and subsequently ET for forestry species, hybrids and clones in the region where only LAI data is available. While the conventional K_c estimation approach may be favoured in most instances due to its relative simplicity, the advantages of

adopting machine learning-based approaches is that these techniques can allow for more complex relationships between target and explanatory variables to be more adequately accounted for and represented (Houborg and McCabe, 2017; Hirigoyen et al., 2017).

Furthermore, the ability of these approaches to include additional explanatory variables can prove to be beneficial for the estimation of K_c for different vegetation types and in other environmental settings. For example, Park et al. (2017) showed that the inclusion of soil moisture data with vegetation indices resulted in the improved estimation of K_c as opposed to the use of vegetation indices alone, as in some instances soil water evaporation may be a large contributor to evapotranspiration.

A major limitation of the methods employed in this study was the assumption that there was no limit on water availability and ET was occurring at potential rates. While it was difficult to ascertain whether this was the case from the comparisons between the measured and estimated ET, this assumption can prove to be problematic when using K_c estimates derived from these methods for hydrological modelling purposes. During water limited conditions hydrological models are often conceptualized to account for the effects of water stress through the inclusion of a stress coefficient which is used to reduce the potential ET. Subsequently, if the K_c estimates used in a hydrological model have been derived during water limited conditions, this may result in an underestimation of ET once water availability has been accounted for. A further limitation of the study was the reliance on in-situ measurements to estimate K_c as a function of satellite-based LAI estimates, as this may limit the feasibility of applying these methods in regions where this data is unavailable. In such instances the use of satellite-derived estimates of ET and ET_0 may represent the most pragmatic approach to acquire estimates of K_c for non-agricultural and natural vegetation.

Notwithstanding the limitations of the methods presented in this study, the results presented herein have demonstrated the utility of using satellite-derived estimates of LAI for the estimation of K_c . Furthermore, the ability of machine learning based approaches to more adequately account for complex relationships between variables can be invaluable when attempting to estimate K_c by extrapolating K_c -LAI models to ungauged sites where only satellite-derived estimates of LAI can be acquired.

6.3.5 Conclusion

The general lack of K_c values for non-agricultural and natural vegetation hinders the application of the reference ET- K_c approach which many hydrological models utilise for the estimation of ET. To address this limitation in this study we explored the utility of utilizing satellite-derived LAI estimates to estimate K_c with a particular focus on forestry. The results of these investigations were quite promising and demonstrated that the use of geospatial cloud computing and machine-learning based approaches provides a robust and efficient means of handling large volumes of data and optimally utilizing this data. Furthermore, the development of a generic K_c -LAI model in this study can be quite useful for future hydrological modelling applications in the region pertaining to forestry as it will allow for the requisite K_c values to be seamlessly generated for the various commercial forest species, clones and hybrids using easily accessible and readily available satellite-based estimates of LAI. This in turn may allow for the improved understanding and estimation of the hydrological impacts of commercial forestry in the region, which is urgently required and necessary to improve the management and regulation of this activity.

6.4 Crop coefficients for various commercial tree species for use in The Acru agrohydrological model

6.4.1 Introduction

Previous studies (e.g. Gush et al., 2002) concerning the water use of commercial tree species only covered three species, namely *Eucalyptus grandis*, *Pinus patula* and *Acacia mearnsii*. Over time the number of species, clones and hybrids grown by the forestry industry has expanded and will continue to expand with improvements in tree breeding. During the initial phases of the project, an exercise was undertaken with the Institute for Commercial Forestry (ICFR) to look at which species were being grown and the extent of those species to assist in determining the crucial species that should be included. Only at the pulpwood stands were included.

The dominant eucalypt species, in terms of current planted area across South Africa is *E. dunnii*. This species occupies the largest area across South Africa irrespective of genera. The next dominate eucalypts, occupying similar areas, are *E. grandis* and *E. grandis x E. urophilla* (Table 6-3) and these each occupy approximately half the area of *E. dunnii*. The dominant pine species, in terms of current planted area across South Africa, is *P. patula* with *P. elliottii* (Table 6-3) occupying approximately half the area that *P. patula* does. The next pine species in terms of area occupies a small fraction in comparison to *P. patula* and *P. elliottii*. Following from this, the growth of commercial tree species across the ICFR climate zones as defined by Smith et al. (2005) was considered.

Table 6-3: Planted areas of eucalypt and pine for the large-scale growers (Source: ICFR, 2018)

Eucalypt species	Area (ha)	Pine Species	Area (ha)
<i>E. dunnii</i>	125 659	<i>P. patula</i>	106 044
<i>E. grandis</i>	67 428	<i>P. elliottii</i>	54 232
<i>E. grandis x E. urophilla</i>	66 238	<i>P. elliottii x P. caribaea</i>	9 971
<i>E. grandis x E. nitens</i>	32 717	<i>P. patula x P. tecunumanii</i>	7 541
<i>E. macarthurii</i>	22 555	<i>P. taeda</i>	7 197
<i>E. nitens</i>	18 720	<i>P. greggii</i>	2 111
<i>E. smithii</i>	14 872	Other pines	1 149
<i>E. benthamii</i>	11 360	Mixed stands	807
<i>E. grandis x E. camaldulensis</i>	7 463	<i>P. radiata</i>	755
Other eucalypts	3 220	<i>P. caribaea</i>	328
Mixed stands	1 186	<i>P. tecunumanii</i>	177
<i>E. badjensis</i>	1 077		

The distribution of commercial tree stands across the climate zones was first considered. Two climate zones, viz. the warm temperate dry (22%) and warm temperate moist (21%), account for 43% of the area planted to commercial forestry currently in South Africa (Table 6-4). Following from that the distribution of the species across the climate zones was determined. As noted above, *E. dunnii* is a dominant species based on area planted, the climate zones in which the species are predominantly planted are the warm temperate dry and warm temperate moist climate zones include (Table 6-5). *E. grandis x E. urophilla* in the subtropical area appears to be quite dominant, this is due to it being the one of the few species grown there whereas in other climate areas a broad range of species are grown. *P. patula* is the most dominant pine across the cool temperate and warm temperate climate zones regardless of the MAP division. *P. elliottii* in the warm temperate moist climate zone is the next most common, occupying 2.6% of the commercial forestry area (Table 6-5). The area of pines in the Sub-tropical zone were minor.

Table 6-4: Planted areas classified according to the ICFR defined climate zones (Source: ICFR, 2018)

Climate Zone		Area (ha)	%
Temperature Zone	Rainfall Zone		
Warm temperate	Dry	123 943	22
Warm temperate	Moist	117 574	21
Cool temperate	Moist	75 808	13
Warm temperate	Wet	74 542	13
Cool temperate	Dry	49 567	9
Cool temperate	Wet	42 139	7
Sub-tropical	Wet	34 266	6
Sub-tropical	Dry	29 812	5
Sub-tropical	Moist	15 157	3

6.4.2 Methodology and Species included

The MLBM as described in Section 6.3 was used to derive K_c values for the 15 sites that were used in the Section 5.4 (demonstrating obtaining moderate resolution LAI values from coarser spatial resolution products). With using an LAI based approach, the record of LAI obtained from the satellite imagery needs to be as long as possible. Furthermore, the site or in this case compartment had to be as large as possible. Together with ICFR, a compartment database that gave the compartment size, species and age, was used to select appropriate sites. Not all the forestry species could be included, as for some suitable compartments where the trees had been planted a few years back to give a long enough record of LAI could not be identified. However, sites to represent the dominant species were included.

Further, to determine whether changes were evident between species grown in the different ICFR climate zones as defined by Smith *et al.* (2005), sites in two climate zones were chosen for three of the species. The species for which crop coefficients were determined and the ICFR zones in which the sites were located are provided in Table 6-6.

For each of the sites, MODIS LAI (MCD15A3H V6 level 4, 500 m spatial and 4-day temporal resolution) image collections were accessed and then filtered to select good quality images for each study site and for a particular date range (dependent on tree age within the period 2002-2021). Similarly, Landsat 7 and 8 (Collection 1 Tier 1 calibrated top-of-atmosphere reflectance, 30 m spatial and 16-day temporal resolution), as well as Sentinel-2 (MultiSpectral Instrument, Level-1C, 10 m spatial and 5-day temporal resolution) collections were then respectively imported directly into GEE where the NDVI and EVI for these was generated. The MLBM as described in Section 5.4 was then used to estimate LAI values from the Landsat and Sentinel-2 VI's. Following which the MLBM was applied to estimate the K_c values for the 15 sites for the three LAI products. The K_c values were averaged monthly.

VOLUME 2: WATER USE ESTIMATION OF SFRA SPECIES

Table 6-5: Planted areas according to ICFR Climate zone and species only shown for those that account for more than 1% of the growth area (Source: ICFR, 2018)

Climate Zone		Species	Area (ha)	%
Temperature Zone	Rainfall Zone			
Warm Temperate	Dry	<i>E. dunnii</i>	42 811	7.6
Warm Temperate	Moist	<i>E. dunnii</i>	36 783	6.5
Sub-tropical	Wet	<i>E. grandis</i> x <i>E. urophilla</i>	29 826	5.3
Warm Temperate	Dry	<i>E. grandis</i>	26 457	4.7
Cool Temperate	Moist	<i>P. patula</i>	23 043	4.1
Warm Temperate	Wet	<i>E. dunnii</i>	20 421	3.6
Warm Temperate	Moist	<i>P. patula</i>	18 822	3.3
Sub-tropical	Dry	<i>E. grandis</i> x <i>E. urophilla</i>	18 710	3.3
Warm Temperate	Moist	<i>P. elliottii</i>	18 693	3.3
Warm Temperate	Dry	<i>P. patula</i>	18 137	3.2
Cool Temperate	Dry	<i>P. patula</i>	18 073	3.2
Warm Temperate	Moist	<i>E. grandis</i>	17 099	3.0
Warm Temperate	Wet	<i>E. grandis</i>	16 749	3.0
Cool Temperate	Wet	<i>P. patula</i>	16 106	2.9
Warm Temperate	Dry	<i>P. elliottii</i>	14 557	2.6
Warm Temperate	Wet	<i>P. patula</i>	10 903	1.9
Cool Temperate	Moist	<i>E. grandis</i> x <i>E. nitens</i>	10 020	1.8
Cool Temperate	Moist	<i>E. dunnii</i>	9 560	1.7
Sub-tropical	Moist	<i>E. grandis</i> x <i>E. urophilla</i>	8 114	1.4
Cool Temperate	Moist	<i>E. macarthurii</i>	7 958	1.4
Cool Temperate	Moist	<i>P. elliottii</i>	6 764	1.2
Warm Temperate	Moist	<i>E. grandis</i> x <i>E. nitens</i>	6 629	1.2
Warm Temperate	Wet	<i>E. smithii</i>	6 603	1.2
Warm Temperate	Wet	<i>P. elliottii</i>	6 236	1.1
Cool Temperate	Dry	<i>E. macarthurii</i>	6 168	1.1
Warm Temperate	Dry	<i>E. grandis</i> x <i>E. nitens</i>	6 015	1.1
Cool Temperate	Moist	<i>E. benthamii</i>	5 802	1.0
Cool Temperate	Wet	<i>E. nitens</i>	5 802	1.0
Cool Temperate	Moist	<i>E. nitens</i>	5 525	1.0
Cool Temperate	Dry	<i>E. nitens</i>	5 381	1.0

Table 6-6: The commercial forestry species and the ICFR climate zone of the sites for which crop coefficients were estimated

Eucalypt species	ICFR Climate Zone	Pine species	ICFR Climate Zone
<i>E. dunnii</i>	Warm Temperate Dry	<i>P. patula</i>	Warm Temperate Moist
<i>E. grandis</i>	Warm Temperate Moist	<i>P. patula</i>	Cool Temperate Moist
<i>E. grandis</i>	Warm Temperate Dry	<i>P. elliottii</i>	Warm Temperate Dry
<i>E. grandis</i> x <i>E. urophilla</i>	Warm Temperate Moist	<i>P. elliottii</i> x <i>P. caribaea</i>	Warm Temperate Moist
<i>E. grandis</i> x <i>E. nitens</i>	Cool Temperate Moist	<i>P. taeda</i>	Warm Temperate Moist
<i>E. grandis</i> x <i>E. nitens</i>	Warm Temperate Dry		
<i>E. macarthurii</i>	Cool Temperate Moist	Acacia Species	ICFR Climate Zone
<i>E. nitens</i>	Cool Temperate Moist	<i>Acacia Mearnsii</i>	Warm Temperate Dry
<i>E. benthamii</i>	Cool Temperate Moist		

6.4.3 Results and Discussion

The long term, averaged monthly K_c vales derived using the MLBM and the MODIS LAI inputs for the 15 sites are shown in Table 6-7, with the monthly averaged K_c estimates derived with the MLBM and Landsat and Sentinel-2 LAI estimates shown in Table 6-8 and Table 6-9, respectively. The K_c values are all above 1 regardless of species and LAI product used. The K_c values vary only slightly through the year, dropping off slightly in the late winter and spring months. Figure 6-5 illustrates the variation in the K_c values estimated per species and between the LAI products used. The K_c estimating using the three LAI products are generally similar, and the variation between the maximum and minimum K_c values across all species and LAI products is 0.15. The greatest variation between the maximum and minimum K_c value for a species is for *E. grandis x nitens* in both a warm temperate dry (WTD) and cool temperate moist (CTM) climate zone, and when using the Landsat or Sentinel-2 LAI products. Overall, the variation between the minimum and maximum K_c values was less when using the MODIS LAI product. Negligible variation occurred between the minimum and maximum K_c values for *E. grandis* warm temperate moist (WTM), *E. grandis x urophylla* WTM and *P. elliottii x caribaea* WTM.

Table 6-7: The monthly averaged K_c values derived using the MLBM and the MODIS LAI inputs for the 15 sites

Species	Climate	Jan	Feb	Mar	Apr	May	Jun	Jul	Aug	Sep	Oct	Nov	Dec
<i>A. mearnsii</i>	WTD	1.21	1.20	1.21	1.22	1.25	1.25	1.11	1.10	1.16	1.16	1.06	1.18
<i>E. benthamii</i>	CTM	1.20	1.20	1.20	1.15	1.25	1.09	1.14	1.16	1.15	1.11	1.24	1.20
<i>E. dunnii</i>	WTD	1.20	1.19	1.20	1.20	1.20	1.23	1.09	1.24	1.14	1.17	1.15	1.21
<i>E. grandis</i>	WTD	1.09	1.21	1.20	1.15	1.17	1.17	1.13	1.08	1.07	1.14	1.22	1.20
<i>E. grandis</i>	WTM	1.18	1.18	1.18	1.18	1.18	1.18	1.21	1.21	1.20	1.21	1.18	1.18
<i>E. grandis x E. nitens</i>	WTD	1.24	1.21	1.22	1.22	1.25	1.28	1.20	1.23	1.15	1.19	1.11	1.24
<i>E. grandis x E. nitens</i>	CTM	1.23	1.22	1.22	1.22	1.20	1.29	1.20	1.23	1.20	1.09	1.21	1.21
<i>E. grandis x E. urophylla</i>	WTM	1.20	1.18	1.18	1.18	1.18	1.18	1.20	1.23	1.23	1.23	1.23	1.23
<i>E. macathurii</i>	CTM	1.15	1.15	1.22	1.15	1.25	1.10	1.11	1.12	1.06	1.13	1.11	1.18
<i>E. nitens</i>	CTM	1.15	1.19	1.15	1.22	1.16	1.16	1.08	1.07	1.07	1.14	1.22	1.19
<i>P. Elliottii</i>	WTD	1.24	1.23	1.20	1.04	1.15	1.24	1.12	1.09	1.16	1.27	1.15	1.15
<i>P. elliottii x P. caribaea</i>	WTM	1.18	1.18	1.18	1.23	1.21	1.20	1.21	1.21	1.20	1.20	1.23	1.18
<i>P. patula</i>	WTM	1.21	1.21	1.20	1.24	1.19	1.08	1.13	1.13	1.15	1.17	1.14	1.15
<i>P. patula</i>	CTM	1.22	1.22	1.21	1.21	1.23	1.25	1.11	1.16	1.09	1.25	1.20	1.29
<i>P. taeda</i>	WTM	1.22	1.21	1.20	1.20	1.20	1.21	1.22	1.16	1.13	1.21	1.29	1.22

Table 6-8: The monthly averaged K_c values derived using the MLBM and the Landsat LAI inputs for the 15 sites

Species	Climate	Jan	Feb	Mar	Apr	May	Jun	Jul	Aug	Sep	Oct	Nov	Dec
<i>A. mearnsii</i>	WTD	1.20	1.20	1.21	1.25	1.24	1.19	1.09	1.15	1.07	1.21	1.25	1.19
<i>E. benthamii</i>	CTM	1.19	1.19	1.20	1.21	1.21	1.24	1.20	1.14	1.09	1.20	1.22	1.19
<i>E. dunnii</i>	WTD	1.16	1.24	1.16	1.22	1.16	1.20	1.24	1.16	1.15	1.20	1.20	1.05
<i>E. grandis</i>	WTD	1.22	1.08	1.05	1.22	1.08	1.08	1.15	1.20	1.20	1.15	1.20	1.20
<i>E. grandis</i>	WTM	1.18	1.18	1.18	1.18	1.18	1.18	1.21	1.23	1.23	1.23	1.23	1.23
<i>E. grandis x E. nitens</i>	WTD	1.21	1.27	1.28	1.20	1.20	1.27	1.23	1.21	1.19	1.05	1.24	1.22
<i>E. grandis x E. nitens</i>	CTM	1.24	1.20	1.20	1.28	1.23	1.20	1.20	1.23	1.19	1.04	1.22	1.24
<i>E. grandis x E. urophylla</i>	WTM	1.21	1.21	1.20	1.20	1.19	1.20	1.23	1.20	1.23	1.20	1.21	1.23
<i>E. macathurii</i>	CTM	1.27	1.25	1.24	1.25	1.25	1.25	1.24	1.20	1.16	1.16	1.21	1.25
<i>E. nitens</i>	CTM	1.19	1.06	1.06	1.25	1.25	1.25	1.10	1.08	1.15	1.10	1.10	1.25
<i>P. Elliottii</i>	WTD	1.16	1.18	1.22	1.21	1.19	1.20	1.24	1.17	1.18	1.06	1.20	1.16
<i>P. elliottii x P. caribaea</i>	WTM	1.19	1.18	1.18	1.18	1.18	1.18	1.19	1.21	1.23	1.21	1.20	1.18
<i>P. patula</i>	WTM	1.11	1.15	1.22	1.15	1.21	1.17	1.10	1.14	1.13	1.15	1.11	1.10
<i>P. patula</i>	CTM	1.28	1.27	1.20	1.20	1.27	1.23	1.26	1.22	1.19	1.18	1.28	1.25
<i>P. taeda</i>	WTM	1.21	1.20	1.21	1.20	1.20	1.28	1.19	1.06	1.21	1.21	1.21	1.20

Table 6-9: The monthly averaged K_c values derived using the MLBM and the Sentinel-2 LAI inputs for the 15 sites

Species	Climate	Jan	Feb	Mar	Apr	May	Jun	Jul	Aug	Sep	Oct	Nov	Dec
<i>A. mearnsii</i>	WTD	1.19	1.21	1.21	1.21	1.21	1.19	1.09	1.27	1.16	1.10	1.21	1.22
<i>E. benthamii</i>	CTM	1.19	1.05	1.08	1.19	1.20	1.14	1.19	1.19	1.14	1.09	1.19	1.15
<i>E. dunnii</i>	WTD	1.14	1.16	1.23	1.11	1.18	1.24	1.22	1.15	1.15	1.20	1.21	1.18
<i>E. grandis</i>	WTD	1.04	1.24	1.21	1.25	1.18	1.22	1.21	1.20	1.23	1.19	1.09	1.20
<i>E. grandis</i>	WTM	1.21	1.19	1.18	1.18	1.20	1.19	1.21	1.23	1.20	1.23	1.20	1.20
<i>E. grandis x E. nitens</i>	CTM	1.05	1.29	1.27	1.20	1.24	1.25	1.23	1.21	1.21	1.09	1.25	1.23
<i>E. grandis x E. nitens</i>	WTD	1.25	1.21	1.25	1.20	1.20	1.22	1.29	1.20	1.23	1.18	1.15	1.04
<i>E. grandis x E. urophylla</i>	WTM	1.23	1.23	1.20	1.20	1.19	1.21	1.20	1.23	1.22	1.23	1.22	1.21
<i>E. macathurii</i>	CTM	1.21	1.09	1.17	1.18	1.17	1.27	1.27	1.22	1.16	1.11	1.22	1.22
<i>E. nitens</i>	CTM	1.18	1.08	1.09	1.09	1.11	1.14	1.09	1.11	1.14	1.16	1.09	1.15
<i>P. Elliottii</i>	WTD	1.08	1.24	1.21	1.25	1.21	1.24	1.15	1.19	1.19	1.15	1.23	1.20
<i>P. elliotii x P. caribaea</i>	WTM	1.20	1.21	1.21	1.21	1.23	1.22	1.23	1.22	1.20	1.20	1.23	1.20
<i>P. patula</i>	WTM	1.19	1.14	1.26	1.24	1.20	1.16	1.15	1.13	1.12	1.13	1.13	1.14
<i>P. patula</i>	CTM	1.21	1.23	1.24	1.27	1.25	1.21	1.19	1.23	1.17	1.06	1.19	1.20
<i>P. taeda</i>	WTM	1.20	1.20	1.21	1.22	1.27	1.21	1.23	1.22	1.22	1.24	1.28	1.24

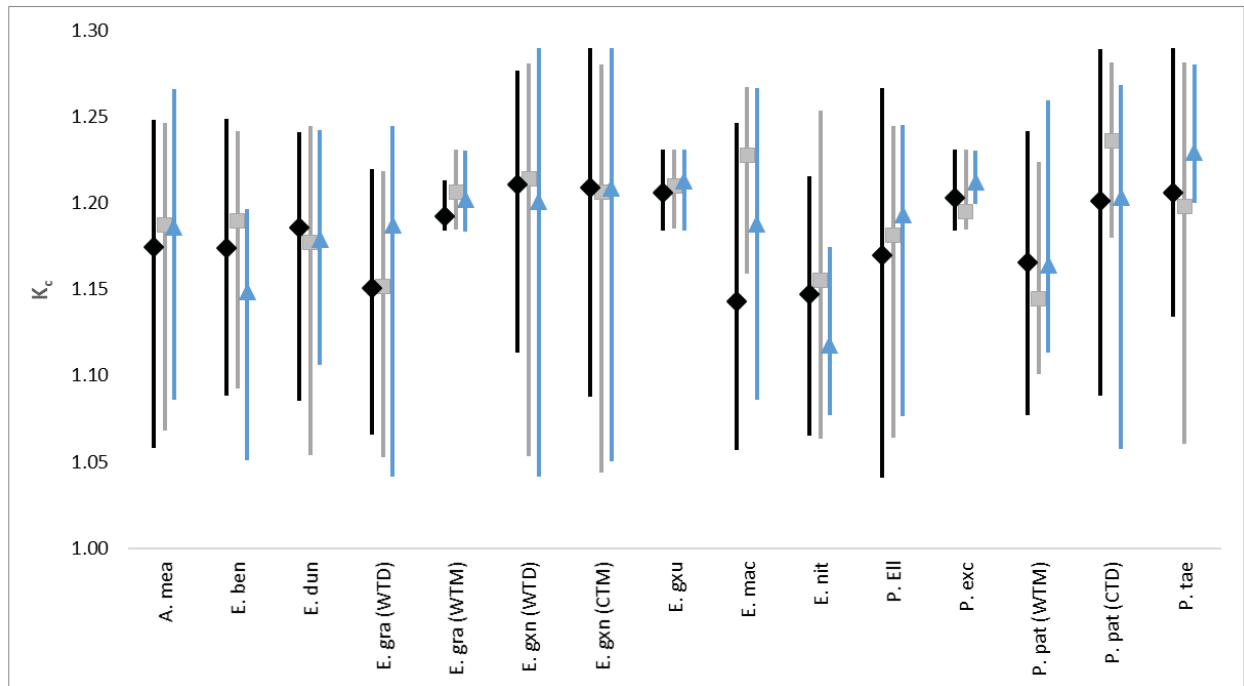


Figure 6-5: Maximum (top of line), minimum (bottom of line) and average (marker) K_c values estimated with the MODIS LAI (black), Landsat LAI (grey) and Sentinel LAI (blue)

The K_c values estimated using MODIS LAI will be the primary set of K_c values used. It must be noted that these are FAO-reference potential related, non-standard K_c values. It cannot be assumed that the time series of LAI values captured non-water stressed conditions. LAI is correlated to rainfall, however, thus the average rainfall pattern over the period the LAI values span will affect them. The response of LAI to rainfall is relatively slow unlike ET_c where there may be a more rapid increase following the vegetation receiving rainfall.

CHAPTER 7. OTHER ACRU INPUT PARAMETERS

R.P. Kunz¹, M.L. Toucher^{1,2} and S. Gokool¹

¹ Centre for Water Resources Research, University of KwaZulu-Natal, Pietermaritzburg

² South African Environmental Observation Network

7.1 Introduction

Since land cover and land use play a significant role in partitioning rainfall into the components of interception, plant and soil water evaporation, infiltration, runoff and recharge, variables relating to the vegetation and its water use are required for hydrological modelling applications. These land cover and land use processes can be grouped functionally into above-ground attributes, ground-surface attributes and below-ground attributes.

The above-ground attributes include the biomass which is determined by the vegetation type and plant structure. Biomass, which varies seasonally and is dependent on climate related factors, primarily determines the maximum evapotranspiration rates (i.e. K_c as discussed in Chapter 6) and the canopy interception losses. The latter variable is either input as a monthly vegetation interception loss (VEGINT in mm.rainday⁻¹) or is calculated using the monthly input leaf area indices (LAI). Plant structure also determines the shading of the soil surface by the vegetation. Water use of the vegetation layer is determined using a monthly crop coefficient (called CAY in ACRU) as explained in Chapter 6.

The ground-surface attributes include (a) the infiltration properties of the soil, which in turn is a controlling factor of the initial abstraction of rainfall before the generation of stormflow (represented in the ACRU model through the coefficient of initial abstraction, COIAM); and (b) the presence and amount of litter and/or mulch (represented as percentage surface cover, PCSUCO), which has the potential to reduce and/or prevent soil erosion and soil water evaporation losses (Schulze, 2007).

The below-ground related attributes include two root-specific attributes that both contribute to determining the patterns of soil water uptake by the vegetation, viz. the seasonal variation of the 1) fraction of active roots in the topsoil horizon (ROOTA), and 2) the degree of root colonisation in the subsoil (COLON) (Schulze, 2004). The onset of plant water stress is also considered to be a below-ground attribute related to vegetation. Within ACRU, the onset of water stress is considered to be the fraction of the soil's plant available water (PAW) at which total evaporation is assumed to drop below maximum evaporation due to drying of the soil. This fraction of PAW is termed CONST in the model.

Therefore, in addition to the monthly K_c (CAY) values, the following parameters were determined using remotely sensed or field-based data (where possible) via a clearly documented and repeatable methodology: VEGINT, ROOTA, COLON, CONST, COIAM and PCSUCO. The methodology used is described in the sections that follow.

7.2 Canopy Interception Loss

Interception is a threshold process, meaning that a certain amount of water is required to fill the canopy storage deficit prior to successive processes such as throughfall, infiltration and runoff occurring (Bulcock and Jewitt, 2012). Thus, in hydrological modelling, it should be one of the first processes considered. However, it is often ignored (Gerrits et al., 2010, Bulcock, 2011) or lumped with total evaporation (Savenije, 2004) as it considered a small component of total evaporation. Interception loss is particularly important in tall vegetation such as forests where evaporation rates of intercepted water are high due to low aerodynamic resistance and high surface roughness. Unlike short vegetation, evaporation rates from intercepted water from tall vegetation exceeds transpiration rates under identical conditions because there is no physiological control by the plants. Therefore, interception is a substantial net addition to actual evapotranspiration (Muzylo et al., 2009).

Two methods of determining canopy interception loss values are described below, viz. 1) the simplistic Von Hoyningen-Huene Method and 2) the more complex “variable storage Gash model”. Importantly, LAI is a primary input to both methodologies.

7.2.1 Methodology

7.2.1.1 The Von Hoyningen-Huene Method

As outlined in Schulze (1995), Von Hoyningen-Huene (1983) related the interception loss (mm.rainday⁻¹) of a number of agricultural crops to gross rainfall (P_g), and LAI as:

$$I_t = 0.30 + 0.27P_g + 0.13LAI - 0.013P_g^2 + 0.0285P_g \cdot LAI - 0.007LAI^2 \quad (7.1)$$

This is the method currently available as an option in the ACURU model, and is preferred over the alternative, which is fixed monthly “interception per rainday” values. The Von Hoyningen-Huene equation has been found to only be “stable” for gross daily rainfall amounts of less than 18 mm above which no further canopy interception is assumed to occur. When investigating canopy interception loss values for the CWRR clusters, Toucher et al. (2020) found no relationship between annual canopy interception losses derived using the Von Hoyningen-Huene method and annual precipitation, because annual canopy interception loss values were all less than 25 mm, due to gross rainfall being “capped” at 18 mm per day. For commercial tree species, the annual sum of monthly canopy interception loss values ranged from 22 mm (*E. nitens* in zone CTM) to 43 mm (*E. grandis* in zone WTM). Of the 15 tree species considered with MODIS LAI data, nine produced more than 25 mm of annual interception loss. Although the Von Hoyningen-Huene method is simplistic and ignores the evaporation loss during the rainfall event, Schulze et al. (1995) showed it adequately estimated the interception loss of a *Pinus patula* stand.

7.2.1.2 The variable storage Gash model

The variable storage Gash model was developed by Bulcock (2011) and is a modified version of the original (Gash, 1979) and revised (Gash et al., 1995) models. Bulcock (2011) used the variable storage Gash model to estimate monthly interception losses for eucalypts, pines and wattle. The model was also used to derive monthly interception loss values for the 121 CWRR natural vegetation clusters (Toucher et al., 2020), as well as for sorghum and soybean (Kunz et al., 2020). The reader is referred to Appendix M of the latter report for a detailed description of the Gash interception model.

The maximum storage capacity (S_c^{max}) represents the rainfall amount required to wet the canopy with droplets of almost “zero” kinetic energy, which can occur when the rainfall intensity is less than

0.36 mm h⁻¹ (Calder, 1996). This variable can be estimated from LAI as described by Van Dijk and Bruinzeel (2001a; 2001b). However, Toucher et al. (2020) obtained S_c^{max} using the WFlow_Sbm model (Arnal, 2014), which calculated representative values for the leafy and woody portions of each natural vegetation cluster. Bulcock (2011; refer to p79 and p108) derived S_c^{max} from the product of LAI and maximum elemental storage (v_e^{max}), with the latter variable set to 0.24, 0.51 and 0.63 for eucalypts, pines and wattle, respectively. In this study, the method utilised by Bulcock (2011) was adopted. Bulcock (2011) set the light extinction coefficient (k ; Equation 35 in Kunz et al., 2020) to 0.5 for each genus, whereas in this study, k was set to

- 0.5 for eucalypts (Gazarini et al., 1990; Bulcock 2011),
- 0.6 for pines (Sampson and Lee Allen, 1998; Vose et al., 1995), and
- 0.4 for wattle (Forrester et al., 2014).

7.2.1.3 Estimation of VEGINT per quinary catchment

For each quinary catchment, monthly estimates of interception loss were determined for each 50-year period (1950 to 1999) using the two above-mentioned methods that require daily climate and monthly LAI as input. From this, long-term monthly means were calculated, together with other useful statistical indicators such as coefficient of variation and the 10th, 50th and 90th percentiles. This was repeated for each set of monthly LAI values obtained from the three remote sensing platforms (MODIS, Landsat and Sentinel2) for each of the 15 forest species, hybrids and clones.

7.2.2 Results and Discussion

As noted by Toucher et al. (2020), the variable storage Gash model produces much higher monthly interception losses than the Von Hoyningen-Huene method across the majority of the 5838 quinaries. One of the main reasons for this is the “capping” of daily rainfall to 18 mm only for the Von Hoyningen-Huene method. The difference in mean monthly interception losses is illustrated for (a) *E. grandis* (WTD1), (b) *P. patula* (WTM4), and (c) *A. mearnsii* (WTD3) in the graphs below for both January (Figure 7.1) and July (Figure 7.2). Although the quinary averaged interception loss for January is 1.76 (VHH) vs 3.57 (VSG) mm.rainday⁻¹, the highest values of 2.21 (VHH) vs 9.60 (VSG) mm.rainday⁻¹ were obtained in quinaries 2370 and 2880, respectively. In July, similar quinary averages of 1.30 (VHH) and 1.27 (VSG) mm.rainday⁻¹ were estimated for *E. grandis*, with maximum values of 1.70 (VHH) and 2.86 (VSG) mm.rainday⁻¹. Slightly higher interception losses were simulated for *P. patula*, with quinary averages of 1.83 (VHH) vs 3.98 (VSG) and 1.35 (VHH) vs 1.53 (VSG) mm.rainday⁻¹ for January and July, respectively. Similar higher interception losses were simulated for *A. mearnsii*, with quinary averages of 2.05 (VHH) vs 3.96 (VSG) and 1.41 (VHH) vs 1.46 (VSG) mm.rainday⁻¹ for January and July, respectively.

7.2.3 Conclusion

Based on the graphs shown below, the decision was made to utilise the Von Hoyningen-Huene estimates, which matches the approach taken in the baseline project (Toucher et al., 2020). Hence, the same method was used to estimate VEGINT in ACRU for both natural vegetation and for the forest species, hybrids and clones, thus facilitating a fair comparison.

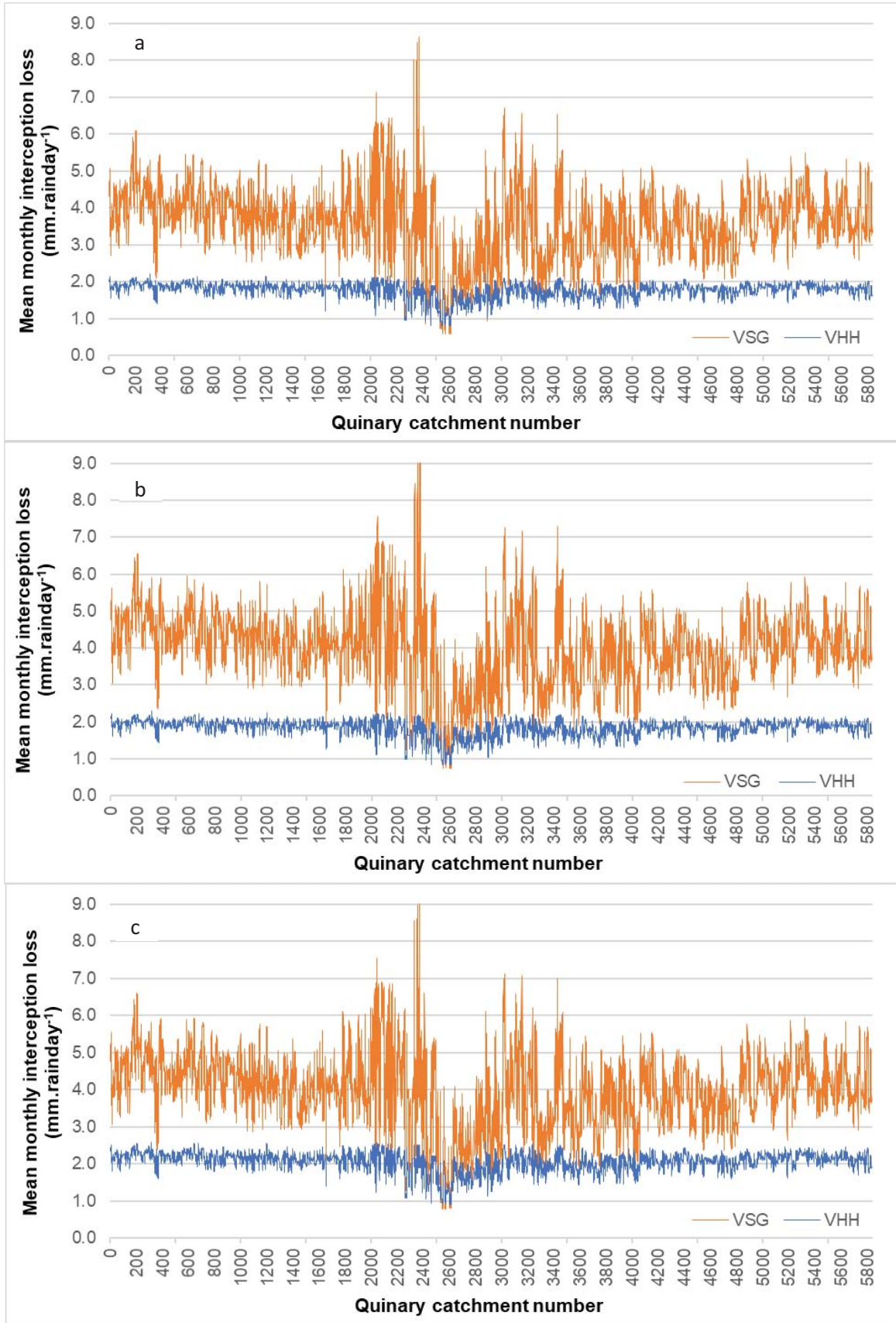


Figure 7-1: Mean monthly interception loss in January for (a) *E. grandis*, (b) *P. patula* and (c) *A. mearnsii*, derived using the Von Hoyningen-Huene (VHH) method and variable storage Gash (VSG) model

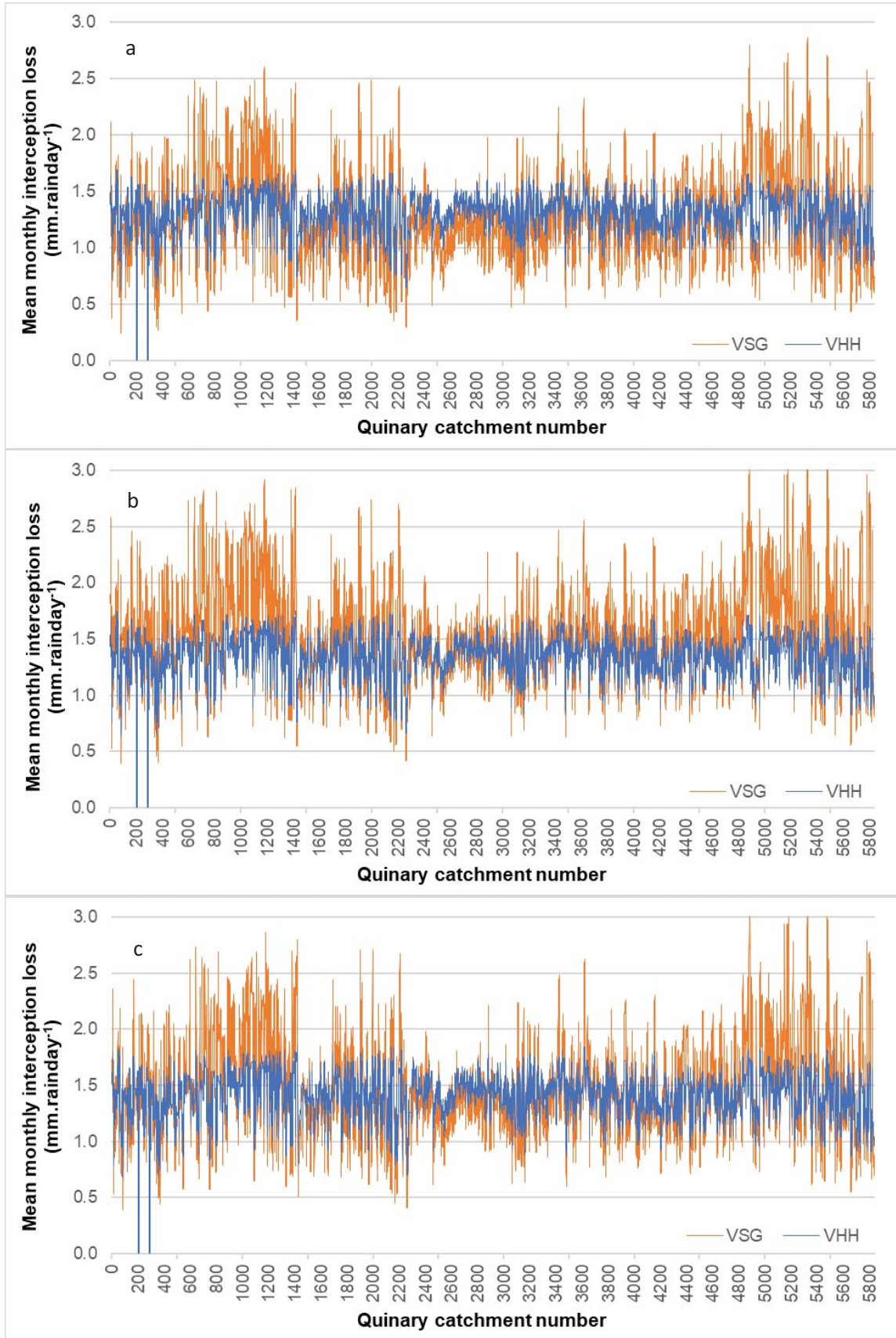


Figure 7-2: Mean monthly interception loss in July for (a) *E. grandis*, (b) *P. patula* and (c) *A. mearnsii*, derived using the Von Hoyningen-Huene (VHH) method and variable storage Gash (VSG) model

7.3 Root specific below ground parameters

Roots tend to grow as deep as is required to adequately anchor the plant/tree, as well as to provide sufficient resources, including both water and nutrients (Schenk and Jackson, 2002). Thus, roots essentially track the availability of water and nutrients across the soil profile (Cheng and Bledsoe, 2002). This is especially true for fine roots, which are primarily responsible for taking up most of the soil water (ACRU FDSS Workshop No3, 1995), and also for obtaining nutrients and oxygen (de Kroon and Visser, 2003; Raz-Yaseef et al., 2013). In comparison, coarse roots are responsible for supporting and anchoring the vegetation, as well as supporting the fine root network (Fogel, 1983). The nature and distribution of the roots through the soil profile at any given time mirrors the transpiration of the vegetation which is governed by the vegetation structure and biomass as well as local site soil conditions including soil temperature, soil water content and nutrient availability (Das and Chaturvedi, 2008). Other factors affecting transpiration include dormancy, senescence, regrowth, growth rates and impeding soil layers. Therefore, changes in vegetation structure and biomass as well as changes in environmental factors, alter vegetation transpiration and result in corresponding changes in root distributions (Day et al., 1996).

In hydrological modelling, the water uptake function of roots needs to be accounted for. Root water uptake by roots is affected by factors including root growth, distribution, colonisation, extension, the differences in the water potentials between plant and soil, the hydraulic conductivity of the soil and the availability of water in the soil. Given the numerous factors affecting root water uptake, it is not a simple matter to attempt to model water uptake. Thus, assumptions, simplifications and generalisations have been made in ACRU to simulate root water uptake.

In ACRU, soil water extraction by roots is considered to occur simultaneously from both soil horizons in proportion to the determined active rooting mass distributions in each horizon, until a soil horizon becomes water limited. Following which plant water uptake is assumed to occur from the wetter soil horizon. Thus, the monthly fraction of active root mass in the A-horizon (ROOTA) is required as an input. This fraction is then used internally to compute the B-horizon root mass (ROOTB). The input ROOTA values need to account for the effect of genetic and environmental factors on transpiration, as well as other factors such as dormancy, senescence, regrowth, growth rates and impeding soil layers. It is important to note, that in the conceptualisation of ACRU, if the parameter describing the fraction of active roots in the A-horizon is ascribed to 1, this designates senescence or no active water uptake by roots from the A-horizon. This essentially means that no transpiration is occurring, only soil water evaporation (Schulze, 1995). The ACRU model also requires the effective rooting depth (EFRDEP) as input. The EFRDEP defines the soil depth to which the effective root system extends within the entire active soil profile (Schulze, 2004b), and is limited to the combined depth of the A and B soil horizons. The last root related input value required is monthly values of the root colonisation of the subsoil horizon (COLON) (ACRU FDSS Workshop No3, 1995), representing the percentage of the subsoil horizon that roots may access the available soil moisture (Summerton, 1995).

Studies related to the roots of the commercial tree species grown in South Africa typically tend to focus on the depth of the tree roots, or the root distribution profile. To note, the studies found were predominantly international studies. Few studies considered the portion of fine active roots in the A-horizon, and those that did defined the fine active roots differently as well as using different methodologies. However, a common finding that emerged from the literature was that a significant portion of the active roots were found in the upper soil horizons. Fredericksen and Zedaker (1995) found that approximately 50% of live fine root biomass was located in the upper 10 cm of soil for young pine-hardwood stands. Similarly, Sudmeyer et al. (2004) concluded that the root density of *P. pinaster*, *P. radiata* and *E. globulus* was greatest in the top 0.5 m of the soil. For *E. grandis*, Laclau et al. (2013) found the majority of fine roots to be in the top

2 m of the soil profile (Figure 7-3). For *E. urophylla*, Teixeira et al. (2002), found that 67% of fine roots were located in the upper 20 cm's of the soil horizon. A further common finding across the studies was that the distribution of the root profile was heavily dependent and influenced by site characteristics (Colter Burkes et al., 2002).

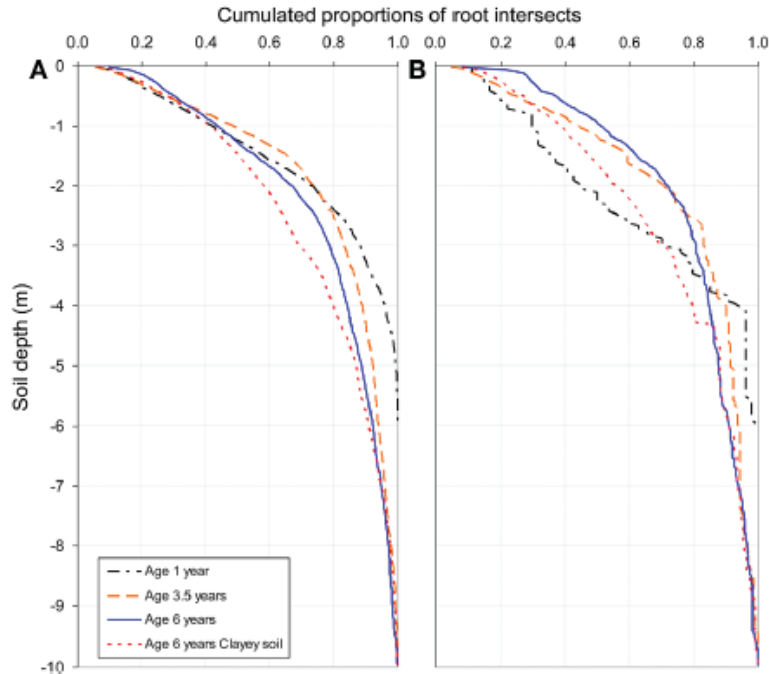


Figure 7-3: Cumulative distribution of (A) fine root intersects (diameter less than 1 mm) and (B) medium root intersects (diameter 1-3 mm) down to a depth of 10 m, from observations on 2-6 soil profiles at each *E. grandis* stand (Laclau et al., 2013).

The sensitivity study presented in Toucher et al. (2020) showed that simulated streamflow and baseflow were only slightly sensitive to changes in ROOTA, with a 50% change in ROOTA altering simulated streamflow by only 12% and baseflow by 7%. Only when ROOTA is 1 (i.e. no transpiration from the A-horizon) is the influence of ROOTA on streamflow simulation significant. Using the literature available and given the limited information relating the fine root distribution, the site dependence of the rooting distribution and the low sensitivity of the ACURU model to the parameter, a monthly ROOTA value of 0.65 across all tree species was selected.

In ACURU, the EFRDEP is limited to combined depth of the A and B soil horizons as determined from the Land Type maps. Setting EFRDEP to 0 defaults the EFRDEP to combined depth of the input soil horizons (i.e. the maximum depth permitted in the model). The combined soil depths of the A and B horizons extracted from the Land Type maps do not exceed 3 m. However, several studies provided evidence of active root depths for the commercial tree species grown in South Africa to depths of 8 m and deeper. Therefore, the EFRDEP for all the tree species was set to 0 to default to the maximum permitted effective root depth.

The last root related input required by ACURU is COLON, defined as the percentage of any given soil horizon to which roots may access the available soil moisture in that horizon (Summerton, 1995). A COLON value of 100% for a given soil horizon implies that the roots in that horizon can access water from 100% of the horizon, provided water is available in the soil. Within the ACURU model, the root colonisation of the topsoil

A-horizon is assumed to be 100% and thus, monthly input values of COLON are only required for the B-horizon (ACRU FDSS Workshop No3, 1995). In this study, COLON was assumed to be 100% for all tree species, hybrids and clones, meaning the tree roots can also access 100% of the soil water stored in the B-horizon. This assumption is deemed valid considering the maximum soil depth is limited to 1.2 m.

7.4 Fraction of plant available water at which plant stress occurs

Within ACRU, onset of plant water stress is considered to be a fraction of plant available water (PAW) of the soil horizon at which total evaporation is assumed to drop below maximum evaporation. The ACRU input variable to represent this fraction of PAW is CONST. As a result of soil water uptake by vegetation, the water content in the root zone dries out. As the soil becomes progressively drier, the forces holding the remaining water to the soil particles becomes greater, lowering its potential energy and making it more difficult for the roots to extract the remaining water. Eventually a point is reached (defined as permanent wilting point or PWP), where the vegetation cannot extract anymore of the remaining water from each soil horizon. Prior to the PWP being reached, vegetation water use is drastically reduced due to the forces holding the remaining water to the soil particles. The threshold of available soil water at which vegetation water use is reduced and plant stress sets in, is dependent on the vegetation nature and type. As CONST approaches a maximum value of 0.9, it indicates the vegetation type is extremely sensitive to water stress and thus, is not drought tolerant.

No field-based studies could be found that determined the fraction of available soil water at which the onset of plant water stress occurs in commercial tree species. A relevant study by Dye (1996) investigated the relation between transpiration rate and soil water availability at two *Eucalyptus grandis* sites. Plastic sheeting was placed over the soil surface at both sites to prevent soil water recharge, which allowed the tree roots to continuously deplete the soil water. Dye (1996) found that declining soil water contents did not cause severe stress in the trees at either site despite the study commencing at a time of severe drought (1991/1992). Given the lack of available information, the FAO 56's (Allen et al., 1998) chapter on crop evapotranspiration under soil water stress was considered.

Allen et al. (1998) provides average fractions of total available soil water content (called the depletion fraction or p) that can be depleted from the root zone before plant stress occurs for various crops and vegetation types. As CONST is the fraction of plant available water in a soil horizon when total evaporation is reduced, it can be defined as the inverse of p , i.e. $CONST = 1 - p$. According to Allan et al. (1998), p ranges from 0.1 to 0.8 and provided a value of 0.7 for conifer trees ($CONST = 0.3$), compared to 0.2 ($CONST = 0.8$) for drought sensitive vegetable crops.

Using these values as limits for CONST values, as well as the findings by Dye (1996), the CONST values for the three commercial tree genera were set as

- 0.2 for eucalypts,
- 0.3 for pines, and
- 0.4 for wattle.

7.5 Coefficient of initial abstraction

In the ACRU model, the coefficient of initial abstraction (COIAM) represents the initial abstractions before stormflow commences, which consist mainly of interception, infiltration and depression storages. The internationally used default value for COIAM is 0.2 (e.g. Hawkins *et al.*, 2002). The relationship between the ratio of initial abstractions with soil surface infiltrability, soil type, antecedent moisture condition, rainfall

amount and intensity has been described extensively in literature (e.g. Hawkins et al., 2002; Mishra and Singh, 2002; Yuan et al., 2012; Kamuju, 2015). However, the uncertainty surrounding the parameterisation of this variable has similarly been extensively noted (e.g. Hawkins et al., 2002; Mishra and Singh, 2002; Yuan et al., 2012; Kamuju, 2015). Given this and the relative insensitivity of streamflow to this variable (as shown in the sensitivity study in Toucher et al. 2020), the working rules established by Schulze (2004) for COIAM linked to rainfall intensity and seasonality and work by Arnold (1981), Schulze (1984), Jewitt (1991) and Topping (1993) were adopted in this study. These working rules were also used to determine the COIAM parameters for the CWRR clusters.

The working rule defined by Schulze (2004) that is relevant to commercial tree species is:

- For dense forests COIAM = 0.35 throughout the year, because the deep litter layer enhances initial infiltration before stormflow commences.

Thus, the COIAM value was set to 0.35 for all months across all tree species.

7.6 Percentage surface cover

Soil water evaporation losses are suppressed in the ACRU model by the variable defined as the percentage surface cover (PCSUCO). PCSUCO suppresses soil water evaporation losses in a linear relationship such that complete cover still allows for 20% soil water evaporation. This variable, which is expressed as a percentage, accounts for the surface cover which includes mulch, litter and stone/rock. Plant litter is recognised to play a major role in

- protecting the soil surface; and
- reducing the evaporation from the ground surface by covering the soil surface and having a high porosity which limits the capillary rise of liquid water from the soil underneath (Sakaguchi and Zeng, 2009).

Schulze (2004) assumed that a greater above-ground biomass resulted in higher litter cover, and through consultation with the National Biodiversity Institute Schulze (2004) used a sigmoidal relationship between PCSUCO and maximum crop coefficient (K_c), simplified into the following:

- For K_c between 0.20 and 0.40, $PCSUCO = 100(K_c - 0.2)$
- For K_c between 0.40 and 0.85, $PCSUCO = 20 + 177.8(K_c - 0.4)$
- For K_c greater than 0.85, $PCSUCO = 100$

This rule was adopted in this study to estimate monthly PCSUCO values, as it was also used to determine monthly PCSUCO values for each Acocks (1988) Veld Type, as well as for each CWRR cluster (Toucher et al., 2020). As the highest monthly K_c value for the various commercial tree species always exceeds 0.85, the PCSUCO value across all months for all tree species was set to 100%. Since PCSUCO was assumed to be constant over the year, it implies that litter decomposition is not considered.

7.7 Streamflow response parameters

In the ACRU model, streamflow response parameters are used to govern the portion of generated stormflow exiting a catchment on a particular day, as well as the portion of baseflow originating from the groundwater store, which contributes to streamflow.

The soil moisture deficit depth (SMDDEP), also known as the critical stormflow generation depth, represents the soil depth that must be wetted before runoff can occur. This parameter accounts for the dominant runoff producing mechanisms that may vary in different climates, as well as with land use, litter

layer and soil conditions. Hence, streamflow generation is extremely sensitive to SMDDEP, particularly for sites with shallow soils and high rainfall intensities. For all hydrological simulations in this project, SMDDEP was set to the thickness of the topsoil, which is the suggested default value (Smithers and Schulze, 1995). Hence, the effective soil depth from which stormflow is generated is the topsoil depth. Schulze (2011) set SMDDEP to the thickness of the topsoil.

The catchment’s stormflow response fraction (QFRESP) influences the timing of streamflow leaving the catchment, but not the magnitude (or volume) of generated runoff. The value is dependent on, inter alia, topography (i.e. catchments with steep slopes exhibit higher QFRESP values). Schulze (2011) recommends 0.30 as being typical at the spatial scale of quinary catchments and is based on experimental evidence.

The baseflow recession constant (COFRU) determines the fraction of daily groundwater store that is released as baseflow, which then contributes to streamflow. Hence, this parameter controls the rate of baseflow release from the groundwater store. A typical value is 0.009 (or 0.9%) for the quinary catchments (Schulze, 2011).

The above-mentioned parameter values, as suggested by Schulze (2011), were used in this project. These values were also used in Kunz et al. (2015), Kunz et al. (2020), Toucher et al. (2020) and Everson et al. (2021).

7.8 Summary

To summarise, the values used for each of the ACRU input variables are:

CAY	Monthly values derived from MODIS LAI input (refer to Chapter 6)
VEGINT	Mean monthly values determined for each quinary catchment using the Von Hoyningen-Huene, which requires daily rainfall and monthly MODIS LAI as input.
ROOTA	0.65 across all commercial forest species and months.
EFRDEP	0 (defaults to depth of A- and B-horizon)
CONST	0.2 for eucalypts 0.3 for pines, and 0.4 for wattle
COIAM	0.35
PCSUCO	100%
COLON	100%
SMDDEP	0 (use thickness of the A-horizon)
QFRESP	0.30
COFRU	0.009

CHAPTER 8. MODEL DESCRIPTION AND INPUTS

R.P. Kunz¹ and M.J.C. Horan¹

¹ Centre for Water Resources Research, University of KwaZulu-Natal, Pietermaritzburg

This Chapter describes the ACRU agrohydrological model used in this study. It also provides a brief description of the updated quinary catchment climate and soils database used as input for the ACRU model.

8.1 The ACRU agrohydrological model

Use of the ACRU agrohydrological model for assessment of potential SFRA has been accepted by DWS (Gush et al., 2002; Jewitt et al., 2009). More recently the ACRU model has been used in other SFRA studies, to assess the potential impacts of biofuel crop cultivation on streamflow (Kunz et al., 2015; Kunz et al., 2020), and the potential impact of bamboo production on streamflow (Everson et al., 2021). The ACRU model was initially chosen and subsequently accepted because it has been intensively and extensively used and verified in South Africa and utilises a sound set of input databases available in the country. “The ACRU model has been developed and shown to be sensitive to land cover, land use and land management changes and has been used frequently in assessing this impact on runoff” (Schulze, 1995; AT2-10). ACRU is a physical-conceptual model of intermediate complexity, physical in that processes are represented explicitly with initial and boundary conditions and conceptual in that it conceives of a system where important couplings and processes are idealised (Figure 8-1; Schulze, 1995). The ACRU model operates at a daily time step, therefore making optimal use of available climatic information, and making the model suitable in terms of flow regimes and sediment yield, which are highly correlated with individual rainfall events (Schulze, 1995).

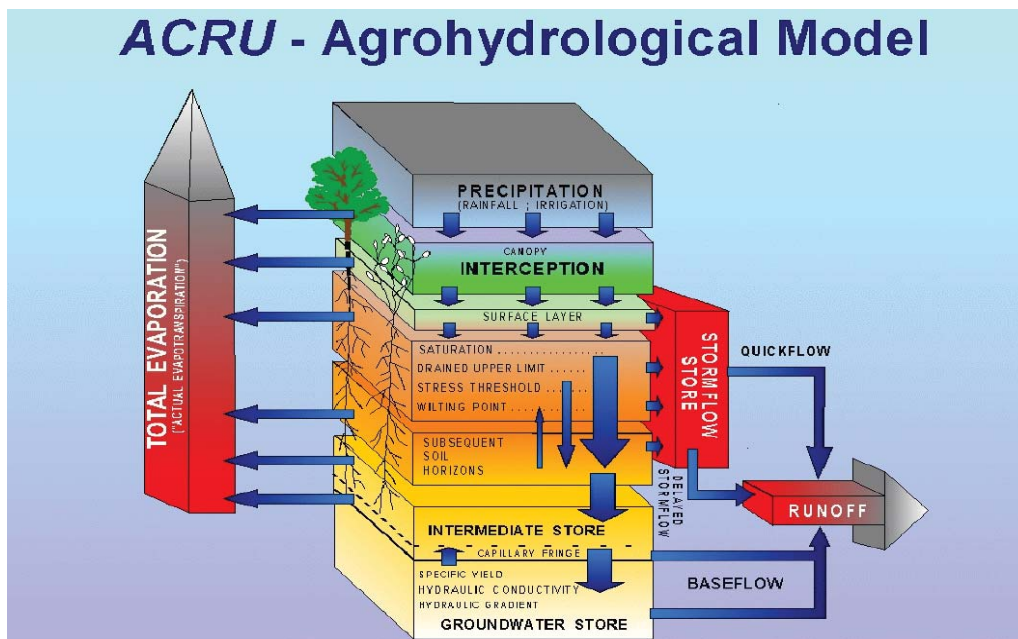


Figure 8-1: Structure of the ACRU agro-hydrological modelling system (Schulze, 1995)

The previous SFRA model output used in the SFRA Utility by Jewitt et al. (2009) were undertaken with ACRU Fortran version 3.31. Since then, significant updates to the ACRU model have taken place. Of significant benefit to this project is the improvements made by Kunz et al. (2020) to ACRU version 3.38 to optimise the speed at which the model runs, as well as significant changes made to the print and statistics utilities to optimise their computational performance and output format. The changes made to optimise ACRU have resulted in the model running 8x faster than the version used in by Jewitt et al. (2009). These improvements allowed for multiple ACRU runs to be undertaken to accommodate the different species.

Since 2009, the ACRU model has been compiled into a Java version. Kunz et al. (2015) highlighted differences in streamflow generated by the Fortran version of ACRU when compared to that from the Java version. One of the reasons for the runoff differences is due to the way in which the two versions adjust the daily crop coefficient within the model. The Fortran version was programmed to reset the daily crop coefficient (K_c) value to that of the monthly input value at the beginning of every month. However, this monthly “resetting” procedure was removed in the Java version, thus allowing the daily K_c value to continue decreasing until recovery from stress begins when the soil water content rises above a threshold value. Kunz et al. (2015) concluded that the Fortran version of the model should be modified to mimic the Java version.

Based on the above recommendation, changes were made to version 3.40 of ACRU to prevent the resetting of the daily K_c value at the beginning of each month. In ACRU, 12 monthly crop coefficients are converted to 366 daily values using Fourier analysis. At the beginning of the simulation (i.e. the first day of Year 1), K_c is set to the daily (i.e. Fourier) value and not the monthly value, which mimics the Java version of ACRU. In addition, daily adjustments made to K_c are limited to Fourier values and not monthly values, which again mimics the Java version. Kunz et al. (2020) investigated the implications of the change for 669 quinary catchments. In total, 169 quinary catchments reflected changes in monthly simulated runoff ranging from 0.01 to 5.84 mm. Changes in annual runoff ranged from 0 to 31.5 mm (or 0 to 48.5%).

For WRC Project No. K5/2833 (Schütte et al., 2021), other significant improvements were made to optimise memory utilisation by the model. This removed the previous limitation where ACRU could only be run for a maximum of 6000 catchments. These improvements were incorporated into ACRU version 3.50, which runs even faster than version 3.38. Additional “tweaks” were made in versions 3.51 and 3.52 to further improve model performance. In summary, ACRU version 3.31 used by Jewitt et al. (2009) took approximately 8.5 hours to complete a national run for all 5838 quinary catchments, whereas version 3.52 used in this study took approximately 23 minutes.

8.2 Updated quinary catchment climate database

The runoff simulated by the ACRU model is extremely sensitive to rainfall input, especially in high-intensity rainfall areas (Schulze, 1995), thus it cannot be over-emphasised that rainfall data used as input for ACRU must be as error-free as possible. Hence, Kunz et al. (2020) invested significant effort into improving the quinary catchments climate database. The full description of the improvements and error checking undertaken are provided in Kunz et al. (2020), with a summary provided below.

In terms of rainfall,

- The driver rainfall station for 11 quaternary catchments (three quinary catchments represent a subdivision of a quaternary) was changed to improve the representation of the rainfall in those catchments.
- The SAWS ID numbers of each of the driver rainfall stations was checked, and 317 SAWS ID numbers were corrected. The ID numbers were used to re-extract the rainfall data from the Lynch (2004)

database. For very few occurrences where the daily value had not been patched by Lynch (2004), these were simply set to 0 mm.

- A total of 13 extreme rainfall events (> 400 mm) were found in the quinary rainfall database. Of these, four values were appropriately corrected when compared to neighbouring gauges.

In terms of temperature,

- The daily temperature dataset deemed representative of each quinary catchment was revised by Kunz et al. (2020) and is now based on observed data, which replaced values derived from the 1'x1' gridded temperature database developed by Schulze and Maharaj (2004).
- A temperature station was selected for the driver rain gauge used for each quinary catchment. The method used to select the temperature station is described in detail in Kunz et al. (2020).
- Following this, a lapse rate adjustment of the temperature data was undertaken. The altitude difference between the temperature station and the average value for each quinary catchment was used to calculate representative temperature values for each catchment. This was achieved using the adiabatic lapse rates corresponding to the region in which the temperature station was located.

Following the revisions to the rainfall and temperature datasets, daily reference evapotranspiration (ET_0 in mm) were calculated using the FAO56 version of the Penman-Monteith equation (Allen et al., 1998). The required inputs of daily solar radiation, as well as relative humidity (maximum and minimum) values, were generated from the revised temperature values using the method described by Schulze et al. (2011) and the wind speed was set to a daily default value of 2 m s^{-1} . As ACRU requires A-pan equivalent reference evaporation, FAO-based reference evaporation was adjusted using the method developed by Kunz et al. (2015). This adjustment was based on a modified version of the PenPan equation, which was successfully applied in Australia to estimate A-pan equivalent evaporation. The adjustments suggest that A-pan equivalent evaporation exceeds FAO56 evaporation by a factor ranging from 16 (for summer) to 51% (for winter) for southern Africa. The reader is referred to Kunz et al. (2015) for more detail on the PenPan method.

Using the updated list of rainfall driver stations, a new climate file in ACRU-composite format. Was generated for each quinary catchment by combining daily rainfall (and its quality code) with the lapse rate-adjusted temperatures (and quality codes). The ET_0 data was added to the climate files, which are called *obstmp_xxxx.txt*, where *xxxx* represents the unique quinary catchment identifier (*SUB_CAT*) that ranges from 0001 to 5838.

8.3 Rainfall adjustment

To improve the representativeness of the point rainfall data (observed at a rainfall recording station), monthly rainfall adjustment factors (called CORPPT in ACRU) were applied to the point data. The CORPPT factors used in this study were derived by Kunz et al. (2020) from the revised quinary catchment database and range from 0.50 to 2.00. The values were identical to those developed by Schulze et al. (2011), except for quinary catchments 4175-4177, where slight changes occurred due to the corrections made to extreme rainfall events.

8.4 Adjusting to the crop coefficients to a-pan reference potential

ACRU requires monthly K_c values calculated using the A-pan as the reference evaporation (E_{PAN}). Since the K_c Forest values are based on FAO56 reference evaporation (E_{REF}), the monthly values were adjusted using a pan coefficient value. Monthly pan coefficients were calculated for each quinary as E_{PAN}/E_{REF} where E_{PAN}

is estimated monthly A-pan equivalent evaporation and E_{REF} is ET_o (i.e. short grass evaporation). Pan coefficients are always greater than 1 as $E_{PAN} > E_{REF}$. Hence, the crop coefficients for the commercial tree species were multiplied by the inverse of the monthly pan coefficients for each quinary to determine pan adjusted crop coefficients as follows:

$$K_{C_PAN} = K_{C_REF} * E_{REF}/E_{PAN} = ET_{FOR}/E_{REF} * E_{REF}/E_{PAN} = ET_{FOR}/E_{PAN} \quad (8.1)$$

Further details on the methodology used can be found in Kunz et al. (2015).

8.5 Improved soils input

For the A- and B-horizons, the Terrain Unit Database (TUDB) described in Chapter 2 contains soil water retention parameters and soil depths for up to five terrain units within each of the 7082 land types across South Africa. This database of 27473 polygons was used to provide improved soils information for each of the 5838 quinaries. This was done using a GIS, where each soil parameter value was first multiplied by a constant to convert into integer format, then the TU polygons were converted from vector (polygon) to raster (grid) format. The quinary catchment boundaries were also converted to raster format and used as a zonal mask to obtain various statistics for each land type and its TUs within each of the 5838 zones. From this, area-weighted soil parameter values were derived for each quinary catchment. The improved soil parameters for South Africa were then merged with previous values that were derived for Lesotho and Eswatini using other soil databases, since land type data does not exist for these two countries. Hence, improved values for PWP, FC and PO were obtained for both soil horizons, as well as depth. Two other ACRU parameters, viz. ABRESP and BFRESP, were also derived for each quinary. These represent the fraction of "saturated" soil water that is redistributed each day from the topsoil into the subsoil horizon, and from the subsoil horizon into the intermediate/ groundwater store.

CHAPTER 9. HYDROLOGICAL IMPACTS OF COMMERCIAL AFFORESTATION

R.P. Kunz¹ and S. Gokool¹

¹ Centre for Water Resources Research, University of KwaZulu-Natal, Pietermaritzburg

9.1 Introduction

Section 36 of the National Water Act (1998) declares land that is used for commercial afforestation a Stream Flow Reduction Activity (SFRA). The declaration was informed and underpinned by the research that has taken place over numerous years starting in 1935 with the establishment of the first forestry research catchment in Jonkershoek, Western Cape. The magnitude of the reduction has been assessed using different tools over time, starting with tools developed from the data from forestry research catchments the Nänni curves (Nänni, 1970), later the Van der Zel Curves (Van der Zel, 1990) which were followed by the CSIR curves (Scott and Smith, 1997). Following the declaration under the NWA of 1998, development of the tools to support the implementation of the declaration continued with Gush et al. (2002) who undertook a verification and modelling exercise using the ACRU agrohydrological model and data from the forestry research catchments. From this work, a set of look-up tables were developed at quaternary catchment scale that express reductions in streamflow (total flow and low flow) caused by the principal commercial forestry genera grown in South Africa (eucalypts, pine and wattle), relative to a baseline flow under indigenous vegetation (considered Acocks Veld Types). Jewitt et al. (2009) developed the SFRA utility and improved the spatial scale of the hydrological modelling from quaternary catchment scale to quinary catchment scale, making use of the quinary catchments database of varying soils and climate. However, only the three commercial forestry genera were represented.

Further to the SFRA Utility, Jewitt et al. (2009) provided a framework for the declaration of a potential candidate SFRA and a framework for the regulation of declared SFRA's. In the framework for the declaration of a potential candidate SFRA, Jewitt et al. (2009) suggested that a 10% reduction in mean annual runoff (MAR) by a land use can be considered a significant reduction or that a 25% reduction of low flows can be considered significant. Low flows are defined as the lowest 25% of the flow regime, or the flow in the driest 3 months of the year.

This project aimed at further improving the SFRA Utility and the data included therein, by broadening the number of species included and making use of the revised climate and soils databases available, as well as undertaking the assessment against the recently developed hydrological baseline, viz. the CWRR clusters. Given the vast changes to the inputs to the ACRU agrohydrological model, this chapter presents the results as simply the quinary catchments where the change in MAR, under the species considered, would be deemed a SFRA ($\geq 10\%$ reduction in MAR).

9.2 Methodology

The ACRU model was used to simulate mean monthly and annual runoff response for:

- baseline conditions (MAR_{BASE}), i.e., the runoff produced from a land cover of natural vegetation (the CWRR clusters), and
- each of the forestry scenarios (MAR_{FOR}), assuming a 100% change in land cover.

This was done using the updated quinary climate database and improved quinary soils database as described in Sections 8.1 and 8.2, respectively. The only variables that were altered between the model runs under the various tree species and the baseline were the vegetation related parameters. The parameter values for the baseline are described in Chapter 4 and those for the forestry runs are given in Chapters 6 and 7. It is important to note that for both baseline conditions and for each forestry scenario, the following was constant (the same):

- version of the ACURU model (version 3.52);
- spatial scale at which the simulations were undertaken (quinary catchment level);
- length of the simulation (1950 to 1999);
- climate files used as input;
- soil parameters used as input; and
- streamflow response variables.

The model was run at the national scale for all 5838 quinaries, regardless of whether commercial forestry could be successfully grown in the quinary. The main reason for running the model for all quinaries was to avoid the scenario where additional model runs may be required for quinaries not previously highlighted as being suitable for forestry production. As tree breeding improves the water use and drought tolerance of species, areas deemed suitable for commercial afforestation may expand and thus, no restrictions were placed for the model runs. Furthermore, due to the significant improvements made to ACURU's performance (cf. Section 8.1 The ACURU agrohydrological model), there is no longer the need to run the model for selected quinaries to minimise computational expense, as was the case in 2009, when the original SFRA model runs were undertaken for approximately 3000 of the 5838 quinaries. Each national run took approximately 23 minutes on a core i9 PC and generated over 8 GB of compressed model output and statistics.

9.3 Results: Quinaries where a more than 10% reduction in MAR occurs

For each quinary, the difference between mean annual runoff generated by the forestry species (MAR_{FOR}) and that for natural vegetation (MAR_{BASE}) was calculated. This difference in annual runoff ($MAR_{BASE} - MAR_{FOR}$) was then expressed as a percentage of the baseline streamflow (MAR_{BASE}). If the difference was above 10%, the quinary was flagged as a potential SFRA candidate. A further change from Jewitt et al. (2009) is that the ACURU modelling was undertaken for all 5838 quinary catchments, not only those deemed climatically suitable for forestry growth. The results shown here are the stream flows produced using vegetation parameters derived from the MODIS LAI values. Maps of the quinary catchments where the change in MAR would be deemed a SFRA ($\geq 10\%$ reduction in MAR) for the four *Pinus* species are shown in Figure 9-1.

In the KwaZulu-Natal, Mpumalanga and Limpopo provinces where the *Pinus* species are predominately grown, the indication is that all *Pinus* species reduce the MAR by more than 10%. The quinaries where a greater than 10% reduction do not occur correspond with the Savanna cluster 7 or the Indian Ocean Coastal Belt biome. ACURU input parameters (e.g. CAY or K_c , VEGINT and PCSUCO) for *Pinus patula* were derived for both a CTM and WTM site. When using these parameters across all quinaries, a difference is evident in the potential SFRA impact. For *P. patula*, the CTM and WTM parameters resulted in 63.9% and 58.6% of all quinaries experiencing a MAR reduction exceeding 10%, respectively. The *Pinus* species which showed the greatest number of quinaries with $\geq 10\%$ of MAR relative to baseline vegetation was *Pinus elliotii x caribaea*. The LAI values for the *P. exc* site, which correspond to the WTM climate zone, varied little and thus, the K_c values showed little variation (Figure 6-5).

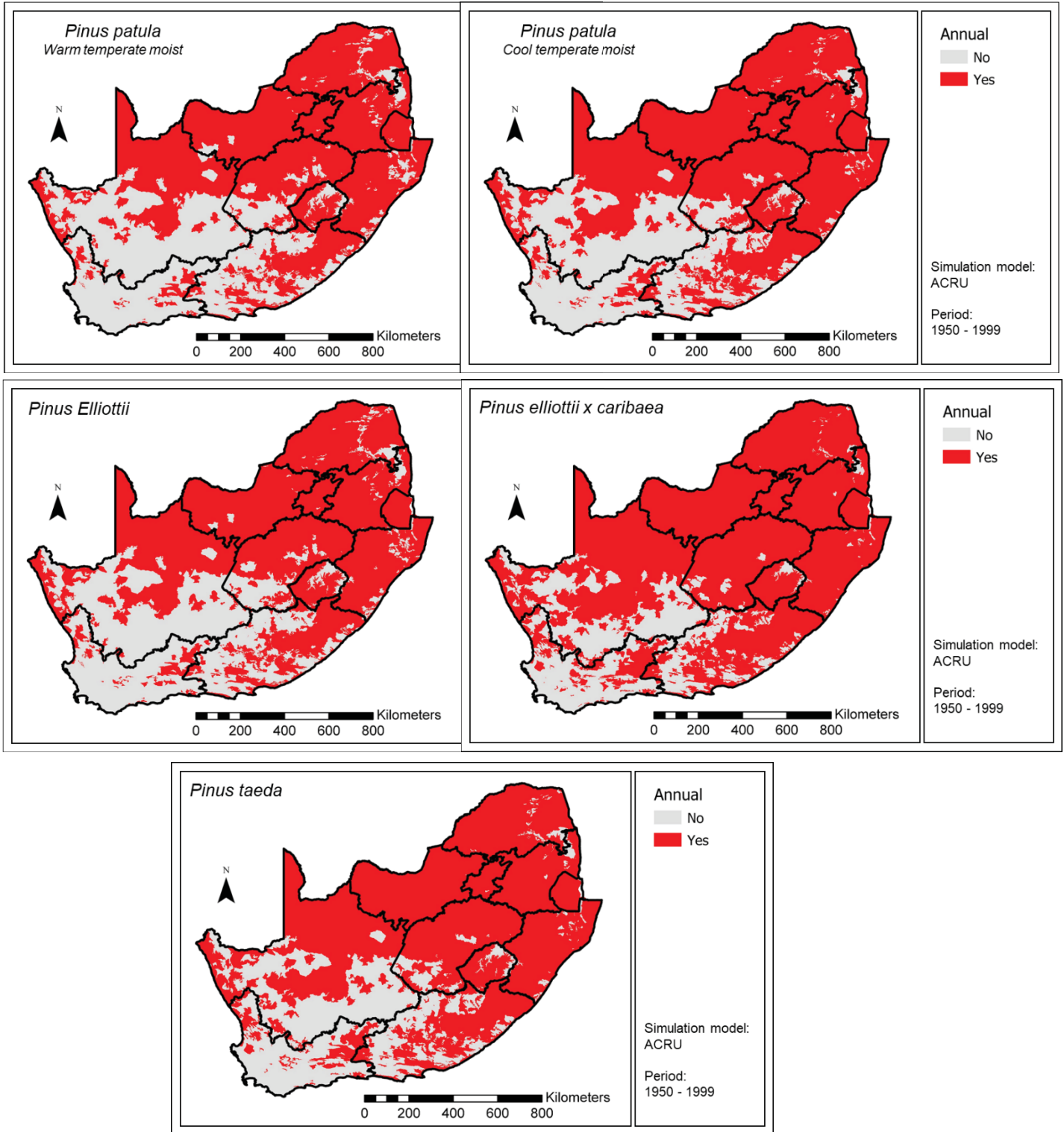
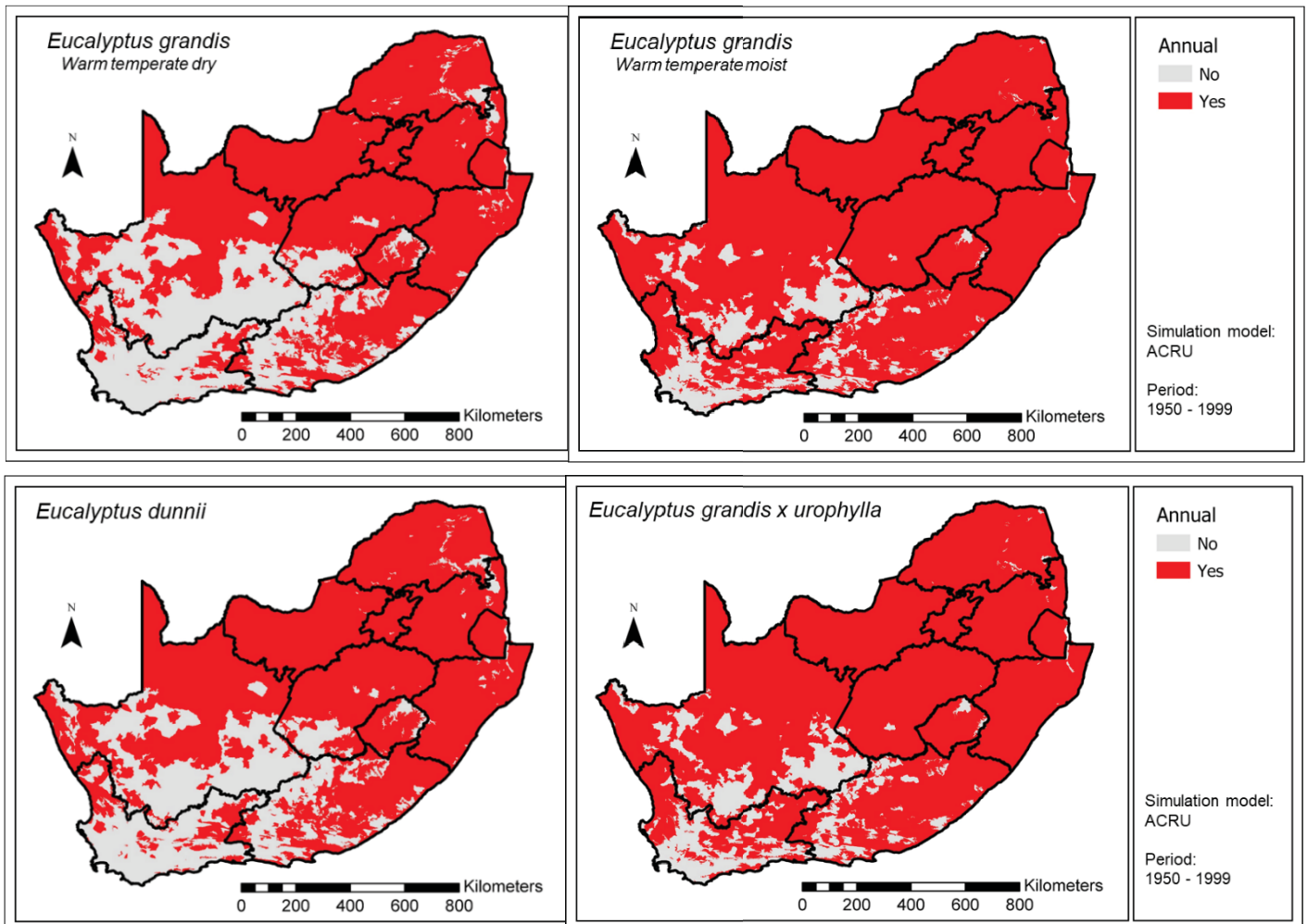


Figure 9-1: Quinary catchments where the change in MAR under *Pinus* species may be deemed a SFRA ($\geq 10\%$ reduction in MAR)

Maps of the quinary catchments where the change in MAR could be deemed a SFRA ($\geq 10\%$ reduction in MAR) for the seven *Eucalyptus* species are shown in Figure 9-2. In the KwaZulu-Natal, Mpumalanga and Limpopo provinces where the *Eucalyptus* species are predominately grown, the indication is that all *Eucalyptus* species reduce the MAR by more than 10%. As with the *Pinus* species, the quinaryes where a greater than 10% reduction do not occur correspond with the Indian Ocean Coastal Belt biome (Savanna cluster 7).

LAI and K_c values for *Eucalyptus grandis* were derived for both a WTD and WTM site, whilst for *Eucalyptus grandis x nitens*, values were developed for a CTM and WTD site. No difference is evident between the CTM and WTD *Eucalyptus grandis x nitens* parameters (Figure 9-2). However, a difference is evident between the WTD and WTM *E. grandis* parameters, with the latter parameters producing a $\geq 10\%$ reduction of MAR (relative to the baseline) in 83.6% of all quinaryes. Across all the species considered, this represented the highest number of quinaryes to fall into the SFRA category. Since the WTM site is wetter than the WTD site, the variation in LAI values was minimal, and subsequently the variation in K_c values was also minimal (Figure 6-5). Using the WTD parameters for *E. grandis*, 65.3% of quinaryes show a $\geq 10\%$ reduction of MAR relative to the baseline. Using the parameters for *E. gxu*, 81.9% of quinaryes exhibit a SFRA impact, i.e. the second largest impact following *E. grandis* (WTM zone). Similarly, the LAI values and subsequent K_c values for *E. gxu* showed little variation, as the site also fell within the WTM climate zone.



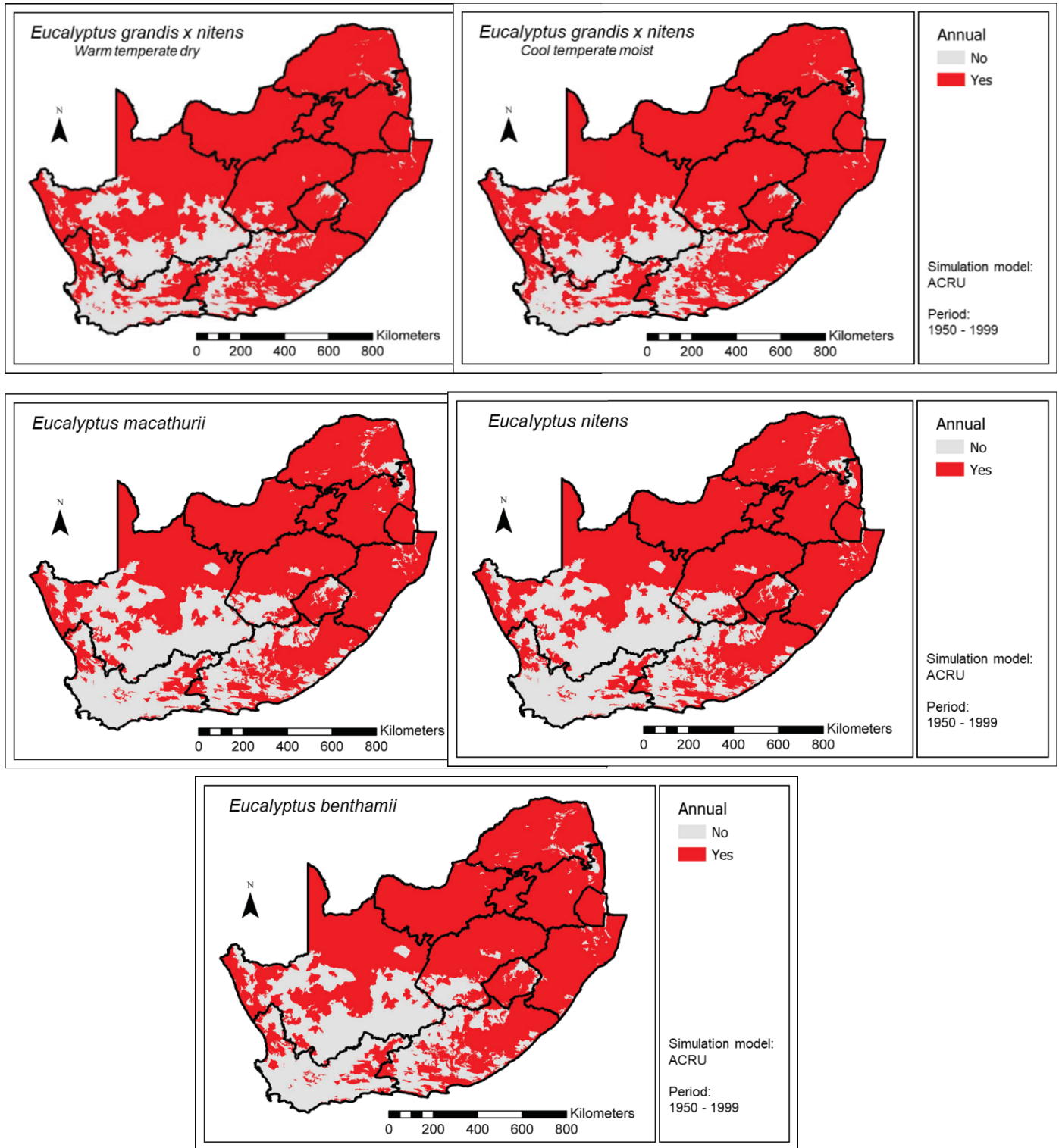


Figure 9-2: Quinary catchments where the change in MAR under *Eucalyptus* species may be deemed a SFRA ($\geq 10\%$ reduction in MAR)

A map showing the quinary catchments where the change in MAR could be deemed a SFRA ($\geq 10\%$ reduction in MAR) for *Acacia mearnsii* is shown in Figure 9-3. Of all the commercial forestry species considered, using the parameters for *Acacia mearnsii* resulted in the lowest proportion of quinary to be affected by commercial afforestation. The average K_c value for *Acacia mearnsii* and the range of values did not differ significantly from the other commercial forestry species. The CONST value (fraction of plant available water at which stress occurs) for *Acacia mearnsii* was set at 0.4 which is the same value used across all the baseline vegetation clusters.

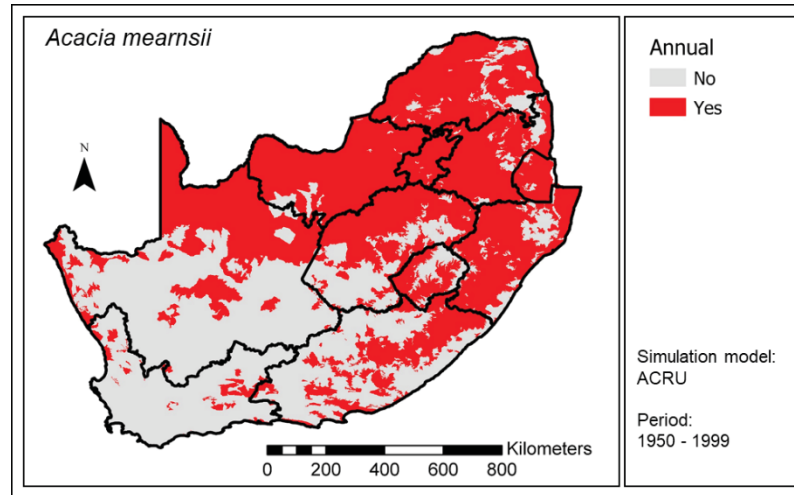


Figure 9-3: Quinary catchments where the change in MAR under *Acacia mearnsii* may be deemed a SFRA ($\geq 10\%$ reduction in MAR)

9.4 Results: influence of the different LAI products

The above results were produced using the K_c parameters derived using the MODIS LAI values. As shown in Figure 6-5, K_c derived from Landsat and Sentinel-2 LAI values appear similar. However, the influence through the model to the streamflow output was considered, given the known sensitivity of the model to changes in K_c . The comparison was undertaken based on the number of quinary which resulted in a $\geq 10\%$ reduction in MAR relative to baseline vegetation. For this comparison, two species and one hybrid were chosen, as they exhibited the largest differences in MODIS and Landsat LAI values, viz. *E. grandis* (WTD climate zone), *P. patula* (CTM climate zone) and *P. exc* (WTM climate zone). The latter had a narrow range of K_c values, whereas *P. patula* showed a larger variation in the range of K_c values (Figure 6-5).

For *E. grandis*, MODIS and Landsat K_c values resulted in 65.3% and 67.4% of all quinary exhibiting a significant SFR, respectively. For *P. exc*, a similar result was obtained (73.4 and 75.8%) and the small differences in percentages were deemed negligible. The largest percentage difference was found for *P. patula* (63.9% vs 66.8% for MODIS and Landsat K_c values). The MODIS range of K_c values was smaller than that of the Landsat K_c values for *P. patula*.

For the primary basins in which commercial trees are primarily grown, negligible differences were also found between the percentage of quinary showing a $\geq 10\%$ reduction in MAR relative to baseline vegetation under the two different sets of K_c values (Figure 9-4). Slight differences in percentages were noted for *P. patula*, with the greatest difference in primary U of 3.2%, which equates to six quinary. Overall, the influence of the LAI product used can be considered negligible.

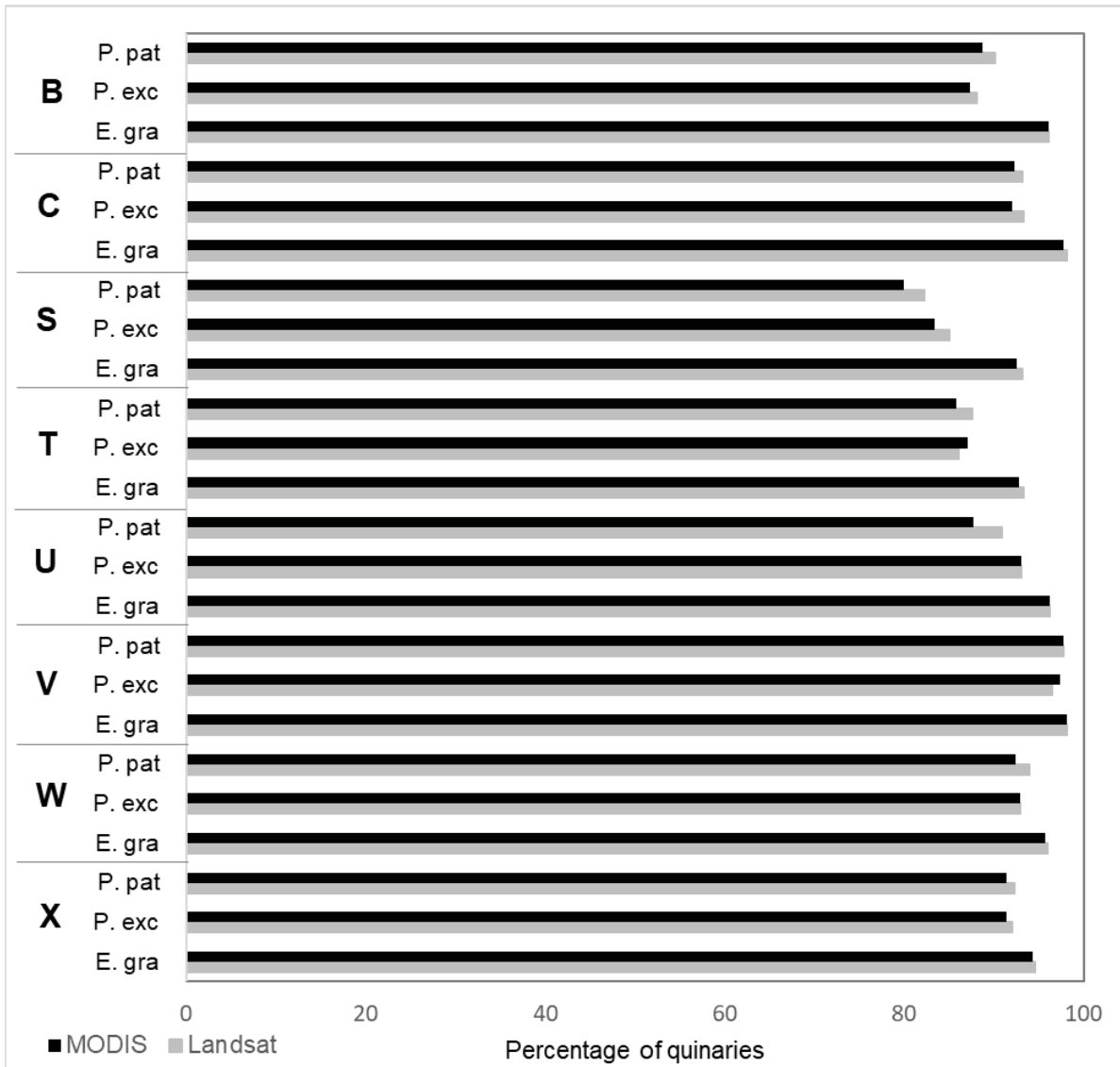


Figure 9-4: Percentage of quinary catchments per primary basin where the change in MAR estimated using K_c values derived with either MODIS or Landsat under *P. patula*, *P. exc* and *E. grandis* may be deemed a SFRA ($\geq 10\%$ reduction in MAR)

CHAPTER 10. SFRA UTILITY

S.L.C. Thorton-Dibb¹

¹ Centre for Water Resources Research, University of KwaZulu-Natal, Pietermaritzburg

10.1 Background and introduction

An initial version of the SFRA Utility was developed in 2009 as part of the SFRA project (Jewitt et al., 2009). The first version consisted of a Microsoft Access database as the backend and a frontend written in the Microsoft C# programming language. The utility was compressed and packaged onto a CD for distribution. The backend required the conversion of output generated by the ACRU model runs into the format and structure required by MS Access. This was identified as an unnecessary step that required considerable time and computing resources. Hence, the second version of the SFRA Utility that was distributed to the DWS consisted of a smaller Microsoft Access database, which was utilised for the configuration of the utility and the modelled time series data.

Kunz et al. (2015) made numerous modifications to the SFRA Utility to improve its performance and to facilitate the dissemination of ACRU output related to the water use of selected biofuel crops. They noted that use of the Microsoft Access database caused installation problems on certain PCs and thus, replaced the configuration database with an XML file to avoid the known installation problems. Additional ACRU output variables were made available to the user of the utility when compared to the original, which defaulted to only the unit streamflow from a catchment (called SIMSQ in ACRU). The addition of additional variables added more storage space requirements and complexity to the utility, as well as issues with units and aggregation of data from daily to monthly level. More options were also added to the statistical calculations done by the utility, i.e. user-selected start of the hydrological year.

10.2 Recent updates to the SFRA Utility

For this project, further improvements were made to the version of the SFRA Utility developed by Kunz et al. (2015). Core to the utility is the data simulated by the ACRU model. As these datasets grow through the addition of more land cover scenarios, the decision was made to store the monthly time series data produced by ACRU's post-processing software, as opposed to the raw daily time series files outputted by ACRU. This required a complete restructuring of the data reading and aggregation processes within the utility. Further development has also been focused on restructuring and updating the code base from the original .NET Framework 2.0 technology, since it is becoming increasingly difficult to deploy software requiring these older technologies onto newer computing systems. The original map interface was dependant on this older framework and thus, was removed from the utility as it would only hamper the installation and was not deemed necessary to correctly use SFRA Utility.

10.3 Recommendations

Further work on decoupling the various components of the software utility is recommended. A more robust API backend is required that would facilitate the development of the utility frontend on a Web based platform. This web-based frontend would access a central backend database, thus making it much easier to update the database and to roll out improvements to the frontend.

CHAPTER 11. GENUS ASSESSMENT UTILITY USER MANUAL (VERSION 2.0.0.2)

11.1 Introduction

The Genus Assessment Utility is a product of WRC Project No. K5/2791, which was completed in 2022. The utility is a software tool that was created to allow a user to view, extract and make comparisons of different *ACRU* model simulations.

11.1.1 Installation

The Genus Assessment Utility is a software tool designed to run on a PC/laptop running the Microsoft Windows operating system.

Minimum PC/laptop requirements:

- PC running Microsoft Windows 7/8/10/11 (32- or 64-bit).
- Please check the Microsoft Web site for updates/patches for the Dot Net Framework.
- 10.6 GB of free disk space.

The Genus Assessment Utility is made up of two parts:

- a) The software utility (application).
- b) The hydroclimatic datasets which contains time series data (i.e. *ACRU* monthly output files) per land use.

Download the installation file called **01_Setup_Genus_Assessment_Utility.msi** from the URL provided. Then download the 16 *_**db.exe** files from the URL provided. Each db.exe file is ~187 MB in size and thus, a total of 2.92 GB of disk space is required to temporarily store these files.

To install the software utility (i.e. part a above):

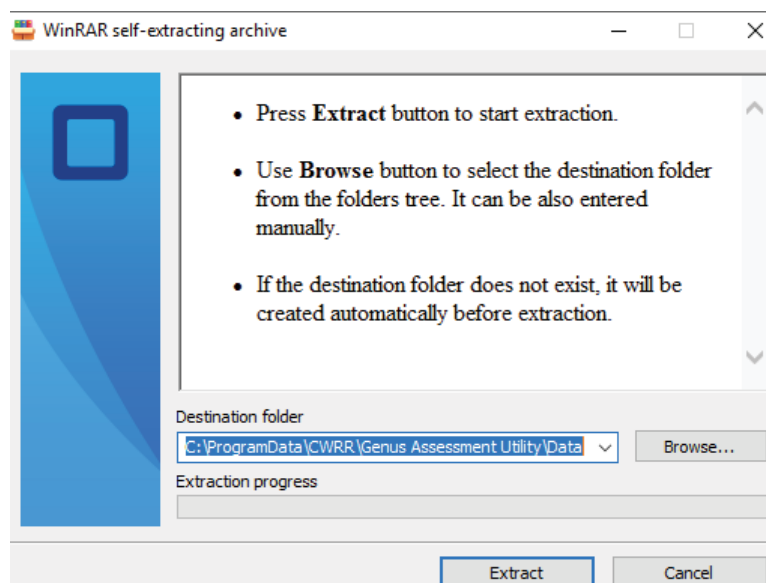
- 1) Double click on **01_Setup_Genus_Assessment_Utility.msi** to install the software utility.
- 2) Click the **Next** button to begin the installation.
- 3) Select the “**I accept the terms in the License Agreement**” option, then click the **Next** button.
- 4) Click the **Typical** button.
- 5) Click the **Install** button to begin the installation.
- 6) This will install the software in the following default folder:
"C:\Program Files (x86)\CWRR\Genus Assessment Utility\"
- 7) Untick the option **Launch Genus Assessment Utility**, then click the **Finish** button.
- 8) The installation folder should contain the following 6 files (7.61 MB):

C:\Program Files (x86)\CWRR\Genus Assessment Utility	
Name	Size
ACRU_bin_tools.dll	34 KB
Genus_assessment_utility.exe	4 240 KB
Genus_assessment_utility.exe.config	1 KB
Genus_Assessment_Utility_Help.pdf	1 557 KB
TeeChart.Lite.dll	908 KB
utility_db.xml	1 056 KB

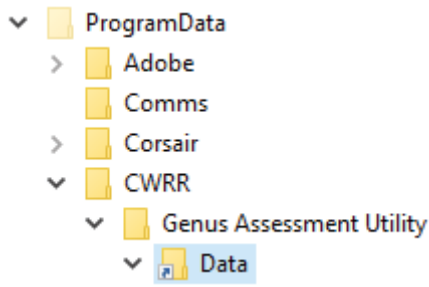
To install the hydroclimatic datasets (i.e. part b above):

- 1) Make sure there is sufficient hard disk space to extract the time series data for all required land uses. Each extracted dataset contains 5838 files requiring ~684 MB of disk space. All 16 datasets will occupy 10.6 GB of disk space.
- 2) To install the baseline (natural vegetation) dataset, double click on the **02_obstmp_nat_veg_db.exe** file that was previously downloaded.
- 3) Unpack all 5838 s*.csv files to the following folder:
C:\ProgramData\CWRR\Genus Assessment Utility\Data

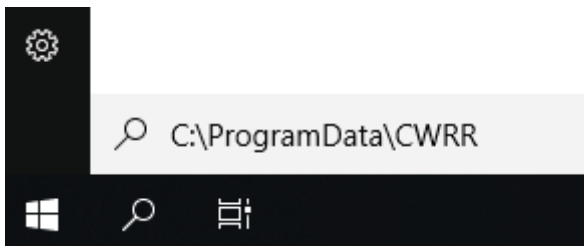
If needed, copy and paste this link into the window called “Destination folder”.



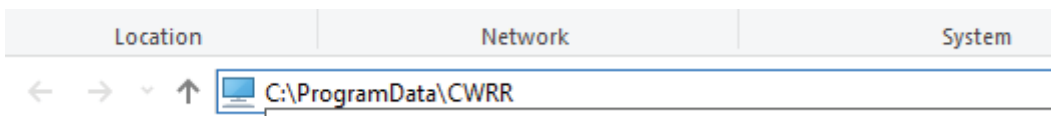
Alternatively, click the Browse... button and navigate to the above folder.



If the C:\ProgramData folder is hidden in Windows File Explorer, click on search  icon on the taskbar and type C:\ProgramData\CWRR, then press the Enter key:



Alternatively, type C:\ProgramData\CWRR into Windows File Explorer, followed by the Enter key:



It is also possible to search the Internet on how to permanently unhide the C:\ProgramData folder.

- 4) Double click on **03_obstmp_m4a_mea_db.exe** and follow the instructions above.
- 5) It is recommended that the user then checks if the utility runs correctly by double clicking on the **Genus_assessment_utility.exe** icon created on the user's desktop.
- 6) If the following error message appears, it indicates the baseline (natural vegetation) dataset was not installed correctly, i.e. the following folder contains no s*.csv files:

C:\ProgramData\CWRR\Genus Assessment Utility\Data\obstmp_nat_veg\05_mth

Timeseries Error



Could Not Locate Timeseries Data for Variable: SIMSQ in:
Natural Vegetation (CWRR clusters)

Please ensure that the data files have been extracted to the
data folder: C:\ProgramData\CWRR\Genus Assessment
Utility\data\data\

File: C:\ProgramData\CWRR\Genus Assessment
Utility\data\obstmp_nat_veg\05_mth\s00001.csv
does not exist.

OK

- 7) A similar error message may appear if the *Acacia mearnsii* dataset was not installed correctly, i.e. the following folder contains no s*.csv files:

C:\ProgramData\CWRR\Genus Assessment Utility\Data\obstmp_m4a_mea\05_mth

- 8) If no issues were found and the utility runs, the 14 remaining dataset files (one for each land use) can then be installed.

Monthly SIMSQ (mm) A10A1 (0001) Natural vegetati		Monthly SIMSQ (mm) A10A1 (0001) Acacia mearnsii		Monthly Change in SIMSQ (m Percentage Change in	
Date	Natural vegetation(2020)	Date	Acacia mearnsii	Date	Change in SIMSQ (m Percentage Change in
1950/01/01	7.59	1950/01/01	3.47	1950/01/01	4.12
1950/02/01	1.23	1950/02/01	0.15	1950/02/01	1.08
1950/03/01	12.23	1950/03/01	2.33	1950/03/01	9.9
1950/04/01	0.43	1950/04/01	0.07	1950/04/01	0.36
1950/05/01	21.44	1950/05/01	19.76	1950/05/01	1.68
1950/06/01	4.24	1950/06/01	3.38	1950/06/01	0.86
1950/07/01	0.05	1950/07/01	0.05	1950/07/01	0
1950/08/01	0.03	1950/08/01	0.04	1950/08/01	-0.01
1950/09/01	0.03	1950/09/01	0.04	1950/09/01	-0.01
1950/10/01	12.11	1950/10/01	7.33	1950/10/01	-4.78
1950/11/01	0.55	1950/11/01	0.18	1950/11/01	0.37
1950/12/01	31.11	1950/12/01	15.9	1950/12/01	15.21
1951/01/01	34.75	1951/01/01	23.72	1951/01/01	11.03
1951/02/01	2.44	1951/02/01	2.86	1951/02/01	-0.42
1951/03/01	4.85	1951/03/01	3.52	1951/03/01	1.33
1951/04/01	7.67	1951/04/01	6.68	1951/04/01	0.99
1951/05/01	67.88	1951/05/01	67.82	1951/05/01	0.06
1951/06/01	5.13	1951/06/01	7.42	1951/06/01	-2.29

- 9) Once the baseline dataset (natural vegetation) and each of the 15 land use data files have been successfully installed, the *_db.exe files can be deleted to save disk space.

- 10) The data folder should contain the following 16 sub-folders (93 408 files; 10.6 GB):

Name	Type
obstmp_m1p_ell	File folder
obstmp_m2e_gxn	File folder
obstmp_m3e_dun	File folder
obstmp_m4a_mea	File folder
obstmp_m5e_gxu	File folder
obstmp_m6p_tae	File folder
obstmp_m7p_pat	File folder
obstmp_m8p_exc	File folder
obstmp_m9e_gra	File folder
obstmp_mae_gra	File folder
obstmp_mbp_pat	File folder
obstmp_mce_nit	File folder
obstmp_mde_mac	File folder
obstmp_mee_gxn	File folder
obstmp_mfe_ben	File folder
obstmp_nat_veg	File folder

Advanced options

The following should only be attempted if necessary. It is strongly recommended that the user is assisted by an IT professional.

If storage space is an issue on the PC/laptop’s C: drive, it is possible to change the location of the database folder, which by default is:

C:\ProgramData\CWRR\Genus Assessment Utility\Data

This can be achieved in one of two ways, both of which require **Administrator privileges**. The first method is preferred and is easier to implement.

- a) Method 1: Move the file called *utility_db.xml* from the installation folder (e.g. *C:\Program Files (x86)\CWRR\Genus Assessment Utility*) to the user’s desktop.

Create a backup copy of this file called *utility_db_bak.xml*.

Edit the *utility_db.xml* file with an XML editor (e.g. XML Notepad 2007) or a standard text editor (e.g. Notepad), search for the tag called “<DataPath>” and manually change the path of the database folder.

The utility will work with both a local (e.g. *D:\CWRR\GeX_Utility\Data*) and UNC path name (e.g. *\\<fileserv_name>\<path>\Data*).

Move *utility_db.xml* back to the installation folder.

Run the utility to make sure it functions properly, i.e. an error message titled "Could Not Locate Time Series Data..." does not occur [see point 6) and 7) above].

- b) Method 2: Copy the **Data** folder in C:\ProgramData\CWRR\Genus Assessment Utility to the desired location, e.g. D:\CWRR\GeX_Utility. This can be achieved using the following DOS commands:

```
cd "C:\ProgramData\CWRR\Genus Assessment Utility"  
xcopy /I Data "D:\CWRR\GeX_Utility\Data"
```

Rename the **Data** folder in C:\ProgramData\CWRR\Genus Assessment Utility to **Data_bak**. This can be achieved using the following DOS commands:

```
cd "C:\ProgramData\CWRR\Genus Assessment Utility"  
rename Data Data_bak
```

Create a symbolic link from the default folder to the desired physical location of the database. This can be achieved using the following DOS commands:

```
cd "C:\ProgramData\CWRR\Genus Assessment Utility"  
mklink /J Data "D:\CWRR\GeX_Utility\Data"
```

Run the utility to make sure it functions properly. If so, the **Data_bak** folder can be deleted.

It is also possible to move the database folder to a network drive. For this option, the Systems Administrator of the fileserver needs to provide the necessary assistance. The Systems Administrator needs to create a read-only folder called **Data** on the fileserver where the database can be stored, e.g. \\<fileserver_name>\<path>\Data

The **Data** folder on the fileserver must then be populated with data by extracting the 16 *.db.exe files to this folder.

Then, a symbolic link must be created from the default folder to the network folder. This can be achieved using the following DOS commands:

```
cd "C:\ProgramData\CWRR\Genus Assessment Utility"  
mklink /D Data "\\<fileserver_name>\<path>\Data"
```

If an error occurs when creating the symbolic link, the following DOS command can be used to assess if the user has permission to create "Local to remote symbolic links", i.e. this option should be enabled:

```
fsutil behavior query SymlinkEvaluation
```

To enable "Local to remote symbolic links", the following DOS command can be used:

```
fsutil behavior set SymlinkEvaluation L2R:1
```

11.2 Using the Genus Assessment Utility

The **Genus_Assessment_UTILITY.exe** is run by:

- selecting the shortcut from Start...Programs...CWRR (Windows 7),
- selecting the shortcut from Start  and looking under G (Windows 10),
- clicking on search  and typing genus, or
- double-clicking the shortcut on the user's Desktop.

The User Interface (UI) is shown in Figure 11-1 and requires the user to provide the following 5 inputs to indicate the:

- 'current' land use (default is natural vegetation to represent baseline conditions),
- proposed land use (forestry species or hybrid),
- hydrological variable of interest (default is simulated runoff; called *SIMSQ* in *ACRU*),
- quinary sub-catchment to be assessed (e.g. A10A1 or sub-catchment number 0001),
- start month of the hydrological year (for statistical calculations).

The main UI comprises of:

- **User Selection Controls** as displayed in Figure 11-2 and described in Table 11-1, and
- *Display Option Tabs* as shown in Figure 11-3 and described in Table 11-2.

In this manual, the **User Selection Controls** (e.g. drop-down lists and buttons) are highlighted in **bold**, whereas the *Display Option Tabs* are highlighted in *italics*.

VOLUME 2: WATER USE ESTIMATION OF SFRA SPECIES

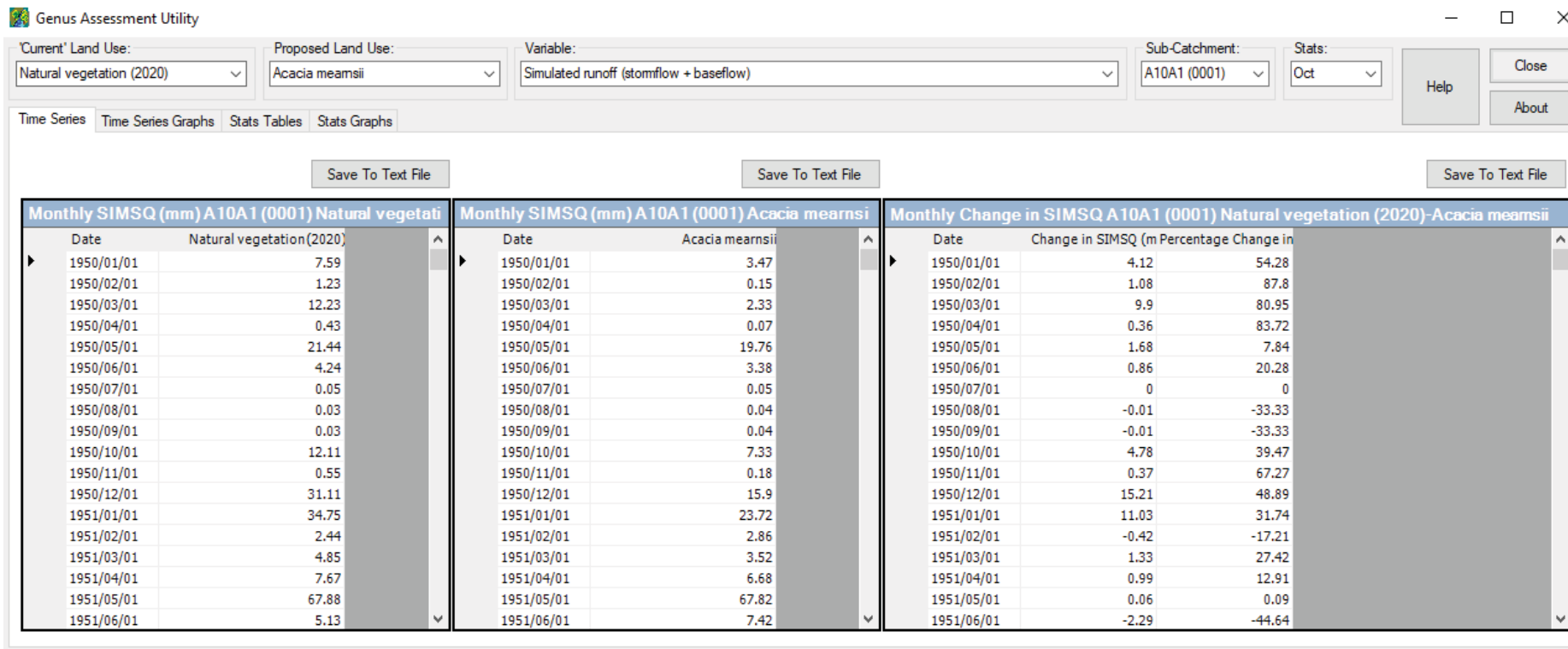


Figure 11-1: Genus Assessment Utility's User Interface

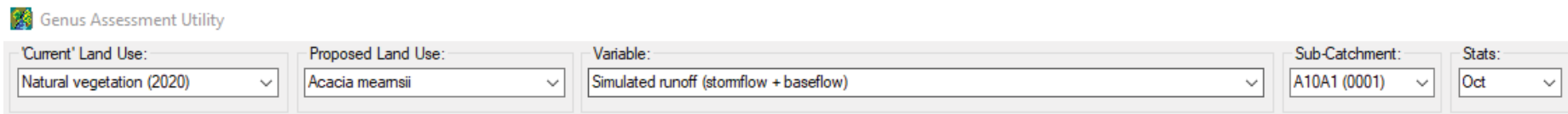


Figure 11-2: Genus Assessment Utility's User Selection Controls

VOLUME 2: WATER USE ESTIMATION OF SFRA SPECIES

Table 11-1: Description of each User Selection Control

User Selection Control	Description
'Current' Land Use	Baseline land use to be compared against
Proposed Land Use	Proposed land use to be analysed
Variable	Output variable to be analysed (as listed in Table 11.3)
Sub-Catchment	The particular quinary sub-catchment to be analysed
Stats	Start month for the hydrological year (October is the default)



Figure 11-3: Assessment Utility's Display Option Tabs

Table 11-2: Description of each Display Option Tab

Display Option Tab	Description
<i>Time Series</i>	Tables of the baseline land use, proposed land use and differences
<i>Time Series Graphs</i>	Graphs of the baseline and proposed land use
<i>Stats Tables</i>	Calculated statistics displayed as a table
<i>Stats Graphs</i>	Calculated statistics displayed as a graph

11.2.1 User Selection Controls

This section is a brief overview of how to use the **User Selection Controls**. First, select from the **'Current' Land Use** options (Figure 11-4a). Next, populate the **Proposed Land Use** with the desired option as shown in the example given in Figure 11-4b.

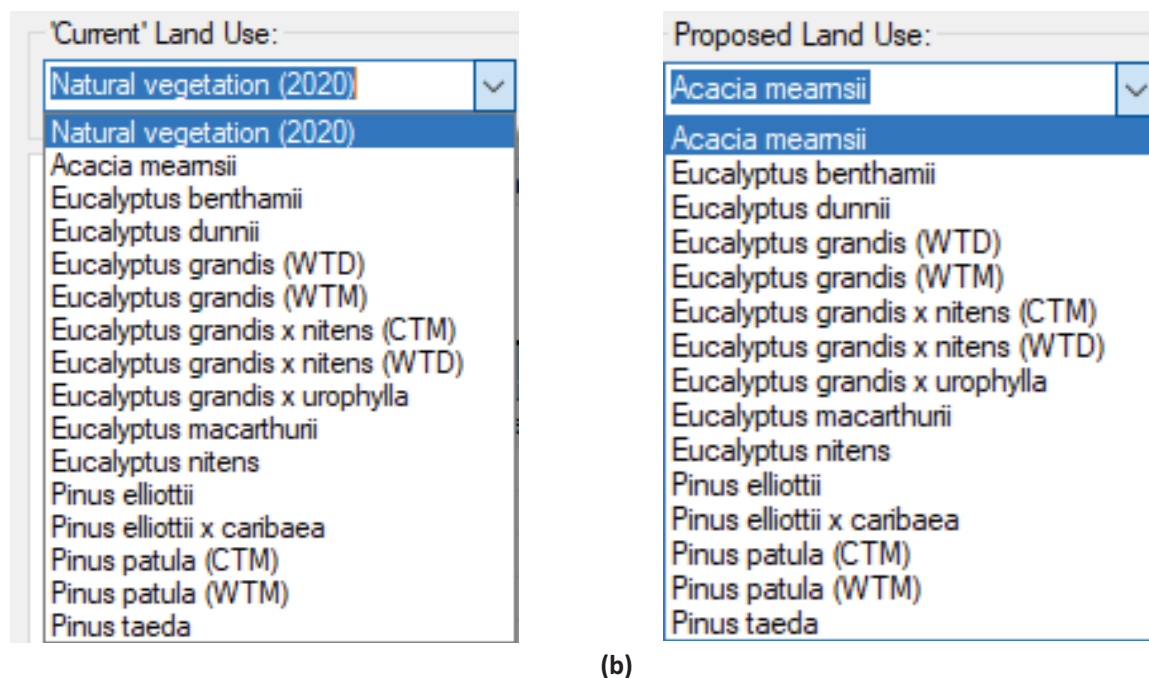


Figure 11-4: Genus Assessment Utility's (a) 'Current' Land Use, and (b) Proposed Land Use selectin options under User Selection Control

Thereafter, select the desired output variable (see Table 11-3) from the **User Selection Control** called **Variable** as shown in Figure 11-5. The output variable selected by default is the runoff (stormflow + baseflow) simulated by ACRU (called *SIMSQ*). It is the estimated runoff generated in the selected quinary sub-catchment only and thus, excludes all contributions from upstream sub-catchments.

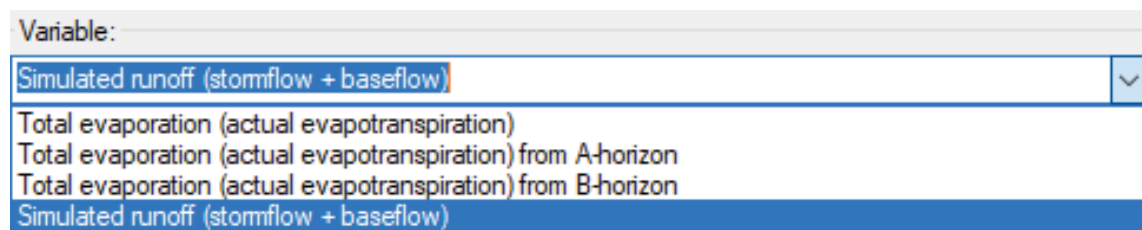


Figure 11-5: Genus Assessment Utility's variable selection from User Selection Control

Table 11-3: Description (and units) of each output variable

Variable	Description	Aggregation	Units
<i>AET</i>	Total evaporation (i.e. actual evapotranspiration) $AET = AET\ 1 + AET\ 2$	Sum	mm
<i>AET1</i>	Total evaporation (actual evapotranspiration) from A-horizon	Sum	mm
<i>AET2</i>	Total evaporation (actual evapotranspiration) from B-horizon	Sum	mm
<i>SIMSQ</i>	Simulated runoff (stormflow + baseflow) from the sub-catchment, excluding upstream contributions	Sum	mm

Finally, select the specific **Sub-Catchment** to be analysed from the **User Selection Control** as shown in Figure 11-6a below. Alternatively, you can start inputting a particular sub-catchment name and the list will be filtered according to provided search characters (Figure 11-6b).

VOLUME 2: WATER USE ESTIMATION OF SFRA SPECIES

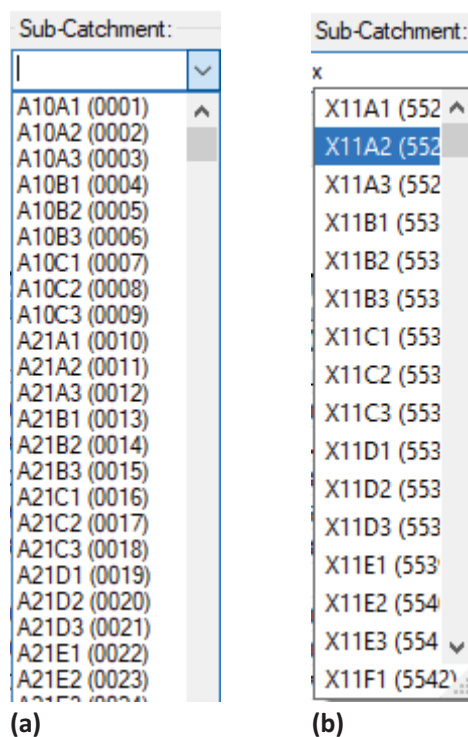


Figure 11-6: Sub-Catchment (a) User Selection Control, and (b) search feature

The utility then loads the monthly time series data for both selected scenarios (**'Current' Land Use** and **Proposed Land Use**). This enables the data comparison for the selected **Sub-Catchment** and the statistical analysis to be performed. The utility also calculates the change (i.e. **Proposed Land Use** – **'Current' Land Use**), which is expressed as either an absolute difference (in mm) or as a percentage change relative to **'Current' Land Use** (c.f. **Section 11.2.2.1** below for more information).

11.2.2 Display Option Tabs

The *display option tabs* enable simple navigation between the simulated time series (data & graphs) and statistics (data & graphs).

11.2.2.1 Time series

The *Time Series* tab displays the monthly time series data for the selected sub-catchment's '**Current**' Land Use and **Proposed Land Use** in tabular format (Figure 11-7), as well as the calculated difference (i.e. **Proposed Land Use** – '**Current**' Land Use). These tables can be exported to comma delimited files (.CSV) by selecting the corresponding **Save To Text File** button.

The screenshot shows a software interface with three data tables. Each table has a 'Save To Text File' button above it. The tables are:

Monthly SIMSQ (mm) A10A1 (0001) Natural vegetati	
Date	Natural vegetation(2020)
1950/01/01	7.59
1950/02/01	1.23
1950/03/01	12.23
1950/04/01	0.43
1950/05/01	21.44
1950/06/01	4.24
1950/07/01	0.05
1950/08/01	0.03
1950/09/01	0.03
1950/10/01	12.11
1950/11/01	0.55
1950/12/01	31.11
1951/01/01	34.75
1951/02/01	2.44
1951/03/01	4.85
1951/04/01	7.67
1951/05/01	67.88
1951/06/01	5.13
1951/07/01	13.7

Monthly SIMSQ (mm) A10A1 (0001) Acacia mearnsii	
Date	Acacia mearnsii
1950/01/01	3.47
1950/02/01	0.15
1950/03/01	2.33
1950/04/01	0.07
1950/05/01	19.76
1950/06/01	3.38
1950/07/01	0.05
1950/08/01	0.04
1950/09/01	0.04
1950/10/01	7.33
1950/11/01	0.18
1950/12/01	15.9
1951/01/01	23.72
1951/02/01	2.86
1951/03/01	3.52
1951/04/01	6.68
1951/05/01	67.82
1951/06/01	7.42
1951/07/01	14.1

Monthly Change in SIMSQ A10A1 (0001) Natural vegetation (2020)-Acacia meamsii		
Date	Change in SIMSQ (m	Percentage Change in
1950/01/01	4.12	54.28
1950/02/01	1.08	87.8
1950/03/01	9.9	80.95
1950/04/01	0.36	83.72
1950/05/01	1.68	7.84
1950/06/01	0.86	20.28
1950/07/01	0	0
1950/08/01	-0.01	-33.33
1950/09/01	-0.01	-33.33
1950/10/01	4.78	39.47
1950/11/01	0.37	67.27
1950/12/01	15.21	48.89
1951/01/01	11.03	31.74
1951/02/01	-0.42	-17.21
1951/03/01	1.33	27.42
1951/04/01	0.99	12.91
1951/05/01	0.06	0.09
1951/06/01	-2.29	-44.64
1951/07/01	-0.4	-2.92

Figure 11-7: Genus Assessment Utility's *Time Series* tab (data for illustration purposes only)

11.2.2.2 Time series graphs

The *Time Series Graphs* tab displays the time series for the selected sub-catchment's '**Current**' Land Use and **Proposed Land Use** in graphical format (Figure 11-8).

The graphical view option has various buttons (   ) to enable closer inspection of the time series.

The time series graph can also be navigated by various left and right mouse clicks:

- Reset graph - Double click on the graph, or press the **Reset** button
- Pan graph - Right click, hold and drag mouse
- Zoom graph - Left click, hold and drag mouse or press the **Zoom** button

VOLUME 2: WATER USE ESTIMATION OF SFRA SPECIES

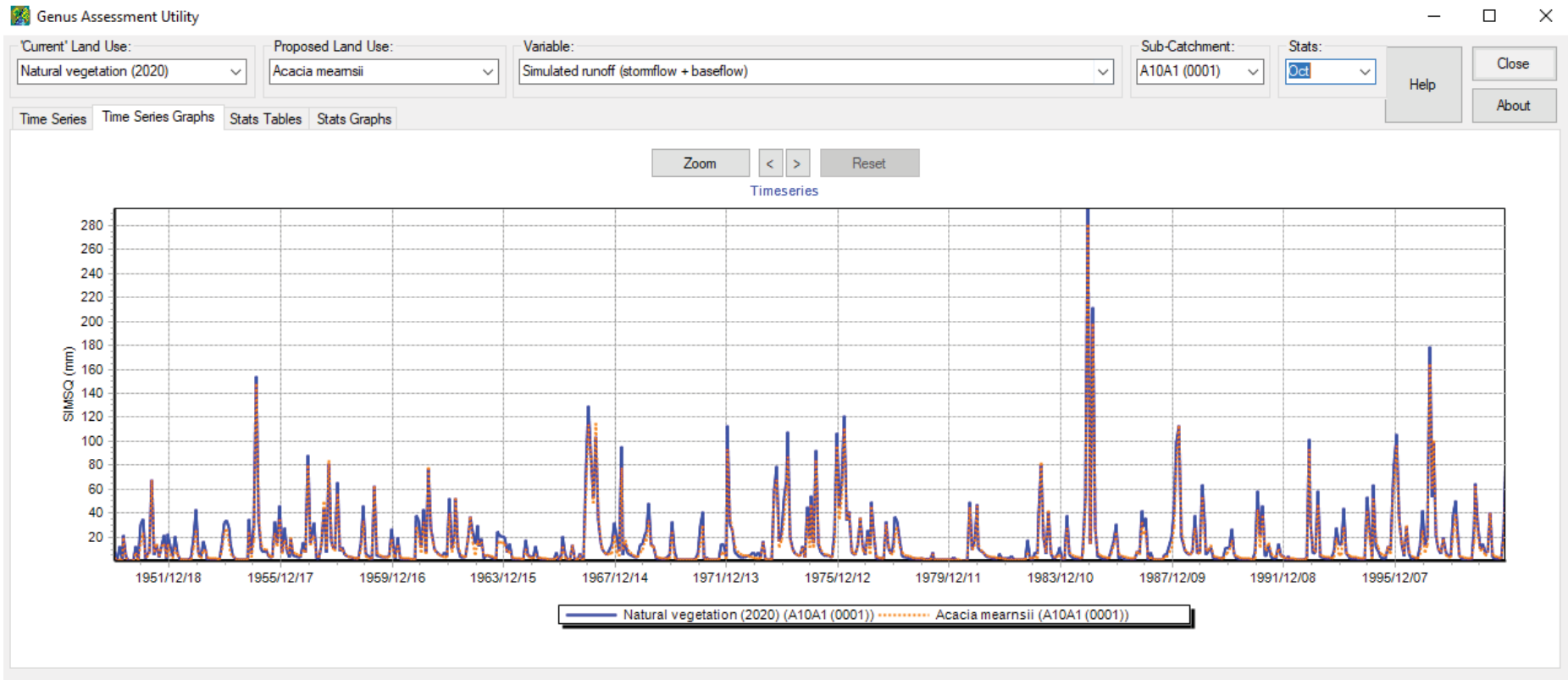


Figure 11-8: Genus Assessment Utility's *Time Series Graphs* tab (data for illustration purposes only)

11.2.2.3 Stats tables

Statistics are calculated on the monthly data. The start month for the calculation of annual statistics can be selected from the **Stats** drop-down option. These statistics can also be exported as comma separated (CSV) files by clicking the **Save to Text File** button.

The *Stats Tables* tab displays the calculated statistics in tabular format for the selected sub-catchment's:

VOLUME 2: WATER USE ESTIMATION OF SFRA SPECIES

- ‘Current’ Land Use (Figure 11-9), or
- Proposed Land Use (Figure 11-10), or
- absolute difference in mm (i.e. ‘Current’ Land Use – Proposed Land Use in Figure 11-11), or
- percentage change relative to the current land use (i.e. ‘Current’ Land Use – Proposed Land Use as% in Figure 11-12).

‘Current’ Land Use – Proposed Land Use (as %) is calculated by first determining the absolute difference in monthly and annual mean values (i.e. ‘Current’ Land Use – Proposed Land Use, which is then divided by the ‘Current’ Land Use means and multiplied by 100 to obtain the percentage change values. Differences expressed in relative terms are only available for the mean values, i.e. they cannot be calculated for the percentiles.

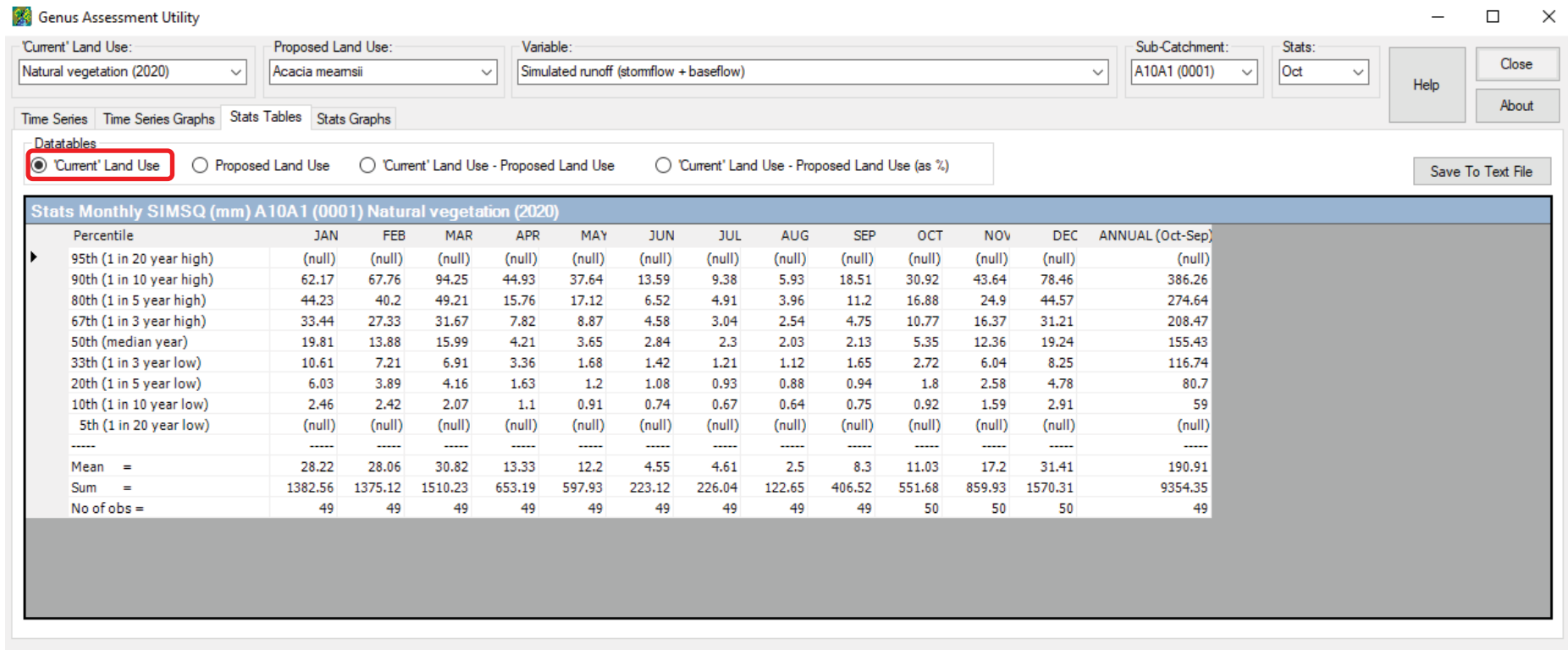


Figure 11-9: Stats Tables tab (‘Current’ Land Use, data for illustration purposes only)

VOLUME 2: WATER USE ESTIMATION OF SFRA SPECIES

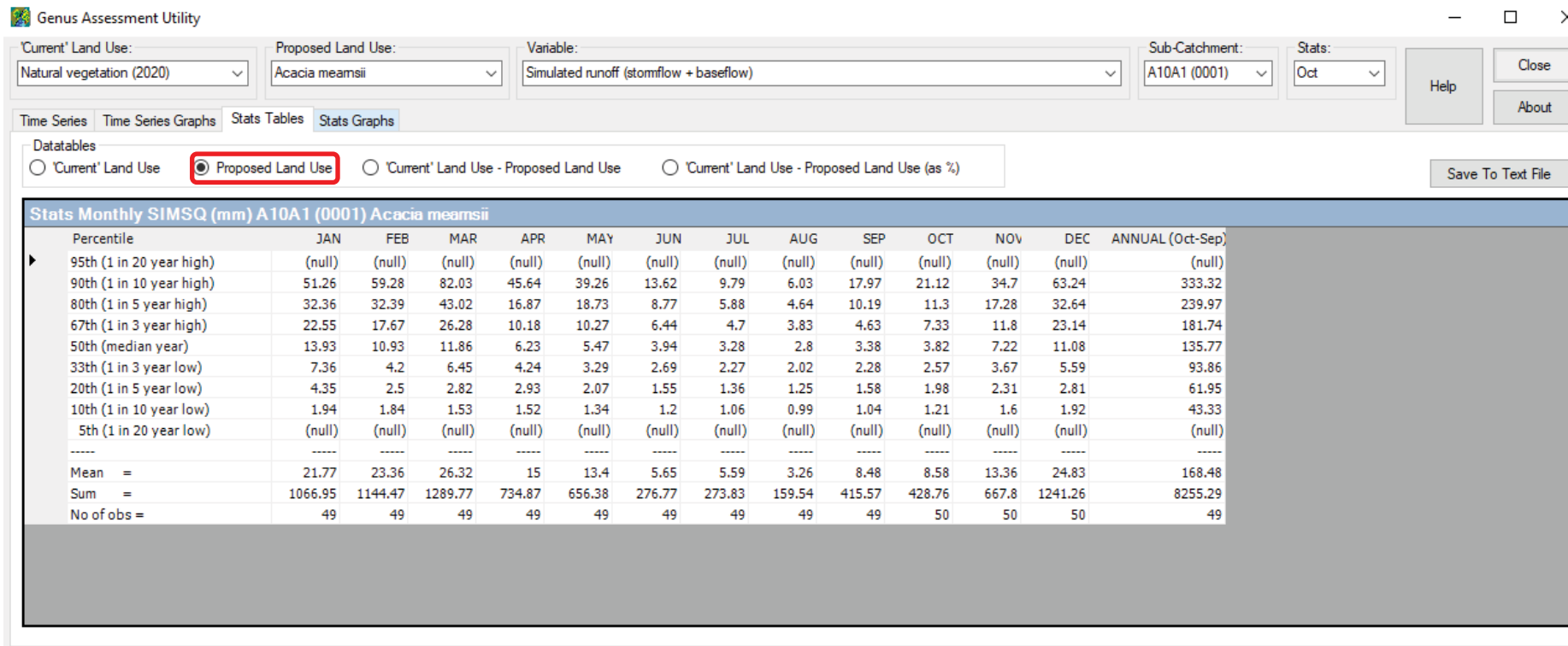


Figure 11-10: Stats Tables tab (Proposed Land Use, data for illustration purposes only)

VOLUME 2: WATER USE ESTIMATION OF SFRA SPECIES

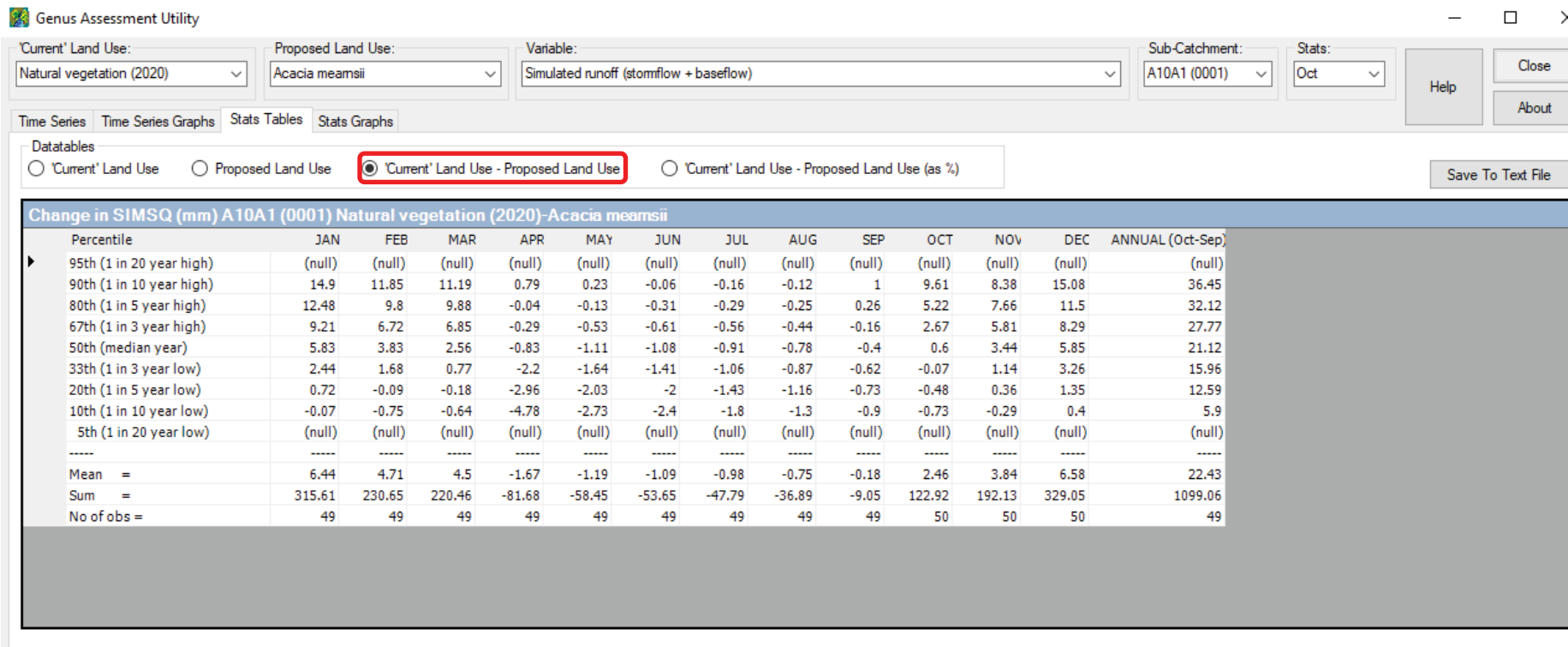


Figure 11-11: Stats Tables tab ('Current' Land Use – Proposed Land Use, data for illustration purposes only)

VOLUME 2: WATER USE ESTIMATION OF SFRA SPECIES

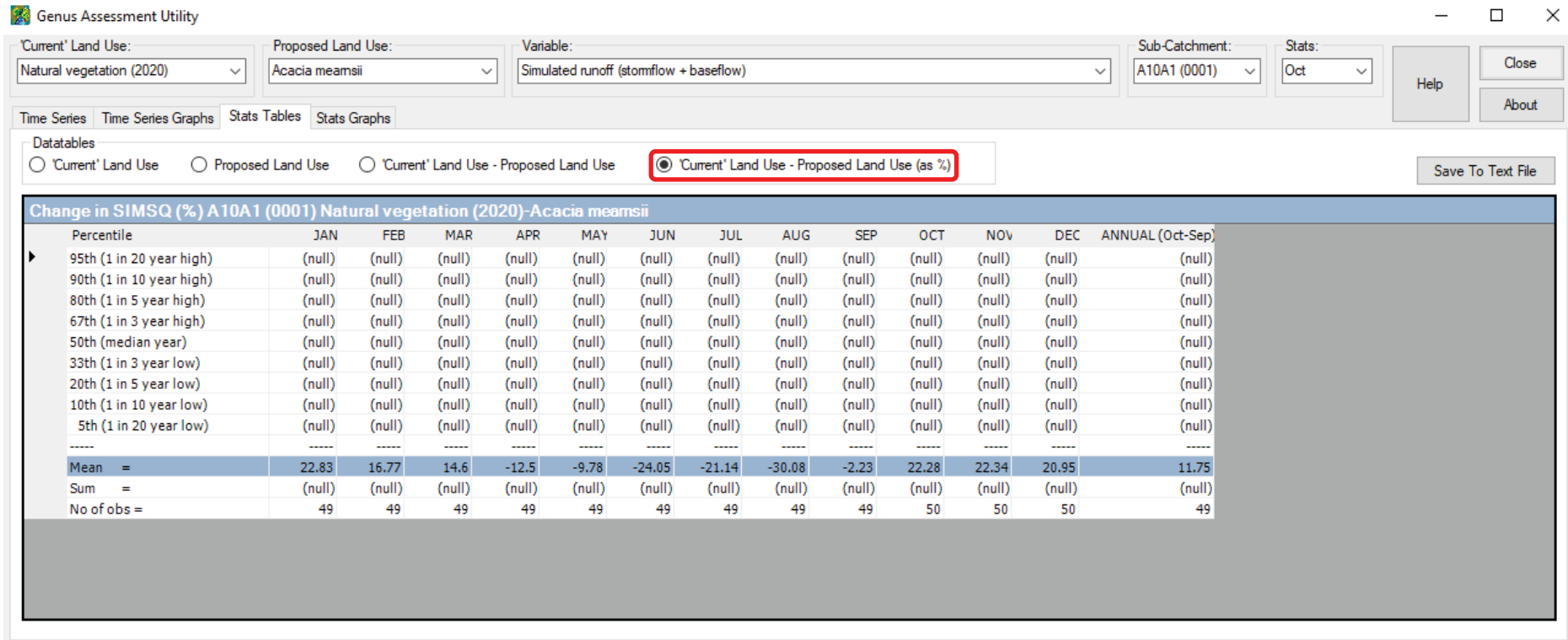


Figure 11-12: Stats Tables tab ('Current' Land Use – Proposed Land Use (as %), data for illustration purposes only)

11.2.2.4 Stats graphs

The Stats Graphs tab displays the probability of exceedance values in graphical format. The Graph Options (All: Jan: ... Dec:) enables annual and/or monthly curves to be switched on/off in the display. The graphs corresponding to the selection made on the Stats Tables tab are plotted on this tab, with the exception of 'Current' Land Use – Proposed Land Use (as %), since relative changes cannot be calculated for percentile values. An Example of a 'Current' Land Use graph is displayed in Figure 11-13.

VOLUME 2: WATER USE ESTIMATION OF SFRA SPECIES

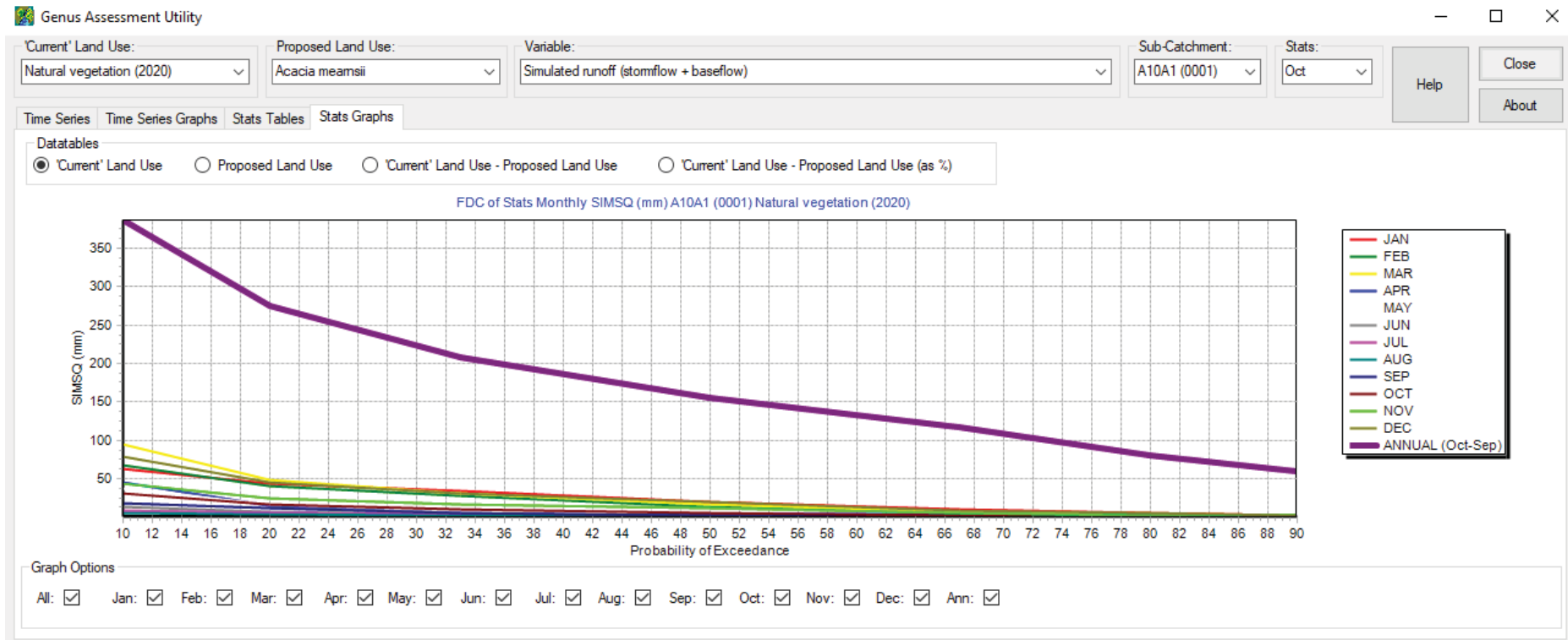


Figure 11-13: Stats Graphs tab ('Current' Land Use, data for illustration purposes only)

11.2.3 Interpreting of results

11.2.3.1 Calculating annual reductions in stream flow

To determine if a particular land use is a potential stream flow reduction activity (SFRA):

- Select **Natural vegetation** as the 'Current' Land Use.
- Then select the **Proposed and Use**, e.g. *Acacia meamsii*.

VOLUME 2: WATER USE ESTIMATION OF SFRA SPECIES

- Thereafter, select the *Stats Tables* tab and the '**Current**' Land Use – **Proposed Land Use as %** option.
- The reduction in mean annual runoff (MAR), expressed as a percentage relative to the current land use, is given in the row called **Mean =** and the column headed **ANNUAL**.
- In the example shown in Figure 11-12 above, the relative annual reduction is 11.75%. According to Jewitt et al. (2009), relative reductions in MAR of 10% or greater may be declared as a SFRA.
- This value is calculated as the difference in MAR (22.43 mm; Under the *Stats Tables* tab, select the '**Current**' Land Use – **Proposed Land Use** option), expressed as a percentage relative to the current land use (190.91 mm; select the '**Current**' Land Use option), i.e. $MAR_{REDN} = 100 \cdot (MAR_{CURR} - MAR_{PROP}) / MAR_{CURR} = 100 \cdot 22.43 / 190.91 = 11.75\%$.
- Hence, the MAR decreased by 22.43 mm from 190.91 mm (MAR_{CURR}) to 168.48 mm (MAR_{PROP}), i.e. less runoff due to a proposed change in land use from natural vegetation to *A. mearnsii*.

11.2.3.2 Calculating monthly reductions for low flow period

To determine the potential impact during the low flow period:

- Select the *Stats Tables* tab and the '**Current**' Land Use option, then click the **Save to Text** File button.
- This creates a .CSV file called "Stats Monthly SIMSQ (mm) A10A1 (0001) Natural Vegetation (CWRR clusters).csv".
- Similarly, select the *Stats Tables* tab and the **Proposed Land Use** option, then click the **Save to Text** File button.
- This creates a .CSV file called "Stats Monthly SIMSQ (mm) A10A1 (0001) Acacia mearnsii.csv".
- Double click on the "Stats Monthly SIMSQ (mm) A10A1 (0001) Natural Vegetation (CWRR clusters).csv" file to open it in MS Excel.
- Delete the **ANNUAL** column, then copy the **JAN** and **FEB** columns and paste them directly after the **DEC** column.
- Create a new row with the heading **Low Flow Total (LFT)**, which sums the mean monthly runoff (MMR) over three months, i.e. $LFT_{JAN} = MMR_{JAN} + MMR_{FEB} + MMR_{MAR}$. Copy and paste this formula to generate the totals for **FEB** to **ANNUAL**.
- Identify the start of the low flow quartile as the smallest LFT value, i.e. June's value of 11.66 mm ($LFT_{JUN} = MMR_{JUN} + MMR_{JUL} + MMR_{AUG} = 4.55 + 4.61 + 2.50 = 11.66$ mm).
- Double click on the "Stats Monthly SIMSQ (mm) A10A1 (0001) Acacia mearnsii.csv" file and calculate the LFT value for the same month (June), i.e. $LFT_{JUN} = 14.50$ mm for *A. mearnsii*.
- Finally calculate the difference in LFT ($11.66 - 14.50 = -2.84$ mm), expressed as a percentage relative to the current land use LFT (11.66 mm), i.e. $LFT_{REDN} = 100 \cdot (LFT_{CURR} - LFT_{PROP}) / LFT_{CURR} = 100 \cdot (11.66 - 14.50) / 11.66 = -24.36\%$.
- According to Jewitt et al. (2009), relative reductions in LFT of 25% or greater may be declared as a SFRA. For this example, there is no impact on the low flow quartile.

		B	C	D	E	F	G	H	I	J	K	L	M	N	O
A		JAN	FEB	MAR	APR	MAY	JUN	JUL	AUG	SEP	OCT	NOV	DEC	JAN	FEB
1															
2	Mean =	28.22	28.06	30.82	13.33	12.20	4.55	4.61	2.50	8.30	11.03	17.20	31.41	28.22	28.06
3	Low flow total (Nat veg)	87.10	72.21	56.35	30.08	21.36	11.66	15.41	21.83	36.53	59.64	76.83	87.69		
4															
5	Mean =	21.77	23.36	26.32	15.00	13.40	5.65	5.59	3.26	8.48	8.58	13.36	24.83	21.77	23.36
6	Low flow total (Aca mea)	71.45	64.68	54.72	34.05	24.64	14.50	17.33	20.32	30.42	46.77	59.96	69.96		
7															
8	Difference in LFTs (in mm)	15.65	7.53	1.63	-3.97	-3.28	-2.84	-1.92	1.51	6.11	12.87	16.87	17.73		
9	Relative difference in LFTs (in %)	17.97	10.43	2.89	-13.20	-15.36	-24.36	-12.46	6.92	16.73	21.58	21.96	20.22		

Figure 11-14: Calculation of the relative reduction in low flow totals of monthly runoff for quinary A10A1 (0001) for a proposed land use change from natural vegetation to *A. mearnsii*

11.2.3.3 Percentile values and flow duration curve

Under the *Stats Tables* tab, the percentiles represent the probability that a runoff value will *not* be exceeded in any given year. For example, the 10th percentile annual runoff for natural vegetation in quinary A10A1 (0001) is 59 mm (Figure 11-9). This means that 10% of all annual runoff values will be less than 59 mm and represents the driest year that can be expected to occur only once in a 10-year period. In other words, in 10% of the years on record, the annual rainfall total will not exceed 59 mm. Hence, 90% of all runoff values will higher than 59 mm, which represents the probability that a runoff value is exceeded. Under the *Stats Graphs* tab, the flow duration curve (FDC) shows the probability of exceedance and thus, 90% of all annual runoff values will exceed 59 mm (Figure 11-13). In other words, the probability of exceedance = 100 – nth percentile (probability of non-exceedance).

Similarly, the 90th percentile annual runoff is 386 mm and represents the wettest year in 10 (Figure 11-9). This means that 90% of annual runoffs will be less than this value, i.e. the annual rainfall total will not exceed 386 mm in 10% of the years on record. Hence, 10% of all runoff values will exceed 386 mm, as shown on the FDC (Figure 11-13).

The 5th and 95th percentiles can only be calculated if there are more than 50 years of data. If January is selected as the start month of the hydrological year, then the number of annual observations is 50 since the climate record spans the period 1950 to 1999. If October is selected as the start of the hydrological year, the number of annual values becomes 49. Hence, the 5th and 95th percentiles cannot be calculated.

11.2.3.4 Understanding differences

Under the *Stats Tables* tab, the '**Current**' Land Use – **Proposed Land Use** options (in mm or %) can show both positive and/or negative values. For simulated runoff (*SIMSQ* variable in *ACRU*), positive values indicate a reduction in runoff ($MAR_{PROP} < MAR_{CURR}$) that may result from the current to proposed land use change, i.e. less runoff may be generated due to the change in land use. On the other hand, negative values indicate that more runoff may be generated by the land use change ($MAR_{PROP} > MAR_{CURR}$).

For the simulated total evaporation variable (*AET* variable in *ACRU*), negative values indicate higher evaporative losses from the proposed land use, compared to the current land use, i.e. ($AET_{PROP} > AET_{CURR}$). Higher evaporation from the vegetation and soil layers means less runoff may occur. On the other hand, positive values indicate that the land use change may result in lower evaporative losses (i.e. $AET_{PROP} < AET_{CURR}$) and potentially, more runoff generation.

CHAPTER 12. CONCLUSIONS & RECOMMENDATIONS

12.1 Conclusions

The improvements and revisions to ACRU that were made over the past 10 years, as well as the improvements and revisions to the quinary catchments climate database that is used as input to ACRU, have been incorporated into the model runs undertaken to simulate the streamflow response under commercial tree species and under baseline vegetation. This alone was a needed step forward to bring the simulations under commercial tree species into alignment with other national scale simulations for the impacts of biofuel crops (Kunz et al., 2020), climate change impacts (Schütte et al., 2021), bamboo impacts (Everson et al., 2021) and those that will be used in the ongoing WRC project titled “Development of Datasets for Multi-Scale Water Resource Assessments towards a Water Secure South Africa”.

A significant advancement in this project was the improvements made to the quinary soils database used as input to the ACRU model. Soils play a critical role in the regulation and generation of catchment hydrological responses; thus, detailed catchment scale soils data is required as input to generate satisfactory results. In previous studies where the streamflows under commercial trees have been simulated, area-averaged land type information was used. A South African soils terrain unit database was developed which provided the key soil physical attributes required as ACRU model input. There was substantial gain in spatial resolution made by using the TU level information compared with the use of only land type information.

A recent WRC project (No. K5/2437) provided a revised hydrological reference baseline, together with the associated vegetation water use parameters required as input by ACRU. The baseline vegetation, termed the CWRR clusters, was a hydrological grouping of the SANBI (2012) vegetation units. The approach to develop the vegetation water use parameters was to use field based or remotely sensed data where possible, and to use a repeatable methodology. The crop coefficients were ultimately derived from remotely sensed LAI values. During that project, only a preliminary assessment was undertaken to determine the impacts of commercial trees on streamflow under this revised baseline, compared to the previous baseline based on Acocks Veld Types. The SANBI vegetation map has become the accepted natural vegetation map for South Africa by other disciplines, and the biome concept as well as the typical vegetation structures within those, have become commonly understood and referred to. Therefore, the move to the CWRR clusters derived from the SANBI vegetation map is a necessary step forward. Further to that, the documented and repeatable method used to derive the vegetation water use parameters allows for alignment across water use parameters for other land cover and land use types.

A significant component of this project focused on field-based studies to improve the understanding of the water use of commercial tree species. The methods and findings of these field-based water use studies are contained in Deliverable 8 of this project, which accompanied this final report. From the literature and the experiences gained in the field-based component of this project, the influence of site characteristics on the growth, rooting patterns and the water use of commercial tree species was illustrated. Sites with shallow soils or those in rain shadows will have different growth characteristics to those on wetter slopes or more favourable soils. Further, the growth patterns may even vary across a compartment due to variations in slope and soils. For determining the impacts of commercial tree species on streamflow generation, a broad picture, representative of large portions of the area under that commercial tree species, is needed. Thus,

field-based studies to understand water use and determine LAI pose significant challenges. The field-based studies, dependent on the methodology used, range from being representative of a compartment, to a small set of trees within the compartment. For example, use of an eddy covariance system to estimate evapotranspiration over a stand of trees will provide an estimate of the water use of the compartment, whereas the use of sap flow methodology (e.g. heat pulse velocity method) will provide estimates of transpiration for the trees instrumented, which then need to be scaled up to the compartment scale. Often the method chosen is based more on costs and on logistics when measuring trees than other factors. The logistics of measuring in tree compartments are complex given the height of the trees and risks associated with fire, theft and vandalism. When combined with the need to find an ideal site, the complexity is compounded. Added to this is the significant cost of field-based measurements, regardless of site, which also limits the number of sites that can be instrumented.

Based on the above, a method for developing a LAI database and determining K_c values that were more broadly representative of trees within a large compartment was investigated and developed. Several different paths were considered, however, the method chosen took advantage of the recent advancements in geospatial cloud-based computing platforms, most notably Google Earth Engine and machine learning. Since the methodology used to derive vegetation water use parameters for the CWRR clusters used remotely sensed LAI values, and literature supported a relationship between tree water use and leaf area, an approach that used LAI to determine the K_c values for commercial tree species was considered. This project also considered that the spatial resolution of the MODIS LAI product may be too coarse. Thus, a method to derive moderate resolution LAI values from coarser spatial resolution products was investigated. Although this method proved promising, the MODIS LAI product was preferred over the additional uncertainty introduced in deriving a moderate resolution LAI. The K_c values estimated from MODIS LAI using machine learning showed good correlation to K_c values calculated from observed data. However, similar to the challenges experienced in the baseline project, very few datasets of total evaporation were available over commercial trees to develop and validate the model for determining K_c from LAI. Data for only two species grown at the same site was available. However, like the baseline project, the method is documented, repeatable and is consistent across species. As more data becomes available, the water use parameters can be refined. The data is not necessarily only total evaporation data, since greater access to the commercial forestry industry's compartment database, to expand the sites for which LAI records are obtained, could help refine the parameters.

Through the project, the required ACRU input vegetation parameters for seven *Eucalyptus*, four *Pinus* and *Acacia mearnsii* were derived. All of the estimated monthly K_c values were above 1, and both the month-by-month variation in K_c values for a specific species and between species was low. Generally, the K_c values for sites in the WTM climate zone had the smallest variation in the monthly values. ACRU model simulations were undertaken with version 3.52 (enhanced performance), the updated South African TU database, revised quinary catchments climate database, using the derived vegetation water use parameters for the 11 species, hybrids and clones, as well as the vegetation water use parameters for the CWRR clusters. All model inputs were held constant between the runs, except for the vegetation water use parameters. A comparison to the ACRU output in the previous SFRA utility developed in 2009 were not undertaken due to the extent of the changes made to the 1) ACRU model, 2) climate and soils databases used as input, 3) changes in the reference land cover, and 4) methodology used to derive water use parameters. Further, these database updates and the use of a consistent and repeatable methodology to determine the vegetation water use parameters across both the land use of impact and the reference, represent a step forward in the science that can be used to support the implementation of the declaration of land used for commercial afforestation as a SFRA.

12.2 Recommendations

The various approaches developed and implemented in this study are by no means considered “exhaustive”. Although much effort was spent on producing simulated output that is considered reliable and error-free, the following suggestions would further improve the accuracy of modelled results:

- The root zone storage concept showed potential and therefore warrants further investigation, with the aim of using it within the ACRU modelling framework to further improve root water uptake, as well as to overcome the paucity of available rooting information.
- More process-based research is needed to improve ACRU’s ability to simulate deep-rooted vegetation. This problem is further compounded by the land type soils data, which is limited to a standard auger depth of only 1.2 m.
- The ACRU model should be modified to replace the A-pan as its reference evaporation standard, and rather use FAO56 (i.e. Penman-Monteith) reference evapotranspiration. This would negate the need to adjust FAO56-derived K_c values to A-pan equivalent values.
- It is clear that additional and reliable measurements of tree water use are required to further improve the derivation of crop coefficients from LAI. Additional data would strengthen the machine learning algorithms developed in this project.
- Further investigation is needed to determine why the variable storage Gash model produces significantly higher vegetation interception losses when compared to the Von Hoyningen-Huene method. This will require additional field-based measurements of interception from forest canopies, which can then be used to validate simulated results. Of particular importance is the need to estimate the element storage volume of each tree species.
- In 2019, the WRC funded a project to extend the quinary subcatchment climate database beyond 1999 and up to 2019 (i.e. by an additional 20 years). Once this work has been completed, the simulation modelling undertaken in this project should be revised.

Reflecting on the project as a whole, the following recommendations are made:

- There is a need for agreement on the best measure of forestry water use. Should the measurement be of just the water use of the trees (i.e. green water) or of the water productivity which includes soil water evaporation and intercepted water? Jewitt et al. (2009) suggested that changes in green water flows be used in the declaration of a land use as a SFRA but that the impact on blue water flows be used in regulation. The measurement approaches that would be used for each aspect differ considerably, with the first a transpiration measurement while the latter requires measurements that consider all components of the water balance, specifically those relevant to the modification of the land cover by the SFRA or candidate SFRA activity.
- Agreement on scale also needs to be reached. The field-based components of the project provided further evidence of the site-specific nature of tree water use. Measurement the scale of a tree (or cluster of trees) is valuable in terms of tree level water use and process understanding. However, these site-specific findings that are possibly broadly not applicable are difficult and probably not applicable to be incorporated into modelling that is undertaken at a broader quinary catchment scale with supporting databases of that resolution. What is a practical and realistic scale at which field based measurements can be made that can be captured in the modelling? Measurements at a valley scale using methods that capture evapotranspiration at that scale as well as monitoring of the components of the water balance may be the way forward. At this scale there would be averaging out of the “extreme” site variations. Finding a valley site with one commercial forestry species dominating would be challenging and the measurement design costly.

- Across both this project and the baseline project, the paucity of evapotranspiration data was noted. For natural vegetation, the number of datasets available has increased as these will continue to increase with the Expanded Freshwater and Terrestrial Observation network program establishing monitoring infrastructure in selected landscapes. This investment focused on instrumentation platforms by the Department of Science and Technology to under the impacts of global change on our environments shows a recognition of the need for long term field-based data for process understanding and development of an evidence base to support decisions. By utilising the data from these infrastructure platforms, the process level understanding of vegetation water use and the parameterisation for use in models can be improved. Allowing for an improved simulation of the baseline of reference conditions to be made. Opportunities to ensure aligned improvements in tree water use understanding need to be explored.
- Given the repeatable method derived in this project, it is suggested that 5-year updates that utilise any additionally available field-based datasets, additional LAI sites and any quinary database or model updates be undertaken, and this be aligned with similar updates to the baseline.

CHAPTER 13. REFERENCES

- Acocks JPH. 1953. Veld Types of South Africa. Memoirs of the Botanical Society, 28. Botanical Research Institute, Pretoria, South Africa.
- Acocks JPH. 1988. Veld Types of Southern Africa. Botanical Survey of South Africa Memoirs, Vol. 57. Botanical Research Institute, Pretoria, South Africa.
- ACRU FDSS Workshop No3. 1995. Institute for Commercial Forestry Research, Pietermaritzburg, RSA, October 1995.
- Afzal M, Ragab R, Blake J, Black A and McEwen L. 2018. April Impacts of the climatic change on the hydrology of the Eden catchment in Scotland UK using DiCaSM model approach. EGU General Assembly Conference Abstracts (Vol 20 p 9346).
- Albaugh JM, Dye PJ and King JS. 2013. Eucalyptus and Water Use in South Africa. International Journal of Forestry Research, DOI: 10.1155/2013/852540.
- Alexandridis T, Ovakoglou G and Clevers JPGW. 2019. Relationship between MODIS EVI and LAI across time and space. Geocarto International: 1-15. doi: 10.1080/10106049.2019.1573928.
- Alexandridis T, Stavridou D, Strati S, Monachou S and Silleos N. 2013. LAI Measurement with Hemispherical Photographs at Variable Conditions for Assessment of Remotely Sensed Estimations. ESA Living Planet Symposium, 252. Edinburgh, United Kingdom.
- Al-Kaisi M, Brun LJ and Enz JW. 1989. Transpiration and Evapotranspiration from Maize as Related to Leaf Area Index. Agricultural and Forest Meteorology, 48: 111-116.
- Allen RG, Pereira LS, Raes D and Smith M. 1998. Crop evapotranspiration – Guidelines for computing crop water requirements. FAO Irrigation and drainage paper 56, ISBN 92-5-104219-5.
- Allen RG, Pereira LS, Smith M, Raes D and Wright JL. 2005. FAO-56 dual crop coefficient method for estimating evaporation from soil and application extensions. Journal of irrigation and drainage engineering, 131(1): 2-13.
- Allen RG, Pereira LS, Howell TA and Jensen ME. 2011. Evapotranspiration information reporting: I. Factors governing measurement accuracy. Agricultural Water Management 98: 899-920. doi: 10.1016/j.agwat.2010.12.015.
- Angus GR. 1987. A distributed version of the ACRU model. Unpublished MScEng dissertation. University of Natal, Pietermaritzburg, Department of Agricultural Engineering. pp 137.
- Angus GR and Schulze RE. 1990. A hydrological interpretation of soil information from the SIRI Land Type survey. *Agricultural Engineering in South Africa*, 22, 178-192.
- Arnal L. 2014. An intercomparison of flood forecasting models for the Meuse River basin. MSc dissertation, Deltares, Vrije Universiteit, Amsterdam, The Netherlands.
- Arnold H. 1981. Suggested Modification to the Estimation of Runoff Volume by the SCS Model. Unpublished MScEng dissertation. University of Natal, Pietermaritzburg, RSA, Department of Agricultural Engineering. pp 119.
- Baroni G, Facchi A, Gandolfi C, Ortuani B, Horeschi D and Van Dam JC. 2010. Uncertainty in the determination of soil hydraulic parameters and its influence on the performance of two hydrological models of different complexity. *Hydrology and Earth System Sciences*, 14(2): 251-270.
- Bates HW. 1921. The naturalist on the river Amazons. London

- Beeri O, Netzer Y, Munitz S, Mintz DF, Pelta R, Shilo T, Horesh A and Mey-tal S. 2020. Kc and LAI Estimations Using Optical and SAR Remote Sensing Imagery for Vineyards Plots. *Remote Sensing* 2020 (12). doi:10.3390/rs12213478.
- Berling DJ and Berner RA .2005. Feedbacks and the coevolution of plants and atmospheric CO₂. *Proceedings of the National Academy of Sciences of the United States of America*, 102: 1302-1305.
- Beukes H. 2018. Personal communication with RE Schulze.
- Bian Z, Gu J, Zhao J, Pan Y, Li Y, Zeng C and Wang L. 2018. Simulation of evapotranspiration based on leaf area index, precipitation and pan evaporation: A case study of Poyang Lake watershed, China. *Ecohydrology and Hydrobiology*, 178: 1-10.
- Blasone RS, Vrugt JA, Madsen H, Rosbjerg D, Robinson BA and Zyvoloski GA. 2008. Generalized likelihood uncertainty estimation (GLUE) using adaptive Markov Chain Monte Carlo sampling. *Advances in Water Resources*, 31(4): 630-648.
- Bleby TM, Mcelrone AJ and Jackson RB. 2010. Water uptake and hydraulic redistribution across large woody root systems to 20 m depth. *Plant Cell & Environment*, 33(12): 2132-2148.
- Bonan GB. 1993. Importance of leaf area index and forest type when estimating photosynthesis in boreal forests. *Remote Sensing of Environment*. 43: 303-314.
- Bulcock HH. 2011. An assessment of canopy and litter interception in commercial forest plantations and an indigenous forest in the KwaZulu-Natal Midlands, South Africa. PhD thesis, School of Bioresources Engineering and Environmental Hydrology, University of KwaZulu-Natal, Pietermaritzburg, South Africa.
- Bulcock HH and Jewitt GPW. 2012. Modelling canopy and litter interception in commercial forest plantations in South Africa using the variable storage Gash model and idealised drying curves. *Hydrology and Earth Systems Science*. 16: 4693-4705.'
- Calder IR. 1996. Dependence of rainfall interception on drop size: 1. Development of the two-layer stochastic model. *Journal of Hydrology* 185 (1–4) 363–378.
- Chen H, Huang JJ and McBean E. 2020. Partitioning of daily evapotranspiration using a modified shuttleworth-wallace model, random Forest and support vector regression, for a cabbage farmland. *Agricultural Water Management* 228.
- Chen L and Wang L. 2018. Recent advance in earth observation big data for hydrology. *Big Earth Data* 2(1): 86-107. doi: 10.1080/20964471.2018.1435072.
- Chen Y, Zhang W, Hu R, Qi J, Shao J, Li D, Wan P, Qiao C, Shen A and Yan G. 2018. Estimation of forest leaf area index using terrestrial laser scanning data and path length distribution model in open-canopy forests. *Agricultural and Forest Meteorology*, 263: 323-333.
- Cheng XM, and Bledsoe CS. 2002. Contrasting seasonal patterns of fine root production for blue oaks (*Quercus douglasii*) and annual grasses in California oak woodland. *Plant Soil*, 240(2): 263-274, doi:10.1023/A:1015723314433.
- Clevers JGPW, Kooistra L and Van den Brande MMM. 2017. Using Sentinel-2 Data for Retrieving LAI and Leaf and Canopy Chlorophyll Content of a Potato Crop. *Remote Sensing* 9. doi:10.3390/rs9050405.
- Clulow AD, Everson CS and Gush MB. 2011. The long-term impact of *Acacia mearnsii* trees on evaporation, streamflow and groundwater resources, WRC Report No. TT 505/11, ISBN 978-1-4312-0020-3, Water Research Commission, Pretoria, South Africa.

- Cohen WB, Maiersperger TK, Gower ST and Turner DP. 2003. An improved strategy for regression of biophysical variables and Landsat ETM+ data. *Remote Sensing of Environment* 84(4):561-571.
- Collins DBG and Bras RL. 2007. Plant rooting strategies in water-limited ecosystems. *Water Resources Research*, 43(W06407): 1-10.
- Colter Burkes E, Will RE, Barron-Gafford GA, Teskey RO and Shiver B. (2003). Biomass partitioning and growth efficiency of intensively managed *Pinus taeda* and *Pinus elliottii* stands of different planting densities. *Forest Science*, 49(2), 224-234.
- Coppin NJ and Richards IG. 1990. Use of vegetation in civil engineering (pp 23-36). London: Construction Industry Research and Information Association.
- Corbari C, Ravazzani G, Galvagno M, Cremonese E and Mancini M. 2017. Assessing Crop Coefficients for Natural Vegetated Areas Using Satellite Data and Eddy Covariance Stations. *Sensors* 2017 (17). doi:10.3390/s17112664.
- D'Agostino DR, Trisorio LG, Lamaddalena N and Ragab R. 2010. Assessing the results of scenarios of climate and land use changes on the hydrology of an Italian catchment: modelling study. *Hydrological processes*, 24(19): 2693-2704.
- Da Silva EV, Bouillet JP, De Moraes Gonçalves JL, Junior CHA, Trivelin PCO, Hinsinger P, Jourdan C, Nouvellon Y, Stape JL and Laclau JP. 2011. Functional specialization of *Eucalyptus* fine roots: contrasting potential uptake rates for nitrogen, potassium and calcium tracers at varying soil depths. *Functional Ecology*, 25(5): 996-1006.
- Day FP, Weber EP, Hinkle CR and Drake BG. 1996. Effects of elevated atmospheric CO₂ on fine root length and distribution in an oak-palmetto scrub ecosystem in central Florida. *Glob. Change Biol.*, 2(2): 143-148, doi:10.1111/j.1365-2486.1996.tb00059.x.
- De Boer-Euser T, McMillan HK, Hrachowitz M, Winsemius HC and Savenije HH. 2016. Influence of soil and climate on root-zone storage capacity. *Water Resources Research*, 52(3): 2009-2024.
- De Boer-Euser T, Meriö LJ and Marttila H. 2019. Understanding variability in root zone storage capacity in boreal regions, *Hydrology 10 and Earth System Sciences*, 23 (1): 125-138.
- De Kroon H and Visser EJW. (Eds). 2003. *Root Ecology*. Springer-Verlag, London Ltd., Berlin Germany. 235-250.
- Department of Water Affairs (DWA). 2012. Business Case for the Inkomati-Usuthu Catchment Management Agency.
- Department of Water Affairs (DWA). 2013. Business Case for the Pongola-Umzimkulu Catchment Management Agency.
- Department of Water Affairs (DWA). 2020. Spatial data catalogue. Accessed 02 September 2021. <https://gia.dws.gov.za/DWSPortalApplication/>.
- DWS (Department of Water and Sanitation) 2016. Policy position on water use in bio-fuel production in South Africa. Department of Water and Sanitation (DWS), Pretoria, RSA.
- Descheemaeker K, Raes D, Allen R, Nysen J, Poesen J, Muys B, Haile M and Deckers J. 2011. Two rapid appraisals of FAO-56 crop coefficients for semiarid natural vegetation of the northern Ethiopian highlands. *Journal of Arid Environments* 75 (4): 353-359. doi.org/10.1016/j.jaridenv.2010.12.002.
- Dube T, Pandit S, Shoko C, Ramoelo A, Mazvimavi D and Dalu T. 2019. Numerical Assessments of Leaf Area Index in Tropical Savanna Rangelands, South Africa Using Landsat 8 OLI Derived Metrics and In-Situ Measurements. *Remote Sensing* 11. doi:10.3390/rs11070829.

- Dupuy L, Gregory PJ and Bengough GA. 2010. Root growth models: towards a new generation of continuous approaches. *Journal of Experimental Botany*, 61(8): 2131-2143.
- Dye PJ. 1996. Response of *Eucalyptus grandis* trees to soil water deficits. *Tree Physiology*, 16(1-2), 233-238.
- Dye P and Versfeld D. 2007. Managing the hydrological impacts of South African plantation forests: An overview. *Forest Ecology and Management* 251(2007): 121-128.
- Dye PJ and Bosch JM. 2000. Sustained water yield in afforested catchments – the South African experience. In: von Gadow KP, Pukkala T, Tome M. *Sustainable Forest Management*. Netherlands: Kluwer Academic Publishers. pp 99-120.
- Eagleson PS. 1982. Ecological optimality in water-limited natural soil-vegetation systems: 1 Theory and hypothesis. *Water Resources Research*, 18(2): 325-340.
- Everson CS, Toucher M, Vather T, Mfeka S, Lawrence K, Horan R, Govender J, Gray B, Ramjeawon M and Aldswaorth T. 2018. Continued hydrometeorological monitoring at the Two Streams Catchment for the clear felling of the *Acacia mearnsii* stand. Water Research Commission (WRC), Pretoria, RSA. WRC Project No. K5/2780. ISBN 978-1-4312-0020-3.
- Everson CS, Gumede MP, Everson TM, Clulow AD and Kunz RP. 2021. Quantification of the evapotranspiration and stream flow reduction caused by Bamboo species on water resources in South Africa. Water Research Commission (WRC), Pretoria, RSA. WRC Project No. K5/2792.
- Fan J, Zheng J, Wu L and Zhang F. 2021. Estimation of daily maize transpiration using support vector machines, extreme gradient boosting, artificial and deep neural networks models. *Agricultural Water Management* 245.
- Fan Y, Miguez-Macho G, Jobbágy EG, Jackson RB and Otero-Casal C. 2017. Hydrologic regulation of plant rooting depth. *Proceedings of the National Academy of Sciences*, 114(40): 10572-10577.
- Fang H, Baret H, Plummer S and Schaepman-Strub D. 2019a. An Overview of Global Leaf Area Index (LAI): Methods, Products, Validation, and Applications. *Reviews of Geophysics* 57. doi.org/10.1029/2018RG000608.
- Fang H, Li W, Wei S and Jiang C. 2014. Seasonal variation of leaf area index (LAI) over paddy rice fields in NE China: Intercomparison of destructive sampling, LAI-2200, digital hemispherical photography (DHP), and AccuPAR methods. *Agricultural and Forest Meteorology* 198-199: 126-141. doi.org/10.1016/j.agrformet.2014.08.005.
- Fang H, Zhang Y, Wei S, Li W, Ye Y, Sun T and Liu W. 2019b. Validation of global moderate resolution leaf area index (LAI) products over croplands in northeastern Chinas. *Remote Sensing of Environment* 233. doi.org/10.1016/j.rse.2019.111377.
- FAO Regional Office for Asia, 2006. *Rapid Growth of Selected Asian Economies: Lessons and Implications for Agriculture and Food Security*. Food & Agriculture Organisation, Bangkok.
- Feddes RA, Hoff H, Bruen M, Dawson T, De Rosnay P, Ditmeyer P, Jackson RB, Kabat, P, Kleidon A, Lilly A and Pitman AJ. 2001. Modeling root water uptake in hydrological and climate models. *Bulletin of the American meteorological society*, 82(12): 2797-2810
- Feng Y, Cui N, Gong D, Wang H, Hao W and Mei X. 2016. Estimating rainfed spring maize evapotranspiration using modified dual crop coefficient approach based on leaf area index. *Transactions of the Chinese Society of Agricultural Engineering* 32: 90-98.
- Fenicia F, Kavetski D and Savenije HH. 2011. Elements of a flexible approach for conceptual hydrological modeling: 1 Motivation and theoretical development. *Water Resources Research*, 47(11): 1-13.

- Fensholt R, Sandholt I and Rasmussen MS. 2004. Evaluation of MODIS LAI, fAPAR and the relation between fAPAR and NDVI in a semi-arid environment using in situ measurements. *Remote Sensing of Environment* 91(3-4): 490-507.
- Fogel R. 1983. Root turnover and productivity of coniferous forests. *Plant and Soil*, 71(1-3): 75-85. doi:10.1007/BF02182643.
- Forrester DI, Guisasola R, Tang X, Albrecht AT, Dong TL and le Maire G. 2014. Using a stand-level model to predict light absorption in stands with vertically and horizontally heterogeneous canopies. *Forest Ecosystems* 1:17. 19 pp.
- Frake AN, Peter BG, Walker ED and Messina JP. 2020. Leveraging big data for public health: Mapping malaria vector suitability in Malawi with Google Earth Engine. *PLoS ONE* 15(8): e0235697. doi.org/10.1371/journal.pone.0235697.
- Fredericksen TS, Zedaker SM. Fine root biomass, distribution, and production in young pine-hardwood stands. *New Forest* 10, 99-110 (1995). <https://doi.org/10.1007/BF00034178>
- FSA 2016. Forestry South Africa. 15th Annual report. <http://www.forestry.co.za/fsa-annual-reports/>
- Ganguly S, Nemani RR, Zhang G, Hashimoto H, Milesi C, Michaelis A, Wang WL, Votava P, Samanta A, Melton F, Dungan JL, Vermote E, Gao F, Knyazikhin Y and Myneni RB. 2012. Generating global leaf area index from landsat: Algorithm formulation and demonstration. *Remote Sensing of Environment*. 122: 185-202.
- Gao F, Anderson MC, Kustas WP and Wang YJ. 2012. Simple method for retrieving leaf area index from landsat using modis leaf area index products as reference. *Journal of Applied Remote Sensing* 6.
- Gao H, Hrachowitz M, Schymanski SJ, Fenicia F, Sriwongsitanon N and Savenije HHG. 2014. Climate controls how ecosystems size the root-zone storage capacity at catchment scale. *Geophysical Research Letters*, 41(22): 7916-7923.
- Gao X, Dirmeyer PA, Guo Z and Zhao M. 2008. Sensitivity of land surface simulations to the treatment of vegetation properties and the implications for seasonal climate prediction. *Journal of Hydrometeorology* 9: 348-366.
- Gash JHC. 1979. An analytical model of rainfall interception by forests. *Quarterly Journal of the Royal Meteorological Society* 105 (443) 43-55.
- Gash JHC, Lloyd CR and Lachaud G. 1995. Estimating sparse forest rainfall interception with an analytical model. *Journal of Hydrology* 170 (1-4) 79-86.
- Gazarini LC, Araujo MCC, Borralho N and Pereira JS. 1990. Plant area index in Eucalyptus globulus plantations determined indirectly by a light interception method. *Tree Physiology* 7: 107-113. Gentine P., D'Odorico P., Lintner B.R., Sivandran G. and Salvucci G., 2012. Interdependence of climate, soil, and vegetation as constrained by the Budyko curve. *Geophysical Research Letters*, 39(L19404):1-9.
- Gerrits AMJ, Pfsiter L and Savenije HHG. 2010. Spatial and temporal variability of canopy and forest floor interception in a beech forest. *Hydrological Processes*, 24: 3011-3025.
- Gholz HL. 1982. Environmental limits on aboveground net primary production, leaf area, and biomass in vegetation zones of the Pacific Northwest. *Ecology*, 63:469-481.
- Gimbel KF, Felsmann K, Baudis M, Puhlmann H, Gessler A, Bruelheide H, Kayler ZE, Ellerbrock RH, Ulrich A, Welk E and Weiler M. 2015. Drought in forest understory ecosystems-a novel rainfall reduction experiment. *Biogeosciences*, 12(4): 961-975.

- Glenn EP, Neale CMU, Hunsaker DJ and Nagler PL. 2011. Vegetation index-based crop coefficients to estimate evapotranspiration by remote sensing in agricultural and natural ecosystems. *Hydrological Processes* 2011 (25): 4050-4062.
- Global climate change research community GCOS. 2011. Systematic observation requirements for satellite-based products for climate, 2011 Update, Supplemental Details to the Satellite-Based Component of the Implementation Plan for the Global Observing System for Climate in Support of the UNFCCC (2010 Update). Retrieved from <http://www.wmo.int/pages/prog/gcos/Publications/gcos-154.pdf>.
- Gorelick N, Hancher M, Dixon M, Ilyushenko S, Thau D and Moore R. 2017. Google Earth Engine: Planetary-scale geospatial analysis for everyone. *Remote Sensing of Environment* 202: 18-27.
- Grier CC and Running SW 1977. Leaf area of mature northwestern coniferous forests: relation to site water balance. *Ecology*, 58:893-899.
- Gu J, Zheng X, Wang Y, Ding W, Zhu B, Chen X, Wang Y, Zhao Z, Shi Y and Zhu J. 2007. Regulatory effects of soil properties on background N₂O emissions from agricultural soils in China. *Plant and Soil*, 295(1-2): 53-65.
- Gush M. 2016. Provision of expert opinion and advice in regard to proposed commercial forestry Genus Exchange regulations. CSIR REPORT FSA-1/2016.
- Gush MB and Moodley M. 2007. Water use assessment of *Jatropha curcas*. In: Holl M, Gush MB, Hallows J and Versfeld DB (eds.) *Jatropha curcas in South Africa: An Assessment of its Water Use and Bio-Physical Potential*. WRC Report No. 1497/1/07 (Chapter 4). Water Research Commission, Pretoria, RSA.
- Gush MB, Scott DF, Jewitt GPW, Schulze RE, Lumden T, Hallows LA, Görgens AHM. 2002. Estimation of streamflow reduction resulting from commercial afforestation in South Africa. WRC Report No. TT173/02. Pretoria: Water Research Commission.
- Hammond EH. 1964. Analysis in properties of landform geography: An application to broad-scale land form mapping. *Annals, Association of American Geographers*, 54, 11-19.
- Hatton T, Reece P, Taylor P and McEwan K. 1998. Does leaf water efficiency vary among eucalypts in water-limited environments? *Tree Physiology*, 18: 529-536.
- Hawkins RH, Jiang R, Woodward DE, Hjelmfelt AT and Van Mullem JA. 2002. "Runoff Curve Number Method: Examination of the Initial Abstraction Ratio". Proceedings of the Second Federal Interagency Hydrologic Modeling Conference, Las Vegas, Nevada. U.S. Geological Survey. doi:10.1111/j.1752-1688.2006.tb04481.x
- Hirigoyen A, Acosta-Muñoz C, Salamanca AJA, Varo-Martinez MA, Rachid-Casnati C, Franco J and Navarro-Cerrillo. A machine learning approach to model leaf area index in Eucalyptus plantations using high-resolution satellite imagery and airborne laser scanner data. *Annals of Forest Research* 64(2): 165-183. doi.org/10.15287/afr.2021.2073.
- Houborg R and McCabe MF. 2017. A hybrid training approach for leaf area index estimation via Cubist and random forests machine-learning. *ISPRS Journal of Photogrammetry and Remote Sensing* 135: 173-188. doi.org/10.1016/j.isprsjprs.2017.10.004.
- Hunnik JE, Eekhout JPC, De Vente J, Contreras S, Droogers P and Baille A. 2017. Hydrological Modelling Using Satellite-Based Crop Coefficients: A Comparison of Methods at the Basin Scale. *Remote Sensing* 9. doi:10.3390/rs9020174.
- Hutson JL. 1984. *Estimation of Hydrological Properties of South African Soils*. PhD thesis, University of Natal, Pietermaritzburg/RSA, Department of Soil Science and Agrometeorology. pp 232.

VOLUME 2: WATER USE ESTIMATION OF SFRA SPECIES

- Irmak S and Djaman K. 2016. Daily reference evapotranspiration estimation under limited data in Eastern Africa. *Journal of Irrigation and Drainage Engineering*, 143(4): 601-605.
- Jewitt GPW 1991. Process studies for the simulation modelling of forest hydrological processes. Unpublished MSc dissertation. Department of Agricultural Engineering, University of Natal, Pietermaritzburg, RSA.
- Jewitt GPW, Lorentz SA, Gush MB, Thornton-Dibb S, Kongo V, Wiles L, Blight J, Stuart-Hill SI, Versfeld D and Tomlinson K. 2009. Methods and guidelines for the licensing of SFRA with particular reference to low flows. Report No. 1428/1/09. Water Research Commission, Pretoria, RSA.
- Jewitt G and Schulze RE. 1999. Verification of the ACRU model for forest hydrology applications. *Water SA*, 25: 483-489.
- Jonckheere I, Fleck S, Nackaerts K, Muys B, Coppin P, Weiss M and Baret F. 2004. Review of methods for in situ leaf area index determination Part I. Theories, sensors and hemispherical photography. *Agricultural and Forest Meteorology*, 121: 19-35.
- Jung JKHM and McCouch SRM. 2013. Getting to the roots of it: genetic and hormonal control of root architecture. *Frontiers in plant science*, 4(1): 1-32.
- Kar G, Kumar A and Martha M. 2007. Water use efficiency and crop coefficients of dry season oilseed crops. *Water Technology Center for Eastern Region (ICAR)*, 87: 73-82.
- Kamuju N. 2015. Sensitivity of Initial Abstraction Coefficient on Prediction of Rainfall-Runoff for Various Land Cover Classes of Ton Watershed Using Remote Sensing & GIS Based Rinspe Model. *IJSRST*, 1(5): 213-221.
- Kapangazwiri E, Kahinda JM, Dziki S, Ramoelo A, Cho M, Mathieu R, Naidoo M, Seetal A and Pienaar H. 2017. Validation and verification of lawful water use in South Africa: An overview of the process in the KwaZulu-Natal Province. *Physics and Chemistry of the Earth*. doi.org/10.1016/j.pce.2017.12.002.
- Kelley G, Eamus D, O'Grady A and Hutley L. 2007. A comparison of tree water use in two contiguous vegetation communities of the seasonally dry tropics of northern Australia: The importance of site water budget to tree hydraulics. *Australian Journal of Botany*, DOI: 10.1071/BT07021.
- King LC 1953. Canons of landscape evolution. *Bulletin of the Geological Society of America*, 64, 721-752.
- Kleidon A. 2004. Beyond Gaia: Thermodynamics of life and Earth system functioning. *Climatic Change*, 66(3): 271-319.
- Kleidon A and Heimann M. 1998. A method of determining rooting depth from a terrestrial biosphere model and its impacts on the global water and carbon cycle. *Global Change Biology*, 4(3): 275-286.
- Knyazikhin YJ, Glassy JL, Privette YT, Lotsch A, Zhang Y, Wang Y, Morisette JT, Votava P and Myneni RB. 1999. "MODIS leaf area index (LAI) and fraction of photosynthetically active radiation absorbed by vegetation (FPAR) product (MOD15) algorithm theoretical basis document." Theoretical Basis Document, NASA Goddard Space Flight Center, Greenbelt, MD20771.
- Kristensen KJ. 1974. Actual evapotranspiration in relation to leaf area. *Nordic Hydrol.*, 5: 173-182.
- Kruger GP. 1973. Konsepte, tegnieke en prosedures vir die globale hulpbronopnameprogram (terrain). Soil and Irrigation Research Institute, Report No. 154/73/784. Department of Agricultural Technical Services, Pretoria/RSA.
- Kuenene BT, Van Huyssteen CW and Hensley M. 2009. September Soil water saturation in the Cathedral Peak VI catchment KwaZulu-Natal. *South African Journal of Geology*, 114 (3): 525-534.

- Kuhn M. 2008. Building Predictive Models in R Using the caret Package. *Journal of Statistical Software* 28(5).
- Kumar CP. 1977. Estimation of Natural Ground Water Recharge. *ISH Journal of Hydraulic Engineering*, 3(1): 61-74.
- Kunz RP, Davis NS, Thornton-Dibb SLC, Steyn JM, Du Toit ES and Jewitt GPW. 2015. Assessment of biofuel feedstock production in South Africa: Atlas of water use and yield of biofuel crops in suitable growing areas, Volume 3. WRC Report No. TT 652/15, Water Research Commission (WRC), Pretoria, South Africa.
- Kunz R, Masanganise J, Reddy K, Mabhaudhi T, Lembede L, Naiken V and Ferrer S. 2020. Water use and yield of soybean and grain sorghum for biofuel production. WRC Report No. 2491/1/20, Water Research Commission (WRC), Pretoria, South Africa.
- Laio F, Porporato A, Ridolfi L and Rodriguez-Iturbe I. 2001. Plants in water-controlled ecosystems: active role in hydrologic processes and response to water stress: II Probabilistic soil moisture dynamics. *Advances in Water Resources*, 24(7): 707-723.
- Laio F. 2006. A vertically extended stochastic model of soil moisture in the root zone. *Water Resources Research*, 42(2): 1-10.
- Laclau JP, Silva EAD, Rodrigues Lambais G, Bernoux M, Le Maire G, Stape JL, ... & Nouvellon Y. (2013). Dynamics of soil exploration by fine roots down to a depth of 10 m throughout the entire rotation in *Eucalyptus grandis* plantations. *Frontiers in plant science*, 4, 243.
- Legesse D, Vallet-Coulomb C and Gasse F. 2003. Hydrological response of a catchment to climate and land use changes in Tropical Africa: case study South Central Ethiopia. *Journal of Hydrology*, 275(1-2): 67-85.
- Li F and Ma Y. 2019. Evaluation of the Dual Crop Coefficient Approach in Estimating Evapotranspiration of Drip-Irrigated Summer Maize in Xinjiang, China. *Water* 2019 (11). doi:10.3390/w11051053.
- Li Z, Yang Y, Kan G and Hong Y. 2018. Study on the Applicability of the Hargreaves Potential Evapotranspiration Estimation Method in CREST Distributed Hydrological Model (Version 3.0) Applications. *Water* 10(12). doi.org/10.3390/w10121882.
- Liu Y and Luo Y. 2010. A consolidated evaluation of the FAO-56 dual crop coefficient approach using the lysimeter data in the North China Plain. *Agricultural Water Management*, 97(1): 31-40.
- Liu C, Sun G, McNulty SG, Noormets A and Fang Y. 2017. Environmental controls on seasonal ecosystem evapotranspiration/potential evapotranspiration ratio as determined by the global eddy flux measurements. *Hydrological Earth System Sciences* 21: 311-322. doi:10.5194/hess-21-311-2017.
- Liu Y, Pereira LS and Fernando RM. 2006. Fluxes through the bottom boundary of the root-zone in silty soils: parametric approaches to estimate groundwater contribution and percolation. *Agricultural Water Management*, 84(1-2): 27-40.
- Liu Z, Chen JM, Jin G and Qi Y. 2015. Estimating seasonal variations of leaf area index using litterfall collection and optical methods in four mixed evergreen-deciduous forests. *Agricultural and Forest Meteorology*, 209-210: 36-48.
- Lobet G, Couvreur V, Meunier F, Javaux M and Draye X. 2014. Plant water uptake in drying soils. *Plant physiology*, 164(4): 1619-1627.
- MacVicar CN, De Villiers JM, Loxton RF, Verster E, Lambrechts JN, Merryweather FR, le Roux J, Van Rooyen TH and Harmse HJ von M. (1977) *Soil Classification – A Binomial System for South Africa*.

- Department of Agricultural Technical Services, Soil and Irrigation Research Institute, Pretoria, RSA. pp 150.
- MacVicar CN, Scotney DM, Skinner TE, Niehaus HS and Loubser JH. 1974. A classification of land (climate, terrain form, soil) primarily for rainfed agriculture. *South African Journal of Agricultural Extension*, 3, 21-24.
- Maeght J-L, Rewald B and Pierret A. 2013. How to study deep roots—and why it matters. *Frontiers in plant science*, 13(4): 299-313.
- Mahe G, Paturel JE, Servat E, Conway D and Dezetter A. 2005. The impact of land use change on soil water holding capacity and river flow modelling in the Nakambe River Burkina-Faso. *Journal of Hydrology*, 300(1-4): 33-43.
- Mao G and Liu J. 2019. A hydrological model for root zone water storage simulation on a global scale. *Geoscientific Model Development Discussions* (under review). 1-32.
- Mayer Z. 2013. CaretEnsemble: framework for combining caret models into ensembles. [R Package Version 1.0].
- McNamara MA. 2018. Determination of below-ground vegetation and water use model parameters for a revised South African hydrological baseline land cover. MSc dissertation. University of KwaZulu-Natal, South Africa.
- Meyer LH, Heurich M, Beudert B, Premier J and Pflugmacher D. 2019. Comparison of Landsat-8 and Sentinel-2 Data for Estimation of Leaf Area Index in Temperate Forests. *Remote Sensing* 11. doi:10.3390/rs11101160.
- Middinti S, Thumaty KC, Gopalakrishnan R, Jha CS and Thatiparthi BR. 2017. Estimating the leaf area index in Indian tropical forests using Landsat-8 OLI data. *International Journal of Remote Sensing* 38(23): 6769-6789. doi: 10.1080/01431161.2017.1363436.
- Milly PCD. 1994. Climate soil water storage and the average annual water balance. *Water Resources Research*, 30(7): 2143-2156.
- Mishra SK and Singh VP. 2002. "SCS-CN-based hydrologic simulation package". In: *Mathematical Models in Small Watershed Hydrology and Applications* Water Resources Publications Edited by: Singh, V.P. and Frevert, D.K. 391-464.
- Monteith JL. 1965. Evaporation and the Environment. 19th Symposia of the Society for Experimental Biology, 19: 205-234.
- Montenegro A and Ragab R. 2010. Hydrological response of a Brazilian semi-arid catchment to different land use and climate change scenarios: a modelling study. *Hydrological Processes*, 24(19): 2705-2723.
- Montenegro S and Ragab R. 2012. Impact of possible climate and land use changes in the semi arid regions: A case study from North Eastern Brazil. *Journal of Hydrology*, 434: 55-68.
- Morris F, Toucher MW, Clulow A, Kusangaya S, Morris C and Bulcock H. 2016. Improving the understanding of rainfall distribution and characterisation in the Cathedral Peak catchments using a geo-statistical technique. *Water SA*, 42(4): 684-693.
- Mucina L and Rutherford MC. 2006. The vegetation of South Africa, Lesotho and Swaziland. *Strelitzia* 19. South African National Biodiversity Institute, Pretoria, South Africa.
- Muzylo A, Llorens P, Valente F, Keizer JJ, Domingo F and Gash JHC. 2009. A review of rainfall interception modelling. *Journal of Hydrology*, 370: 191-206.

- Myneni RB, Hoffman S, Knyazikhin Y, Privette JL, Glassy J, Tian Y, Wang Y, Song X, Zhang Y, Smith GR, Lotsch A, Friedl M, Morisette JT, Votava P, Nemani RR and Running SW. 2002. Global products of vegetation leaf area and fraction absorbed PAR from year one of MODIS data. *Remote Sensing of Environment* 83: 214-231.
- Nänni UW. 1970. Trees, water and perspective. *South African Forestry Journal* 75: 9-17.
- Ndlovu MS and Demlie M. 2020. Assessment of Meteorological Drought and Wet Conditions Using Two Drought Indices Across KwaZulu-Natal Province, South Africa. *Atmosphere* 11. doi:10.3390/atmos11060623.
- Nemani RR and Running SW. 1989. Testing a theoretical climate soil-leaf area hydrologic equilibrium of forests using satellite data and ecosystem simulation. *Agric. For. Meteorol.* 44:245-260.
- Netzer Y, Munitz S, Shtein I and Schwartz A. 2019. Structural memory in grapevines: early season water availability affects late season drought stress severity. *European Journal of Agronomy* 105: 96-103. doi:10.1016/J.EJA.2019.02.008.
- Ngubo CZ, Demlie M and Lorentz S. 2020. Investigation of hydrological processes and the impacts of *Acacia mearnsii* plantations on groundwater in secondary aquifers: Case study at the two-stream research catchment, South Africa. *Journal of Hydrology: Regional Studies* 40. doi.org/10.1016/j.ejrh.2022.101018.
- Nijzink R, Hutton C, Pechlivanidis I, Capell R, Arheimer B, Freer J, Han D, Wagener T, McGuire K, Savenije H and Hrachowitz M. 2016. The evolution of root-zone moisture capacities after deforestation: a step towards hydrological predictions under change? *Hydrology and Earth System Sciences*, 20(12): 4775-4799.
- O'Grady AP, Eamus D and Hutley LB. 1999. Transpiration increases during the dry season: patterns of tree water use in eucalypt open-forests of northern Australia. *Tree Physiol*, 19: 591-598.
- O'Grady AP, Carter JL and Bruce J. 2011. Can we predict groundwater discharge from terrestrial ecosystems using existing eco-hydrological concepts? *Hydrol. Earth Syst. Sci.*, 15: 3731-3739.
- Orth R, Staudinger M, Seneviratne SI, Seibert J and Zappa M. 2015. Does model performance improve with complexity? A case study with three hydrological models. *Journal of Hydrology*, 523(1): 147-159.
- Ovakoglou G, Alexandridis TK, Clevers JPW and Gitas IZ. 2020. Downscaling of MODIS leaf area index using landsat vegetation index. *Geocarto International*. doi: 10.1080/10106049.2020.1750062.
- Padalia H, Sinha SK, Bhawe V, Trivedi NK and Kumar S. Estimating canopy LAI and chlorophyll of tropical forest plantation (North India) using Sentinel-2 data. *Advances in Space Research* 65: 458-469.
- Padarian J, Minasny B and McBratney, AB. 2015. Using Google's cloud-based platform for digital soil mapping. *Computers & Geosciences* 83: 80-88.
- Pappenberger F and Beven KJ. 2006. Ignorance is bliss: Or seven reasons not to use uncertainty analysis. *Water resources research*, 42(W05302): 1-8.
- Park J, Baik J and Choi M. 2017. Satellite-based crop coefficient and evapotranspiration using surface soil moisture and vegetation indices in Northeast Asia. *CATENA* 156: 305-314.
- Pasqualotto N, Delegido J, Wittenberghe SV, Rinaldi M and Moreno J. 2019. Multi-Crop Green LAI Estimation with a New Simple Sentinel-2 LAI Index (SeLI). *Sensors* 19. doi:10.3390/s19040904.
- Peduzzi A, Wynne RH, Fox TR, Nelson RF and Thomas VA. 2012. Estimating leaf area index in intensively managed pine plantations using airborne laser scanner data. *Forest Ecology and Management*, 270: 54-65.

- Pereira L, Paredes P, Hunsaker DJ, López-Urrea R and Mohammadi Shad Z. 2021. Standard single and basal crop coefficients for field crops. Updates and advances to the FAO56 crop water requirements method. *Agricultural Water Management* 243 (2021). doi.org/10.1016/j.agwat.2020.106466.
- Pereira L, Paredes P, Melton F, Johnson L, Wang T, López-Urrea R, Cancelli JJ and Allen RG. 2020. Prediction of crop coefficients from fraction of ground cover and height. Background and validation using ground and remote sensing data. *Agricultural Water Management* 241 (2020).
- Pereira LS, Allen RA, Smith M and Raes D. 2015. Crop evapotranspiration estimation with FAO56: Past and future. *Agricultural Water Management* 147: 4-20. doi.org/10.1016/j.agwat.2014.07.031.
- Pierce LL, Walker J, Dowling TI, McVicar T, Hatton TJ, Running SW and Coughlan JC. 1993. Hydroecological changes in the Murray-Darling Basin: Part 3 – A simulation of regional hydrological changes. *J. Appl. Ecol.*, 30:283-294.
- Pierret A, Maeght JL, Clément C, Montoroi JP, Hartmann C and Gonkhamdee S. 2016. Understanding deep roots and their functions in ecosystems: an advocacy for more unconventional research. *Annals of botany*, 118(4): 621-635.
- Qiao K, Zhu W, Xie Z and Li P. 2019. Estimating the Seasonal Dynamics of the Leaf Area Index Using Piecewise LAI-VI Relationships Based on Phenophases. *Remote Sensing* 11(6). doi.org/10.3390/rs11060689.
- Ragab R. 2012. Challenges and issues on measuring modelling and managing the water resources under changing climate and land use. *Integrated Water Resources Management in the Mediterranean Region*, 1(1): 91-107.
- Raz-Yaseef N, Koteen L and Baldocchi DD. 2013. Coarse root distribution of a semi-arid oak savanna estimated with ground penetrating radar. *J. Geophys. Res. Biogeosci.*, 118: 135-147.
- Reynolds CA, Jackson TJ and Rawls WJ. 2000. Estimating soil water-holding capacities by linking the Food and Agriculture Organization soil map of the world with global pedon databases and continuous pedotransfer functions. *Water Resources Research*, 36(12): 3653-3662.
- Ritchie JT and Burnett E. 1971. Dryland Evaporative Flux in a Subhumid Climate: II. Plant Influences. *Agron.*, 63: 56-62.
- Richter D and Markewitz D. 1995. How Deep Is the Soil? *BioScience*, 45: 600-609.
- Robinson NP, Allred BW, Jones MO, Moreno A, Kimball JS, Naugle DE, Erickson TA and Richardson AD. 2017. A Dynamic Landsat Derived Normalized Difference Vegetation Index (NDVI) Product for the Conterminous United States. *Remote Sensing* 9. doi:10.3390/rs9080863.
- Robock A, Vinnikov KY, Schlosser CA, Speranskaya NA and Xue Y. 1995. Use of midlatitude soil moisture and meteorological observations to validate soil moisture simulations with biosphere and bucket models. *Journal of Climate*, 8(1): 15-35.
- Rodríguez-Iturbe I and Porporato A. 2007. *Ecohydrology of water-controlled ecosystems: soil moisture and plant dynamics*. Cambridge University Press, New York, pp 10-12.
- Sakaguchi K and Zeng X. 2009. Effects of soil wetness, plant litter, and under-canopy atmospheric stability on ground evaporation in the Community Land Model (CLM3.5). *J. Geophys. Res.*, 114. doi:10.1029/2008JD010834.
- Sampson DA and Lee Allen H. 1998. Light attenuation in a fourteen year old loblolly pine stand as influenced by fertilization and irrigation. *Trees* 13: 80-87.
- Savenije HHG. 2004. The importance of interception and why we should delete the term evapotranspiration from our vocabulary. *Hydrological Processes*. 18(8): 1507-1511.

VOLUME 2: WATER USE ESTIMATION OF SFRA SPECIES

- Schenk HJ and Jackson RB. 2002. Rooting depths lateral root spreads and below-ground/above-ground allometries of plants in water-limited ecosystems. *Journal of Ecology*, 90(3): 480-494.
- Schulze RE. 1984. Hydrological Models for Application to Small Rural Catchments in Southern Africa: Refinements and Development. Water Research Commission, Pretoria, RSA, Report 63/2/84. pp 268.
- Schulze RE. 1985. Hydrological characteristics and properties of soils in Southern Africa 1: Runoff response. *Water SA* 11, 121-128.
- Schulze RE. 1995. *Hydrology and Agrohydrology*. Water Research Commission, Pretoria, RSA, TT69/95. pp 552 (ISBN 1 86845 136 4).
- Schulze RE. 2004. Determination of Baseline Land Cover Variables for Applications in Assessing Land Use Impacts on Hydrological Responses in South Africa. In: Schulze, R.E. and Pike, A. (Ed). Development and Evaluation of an Installed Hydrological Modelling System. WRC Report No. 1155/1/04.
- Schulze RE. 2007. Baseline Land Cover. In: Schulze, R.E. (Ed). 2007. South African Atlas of Climatology and Agrohydrology. Water Research Commission, Pretoria, RSA, WRC Report 1489/1/06, Section 3.4.
- Schulze RE, Angus GR and Guy RM. 1991. Making the most of soils information: A hydrological interpretation of southern African soil classifications and data bases. *Proceedings, 5th South African National Hydrology Symposium*, Stellenbosch. NSI, Cape Town, RSA. 3B-2-1 to 3B-2-12.
- Schulze RE and Horan MJC. 2008. Soils: Hydrological Attributes. In: Schulze, R.E. (Ed). 2008. *South African Atlas of Climatology and Agrohydrology*. Water Research Commission, Pretoria, RSA, WRC Report 1489/1/08, Section 4.2.
- Schulze RE, Hutson JL and Cass A. 1985. Hydrological characteristics and properties of soils in southern Africa 2: Soil water retention models. *Water SA* 11, 129-136.
- Schulze RE and Pike A. 2004. Development and Evaluation of an Installed Hydrological Modelling System. Water Research Commission Report 1155/1, Water Research Commission, Pretoria.
- Schwinning S. 2010. The ecohydrology of roots in rocks. *Ecohydrology: Ecosystems, Land and Water Process Interactions, Ecohydrogeomorphology*, 3(2): 238-245.
- Schymanski SJ, Sivapalan M, Roderick ML, Beringer J and Hutley LB. 2008. An optimality-based model of the coupled soil moisture and root dynamics. *Hydrology and earth system sciences*, 12(3): 913-932.
- Scott DF, Le Maitre DC and Fairbanks DHK. 1998. Forestry and streamflow reductions in South Africa: a reference system for assessing extent and distribution. *Water SA* 24: 187-199.
- Scott DF and Smith RE. 1997. Preliminary empirical models to predict reductions in annual and low flows resulting from afforestation. *Water SA*, 23:135-140.
- SCWG (1991) *Soil Classification – Taxonomic System for South Africa*. Department of Agricultural Development, Pretoria, RSA, Soil Classification Working Group.
- Sidhu N, Pebesma E and Câmara G. 2018. Using Google Earth Engine to detect land cover change: Singapore as a use case. *European Journal of Remote Sensing* 51(1): 486-500. doi: 10.1080/22797254.2018.1451782.
- Singh P, Singh A and Upadhyay RK. 2021. A Web Based Google Earth Engine Approach for Irrigation Scheduling in Uttar Pradesh India Using Crop Water Stress Index. *American Journal of Remote Sensing* 9(1): 42-46. doi: 10.11648/j.ajrs.20210901.15.

- SIRI 1989. Land Type Series. Department of Agriculture and Water Supply, Pretoria, RSA, Soil and Irrigation Research Institute. *Memoirs on the Agricultural Natural Resources of South Africa*.
- Shao G, Han W, Zhang H, Liu S, Wang Y, Zhang L and Cui X. 2021. Mapping maize crop coefficient Kc using random forest algorithm based on leaf area index and UAV-based multispectral vegetation indices. *Agricultural Water Management*. doi.org/10.1016/j.agwat.2021.106906.
- South African National Biodiversity Institute (SANBI). 2012. Vegetation map of South Africa, Lesotho and Swaziland. Available from: <http://bgis.sanbi.org/SpatialDataset/Detail/18> [Accessed: 14 October 2016].
- Srinivasan V, Thompson S, Madhyastha K, Penny G, Jeremiah K and Lele S. 2015. Why is the Arkavathy River drying? A multiple-hypothesis approach in a data-scarce region. *Hydrology and Earth System Sciences*, 19(4): 1905-1917.
- Sudmeyer RA, Speijers J and Nicholas BD. (2004). Root distribution of *Pinus pinaster*, *P. radiata*, *Eucalyptus globulus* and *E. kochii* and associated soil chemistry in agricultural land adjacent to tree lines. *Tree physiology*, 24(12), 1333-1346.
- Summerton MJ. 1995. Process and modelling studies in forest hydrology. M.Sc. Dissertation, Dept. Agric. Eng., Univ. of Natal, Pietermaritzburg, RSA
- Teixeira PC, RF Novais and NF Barros. Root growth and distribution of *Eucalyptus urophylla* coppice. *New Zealand Journal of Forestry Science* 32.1 (2002): 16-27.
- Topping CC. 1993. Improving Stormflow Simulation Using Rainfall Intensity Related Initial Abstractions. Unpublished MSc dissertation. University of Natal, Pietermaritzburg, RSA, Department of Agricultural Engineering. pp 175.
- Törnros T and Menzel L. 2014. Leaf area index as a function of precipitation within a hydrological model. *Hydrology Research* 45(4-5). doi.org/10.2166/nh.2013.143.
- Toucher ML and Everson CE. 2018. The expansion of knowledge on evapotranspiration and stream flow reduction of different clones/hybrids to improve the water use estimation of SFRA species (i.e., *Pinus*, *Eucalyptus*, and *Wattle* species). Water Research Commission (WRC) Report, Deliverable 3. WRC Research Project K5/2791.
- Toucher ML, Ramjeawon M, Mcnamara MA, Rouget M, Bulcock H, Kunz RP, Moonsamy J, Mengistu M, Naidoo T and Vather T. 2020. Resetting the baseline land cover against which stream flow reduction activities and the hydrological impacts of land use change are assessed. Draft report for WRC Project No. K5/2437, Water Research Commission, Pretoria, South Africa.
- Troch PA, Martinez GF, Pauwels VR, Durcik M, Sivapalan M, Harman C, Brooks PD, Gupta H and Huxman T. 2009. Climate and vegetation water use efficiency at catchment scales *Hydrological Processes*. An *International Journal*, 23(16): 2409-2414.
- Tron S, Bodner G, Laio F, Ridolfi L and Leitner D. 2015. Can diversity in root architecture explain plant water use efficiency? A modeling study. *Ecological modelling*, 312: 200-210.
- Van der Zel DW. 1995. Accomplishments and dynamics of the South African afforestation permit system. *South African Forestry Journal* 172: 49-58.
- Van Dijk AIJM and Bruijnzeel LA. 2001a. Modelling rainfall interception by vegetation of variable density using an updated analytical model. Part 1. Model description. *Journal of Hydrology* 247 (3–4) 230–238.

- Van Dijk AIJM and Bruijnzeel LA. 2001b. Modelling rainfall interception by vegetation of variable density using an updated analytical model. Part 2. Model validation for a tropical upland mixed cropping system. *Journal of Hydrology* 247 (3–4) 239–262.
- Vather T, Everson CS and Franz T. 2020. The Applicability of the Cosmic Ray Neutron Sensor to Simultaneously Monitor Soil Water Content and Biomass in an *Acacia mearnsii* Forest. *Hydrology* 7(48). doi:10.3390/hydrology7030048.
- Vertessy RA, Benyon RG, O'Sullivan SK and Gribben PR. 1995. Relationships between stem diameter, sapwood area, leaf area and transpiration in a young mountain ash forest. *Tree Physiology*, 15: 559-567.
- Vietz FG. 1972. Water deficits and nutrient availability. *Water deficits and plant growth*,
- Von Hoyningen-Huene J. 1983. Die Interzeption des Niederschlages in landwirtschaftlichen Pflanzenbeständen. Deutscher Verband für Wasserwirtschaft und Kulturbau. Schriften 57 1–66. Verlag Paul Parey, Hamburg Germany.
- Vose JM, Sullivan NH, Clinton BD and Bolstad PV. 1995. Vertical leaf area distribution, light transmittance, and application of the Beer-Lambert Law in four mature hardwood stands in the southern Appalachians. *Canadian Journal of Forestry Research* 25 1036-1043.
- Vrettas MD and Fung IY. 2017. Sensitivity of transpiration to subsurface properties: Exploration with a 1-D model. *Journal of Advances in Modeling Earth Systems*, 9(2): 1030-1045.
- Wagener T, Sivapalan M, Troch P and Woods R. 2007. Catchment classification and hydrologic similarity. *Geography compass*, 1(4): 901-931.
- Wang R, Chen JM, Liu Z and Arain A. 2017. Evaluation of seasonal variations of remotely sensed leaf area index over five evergreen coniferous forests. *ISPRS Journal of Photogrammetry and Remote Sensing*, 130: 187-201.
- Wang Q, Adiku S, Tenhunen J and Granier A. 2005. On the relationship of NDVI with leaf area index in a deciduous forest site. *Remote Sens Environ* 94(2): 244-255.
- Wang-Erlandsson L, Van Der Ent RJ, Gordon LJ and Savenije HHG. 2014. Contrasting roles of interception and transpiration in the hydrological cycle – Part 1: Temporal characteristics over land. *Earth System Dynamics*, 5(2): 441-469.
- Wang-Erlandsson L, Bastiaanssen WG, Gao H, Jagermeyr J, Senay GB, Van Dijk A, Guerschman JP, Keys PW, Gordon LJ and Savenije HH. 2016. Global root-zone storage capacity from satellite-based evaporation. *EGU General Assembly Conference Abstracts* 18.
- Whitley RJ, Zeppel MJB, Armstrong N, Macinnis-Ng C, Yunusa IAM and Eamus D. 2008. A modified JS model for predicting stand-scale transpiration of an Australian native forest. *Plant and Soil.*, 305: 35-47.
- Whitley R, Medlyn B, Zeppel MJB, Macinnis-Ng C and Eamus D. 2009. Comparing the Penman-Monteith equation and a modified Jarvis-Stewart model with an artificial neural network to estimate stand-scale transpiration and canopy conductance. *Journal of Hydrology*, 373: 1-2. 256-266.
- Whitley R, Taylor D, Macinnis-Ng C, Zeppel M, Yunusa I, O'Grady A, Froend R, Medlyn B and Eamus D. 2013. Developing an empirical model of canopy water flux describing the common response of transpiration to solar radiation and VPD across five contrasting woodlands and forests. *Hydrol. Process.*, 27: 1133-1146.

- Yan K, Park T, Yan G, Liu Z, Yang B, Chen C, Nemani RR, Knyazikhin Y and Myneni RB. 2016. Evaluation of MODIS LAI/FPAR Product Collection 6. Part 2: Validation and Intercomparison. *Remote Sensing* 8(6). doi.org/10.3390/rs8060460.
- Yang Y, Donohue RJ and McVicar TR 2016. Global estimation of effective plant rooting depth: Implications for hydrological modeling. *Water Resources Research*, 52(10): 8260-8276.
- Yin G, Li J, Liu Q, Fan W, Xu B, Zeng Y and Zhao J. 2015. Regional Leaf Area Index Retrieval Based on Remote Sensing: The Role of Radiative Transfer Model Selection. *Remote Sensing* 7: 4604-4625. doi:10.3390/rs70404604.
- Yuan Y, Nie W, McCutcheon SC and Taguas EV. 2012. Initial abstraction and curve numbers for semiarid watersheds in Southeastern Arizona. *Hydrological Processes*. DOI: 10.1002/hyp.9592
- Zegre NP. 2008. Local and downstream effects of contemporary forest harvesting on streamflow and sediment yield. PhD dissertation. Oregon State University.
- Zeppel M. 2013. Convergence of tree water use and hydraulic architecture in water-limited regions: a review and synthesis. *Ecohydrol.* 6: 889-900.
- Zhai H, Huang F and Qi H. 2020. Generating High Resolution LAI Based on a Modified FSDAF Model. *Remote Sens* 12. doi:10.3390/rs12010150.
- Zhang J, Wang J, Sun R, Zhou H and Zhang H. 2020. A Model-Downscaling Method for Fine-Resolution LAI Estimation. *Remote Sensing* 12. doi:10.3390/rs12244147.
- Zhang M and Wang S. 2016. A review of precipitation isotope studies in China: Basic pattern and hydrological process. *Journal of Geographical Sciences*, 26(7): 921-938.
- Zhao J, Chen S, Hu R and Li Y. 2017. Aggregate stability and size distribution of red soils under different land uses integrally regulated by soil organic matter, and iron and aluminum oxides. *Soil and Tillage Research*, 167(1): 73-79.
- Zhao L, Xia J, Xu C, Wang Z, Sobkowiak L and Long C. 2013. Evapotranspiration estimation methods in hydrological models. *Journal of Geographical Sciences* 23: 359-369 (2013). doi.org/10.1007/s11442-013-1015-9.
- Zhao Q, Poulson SR, Obrist D, Sumaila S, Dynes JJ, McBeth JM and Yang Y 2016. Iron-bound organic carbon in forest soils: quantification and characterization. *Biogeosciences*, 13(1): 4777-4788.
- Zhu YI, Ren LI, Lui H and Skaggs TH. 2006. Determination of root-zone water storage in a desert woodland using a two-layer moisture balance model *Hydrological Research in China: Process Studies Modelling Approaches and Applications*. IAHS publication, 322 (1):246.

APPENDIX A: Data storage

This research project has generated over 160 GB of compressed data in WinRAR format of input and output files pertaining to the ACRU agrohydrological model. This represents a wealth of simulated data generated from national model runs performed for each of the 5838 quinary catchments (or altitude zones). All simulated datasets described below are stored and archived on a files server located in the ICS Server Room on the University of KwaZulu-Natal's main campus in Pietermaritzburg. The contact person is Richard Kunz (kunzr@ukzn.ac.za).

A.1 ACRU input files

The following model input files were generated to meet the project's objectives:

- a) ACRU climate (.txt) files for each of the 5838 quinaries (altitude zones) based on observed (historical) climate data from 1950-1999 (5838 files: 12.1 GB). This dataset was originally developed by WRC Project No. K5/2491 (Kunz et al., 2020).
- b) Updated ACRU soils information for each of the 5838 altitude zones, which was generated from soil parameters for each land type and terrain unit (.csv file format: 457 KB).
- c) For each of the 15 forestry species/hybrids/clones, unique monthly values were generated for each quinary (altitude zone) for the following parameters: crop coefficients (CAY; 15 files, each 382 KB) and interception loss (VEGINT; 15 files, each 377 KB).
- d) For each of the 15 forestry species/hybrids/clones, unique monthly values were generated the following parameters: leaf area index or LAI (ELAIM; 15 files, each 1 KB).
- e) Unique values were generated for each genus (eucalypts, pines and wattle) for the following parameters: fraction of plant available water at which water stress occurs (CONST; 3 files, each 1 KB).
- f) Generic values (i.e., same values used for each species/hybrid/clone) were generated for the following parameters: coefficient of initial abstraction (COIAM), root colonisation of the B-horizon (COLON), enhanced wet canopy evaporation (FOREST), percentage of surface cover (PCSUCO) and rooting distribution in the A-horizon (ROOTA).
- g) For natural vegetation, the above parameters were developed in WRC Project No. K5/2437 (Toucher et al., 2019).
- h) The above-mentioned parameters were used to create ACRU's main input parameter file called menu (16 files, each 59.4 MB) and ACRU's supplementary input parameter file called suppmenu (16 files, each 2.74 MB).

A.2 ACRU output files

The following model output files were generated for both natural vegetation, as well as for each of the 15 forestry species/hybrids/clones and for each of the 5838 quinaries (altitude zones):

VOLUME 2: WATER USE ESTIMATION OF SFRA SPECIES

- a) Monthly and annual statistics for the following climate variables (1 file; 58.3 MB):
 - i. Raw rainfall (mm; with no adjustment)
 - ii. Adjusted rainfall (mm; with CORPPT adjustment)
 - iii. Daily maximum temperature (°C)
 - iv. Daily minimum temperature (°C)
 - v. Mean temperature (°C)
 - vi. FAO56 reference evapotranspiration (mm; short grass)
 - vii. ASCE reference evapotranspiration (mm; tall grass)
 - viii. A-pan equivalent evaporation (mm; FAO56 * CORPAN)
 - ix. Solar radiation (MJ m² day⁻¹)
 - x. Maximum relative humidity (%)
 - xi. Minimum relative humidity (%)
 - xii. Mean relative humidity (%)
 - xiii. Windrun (km day⁻¹)
 - xiv. No. of rain days > 0 mm
- b) Binary (.BIN) files of daily values for 28 output variables in mm (21 files; 8.12 GB), e.g.
 - i. AET (actual evapotranspiration)
 - ii. ERFL (effective rainfall)
 - iii. QUICKF (quick flow)
 - iv. RUN (base flow)
 - v. SIMSQ (storm flow, i.e. runoff for each individual catchment)
 - vi. CELRUN (stream flow, including all upstream contributions)
- c) Monthly output for each variable from 1950-1999 (21 files; 206 MB)
- d) Annual output for each variable 1950-1999 (21 files; 30.1 MB)
- e) 17 monthly and annual statistics for each variable (21 files; 108 MB) as follows:
 - i. mean
 - ii. variance, standard deviation, coefficient of variation (CV), skewness, kurtosis
 - iii. minimum, maximum, sum
 - iv. number of observations
 - v. percentile values (10, 20, 33, 50, 67, 80, 90)
- f) Extracted statistics (mean, 10th, 50th and 90th percentiles) for each of the 28 variables at a
 - i. monthly level (28 files; 24.7 MB)
 - ii. annual level (28 files; 3.69 MB)
- g) GIS-ready files to assist with analysis mapping (i.e., extracted values for all 5828 quinarries) for the following:
 - i. 14 climate and 38 ACUR variables
 - ii. statistics (mean, 10th, 50th and 90th percentiles)
49 seasons (1 file: 0.4 MB)
29 seasons (1 file: 0.4 MB)
 - iii. monthly (1 file; 4.51 MB) and annual (1 file; 33.9 MB level)
- h) SFRA analysis highlighting the impact of land use change on simulated runoff relative to the baseline, i.e. natural vegetation (7 files; 2.33 MB)

APPENDIX B: New knowledge creation report

Motivation: This to evaluate if the project is on course to deliver on its promises or mandates. If not, what are the challenges and how is the team dealing with the challenges.

WRC Project Number	K5/2791
Project title	The Expansion of Knowledge on Evapotranspiration and Stream Flow Reduction of Different Clones/Hybrids to Improve the Water Use Estimation of SFRA Species (i.e. Pinus, Eucalyptus, and Wattle Species)
Project Leader	Prof A Clulow
Institution/Contractor	University of KwaZulu-Natal
Financial Year	2021/2022

ITEMS	ORIGINAL DESCRIPTION (As reported in the first meeting)	AGREED CHANGES regarding the creation of new knowledge (the WRC should formally authorize any changes)
1. (a) What is the new knowledge created by this project?	Additional water use of some commercial forestry species and improved streamflow estimates	There have been no changes
(b) What/which gap(s) will be filled by the new knowledge?	To provide best possible SFRA estimates including changes between genus and species	There have been no changes
2. What product(s) will be/has been produced?	A methodology for determining leaf area and crop coefficients using Google Earth engine and machine learning. ACRU – improved streamflow reduction estimates through improved soils, canopy interception, natural vegetation coverage and crop co-efficient inputs. SFRA Utility has been updated to include the new ACRU outputs.	There have been no changes
3. How innovative is the new product(s) in no 2 above?	The products make use of the most up-to-date information and technology available to improve SFRA estimates	There have been no changes
4. Who are the users and beneficiaries of the product(s)/output(s)?	DWS and the forestry industry.	There have been no changes
5. How do you know that the users need the product(s) of this project?	There have been increasing calls from landowners requesting crop changes that could not be accommodated with existing tools.	There have been no changes
Research Manager Recommendation	Signature	Date
Executive Manager Approval	Signature	Date

APPENDIX C: Capacity building report

Name	Degree/post	Gender	Race	Commenced	Completed	Title
Nkosinathi Kaptein	PhD	Male	Black	2018	2022	Improved understanding of commercial forestry water use and the hydrological implications
Shaeden Gokool	Post-doctoral researcher	Male	Indian	2020	Ongoing	Leveraging Google Earth engine and machine learning to derive leaf areas index and crop coefficient data for commercial forestry
Robyn Horan	MSc	Female	White	2018	2019	Investigation of the root-zone storage concept for use in the ACRU Model

